TAMPEREEN TEKNILLINEN YLIOPISTO
TAMPERE UNIVERSITY OF TECHNOLOGY

Niina Ahola

In vitro Studies of Bioabsorbable and Antibiotic-Releasing Composites for the Treatment of Osteomyelitis

Julkaisu 1188 • Publication 1188

Tampere 2014

Tampereen teknillinen yliopisto. Julkaisu 1188
Tampere University of Technology. Publication 1188

Niina Ahola

In vitro Studies of Bioabsorbable and Antibiotic-Releasing Composites for the Treatment of Osteomyelitis

Thesis for the degree of Doctor of Science in Technology to be presented with due permission for public examination and criticism in Sähkötalo Building, Auditorium S4, at Tampere University of Technology, on the 14th of February 2014, at 12 noon.

Tampereen teknillinen yliopisto - Tampere University of Technology
Tampere 2014

ISBN 978-952-15-3211-5 (printed)
ISBN 978-952-15-3234-4 (PDF)
ISSN 1459-2045

Abstract

Osteomyelitis is a severe bacterial infection that is considered to be one of the most-difficult-to-treat infections. It causes the destruction of bone tissue and the treatment often includes surgical debridement that creates a defect in the bone. Because there may be bacteria left in the surrounding tissues, long courses of antibiotics are also required. Adequate antibiotic concentrations using oral or intravenous antibiotics may be difficult to achieve because of degenerated blood circulation. Local antibiotic delivery using implanted antibiotic-releasing materials in the defect site provides an efficient way of achieving high local antibiotic concentrations, and also decreases the side-effects that are often associated with oral or intravenous antibiotics.

The objective of this thesis was to develop bioabsorbable and antibiotic-releasing (either rifampicin or ciprofloxacin) composite materials that can be used for the local antibiotic treatment of osteomyelitis and that also include a osteoconductive ceramic component to aid bone healing. Continuous antibiotic delivery for three to six months was requested. The materials developed are to be used together so that the surgeon can decide in which ratio to use them. The materials chosen for the study were medical grade poly(L-lactide-co-ε-caprolactone) as the bioabsorbable polymer matrix, β-tricalcium phosphate (β-TCP) as the osteoconductive ceramic component, and the antibiotics ciprofloxacin and rifampicin that are clinically used as a combination in the treatment of osteomyelitis. All the materials used are approved for clinical use. Ten different composites of these materials plus plain poly(L-lactide-co-ε-caprolactone) were processed using extrusion and cut into pellet shaped samples (diameter approximately 2.5 mm and length 2.5 mm). Four of the composites had no antibiotic component, three composites contained 8 wt-% ciprofloxacin, and three contained 8 wt-% rifampicin. A series of *in vitro* tests (Sörensen phosphate buffer, pH 7.4, 37 °C) were performed to evaluate the hydrolytic degradation and drug release behavior of the manufactured composites. The most promising antibiotic-releasing composites, showing continuous release, were also tested against two common osteomyelitis-causing model bacteria utilizing genetically engineered bioluminescent bacteria.

The antibiotic containing composites with 50 wt-% of β-tricalcium phosphate were the most promising with continuous drug release up to approximately 20 weeks. The antibiotic release occurred in several phases and the release was not similar for the two studied antibiotics. The differences were attributed mainly to different molecular size (ciprofloxacin 331 g/mol and rifampicin 823 g/mol) and differences in water solubility (For rifampicin in water at 30 °C, 1.5-1.7 mg/ml depending on the crystal form (Henwood et al. 2000) and for ciprofloxacin at 37 °C, 0.20 mg/ml at pH 7.8 and 0.22 mg/ml at pH 6.9 (Breda et al. 2009)). The composites containing 50 wt-% β-TCP also showed good effect against the common osteomyelitis-causing bacteria, *Staphylococcus epidermidis* and *Pseudomonas aeruginosa*. The hydrolytic degradation of the polymer

followed first order kinetics and the molar ratio of the comonomers changed, as the degradation proceeded. These composites have great potential to be used in the treatment of osteomyelitis or other bone related infections. In this work, only *in vitro* tests were performed, and thus the next step for these composites is preclinical testing.

Acknowledgements

The work presented in this thesis was performed at the Tampere University of Technology, Department of Biomedical Engineering (Department of Electronics and Communications Engineering from January 1st, 2013).

The work was financially supported by the Finnish Funding Agency for Technology and Innovation (TEKES), National Doctoral Programme of Musculoskeletal Disorders and Biomaterials (TBDP), Emil Aaltonen Foundation, Tampere Science Foundation and Finnish Concordia Fund.

Foremost, I want to express my sincere gratitude to my supervisor, professor Minna Kellomäki for her guidance and support during this work and giving me the opportunity to work in the fascinating world of biomaterials.

I want to thank my co-authors Minna Veiranto, Jaana Rich, Alexander Efimov, Markus Hannula, Jukka Seppälä, Matti Karp and especially Noora Männistö for fruitful co-operation and sharing their expertise with me.

I am very grateful to the official pre-examiners of this thesis, professor Kristiina Järvinen and professor Vasif Hasirci, for their effort and constructive comments for improving the thesis.

All my colleagues at the Biomaterial and tissue engineering group of the former Department of Biomedical Engineering deserve a warm thank you for creating a nice atmosphere for working and taking me as a part of the group when I joined it in 2007. Furthermore, I like to thank Raija Reinikainen, Eija Ahonen and Vuokko Heino for technical help and Jari Viik for help in statistical analysis. I want to thank Suvi Heinämäki for all the help in the lab and for her friendship. I also would like to thank the personnel of Bioretec ltd., especially Kaija Honkavaara for help in the lab and Kalle Räsänen for his expertise in polymer processing. I am very grateful to Peter Heath for language editing and for valuable guidance and discussions about scientific writing.

I owe my deepest gratitude to my parents, Jukka and Marketta Mäkelä, for their love and support throughout the years. I want to thank also the rest of my family and my friends near and far for their support and encouragement through all the bends in the road of this project.

Finally, there are no words to thank enough my dear husband Pasi for his truly endless patience, understanding, love and support. This project would not have been finished without you.

Jimi and Niko, thank you for reminding me every day about what is important in life. You are the best!

Pirkkala, December 2013

Niina Ahola

Table of contents

List of original publications

This thesis is based on the following original publications that are referred to in the text as I-IV. The publications are reproduced with the kind permission of the publisher (Publication I) and according to the Creative Commons Attribution 3.0 Licence (Publications II, III and IV).

I Ahola, N., Veiranto, M., Rich, J., Efimov, A., Hannula, M., Seppälä, J., and Kellomäki, M., Hydrolytic degradation of composites of poly(L-lactide-co-ε-caprolactone) 70/30 and β-tricalcium phosphate, Journal of Biomaterials Applications, 28 (2013), 529-543

II Ahola, N., Männistö, N., Veiranto, M., Karp, M., Rich, J., Efimov, A., Seppälä, J., and Kellomäki, M., An in vitro study of composites of poly(L-lactide-co-ε-caprolactone), β-tricalcium phosphate and ciprofloxacin intended for local treatment of osteomyelitis, Biomatter, 3 (2013), e23162

III Ahola, N., Veiranto., M., Männistö, N., Karp, M., Rich, J., Efimov, A., Seppälä, J., and Kellomäki, M., Processing and sustained in vitro release of rifampicin containing composites to enhance the treatment of osteomyelitis, Biomatter, 2 (2012), 213-225

IV Männistö, N., Ahola, N., Karp, M., Veiranto, M., Kellomäki, M., In vitro bioluminescence used as a method for real-time inhibition zone testing for antibiotic- releasing composites, British Microbiology Research Journal, 4 (2014) 235-254

Author's contribution

I The author planned the research work together with Minna Veiranto and Minna Kellomäki. The materials were processed in collaboration with Bioretec Ltd. The author performed most of the test series and analyzed the samples. Alexander Efimov helped with the NMR analysis. Markus Hannula performed μCT imaging and analyzed the results. The molecular weight measurements were done in collaboration with Jaana Rich. The author interpreted the results and wrote the manuscript as corresponding author. The co-authors commented on the manuscript.

II The author planned the research together with Minna Veiranto and Minna Kellomäki. The materials were processed in collaboration with Bioretec Ltd. The author performed most of the test series and analyzed the samples. Noora Männistö performed the inhibition zone tests with bioluminescent bacteria. Alexander Efimov helped with the NMR analysis. The molecular weight measurements were done in collaboration with Jaana Rich. The author interpreted the results and wrote the manuscript as corresponding author. The co-authors commented on the manuscript.

III The author planned the research together with Minna Veiranto and Minna Kellomäki. The materials were processed in collaboration with Bioretec Ltd. The author performed most of the test series and analyzed the samples. Noora Männistö performed the inhibition zone tests with bioluminescent bacteria. Alexander Efimov helped with the NMR analysis. The molecular weight measurements were done in collaboration with Jaana Rich. The author interpreted the results and wrote the manuscript as corresponding author. The co-authors commented on the manuscript.

IV All the authors took part in the design of the experimental test series. The author supervised the work and Noora Männistö carried out the research work. The manuscript was written jointly by the author and Noora Männistö.

Abbreviations

ATCC	American Type Culture Collection
β-TCP	β-Tricalcium phosphate
BLI	Bioluminescence imaging
CaP	Calcium phosphate
CRP	C-reactive protein
DSC	Differential scanning calorimetry
FDA	Food and drug administration (United States)
GI	Gastrointestinal
GPC	Gel permeation chromatography
HA	Hydroxy apatite
IBTG	Isopropyl-β-D-thiogalaktopyranoside
i.v.	Intravenous
kGy	kiloGray, SI unit for radiation dose
KH_2PO_4	Potassium dihydrogen phosphate
LB	Luria-Bertani –medium
logP	Partition coefficient
MIC	Minimum inhibitory concentration
M_n	Number average molecular weight
M_w	Weight average molecular weight
Na_2HPO_4	Sodium hydrogen phosphate
NMR	Nuclear magnetic resonance
pAT19	Plasmid with erythromycin resistance factor
pCGLS-1	Plasmid with ampicillin resistance factor
PCL	Polycaprolactone
PD	Polydispersity
PLCL	Poly(L-lactide-co-ε-caprolactone)
PLGA	Poly(lactide-co-glycolide)
PMMA	Poly(methyl methacrylate)
pUCP24GW	Plasmid with gentamycin resistance factor
SEC	Size exclusion chromatography
SEM	Scanning electron microscopy
T_g	Glass transition temperature
TGA	Thermogravimetric analysis
T_m	Melting temperature
TMS	Tetramethylsilane
UV	Ultraviolet light
Vis	Visible light

Symbols

A	Area
a	Constant describing the geometrical and structural characteristics of a test specimen
C	Concentration
D	Diffusion coefficient
J	Diffusion flux
k	Constant
l	Thickness of a sample
M_0	Mass of active agent in the system at time t=0
M_t	Mass of active agent released in time t
M_∞	Mass of active agent released at time t=∞
n	Release exponent describing the transport mechanism of released active agent
ñ	Number average sequence length
P	Permeability of a polymer to an active agent
t	Time
x	Position in a sample relative to x-axis
y	Position in a sample relative to y-axis
z	Position in a sample relative to z-axis

Definitions

Allograft	Graft taken from another individual of the same species as the recipient.
Autograft	Graft taken from a source in the individual who receives it. The donor and the recipient are the same.
Bioabsorbable	Capable of being degraded or dissolved and subsequently metabolized within an organism.
Biocompatibility	The ability of a material to perform with an appropriate host response in a specific application.
Biodegradable	Capable of being degraded by biological activity or system.
Biofilm	A coherent cluster of bacterial cells embedded in a matrix that are more tolerant to most antimicrobials and the defense than planktonic bacterial cells. Layer-like aggregation of cells and cellular products attached to a solid surface or substratum.
Biomaterial	Material intended to interface with biological systems to evaluate, treat, augment or replace any tissue, organ or function of the body.
Bolus	A single dose of a drug or other medicinal preparation given all at once.
Degradation	Process of chain cleavage in a polymer.
Erosion	Mass loss.
In vitro	Taking place in a test tube, culture dish, or elsewhere outside a living organism. (Lat. ‘In glass’).
In vivo	Taking place in a living organism (Lat. ‘In a living thing’).
Osteoblast	Bone forming cell.
Osteogenic	Capable of producing bone.
Osteoconductive	Capable of guiding bone growth on a surface.
Osteoinductive	Capable of inducing bone growth.
Prophylaxis	Prevention of disease or control of its possible spread.
Systemic	Affecting the body generally.

1 INTRODUCTION

In the field of biomaterials, drug delivery of various active agents is a very important application area. Traditionally, drug-delivering materials have been developed with optimal drug delivery properties in mind. Nowadays, the development of drug-delivering materials is heading towards multifunctional materials that can also perform other functions in addition to drug delivery. Major interest lies in applications where the goal of the biomaterials is to help the body to heal itself. Such biomaterials may be called third generation biomaterials and they often combine bioabsorbability and bioactivity with other functions such as drug release. (Hench and Polak 2002)

Today, infectious diseases are still a major problem around the world despite the efforts in the development of antibiotics and the treatment methods. Infectious diseases kill more people worldwide than any other single cause (Muñoz-Bonilla and Fernández-García 2012). A disease that is often considered as one of the most difficult-to-treat infections is osteomyelitis (Sia and Berbari 2006). Osteomyelitis is an infection of bone caused by bacteria that are usually very difficult to eradicate from the infected bone tissue (Chihara and Segreti 2010; Sia and Berbari 2006). The disease may lead to amputation or even death. The treatment of osteomyelitis is long and hard for the patient and expensive with long courses of antibiotics. Treatment of chronic osteomyelitis includes a radical surgical debridement of the infected tissue that leaves a defect in the bone called a dead space. The treatment of the dead space has often been done in two stages. The first stage has been to fill the dead space with biostable antibiotic-releasing poly(methyl methacrylate) beads that eradicate the remaining bacteria in the tissues surrounding the dead space. The second stage has been the removal of the antibiotic-releasing beads followed by bone grafting. This method of treatment is not optimal because it involves two surgeries and increases the risks for the patient. Bioabsorbable, osteconductive and antibiotic-releasing composites offer the possibility to treat osteomyelitis in one stage and to reduce both the risks for the patient and the costs. Such materials have been requested in the literature and the research is going on to achieve these goals (Jiang et al. 2012). The development of such bone filling materials has been the goal in this thesis. In addition to the treatment of osteomyelitis, these materials can also be used as prophylaxis to prevent bone related infections.

This thesis consists of a literature review, experimental section, and four original publications. The literature review provides an overview of the field of controlled antibiotic delivery applications intended for the treatment or prevention of bone infections. In addition, the medical background of osteomyelitis and implant-related infections as well as the treatment of them are addressed. In the experimental part, bioabsorbable and antibiotic-releasing composite materials were developed for use as

bone defect filler materials in the treatment of osteomyelitis and other bone related infections. The composites are composed of three FDA-approved components. A bioabsorbable polymer matrix provides bioabsorbability, drug releasing properties and the possibility of healing bone tissue to replace the material. Bioceramic, β-tricalcium phosphate, offers osteoconductivity, e.g. it helps the bone tissue to grow and heal. Two different antibiotics, ciprofloxacin and rifampicin, were released in a continuous manner from the respective composites to eradicate bacteria. The optimal composition was investigated in the *in vitro* test series and the degradation and drug release properties of the materials were tested. The effect of the most promising composites against common osteomyelitis-causing bacteria *Pseudomonas aeruginosa* and *Staphylococcus epiderdmidis* was shown *in vitro* using genetically engineered bioluminescent bacterial strains.

2 LITERATURE REVIEW

2.1 Controlled drug delivery

2.1.1 Controlled drug delivery systems

Medical drugs have been traditionally administered systemically via oral and intravenous (bolus injections or infusions) routes and via intramuscular or subcutaneous injections. In the case of intravenous infusion, a very constant drug concentration in the blood circulation is achieved. When the other administration routes are used, the drug is released immediately and the drug concentration in the body may fluctuate according to the doses taken (Figure 1). Additionally, in cases when the doses are taken too frequently, a toxic level may be reached. For part of the time, however, the drug concentration is still below the minimum effective concentration. If longer time periods with effective drug concentration are desired, the only option is to increase the dose. By doing so, the drug concentration may reach the toxic level and increase the side effects. (Heller 1996) The drawbacks of the traditional delivery routes and not constant drug concentration are toxicity issues (side effects), patient discomfort, and the possible development of bacterial resistance. Moreover, the drug may take a longer time to reach the target and may not reach those areas that lack vascularization (Hanssen 2005; Parker et al. 2011). Additionally, because the whole organism treated with the drug is affected as the drug is distributed throughout the organism, unwanted side effects can increase.

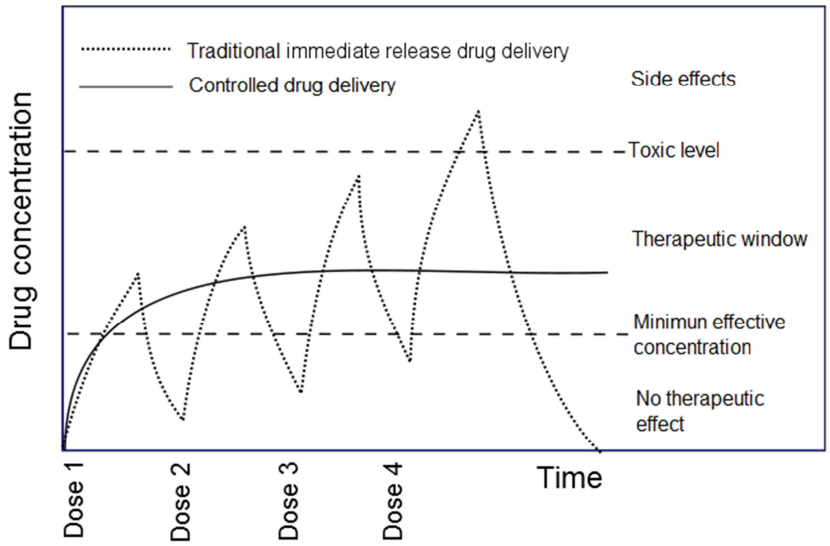

Figure 1. Drug concentration in traditional immediate release drug delivery and controlled drug delivery (modified from (Anonymous2003)).

In controlled drug delivery, the goal may be either to deliver the drug in a controlled manner or to target the delivery locally in the body or both (Anonymous2003). Examples of controlled drug delivery systems are plasters that release analgesic agents, hormones, or nicotine. Examples of targeted drug delivery are antibiotic-releasing poly(methyl methacrylate) (PMMA) beads that release gentamycin antibiotic in bone defects in the treatment of osteomyelitis (Zilberman and Elsner 2008) or contraceptive hormone-releasing intrauterine systems (Luukkainen 1991). Targeted drug delivery may be supplementary to the systemic drug administration or completely replace it (Hanssen 2005). Several benefits can be achieved when drugs are administered either in a controlled manner or targeted to a specific site in the body. These benefits can include: reduced side effects, lower doses, better efficacy of the drugs, and drugs with a narrow therapeutic window or low bioavailability can be administered (Jain et al. 2005; Lao et al. 2011). Drug concentrations on the site of the delivery can be extremely high compared with those concentrations achieved by systemic administration, which increases the efficacy of the treatment. Especially, in the case of antibiotics, the high concentration achieved locally may be critical in eradicating bacteria (Hanssen 2005). However, care must be taken so that the local concentration does not exceed toxic levels and stays above the therapeutical level. Additionally, controlled release technology has the potential to reduce patient compliance problems and the adverse effects that cause roughly 10-14% of the hospitalizations in the U.S. This would mean major savings in the health care sector. (Rothstein and Little 2011) The development of new local delivery methods may also lead to new therapies because local drug delivery allows new administration routes and the possibility to better deliver complex drugs (e.g. proteins), which are normally destroyed in the gastrointestinal tract. From the commercial point of view, new drug delivery methods offer a good investment opportunity for the drug companies when there is a new way of delivery developed for an already existing drug. (Langer 1990)

If the controlled drug delivery system is bioabsorbable, no removal of the device is required, which is an additional advantage. Usually, such systems utilize bioabsorbable polymers that degrade in the body to harmless degradation products that are removed by the body via normal metabolism. Bioabsorbable synthetic polymers can be tailored to meet specific drug release patterns and degradation rates (Mönkäre et al. 2010; Mönkäre et al. 2012; Pulkkinen et al. 2007). The addition of substances other than small molecular weight drugs, such as growth factors and peptides, may also be possible (Hanssen 2005; Mönkäre et al. 2010; Mönkäre et al. 2012; Pulkkinen et al. 2007). Bioabsorbable drug-releasing systems have been developed in various forms. Some examples of these are antibiotic-releasing screws (Veiranto et al. 2002; Veiranto et al. 2004b), bone cements (Ginebra et al. 2012), pellets (Koort et al. 2006; Koort et al. 2008), cylinders (Alvarez et al. 2008), fibers (Nikkola et al. 2008), nanofibers (Kim et al. 2012), and scaffolds (Mouriño and Boccaccini 2010).

In the case of bone related infections, local antibiotic delivery offers a way to overcome the difficulty of administering the drug to infected bone tissue that has poor blood circulation (Alvarez et al. 2008; Castro et al. 2003; Castro et al. 2005; Garvin et al. 1994; Mäkinen et al. 2005a; Mäkinen et al. 2005b; Miyai et al. 2008; Tiainen et al. 2009; Waknis and Jonnalagadda 2011). Previous studies have shown that with the local administration of antibiotics, the drug concentrations in the blood or other tissues are low, at least a decade lower than in the tissues surrounding the locally drug-releasing material (Koort et al. 2005; Koort et al. 2006; Koort et al. 2008). This naturally leads to decreased side effects such as nausea that has been often reported as the cause for the discontinuation of the antibiotic therapy or the continuation of the therapy but with a lower dose. (Bliziotis et al. 2007; Zimmerli et al. 1998)

During the last decades, there have been a large number of scientific articles published regarding controlled drug delivery research and applications. However, only a few products that release drugs locally have reached the commercial stage. This may be due to the complexity of the research area and the numerous factors that influence the release of drug molecules from different polymeric systems. These factors include molar mass and molar mass distribution (polydispersity) of the polymer, permeability, the molecular size of the drug, polymer morphology (Frank et al. 2005; Hurrell and Cameron 2002), the chemical composition of both the polymer and the drug (Frank et al. 2005; Li et al. 1996), the size and shape of the device (Ahola et al. 2003), the porosity of the device, drug load, and drug/polymer interactions. (Lao et al. 2011; Li and Vert 1999; Nair and Laurencin 2007) These factors are very much dependent on each other and cannot be considered separately. Additionally, regulatory procedures and requirements cause the development phase of implantable drug delivery devices to be long and include expensive and time-consuming clinical studies.

Some commercially available antibiotic-releasing products for the targeted drug delivery of bone tissue are collected in Table 1.

Table 1. Examples of commercial antibiotic-releasing products for the treatment or prevention of bone related infections.

Product name	Manufacturer / Distributer	Drug	Matrix	Indication
CiproScrew	Bioretec Ltd.	Ciprofloxacin	PLGA[a]	Fracture fixation in risk patients
Septopal	Biomet Deutschland GmbH	Gentamycin	PMMA[b]	Osteomyelitis
SmartSet GMV SmartSet GHV DePuy 2 Fast Set Bone Cement	DePuy	Gentamycin	PMMA[b]	Second stage of a two-stage revision for total joint arthroplasty, after the initial infection has been cleared.
Simplex P Simplex SpeedSet	Stryker	Tobramycin	PMMA[b] P(MMA-S)[c]	Fixation of prostheses to living bone in the second stage of a two-stage revision for total joint arthroplasty
Refobacin Bone Cements Biomet Bone Cements	Biomet	Gentamycin	PMMA[b]	Primary implantation and revisions
Palacos R+G Palacos MV+G Palacos LV+G	Heraeus Medical	Gentamycin	PMMA[b]	Hip and knee joint replacement

a: poly(lactide-co-glycolide)
b: poly(methyl methacrylate)
c: poly(methyl methacrylate-co-styrene)

2.1.2 Mathematical theory of controlled drug delivery

2.1.2.1 Delivery rates

The pattern of active agent release from a system can vary over a wide range. The three patterns describing the release used most often are zero order release, first-order release, and square-root-of-time release. According to Baker (Baker 1987), these can be presented as follows:

Zero-order release is the simplest case mathematically with constant active agent release and can be described with the following equation (Equation 1):

$$\frac{dM_t}{dt} = k \qquad (1)$$

where M_t is the mass of active agent released, t is time, and k is constant.

In the first order release, the release rate of the active agent declines exponentially (Equation 2)

$$\frac{dM_t}{dt} = kM_0 exp(-kt) \quad (2)$$

where M_0 is the mass of active agent in the system at time t=0.

In the square-root-of-time release pattern, the release rate is proportional to the inverse of the square root of time (Equation 3)

$$\frac{dM_t}{dt} = \frac{k}{\sqrt{t}} \quad (3).$$

2.1.2.2 Models based on diffusion

Controlled delivery systems can be classified according to the mechanism controlling the drug release from the system. The different classes are diffusion controlled, swelling controlled, osmotically controlled, and chemically controlled systems. In this section, only diffusion-controlled systems are addressed. The mathematical models that describe drug release are based on mass transport equations, and they are usually called kinetic models because they describe the time-dependent behavior of the drug release. (Narasimhan et al. 1999)

There are various mathematical models that describe the release of active agents from different kinds of drug release systems. In the case of polymeric materials, the models are often based on Fick's law of diffusion (Lao et al. 2011). Diffusion is a transport process caused by the random motion on the molecular level and it leads to the movement of molecules from the high concentration to the low concentration. Fick introduced this mass transport phenomenon in 1855. (Cussler 2008; Lao et al. 2011)

Fick's first law (Eqation 4) describes the steady state diffusion:

$$J = D\frac{\partial C}{\partial x} \quad (4)$$

where J is the diffusion flux, C is the position dependent drug concentration in the sample, and x is the position (normal to the plane) in the sample, which is assumed to be planar (Narasimhan and Peppas 1997).

Fick's second law describes non-steady diffusion and takes into account the change of the concentration within the diffusion volume with respect to time as well as position (Cussler 2008; Lao et al. 2011). In three dimensions and with rectangular geometry, it has the following form (Crank 1975):

$$\frac{\partial C}{\partial t} = D\left(\frac{\partial^2 C}{\partial x^2} + \frac{\partial^2 C}{\partial y^2} + \frac{\partial^2 C}{\partial z^2}\right) \quad (5)$$

where C is the concentration of the active agent; t, the time; and x, y, and z, the coordinates of the system.

Fick's second law is, however, quite simple. It does not take into account, for example, pressure or osmotic pressure. It can be used when binary mixtures are handled, but it cannot be used for very complex situations (Wesselingh 1993).

The most known model of drug release is the Higuchi model (Equation 6). It describes the drug release from non-degradable, non-porous, film shaped monolithic systems, where the drug is dispersed as particles in the matrix (Higuchi 1963; Siepmann and Peppas 2011). It is based on the Fick's first law of diffusion and it assumes that the dispersed drug particles are smaller in diameter than the thickness of the polymer matrix. In this way, the effects of the edges of the test specimens on the drug release can be ignored. It is also assumes that a pseudo-stationary state is predominant: the drug is dissolved into the matrix from the dispersed particles at the same rate as the drug is leaving the matrix. (Ginebra et al. 2006; Higuchi 1963; Lao et al. 2011; Narasimhan and Peppas 1997; Siepmann and Peppas 2011)

$$M_t = A\sqrt{(2DC_SC_0t)} \qquad (6)$$

where M_t is the active agent released in time t, D is the diffusion coefficient of the drug in the polymer, C_s is the solubility of the active agent in the matrix, C_0 is the initial drug concentration in the sample, and A is the cross-sectional diffusion area.

Exact solutions of Fick's second law have been provided and the solutions have been approximated to allow simpler mathematical equations to be used (Baker 1987; Lao et al. 2011). Two examples of these are Equations 7 and 8. Equation 7 is an approximation of the exact solution to Fick's second law for one-dimensional diffusion in a film-shaped test specimen and assumes a constant diffusion coefficient (Baker 1987; Siepmann and Peppas 2011):

$$\frac{M_t}{M_0} = 4\left(\frac{Dt}{\pi l^2}\right)^{1/2} \qquad (7)$$

where M_0 is the total amount of drug in the sample, M_t is the amount of drug released at time t, D is the diffusion coefficient, and l is the thickness of the sample. The equation is valid for short time periods (usually assumed $0 < \frac{M_t}{M_0} < 0.6$) and in cases when the initial drug concentration in the samples is lower than the solubility limit. Equation 8 is an approximation for the release after 40 % of the active agent has been released and is called a late-time approximation (Baker 1987)

$$\frac{M_t}{M_0} = 1 - \frac{8}{\pi^2}exp\left(\frac{-\pi^2Dt}{l^2}\right) \qquad (8).$$

It can be noted that both Higuchi's equation (Equation 6) and Equation 7 give the release $t^{1/2}$-dependence although the approaches behind these two equations are quite different (Siepmann and Peppas 2011).

Peppas and coworkers introduced the so-called power law (Equation 9) in 1983. It is a semi-empirical model (Lao et al. 2011; Ritger and Peppas 1987) and the Equation has the following form:

$$\frac{M_t}{M_\infty} = at^n \qquad (9)$$

where M_t and M_∞ are the amounts of drug released at time points t and infinity (M_∞ is often assumed to be the same as the drug load in the test specimen), a is a constant describing the geometrical and structural characteristics of the test specimen, and n is the release exponent describing the transport mechanism. This equation is valid for the first 60% of the cumulative release. For thin films, the exponent n has the values of 0.5 for fickian diffusion, $0.5<n<1$ for non-fickian transport and 1 for zero-order release. This equation can also be used for other geometries and, for example, for cylinder n = 0.45 for fickian diffusion, $0.45<n<1$ for non fickian (anomalous) transport, and 1 for zero order release. (Lao et al. 2011; Ritger and Peppas 1987) The power law has been subsequently modified to take into account the lag time and burst effects in the beginning of the release (Kim and Fassihi 1997).

There are severe limitations to the diffusion models presented above. Although drug release is studied from three dimensional structures, the equations are often one-dimensional (Zamoume et al. 2011). The assumption that the diffusion coefficient is constant throughout drug release is erroneous, for example, in cases where polymer degradation changes the diffusion properties (Siepmann and Peppas 2011). In cases where the release period is very short and polymer degradation is negligible, a constant diffusion constant may be valid. Because of the many limitations of the models, extensions have been developed such as the models where diffusion coefficient is not constant (Zamoume et al. 2011). For example, Higuchi's model has been modified to include a diffusion coefficient that changes with time due to polymer degradation (Lao et al. 2011). Zamoume *et al.* have added a geometrical parameter to the diffusion coefficient that takes into account the distance of the drug molecule to the exit point (Zamoume et al. 2011). If the matrix is porous, the diffusion coefficient can be replaced by an effective diffusion coefficient D_{eff}, because porosity obviously plays an important role in the release of active agents from the matrix (Ginebra et al. 2006).

2.1.2.3 Models for bulk degrading polymers

Because the properties of degradable polymers change as the degradation proceeds, polymer degradation and erosion need to be taken into account. In the case of surface eroding polymers, the modeling of drug release is rather easy because of the linear fashion of the polymer erosion. Bulk eroding polymers, on the other hand, make the modeling more complex (Lao et al. 2011).

A widely accepted way that bulk-degrading polymers degrade is according to first order kinetics:

$$\frac{dM_w}{dt} = -kM_w \quad (10),$$

and when integrated, the Equation has the following form:

$$M_{w,t} = M_{w,0}exp(-kt) \quad (11)$$

where $M_{w,t}$ is the polymer molecular weight at time t, $M_{w,0}$ is the initial polymer molecular weight, and k is the degradation rate constant (Lao et al. 2011).

As the polymer degrades, the simplest way of taking the changing permeability of the polymer matrix into account is to add a time-dependent factor to the diffusion coefficient. For example, Heller and Baker modified the Higuchi equation into following form (Baker 1987):

$$\frac{dM_t}{dt} = \frac{A}{2}\left(\frac{2PC_0}{t}\right)^{\frac{1}{2}} \quad (12)$$

where A is the surface area of both sides of the film, P is the time dependent permeability of the drug in the matrix (equal to DC_s in Equation 6), C_0 is the initial drug concentration in the matrix, and M_t is the cumulative released drug at time t. Permeability was assumed to be dependent on the remaining number of bonds in the polymer. Omitting the intermediate steps, the final equation has the following form (Lao et al. 2011):

$$\frac{dM_t}{dt} = \frac{S}{2}\left[\frac{2P_0exp(kt)C_0}{t}\right]^{1/2} \quad (13)$$

where P_0 is the initial drug permeability in the polymer and k is the first order rate constant of the polymer degradation (see Equations 10 and 11).

In another approach, the diffusion coefficient was assumed to be inversely dependent on polymer molecular weight. Additionally, the degradation of the polymer was assumed to occur according to the first order kinetics (Equation 11) (Charlier et al. 2000). The

model was based on the Higuchi model and showed good agreement with the experimental data also with longer times.

Models that rely solely on diffusion are usually good in predicting mono-phasic release (Lao et al. 2011). If the release profile includes more than one phase, it is clear that more complex models are needed that take factors into account other than diffusion and the dependency of the diffusion coefficient on concentration or polymer degradation.

2.1.2.4 Models for multiple release mechanisms

Attempts to describe the drug release kinetics with single mathematical models have proven to be complex due to the multitude of factors that affect polymer-based drug delivery systems. Additionally, the equations are often one-dimensional whereas real systems are three-dimensional. Models for multiple release mechanisms are not further presented here and the interested reader is instructed to read an excellent review by Lao *et al.* (Lao et al. 2011), as a starting point.

Nowadays, powerful software tools are available for the more accurate modeling and simulation of drug release. The tools utilize, for example, finite element method (FEM) (e.g. Comsol Multiphysics) and offer a way to simulate cases where several factors affect the drug release. (Kaunisto et al. 2013; Manzano et al. 2011; Moscicka-Studzinska and Ciach 2012; Thakhiew et al. 2011) As more computing power is available than ever before, the multiphysics models are the next step in the modeling of controlled drug delivery from polymeric systems.

2.2 Bone related infections

2.2.1 Osteomyelitis

Osteomyelitis is a severe bone infection that leads to bone destruction and is considered to be one of the most difficult-to-treat infectious diseases. The disease may become chronic and lead to amputation or even death (Chihara and Segreti 2010; Nandi et al. 2010; Sia and Berbari 2006). The term osteomyelitis is generally used for the condition where bone marrow is infected and the condition where both bone marrow and bone cortex are infected (Walter et al. 2012). The disease is caused by bacteria or other microorganisms, *Staphylococcus aureus* is the most common (60% of cases) (Gautier et al. 2012; Jones et al. 2004; Nandi et al. 2010). *S. aureus* are Gram positive, nonmotile, and non-spore-forming bacteria (Kiedrowski and Horswill 2011). The bacteria also have the ability to adhere to many types of surfaces and to develop biofilm (Harris and Richards 2006; Kiedrowski and Horswill 2011). Other osteomyelitis causing microorganisms include: *Pseudomonas aeruginosa* or other enterobacteria, *Staphylococcus epidermidis*, *Escherichia coli, Aspergillus* spp, and *Mycobacterium avium.* Virtually any organism has the potential to cause osteomyelitis and often the infection is polymicrobial, especially in cases where the bacterial inoculation has been through an open fracture (Chihara and Segreti 2010). Staphylococcal biofilms are very resistant to antimicrobial treatments as well as to host immune defenses (Kiedrowski and Horswill 2011).

Osteomyelitis may be acquired from direct inoculation of the bacteria into the bone, via hematogenous seeding, or contiguous spreading of infection (Sia and Berbari 2006). Additionally, there is an ischemic form of osteomyelitis that is most often related to diabetic foot (Walter et al. 2012). Normal healthy bone is highly resistant to infection, so osteomyelitis often occurs in patients with risk factors such as diabetes, decubitus ulcers, surgery, trauma, malnutrition, kidney or liver failure, respiratory failure, immune deficiency, malignant tumor, or intravenous drug abuse (Chihara and Segreti 2010; Walter et al. 2012). Foreign bodies, e.g. implants and external fracture fixation devices, may also offer a surface for the bacteria to attach to and lead to biofilm formation and finally to osteomyelitis (Kiedrowski and Horswill 2011). Infection rates reported for trauma surgery for the fixing of fractures vary between 1% and 5% for closed fractures and 3% and 50% for open fractures (Walter et al. 2012). Numerous reviews have addressed these problems (Esposito and Leone 2008; Harris and Richards 2006; Jain et al. 2007).

In a biofilm model of osteomyelitis suggested by Walter *et al.*, bacteria are first inoculated at the bone surface and start to form colonies. These colonies produce an extracellular matrix and develop into three-dimensional structures. The matrix acts as a diffusion barrier and protects the bacteria from mechanical influences from the body's own defense mechanisms and from antibiotics. (Walter et al. 2012) A biofilm can be

defined as a “layer-like aggregation of cells and cellular products attached to a solid surface or substratum” (Zoubos et al. 2012). When bacteria attach to a surface (e.g. bone or implant) and start to grow and form biofilm, their phenotype is different from the planktonic, freely suspended bacteria. In biofilms, bacteria communicate via intercellular signals. The good resistance of biofilms against antibiotics and host defense systems is partly due to the slimy and sticky matrix where the bacteria are embedded. The formation and function of biofilms is not, however, fully understood (Zoubos et al. 2012). There is also evidence that biofilms tend to form more easily on hydrophobic surfaces, such as many polymers, glass, and metal, than on hydrophilic surfaces (Zoubos et al. 2012). The formation of biofilms comprises several steps: rapid surface attachment; multi-layered cellular proliferation; and intercellular adhesion in an extracellular polysaccharide matrix (slime) that is excreted by the bacteria (Zimmerli 2006; Zoubos et al. 2012).

Osteomyelitis can be divided into acute and chronic osteomyelitis. There is, however, no uniform clinical definition for chronic osteomyelitis, and it can be difficult to define a threshold when acute infection becomes chronic. Many authors define their own criteria. (Walter et al. 2012) Often, acute osteomyelitis refers to the disease before osteonecrosis has occurred and chronic osteomyelitis to the stage where osteonecrosis, characterized by the presence of necrotic devascularized bone (sequesterum), has occurred (Chihara and Segreti 2010; Mouzopoulos et al. 2011). Osteomyelitis can be classified into several other subgroups according to location, duration of the disease, the microorganism causing the infection, or the route of the infection. According to Sia and Berbari, these can be classified clinically as long-bone osteomyelitis, open-fracture osteomyelitis, vertebral osteomyelitis, and SAPHO syndrome (synovitis, plantar pustulosis, hyperostosis and osteitis) (Sia and Berbari 2006). According to Waldvogel, osteomyelitis classification criteria are the duration of the disease, mechanism of the infection, and the presence of vascular insufficiency (Waldvogel et al. 1970). The Cierny-Mader system classifies osteomyelitis according to the portion of bone affected, the physiological condition of the host, and other risk factors (Cierny 3rd. et al. 2003). Additionally, osteomyelitis in patients with diabetes mellitus, vascular insufficiency, or rheumatoid arthritis can be considered as a special class, because of the challenges in the treatment (Walter et al. 2012).

Diagnosis of osteomyelitis can be challenging because symptoms may be various and subtle. Appropriate diagnosis often requires combination of clinical findings, microbiological cultures of bone biopsies and other samples (sinus tract material, purulent fluid, soft tissues), laboratory tests, and imaging (Mouzopoulos et al. 2011; Sia and Berbari 2006). Symptoms of acute osteomyelitis may include pain, erythema, oedema, warmth, tenderness, necrosis of wound edges, and the abrupt onset of high fever (Mouzopoulos et al. 2011). Symptoms of chronic osteomyelitis may include fever, chills, fatigue, irritability, lethargy, and malaise (Chihara and Segreti 2010;

Mouzopoulos et al. 2011; Walter et al. 2012). The disease may also have quiescent periods of variable duration (Mouzopoulos et al. 2011).

2.2.1.1 Treatment of osteomyelitis

Although osteomyelitis has been known since the early stages of human development, diagnosis and treatment are still a challenge today. One reason for this is the variety of symptoms. With recent developments in antibiotic treatments, however, the haematogenous version of osteomyelitis has been almost completely wiped out in the industrialized world. On the other hand, post-traumatically or post-operatively acquired forms of osteomyelitis are on the increase. (Walter et al. 2012)

Osteomyelitis in children is usually successfully treated with antibiotics without debridement of the infected bone tissue (Pääkkönen and Peltola 2011; Walter et al. 2012). Treatment of osteomyelitis in adults, especially the chronic form, is more difficult, time consuming, and is also expensive (Calhoun and Mader 1997). Treatment often requires surgical intervention (Uckay et al. 2012). Depending on the patient's condition, curative or palliative treatment can be chosen (Walter et al. 2012). These paths of treatment protocols are described in Figure 2. In the curative protocol, the first step includes radical surgery where all the infected tissues (both bone and soft tissues) and possible implants are removed. This protocol follows certain principles: the complete drainage of infected tissue, thorough debridement of necrotic tissue, the removal of possible implants or fixation devices, elimination of the dead space, complete soft tissue coverage and bone/fracture stabilization. (Sia and Berbari 2006; Walter et al. 2012) The surgical treatment is followed by a long course of intravenous or oral antibiotics because bacteria may be left in the surrounding tissues (Kankilic et al. 2011; Parsons and Strauss 2004; Soundrapandian et al. 2007). Another option in the curative approach is amputation, which is very radical, carries high risks, and is very stressful for the patient (Walter et al. 2012).

The relapse rate for osteomyelitis is high (20-30%) (Mouzopoulos et al. 2011; Sia and Berbari 2006; Walter et al. 2012). Usually, the high relapse rate is caused by inadequate debridement of the infected tissues (Mouzopoulos et al. 2011). Additionally, 10-30% of acute osteomyelitis cases become chronic (Walter et al. 2012).

Often, a multidisciplinary approach, meaning co-operation between various healthcare professionals, is emphasized in the treatment of osteomyelitis (Bauer et al. 2012; Mouzopoulos et al. 2011). Such an approach has been rarely reported in scientific literature. In one study by Bauer *et al.*, however, the outcome of a patient suffering from bone and joint infections was significantly improved, when the antibiotic therapy was decided on after a multidisciplinary meeting (Bauer et al. 2012).

There is currently no clear consensus about the optimal duration, route of the antibiotic treatment, or the choice of the antibiotic (Guillaume et al. 2012; Haidar et al. 2010;

Lazzarini et al. 2005; Sia and Berbari 2006; Uckay et al. 2012). In the case of chronic, non-implant related osteomyelitis, the length of the antibiotic therapy after the debridement of the infected tissue has been mainly based on the opinions of experts. No scientific proof or international guidelines have been presented. (Haidar et al. 2010; Lazzarini et al. 2005; Rod-Fleury et al. 2011; Uckay et al. 2012) Lazzarini *et al.* concluded their review about the antibiotic treatment of osteomyelitis: "Despite three decades of research, the available literature on the treatment of osteomyelitis is inadequate to determine the best agent(s), route, or duration of antibiotic therapy." This describes the field well. (Lazzarini et al. 2005)

Usually, the length of the antibiotic treatment in the case of chronic osteomyelitis is 4-6 weeks (Haidar et al. 2010; Mouzopoulos et al. 2011), but treatments also lasting up to three or even six months are used (Uckay et al. 2012). Recently, however, there have been suggestions that properly designed studies should be performed in order to find out the optimal treatment length. These suggestions have been based on the fact that surgical procedures have been improved substantially and thus may justify shorter antibiotic treatments (Haidar et al. 2010; Rod-Fleury et al. 2011). There is also a debate about whether the oral administration of antibiotics could replace the intravenous treatment in some cases and thus avoid the risks of intravenous catheters. This is because nowadays there are antibiotics available that achieve adequate concentrations in bone to eradicate osteomyelitis-causing bacteria. (Spellberg and Lipsky 2012) Some authors suggest that the treatment should be started with intravenous treatment that can be switched to oral treatment later on (Sendi and Zimmerli 2012). In a retrospective clinical study by Rod-Fleury *et al.*, rather short antibiotic therapies were suggested and enhanced cure ratios were not found with oral antibiotic therapy over six weeks or intravenous therapy over one week. It must be noted that some of the subjects of the study were also treated with gentamycin releasing PMMA beads in addition to the antibiotic therapy. (Rod-Fleury et al. 2011)

Prolonged intravenous courses of antibiotic therapy cause several problems including catheter related infections, catheter failures, costly antibiotics and supplies, patient discomfort, and poor patient compliance (Calhoun and Mader 1997). Additionally, the high doses of antibiotics used to achieve effective therapeutic doses at the infection site may lead to systemic toxicity and unwanted side effects. Too long antimicrobial treatment may also enhance the emergence of resistant bacteria (Uckay et al. 2012).

A great challenge in the treatment of osteomyelitis or other bone related infections is the access of the required antibiotic to the site of the infection. The blood circulation in the infected tissue may be severely compromised, and thus orally or intravenously administered antibiotics may not reach the site of infection in the required concentrations. Another challenge is to keep the drug concentration above the therapeutic level and below the toxic level for a long enough time period. (Ginebra et al.

2006) Biofilms make the antibiotic treatment very challenging due to their resistance to antibiotics and also to the host defense (Kiedrowski and Horswill 2011).

Another challenge is how to take care of the dead space in bone tissue that results from surgical debridement of infected tissues. Traditionally, the dead space resulting from the surgical debridement of the infected tissue has been treated using non-biodegradable gentamycin releasing poly(methyl methacrylate) (PMMA) beads that are implanted into the bone defect (Zilberman and Elsner 2008). The beads release gentamycin locally and should kill the remaining bacteria in the bone tissue because high local concentrations of antibiotics can be achieved and systemic complications avoided (Calhoun and Mader 1997). The major drawback in the usage of the PMMA beads is that they are not biodegradable and they require removal, followed by bone grafting (Calhoun and Mader 1997). If left implanted for a long time, the PMMA beads may become surrounded by dense scar tissue and their removal may be very difficult (Hanssen 2005; Nandi et al. 2010). Additionally, they do not completely release the antibiotic, and bead failure has also been reported (McLaren 2004). The initial burst in the antibiotic release is large: 60% of the antibiotic may be released within the first day. After the initial burst, the drug concentrations rapidly fall below therapeutic levels in two to four weeks or even faster (Calhoun and Mader 1997; Li et al. 2010). This means that supplementary systemic antibiotic treatment is often needed because local drug delivery has been suggested to last for at least six to eight weeks (Calhoun and Mader 1997; Li et al. 2010). Other problems associated with the non-biodegradable PMMA beads include: low biocompatibility, thermal damage to the antibiotic during fabrication, poor drug elution properties, and the possibility of resistant bacteria development on the surface of the beads when low levels of drug is released during the latter stages of the release (Nandi et al. 2010; Neut et al. 2001).

In the case of bone defects, the gold standard so far has been the use of autografts. However, tissue availability is limited and harvesting causes local morbidity and increases the risk of infection. (Hench and Polak 2002; Mouriño and Boccaccini 2010; Vallet-Regí and Arcos 2013) One option is the use of allografts or xenografts, but these carry the risks of graft rejection or transfer of pathogens (Mouriño and Boccaccini 2010). Based on these limitations, the interest has lately been towards artificial and synthetic materials. An ideal bone substitute should be biocompatible, bioabsorbable, osteoconductive, osteoinductive, structurally similar to bone, easy to use, cost-effective, and should encourage patient bone regeneration. (Kolk et al. 2012; Mouriño and Boccaccini 2010) In the case of treating the dead spaces resulting from the treatment of chronic osteomyelitis or implant-related infections, antibiotic-releasing properties are also valuable.

Biodegradable, osteoconductive, and antibiotic-releasing composites offer certain advantages in the treatment of chronic osteomyelitis. Antibiotic release can be prolonged to cover the time needed and different polymers offer variable

biodegradability, which in turn offers possibilities to treat various infections. Additionally, there is no need for the surgical operation to remove the implants because bone tissue can grow and replace the implant, as the implant slowly degrades (Calhoun and Mader 1997; Nandi et al. 2010). Antibiotic concentrations in infected bone tissue achieved by locally drug-releasing implants have been found to be several times higher than in the cases of intravenous or oral drug delivery in experimental animal models (Garvin et al. 1994; Hamanishi et al. 1996; Koort et al. 2006; Koort et al. 2008; Lucke et al. 2005; Mäkinen et al. 2005a; Mäkinen et al. 2005b; Miyai et al. 2008). It has been suggested that the antibiotic level at the infection site should be kept at the therapeutic level for at least 6-8 weeks to allow adequate infection control and healing (Calhoun and Mader 1997; Li et al. 2010). The bone reconstruction period is long and it can take 3–4 months to reconstruct an adult bone (Jiang et al. 2012).

There is a treatment algorithm based on osteoconductive antibiotic-releasing bone grafting materials proposed by Mäkinen (Mäkinen 2005). The protocol is presented as one treatment option on the right side of Figure 2. In this algorithm, one step in the treatment, i.e. bone grafting, can be avoided. Because all surgical procedures pose a risk for the patient, this is the preferable direction in the development of new treatment protocols.

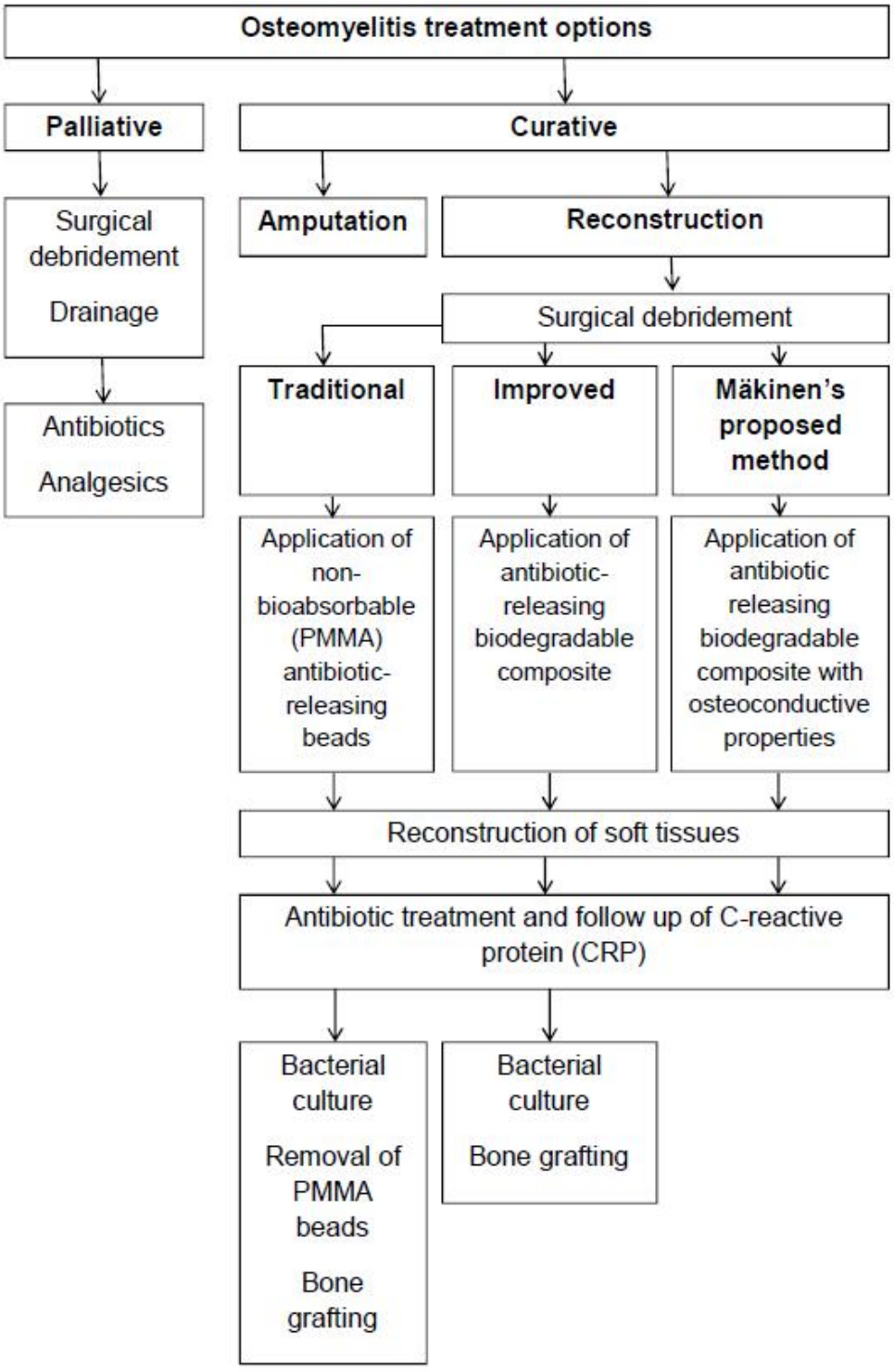

Figure 2. Traditional and new proposed treatment options for the treatment of osteomyelitis (Modified from (Mäkinen 2005) and (Walter et al. 2012)).

2.2.2 Implant-related orthopaedic infections

Prosthetic joints and internal fixation devices (nails, pins, and screws) are the most used implants in modern medicine (Zimmerli and Sendi 2011). They are used to relieve pain, to enable rapid fracture healing, and to improve the mobility and independence of patients (Sendi and Zimmerli 2012). The presence of an implant is known to increase the risk of infection and implant-related infections are a significant problem in modern medicine (Harris and Richards 2006; Zimmerli 2006; Zimmerli and Sendi 2011). Especially, internal fixation devices used in open fractures have high infection rates (30%) (Mouzopoulos et al. 2011; Zimmerli et al. 1998). As an implant is presented to the body, there is a "race for the surface" involving extracellular matrix (ECM) proteins, host cells, and bacteria (Harris and Richards 2006). Depending on the cascade of phenomena on the surface, bacteria may or may not be adhered to the surface layer. A six-hour "decisive period" after surgery has been identified where the success of the implant is determined. During this time, the implant is particularly vulnerable to bacterial adhesion. (Hetrick and Schoenfisch 2006; Zilberman and Elsner 2008) If bacteria are able to adhere on the implant surface, it may lead to bacterial growth, development of a biofilm, and infection. Thus, the prevention of bacterial adhesion on the surface of the implant during or right after the surgery is crucial. Bacteria that are able to grow biofilms typically cause infections associated with implants (Zimmerli 2006). The pathogens encountered most often are *Staphylococcus aureus* and *Staphylococcus epidermidis* (Darouiche 2001). The bacteria may cause infection by direct inoculation during or even before (in the case of open fractures) surgery, post-operatively (e.g. if the wound healing is disturbed), hematogenous seeding, and contiguous spreading from neighboring tissues (Sendi and Zimmerli 2011; Zimmerli and Ochsner 2003; Zoubos et al. 2012).

Implant-related infections involve interaction between three factors: the infecting microorganism, the implant, and the host (Darouiche 2001; Zimmerli 2006). From these, device-related factors are the easiest to modify. Prevention of bacterial adhesion on the surface of the device is the key factor in preventing infection (Darouiche 2001). There are different factors playing a role in the attachment, the proliferation, and the biofilm formation of different bacterial species (Zimmerli 2006). Implant surface chemistry has been observed to influence the bacterial adhesion, e.g. stainless steel has been associated with higher rates of infection than titanium (Harris and Richards 2006; Kiedrowski and Horswill 2011). Bone cements also provide an attractive surface for bacterial adhesion. To prevent this, antibiotics are often mixed with the cements (Kiedrowski and Horswill 2011). In animal models, it has been observed that the presence of a foreign body alone can reduce the number of bacterial cells that are needed to cause infection (Kiedrowski and Horswill 2011; Zimmerli 2006). This is probably due to compromised host defense around the implant (Zimmerli 2006; Zimmerli and Sendi 2011).

Although the implant-related infections are rare, their number is increasing because the number of patients with orthopaedic implants is increasing (Sendi and Zimmerli 2012). Often, antibiotics are administered before and during the operation as prophylaxis, but regardless of this, infections still occur (Schmidmaier et al. 2006). Incidences of implant-related infections vary according to the type and site of operation, trauma, and patient condition (Schmidmaier et al. 2006). Overall, 5% of implants become infected during their lifetime (Walter et al. 2012). Of the patients having primary elective joint replacements, 0.5-1% (Kankilic et al. 2011) or 1-2% (Senneville et al. 2011) become infected, but in patients with diabetes or compromised vascularization the incidences range between 10% and 20%. Of the patients that have a revision surgery or trauma, 2-20% of the cases become infected. (Kankilic et al. 2011) In a retrospective study reported by Achermann *et al.*, it was found that the infection rate concerning elbow prostheses was as high as 7.5 % (Achermann et al. 2011). Bacterial adhesion to the surface of the implant can occur at any time during or after implantation, but the time period with the highest risk is the early postoperative period (Zimmerli 2006). External fracture fixations are less invasive than internal fixation plates, but still possess a risk of pin tract infection. If the infection is untreated, it may lead to osteomyelitis. (Harris and Richards 2006)

Risk factors for orthopaedic-implant-related infections are old age, malnutrition, underlying joint disease, obesity, diabetes mellitus, malignant tumor, remote infection, prior native joint infection, and advanced HIV infection. Patients that have rheumatoid arthritis have a higher risk of prosthetic-joint-associated infection than patients that have osteoarthritis. Additionally, infection of the surgical wound may increase the risk of infection. (Zimmerli 2006)

Diagnosis of implant-related infections can be challenging because of the variety of symptoms (Lazzarini et al. 2005). Typical first symptoms are systemic, such as fever, shivering, and tachycardia (Zimmerli 2006). In addition to these, local signs may be local pain, wound infection, warmth, a wet or gaping wound, and prolonged wound secretion (Zimmerli and Ochsner 2003; Zimmerli 2006). If the early stage infections are treated with short term antibiotics without further diagnostics, the result may be delayed infection with implant loosening, sinus tracts, or hidden abscess (Zimmerli 2006). Persistent or increasing pain and the loosening of the implant may also be signs of an implant-related infection (Zimmerli and Ochsner 2003).

For accurate diagnosis, various methods are used including bacterial cultures on tissue samples as well as explanted implants, laboratory studies, and imaging with different methods (e.g. radiography, computed tomography (CT), ultrasonography, magnetic resonance imaging (MRI), and positron emission tomography (PET)) (Koort et al. 2004; Zimmerli 2006).

As in the case of osteomyelitis, there are no generally accepted criteria for the treatment of implant-related infections nor for the optimal duration of the antimicrobial treatment (Marschall et al. 2013; Zimmerli 2006). Implant-related infections never heal spontaneously (Zimmerli and Sendi 2011). Treatment is usually a combination of surgical treatments with adequate tissue debridement with or without prosthesis removal and prolonged antibiotic therapy (usually intravenous which can be switched to oral antibiotics later on) (Kankilic et al. 2011; Kiedrowski and Horswill 2011; Sendi and Zimmerli 2012; Senneville et al. 2011; Zimmerli 2006). Surgical intervention is not always possible because of the condition of the patient and thus there is a great need to develop less invasive treatment methods (Kiedrowski and Horswill 2011). Overall, the treatment is difficult, often requiring multiple surgeries, which lead to a decrease in quality of life and increase morbidity and mortality (Kankilic et al. 2011). The radical surgical treatment also causes bone and muscle destruction (Zimmerli 2006). There is no consensus whether the implant should be removed or retained in the case of acute infection. If the implant is stable, retaining is suggested (Mouzopoulos et al. 2011). Risk factors favoring implant removal in acute cases are heavy smoking, open fractures, and intramedullary devices (Mouzopoulos et al. 2011). Instead of the radical treatment, it has also been suggested that the patient should be treated with lifelong suppressive oral antimicrobial treatment without surgical intervention (Zimmerli 2006). This is not a curative alternative and may lead to other problems such as resistant bacterial development and toxicity (See Figure 2, palliative treatment route).

Antibiotic treatments of implant-related infections are long. Zimmerli *et al.* have suggested 3-month antibiotic therapy for infected hip prostheses and 6-month therapy for infected knee prostheses. The first two weeks of the treatment should be intravenous and then switched to oral therapy if the antibiotic has good oral bioavailability. In the case of total removal of the foreign material, they suggest that the antimicrobial treatment can be shortened to six weeks. After the infection has been eradicated, re-implantation is possible. (Zimmerli et al. 1998; Zimmerli 2006)

Prosthetic joint loosening may also be caused by mechanical reasons (Darouiche 2001). The particles resulting from the mechanical wear of the prosthesis materials may induce osteolysis and lead to a loosening of the implant. This kind of loosening is called aseptic loosening. Many cases of aseptic loosening are actually caused by bacteria colonized on the surface but are undetected (Darouiche 2001; Zimmerli et al. 2004). This may be due to the difficulties of culturing the bacteria in laboratory conditions (Drancourt et al. 1993).

2.2.3 Antibiotics for bone infections

Antibiotics play a significant role in the treatment of osteomyelitis and implant-related infections. The choice of the antibiotic used in the treatment should be always based on the pathogen and its antimicrobial susceptibility. Gentamycin is a commonly used antibiotic in the treatment of osteomyelitis. (Mouriño and Boccaccini 2010) However, it is not recommended for use with methicillin resistant bacterial strains, due to several reports of gentamycin resistance (Jackson et al. 2011). Prolonged gentamycin use has also been associated with problems such as ototoxicity and nephrotoxicity (Ismail et al. 2012).

In addition to gentamycin, many antibiotics including ciprofloxacin, rifampicin, vancomycin, teicoplanin, and daptomycin are used in the treatment of osteomyelitis (Chang et al. 2011; Mouriño and Boccaccini 2010). Vancomycin is effective against methicillin-resistant *Staphylococcus aureus* (MRSA) (Jackson et al. 2011), but when it is administered intravenously, even in large doses, it does not reach the infection site effectively and may also cause some adverse reactions such as nephrotoxicity, ototoxicity, and gastrointestinal side effects (Gautier et al. 2012; Jiang et al. 2012). Additionally, emerging resistance to vancomycin has been reported (Gautier et al. 2012). The thermal instability of vancomycin restricts its use in applications where high temperatures are used either in the production phase of the drug release system or in the setting reaction of a bone cement. Vancomycin is considered as a last resource antibiotic in severe MRSA infections (Kluin et al. 2009).

An alternative to vancomycin is linezolid, which is a rather new antibiotic and so far the use has been restricted to cases requiring hospitalization. It is not the first choice treatment because it is reserved for more serious cases such as repeated infections caused by methicillin resistant *Staphylococcus aureus*. Linezolid penetrates human tissues easily. (Gautier et al. 2012) Newer antibiotics such as quinupristin and dalfopristin have also shown promising results in the treatment of osteomyelitis caused by resistant bacterial strains (Lazzarini et al. 2005).

2.2.3.1 Ciprofloxacin

Ciprofloxacin belongs to the family of quinolones that are widely used due to their broad spectrum, highly bactericidal activity, and favorable pharmacokinetic properties (Vallet et al. 2011; Van Bambeke et al. 2005). The first antibiotic belonging to this group was nalidixic acid and it was approved in 1962 (Bertino Jr. and Fish 2000). The structure-property relationships of quinolones are well understood and many derivatives of nalidixic acid have entered the market. Ciprofloxacin is a fluorinated derivative of nalidixic acid and it was discovered in 1982 (Arcieri et al. 1989). The chemical structure of ciprofloxacin is presented in Figure 3. It is widely used to treat urinary infections (Fong et al. 1986), osteomyelitis, and other bone and joint infections (Alvarez et al. 2008; Levine and DiBona 2002).

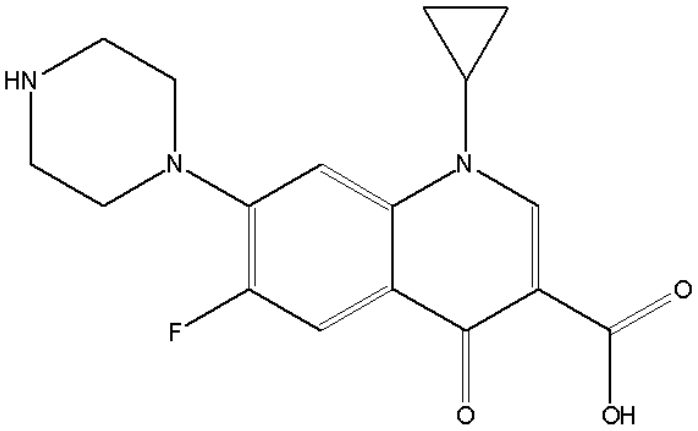

Figure 3. Chemical structure of ciprofloxacin.

The molecular weight of ciprofloxacin is 331.4 g/mol. Solubility in water at 37 °C has been reported to be 0.20 mg/ml at pH 7.8 and 0.22 mg/ml at pH 6.9 (Breda et al. 2009) and a LogP value of 0.28 (Takacs-Novak et al. 1992).

Ciprofloxacin, like many other fluoroquinolones, is available both in oral and parenteral forms (Levine and DiBona 2002). It is well absorbed after oral administration and is widely distributed throughout the body with good tissue penetration (Fong et al. 1986; Levine and DiBona 2002). Blood concentrations achieve similar levels after oral administration than after parenteral administration and peak concentrations are achieved 1-2 hours after administration (Levine and DiBona 2002). This is an advantage because adverse effects and risks of intravenous catheters can be avoided with oral administration (Lazzarini et al. 2005). It also allows the change from intravenous administration to oral administration of the same drug if needed.

The pharmacokinetic features of ciprofloxacin depend strongly on the dosage given to the patient and also on the patient's age (Levine and DiBona 2002; Mitscher 2005). The average volume of distribution of ciprofloxacin is in the order of 2-3 l/kg and the elimination half-life is 3-5 hours (Kettunen 2004). Ciprofloxacin is excreted unchanged by the kidneys, which has raised some ecological concerns (Näslund et al. 2008).

The principle of the action of ciprofloxacin is the inhibition of the bacterial topoisomerase II (DNA gyrase), which triggers cell replication arrest and cell death (Herbold et al. 2001; Holtom et al. 2000; Levine and DiBona 2002). It may also have an effect on bacterial topoisomerase IV. Additionally, ciprofloxacin has been reported to inhibit mammalian topoisomerase II and, due to this, has shown genotoxicity in tests utilizing pro- and eukaryotic cells. It must be noted, however, that several orders of magnitude higher concentrations are needed than for the inhibition of bacterial DNA gyrase. (Herbold et al. 2001)

Ciprofloxacin has a broad spectrum of activity that includes the bacteria that cause the most cases of osteomyelitis, including *Staphylococcus aureus*. Thus, it is one of the

most used antibiotics in the treatment of osteomyelitis. (Castro et al. 2005; Koort et al. 2005; Overbeck et al. 1995; Puga et al. 2012; Tiainen et al. 2012) Good tissue penetration can be achieved even in poorly vascularized areas (Castro et al. 2005; Koort et al. 2005; Puga et al. 2012). Minimum inhibitory concentrations (MIC) against the common osteomyelitis causing bacteria are rather low. The MICs are for *S. aureus* 0.1-1.0 μg/ml (Overbeck et al. 1995; Tiainen et al. 2012), for *S. epidermidis* 0.1-0.8 μg/ml (Chin and Neu 1984), and for *P. aeruginosa* 0.1-1.2 μg/ml (Kwok et al. 1999; MacGowan et al. 1999). Good tissue penetration into the surrounding tissues has also been reported in local administration of ciprofloxacin (Overbeck et al. 1995; Ramchandani and Robinson 1998; Tiainen et al. 2012).

Generally, ciprofloxacin is well tolerated (Bertino Jr. and Fish 2000; Herbold et al. 2001). Adverse effects that have been reported are gastrointestinal effects such as nausea, vomiting and diarrhea, central nervous system effects (convulsive seizures, headache and dizziness), dermatologic effects, (Arcieri et al. 1989; Ball 1989), and changes in blood chemistry (Arcieri et al. 1989). These effects are generally mild and reversible when the treatment is ended (Bertino Jr. and Fish 2000). For intravenously administered ciprofloxacin, local effects at the site of the infusion have been the most reported adverse effects. It has been also reported that there is no correlation between the daily dose of intravenous ciprofloxacin and the occurrence of adverse effects, but there is correlation between the duration of the therapy and the occurrence of adverse effects. (Arcieri et al. 1989)

There are, however, some concerns about ciprofloxacin being toxic to articular cartilage tissue and joints, especially when administered long-term and in high doses (LeBel 1988). The effects have been studied, for example, on adult human cartilage *in vitro* (Menschik et al. 1997; Mont et al. 1996), juvenile beagle dogs (Stahlmann et al. 2000; Von Keutz et al. 2004), and juvenile rats (Li et al. 2004). The results indicate that ciprofloxacin has a toxic effect on chondrocytes, especially at high doses. Ciprofloxacin has been also reported to inhibit the proliferation of osteoblast-like cells *in vitro* (Miclau et al. 1998) and the osteoblastic cells of mouse (Holtom et al. 2000). It has to be noted, however, that these studies have been performed either *in vitro*, or in animal studies, and thus the results cannot be directly translated to human bone and cartilage tissue. Nevertheless, because of these results, ciprofloxacin is not recommended for children, pregnant women, or nursing mothers. (Bertino Jr. and Fish 2000; Hanssen 2005; Levine and DiBona 2002)

2.2.3.2 Rifampicin

Rifampicin is a semisynthetic antibiotic and belongs to the group of rifamycins that are a well-known class of antibiotics. Rifamycins are a subgroup of ansamycins that are named according to the chemical structure where an aromatic moiety is bridged by an aliphatic chain called an *ansa* chain (Lat. handle) (Cellai et al. 1982). Rifampicin shows polymorphism because it exists in three different forms: amorphous and crystalline forms I and II (Agrawal et al. 2004; Freire et al. 2009). This is believed to be because of its complex structure, various possibilities to form hydrogen bonds, conformational exchanges, and ionization states (Henwood et al. 2000). Rifamycins inhibit the bacterial DNA-dependent RNA polymerase and are thus bacteriocidical (Cellai et al. 1982).

A rifampicin molecule is rather large and has a molecular weight of 823 g/mol (Figure 4). Solubility in water at 30 °C has been reported to be 1.5-1.7 mg/ml, depending on the crystal form (Henwood et al. 2000). Rifampicin is considered to be lipophilic with the logP value of 2.7 (Marchidanu et al. 2013).

Rifampicin has been shown to have surprisingly good effect against *staphylococci* in their various modes of growth. It is known to penetrate biofilms well and also to prevent biofilm formation. The reason for this is, however, unknown. (Kiedrowski and Horswill 2011) When rifampicin is used alone, there is rapid development of resistant bacterial strains. Because of this, rifampicin should never be used alone. (Bliziotis et al. 2007; Coiffier et al. 2013; Kiedrowski and Horswill 2011; Perlroth et al. 2008) MIC values reported in the literature for rifampicin are 0.013 μg/ml against *S. aureus* (Guillaume et al. 2012), and 0.015 μg/ml against *S. epidermidis* (Leite et al. 2011). The values against *P. aeruginosa* vary greatly and values of 32-64 μg/ml (Yee et al. 1996) and 8-16 μg/ml (Timurkaynak et al. 2006) have been reported.

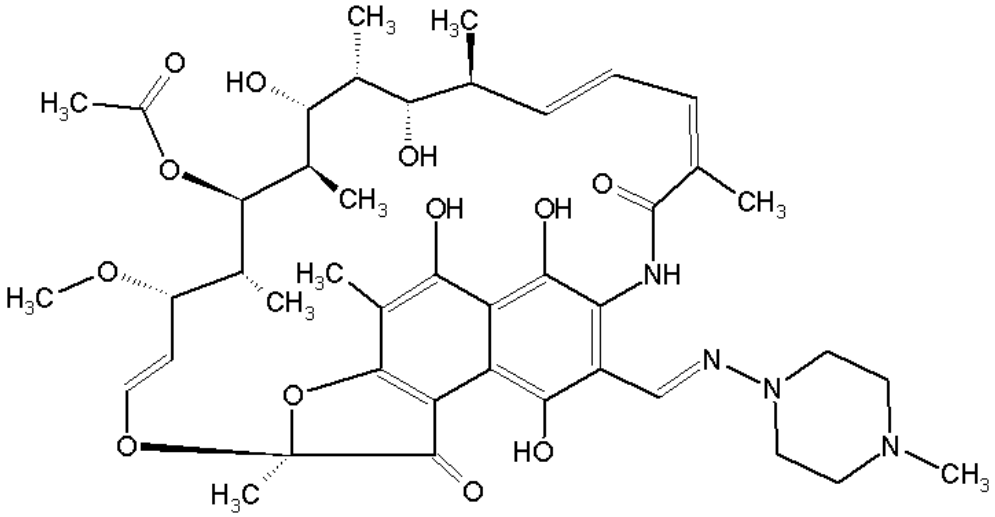

Figure 4. Chemical structure of rifampicin.

Rifampicin is well absorbed from the GI tract and is widely distributed into most body tissues and fluids (Acocella 1978; Roth 1984). Rifampicin penetrates into the bone tissue in relation to the concentration in plasma, which is about half of the rifampicin concentration in plasma. The pharmacokinetics show large variability between individuals. (Pargal and Rani 2001) The elimination of rifampicin from bone is slower than from plasma (Roth 1984), and the biological half-life or rifampicin in plasma has been reported to be 2.5-5.4 hours (Acocella 1978; Pargal and Rani 2001; Sreenivasa Rao et al. 2001). Peak drug concentration in plasma typically occurs 2 hours after oral administration into an empty stomach (Pargal and Rani 2001). Le Guellec *et al.* found that rifampicin stability was better in rifampicin-containing plasma samples taken from patients treated with rifampicin than in plasma samples where rifampicin was added in the laboratory. They suggest possible *in vivo* stabilization of the rifampicin molecule. (Le Guellec et al. 1997)

Because of the good penetration into biofilms, rifampicin has been used together with other antibiotics in the treatment of osteomyelitis and other bone related infections (Bliziotis et al. 2007; Kiedrowski and Horswill 2011; Perlroth et al. 2008). In a recent review by Sendi and Zimmerli, it was said that: “Rifampicin is now a standard combination partner in the treatments of staphylococcal infections.” (Sendi and Zimmerli 2012) The advantages of rifampicin combination therapy have been reported several times in the literature (Coiffier et al. 2013). It has even been suggested that rifampicin should always be used, in combination with other antibiotics, in the cases of implant-related infections because of its excellent efficacy against bacteria adhered to surfaces (Zimmerli 2006). Senneville *et al.* concluded in their retrospective study of prosthetic joint infections caused by *S. aureus* that rifampicin combination therapy was associated with a better outcome for the patients when compared with other antibiotic regimens (Senneville et al. 2011). Perlroth *et al.* have reviewed the use of rifampicin in *Staphylococcus aureus* infections. In general, in *in vivo* and human studies, the combination of ciprofloxacin with rifampicin has been more effective than monotherapy, especially in prosthetic device infections and osteomyelitis. (Perlroth et al. 2008) In a double-blinded randomized clinical trial performed by Zimmerli *et al.*, the efficacy of rifampicin was studied as a supportive antibiotic in implant-related infections. The patients had stable implants that were not removed during the study. The results clearly showed that the outcome was better in the group where patients were treated with rifampicin in addition to other antibiotics (first 2 weeks intravenous flucloxacillin or vancomycin and then switched to oral ciprofloxacin). The treatment was successful even without implant removal. An additional advantage of the combination therapy was the prevention of emerging ciprofloxacin resistance. (Zimmerli et al. 1998) Rifampicin has also been studied together with other fluoroquinolones in the treatment of deep sternal wound infections and studies have shown that using rifampicin together with fluoroquinolones improves the outcome (Khanlari et al. 2010).

2.3 Controlled antibiotic delivery in bone applications

2.3.1 Macroscopic systems

During the last decades, there have been numerous approaches in the local treatment or prophylaxis of bone related infections. Synthetic biodegradable polymers, meaning mostly polymers based on lactide, glycolide, and caprolactone have been extensively studied as drug delivery systems both alone and in composites (Dash and Konkimalla 2012; Makadia and Siegel 2011; Nair and Laurencin 2007). These polymers offer the possibility of tailoring the polymer properties, for example by copolymerization and blending (Albertsson and Varma 2003; Puga et al. 2012; Woodruff and Hutmacher 2010), and they degrade in a tissue environment via hydrolysis and the degradation products are excreted via normal metabolic pathways (Albertsson and Varma 2003). Enzymatic activity may also be involved in the degradation process (Dash and Konkimalla 2012).

An ideal antibiotic-releasing implant for the treatment of bone-related infections should combine antibiotic delivery and bone regeneration. In cases where the size of the bone defect is greater than what the bone is able to heal spontaneously (critical size defect), bone regeneration by other means is crucial (Vallet-Regí and Arcos 2013). The implant material should deliver the antibiotic in a continuous manner and in high enough concentrations. Moreover, it should accommodate the space required (e.g. dead space in osteomyelitis after the debridement of infected tissue) and should provide a structural function (Hanssen 2005). Antibiotic release should occur in a limited time period to prevent the development of resistant bacterial strains (Pavithra and Doble 2008). Because entrance of infectious microorganisms cannot be totally prevented with surgical precision, such implant materials can be used not only for infection treatment but also as prophylaxis (Vallet-Regí and Arcos 2013).

Traditionally, the dead spaces resulting from the surgical treatment of osteomyelitis have been treated using commercial gentamycin releasing PMMA beads (Ginebra et al. 2006). There are several drawbacks related to PMMA beads: they are not degradable in biological systems and require removal. The delivery of other antibiotics such as vancomycin from PMMA beads has also been studied (rat model). The conclusion has been that the drug delivery from the PMMA matrix is not very efficient and also includes a large burst in the beginning of the release period. Moreover, the release falls rapidly to concentrations below MIC (Li et al. 2010). Additionally, bacteria may adhere to the surfaces of the beads despite their antibiotic-releasing nature. In a study by Neut *et al.,* gentamycin releasing beads were retrieved from 20 patients. It was found that 18 of them had bacteria present, although 12 of the patients were considered free of infection. The majority of the isolated bacterial strains were also gentamycin resistant. (Neut et al. 2001)

Interest towards biodegradable alternatives has been growing and systems that both deliver the antibiotic to the site of the infection and help the bone to heal have been requested (Jiang et al. 2012). The challenges facing controlled drug delivery using biodegradable polymers are potential dose dumping if the device does not work properly, inconsistent release, and drug-polymer interactions (Makadia and Siegel 2011).

2.3.1.1 Bone cements

Antibiotic-releasing bone cements are important materials in the treatment and prevention of bone-related infections (Bourne 2004). Today, they represent the gold standard in orthopaedic surgery, for example in the prevention and treatment of infections after total hip and knee arthroplasties (Hanssen 2005; Tan et al. 2012). The very first antibiotic-releasing bone cements were normal PMMA bone cements that were mixed with antibiotics by the surgeons themselves. Buchholz and Engelbrecht had already started the development of antibiotic-releasing bone cements in 1970 (Buchholz and Engelbrecht 1970). In 1977, there were publications about mixing PMMA bone cements with antibiotics (Ger et al. 1977). The antibiotic delivering cements were first utilized as prophylaxis to prevent infections but soon they began to be used in the treatment of implant-related infections and osteomyelitis (Hanssen 2005). Gentamycin and tobramycin are the two antibiotics most used in combination with bone cements (Hanssen 2005). Also, daptomycin, vancomycin, teicoplanin, clindamycin, cephalothin, erythromycin, oxacillin, cefuroxime, colistin, methicillin, tetracycline, lincomycin, dicloxacillin, grepafloxacin, and bactrim have been studied in PMMA bone cements (Bourne 2004; Chang et al. 2011; Efstathopoulos et al. 2008). Antibiotic-releasing PMMA bone cements were subsequently approved for clinical use in Europe and have been used for over two decades (Luginbuehl et al. 2010). In the United States, they were approved in the 2000s, but their use is restricted to joint revisions following the elimination of an active infection (Bourne 2004; Zilberman and Elsner 2008).

PMMA based bone cements are not biodegradable and thus do not provide the possibility of bone regeneration. The porous surface of the cement may also offer a surface where bacteria can attach, and this can lead to serious infections. Drug release kinetics from PMMA cements are rather poor. The antibiotic concentrations released from the PMMA cements are low and may rapidly fall below MIC (Jackson et al. 2011). Additionally, the drug release may not be complete and if prolonged with low antibiotic concentrations, resistant bacterial strains may develop (Jackson et al. 2011; Tan et al. 2012). To overcome these problems, PMMA cements with a chitosan derivative (hydroxypropyltrimethyl ammonium chloride chitosan) have been developed. With these cements, better stem cell proliferation and osteogenic differentiation than pure PMMA cements were found. However, their function in *in vivo* conditions has not been studied yet. (Tan et al. 2012) Additives such as sodium chloride and dextran have been

found to improve the drug release behavior of linezolid, vancomycin and fusidic acid from PMMA cements (Jackson et al. 2011).

Bone cements based on calcium phosphates (CaP) were discovered in the 1980s (Ginebra et al. 2012). Today, there are several commercial varieties available but they do not have antibiotics incorporated in them (Bohner et al. 2005). The main advantages of CaP bone cements over the traditional PMMA cements are bioactivity and osteoconductivity. In addition, the setting reaction is not exothermic making the setting reaction temperature in the tissue environment low, minimizing the risk of tissue damage. This offers the possibility to incorporate heat sensitive drugs or other biomolecules in the cements. CaP cements are bioresorbable and the resorption rate depends on the composition and microstructure. The main drawbacks of these kinds of cements are their poor mechanical properties that limit their use to non-load bearing locations. (Ginebra et al. 2012) Additionally, the incorporation of drugs into calcium phosphate cements may cause changes in the rheological properties of the cements as well as in the setting times, the microstructure of the resulting cement, and the mechanical properties. There are no general rules how this happens because it depends on the molecular structure and the chemical nature of the incorporated drug. (Ginebra et al. 2012; Ginebra et al. 2006; Vallet-Regí and Arcos 2013)

The setting reaction of CaP bone cements is a combination of dissolution and precipitation reactions and the result is very porous cement (Chen et al. 2003; Ginebra et al. 2012). The setting times and the porosity can be modified in several ways such as liquid to powder ratio and the powder size of the ceramic (Bohner et al. 2005; Laycock et al. 2011; Schnieders et al. 2011). Although the highly porous structure compromises the mechanical properties, it also offers some advantages such as enhanced resorbability and an increased ability of the cements to bind drug molecules on their surfaces (Ginebra et al. 2012). Additionally, the drug release properties can be tailored by changing the porosity of the bone cement (Bohner et al. 1997; Schnieders et al. 2011). Drug release from calcium phosphate cements is often characterized by an initial phase as the cement is setting followed by a diffusion-controlled release that is influenced by the material and drug characteristics (Habraken et al. 2007). One method to control the drug release profile and especially the burst in the beginning is to incorporate of the drug into polymer microparticles and then mix them into the cement. This approach can also be used to improve the handling properties of the cements. (Bohner et al. 1997; Habraken et al. 2007; Schnieders et al. 2011).

The use of calcium phosphate cements as drug delivery systems has been extensively reviewed by Ginebra *et al.* (Ginebra et al. 2012; Ginebra et al. 2006). They can be used to deliver not only small molecular size drugs such as most antibiotics, analgesics and anticancer drugs (Ginebra et al. 2012; Otsuka et al. 1997) but also larger molecular size biomolecules such as proteins (Otsuka et al. 1994) and growth factors (Ginebra et al.

2012; Ginebra et al. 2006). However, the drugs to be incorporated in phosphate bone cements that have been studied the most are antibiotics (Ginebra et al. 2012).

Although antibiotic-releasing bone cements have been proven to be very efficient and usable in different bone applications, they are not very widely commercialized (Ginebra et al. 2006). They can be used either in the treatment of bone related infections or as a prophylactic strategy to prevent infections (Bohner et al. 1997; Ginebra et al. 2006). The problems that arise and prevent the use and industrial production of drug-releasing bone cements from being expanded are a lack of knowledge of drugs on the part of implant manufacturing companies and the lack of interest in bone cements of pharmaceutical companies, due to the small market for bone cements (Ginebra et al. 2006).

Bioactive glass cements have also been studied, but the drug release from these cements has been rather short term, maximum 2 weeks, with a large burst in the beginning of the release. The cements were also reported to shrink, which makes them not very useful in filling bone defects. (Otsuka et al. 1992; Otsuka 1994)

2.3.1.2 Bioabsorbable polymeric systems

The bioabsorbable polymers used as matrix materials for controlled antibiotic delivery for bone tissue applications include polylactides (Cao et al. 2012; Veiranto et al. 2002), polycaprolactone (Puga et al. 2012), polyurethanes (Kwok et al. 1999; Li et al. 2010), various copolymers of lactides, glycolide and caprolactone (Calhoun and Mader 1997; Veiranto et al. 2004a; Veiranto et al. 2004b), polyhydroxyalkanoates (Gursel et al. 2002; Gürsel et al. 2001; Korkusuz et al. 2001; Türesin et al. 2001), poly(trimethyl carbonate) (Kluin et al. 2009; Neut et al. 2009), polyanhydrides (Chiu Li et al. 2002; Stephens et al. 2000), and collagen (Ipsen et al. 1991; Knaepler 2012).

Although a great number of studies have been published in the field of antibiotic-delivering materials for bone applications both *in vitro* and in animal models (rat, rabbit), very few materials have reached the commercial market. One example of a commercialized product is ciprofloxacin-releasing bone fixation screw made of poly(lactide-co-glycolide) that can be used as prophylaxis in patients with increased risk factors for developing an infection (Veiranto et al. 2004a; Veiranto et al. 2004b). The Finnish company Bioretec Ltd has commercialized the bone fixation screws.

Local antibiotic-releasing systems based on bioabsorbable polymeric systems have been studied and reviewed by many research groups (Alvarez et al. 2008; Mäkinen et al. 2005b; Miyai et al. 2008; Zilberman and Elsner 2008). However, the drug release properties of these polymers may not be optimal, and often processing methods are used that are either not feasible on an industrial scale or involve the use of solvents that may be a problem if solvent residues remain in the final product (Calhoun and Mader 1997; Cao et al. 2012; Kankilic et al. 2011; Kluin et al. 2009; Puga et al. 2012). Proving that no residues of solvents are present in the final product may be difficult. An additional

challenge is that materials based purely on polymers do not offer osteocoductive properties and thus do not aid bone healing.

Although animal model results concerning polymer based antibiotic-releasing systems have been promising (Calhoun and Mader 1997; Koort et al. 2005; Koort et al. 2006; Koort et al. 2008; Kundu et al. 2012), it has to be noted that that animal models cannot replicate complex human bone infections such as osteomyelitis and implant-related infections (Lazzarini et al. 2005). Animal models have also been criticized because of the initial inoculation used in the infection model. Since it has been suggested that bacteria growing in biofilms cause most bone related infections, the same approach should be also used in animal models to get more consistent results. The initial inoculation in the animal models should be also made using bacteria that are already forming biofilms. (Williams et al. 2012)

Puga *et al.* studied the release of ciprofloxacin hydrochloride from macroscopic systems of a blend of rather low molecular weight PCL (42500 g/mol) and poloxamine, which is a surfactant comprised of a block copolymer of ethylene oxide and propylene oxide. The results clearly showed a dependence of poloxamine in the blend. A higher poloxamine to PCL ratio resulted in faster ciprofloxacin hydrochloride release. The release continued steadily for 60 days and the kinetics fitted best with the Higuchi model. The study also showed promising results in the eradication of *Staphylococcus aureus in vitro* and good compatibility with osteoblasts in cell cultures. (Puga et al. 2012) In a study by Cao *et al.*, levofloxacin-releasing poly(D,L-lactide) beads were reported to release levofloxacin in a continuous manner for 46 days and were effective against *Staphylococcus aureus, Pseudomonas aeruginosa,* and *Escherichia coli* in inhibition zone tests (Cao et al. 2012). Biodegradable vancomycin-releasing polyurethane beads have been developed and studied in a rat model by Li *et al.* The continuous release of vancomycin continued for 8 weeks and the implants were as active against *S. aureus* as PMMA beads. (Li et al. 2010) Vancomycin-releasing beads of poly(DL-lactide-co-glycolide) were studied by Calhoun *et al.*. They used a localized rabbit tibial osteomyelitis model and concluded that biodegradable antibiotic-releasing beads may be more effective than parenteral antibiotic therapy in the treatment of osteomyelitis. (Calhoun and Mader 1997)

The release of gentamycin and vancomycin was studied from poly(trimethyl carbonate) (PTMC) by Kluin *et al.* The advantage of the PTMC polymer is that the degradation products are not acidic. PTMC is also surface eroding in the presence of lipase enzyme. Surface erosion is considered an advantage in controlled drug delivery applications, especially in the delivery of large drug molecules that are not able to diffuse through polymer matrices. Additionally, zero-order release is easier to achieve than by using bulk degrading polymers. The *in vitro* results showed that surface erosion in the presence of lipase enzyme significantly enhanced the release of both vancomycin and gentamycin. The release results were reported up to 30 days. (Kluin et al. 2009)

Natural polymers offer an attractive alternative for drug delivery matrices because of their excellent biocompatibility. However, disadvantages include batch-to-batch variations, poor mechanical properties, and difficulties in processing. Additionally, animal based natural polymers possess the risk of transferring pathogens. Gentamycin-releasing collagen implants have been used clinically both as prophylaxis and in the treatment of osteomyelitis. (Ipsen et al. 1991; Knaepler 2012) When compared with gentamycin-releasing PMMA beads, the collagen implants have been as effective, but fewer re-operations have been needed for the collagen treated group. Collagen has also been claimed to have positive effects on wound healing. (Knaepler 2012)

When ciprofloxacin has been administered locally, good penetration into bone tissue has been observed. Overbeck *et al.* studied ciprofloxacin release from polyglycolide cylinders in rabbits and found that the drug penetration in bone was better than for gentamycin released from PMMA beads. During the first week of implantation, concentrations greater than the MIC of ciprofloxacin against *Staphylococcus aureus* were found at a distance up to 30 mm from the implant. (Overbeck et al. 1995) In a study by Tiainen *et al.*, therapeutic levels of ciprofloxacin were measured in a rabbit model 5 mm away from the implantation site of ciprofloxacin-containing PLGA miniscrews for eight weeks (Tiainen et al. 2012). Ramchandani and Robinson reported therapeutic levels of ciprofloxacin measured at a distance up to 70 mm from PLGA microcapsule implants for six weeks in a rabbit model (Ramchandani and Robinson 1998).

2.3.1.3 Ceramics and glasses

Calcium phosphate ceramics possess excellent properties with regard to bone tissue. Their chemical composition is close to the mineral phase in bone and they have excellent biocompatibility (Bose and Tarafder 2012; Habraken et al. 2007; Vallet-Regí and Ruiz-Hernández 2011). Additionally, they provide osteoconductivity and even osteoinductivity when combined with growth factors, bioactive proteins, or osteogenic drugs (Bose and Tarafder 2012). Ceramics have been used clinically in hip and other joint prosthesis, dental applications, maxillofacial reconstruction, spinal fusion, and as bone defect fillers (Vallet-Regí and Arcos 2013). Depending on the chemical structure and crystal form, calcium phosphate ceramics can be classified as hydroxy apatite (HA), tricalcium phosphate (α-TCP or β-TCP depending on the crystal form), biphasic calcium phosphate (BCP), amorphous calcium phosphate (ACP), carbonated apatite (CA), and calcium deficient HA (Habraken et al. 2007). From these, hydroxy apatite and β-tricalcium phosphate are the most used ones, β-TCP being more resorbable than HA (Bose and Tarafder 2012). They are available as granules, pastes, cements, coatings and porous devices (Vallet-Regí and Arcos 2013). The degradation of calcium phosphate ceramics depends on their composition, crystallinity, crystal form, and phase purity. These ceramics can be processed into various shapes and sizes and antibiotics can be incorporated in them. Also, other drugs and even growth factors have been

incorporated in the ceramics (Bose and Tarafder 2012; Habraken et al. 2007). The major drawback in the use of ceramics is their brittleness, which makes the handling of them challenging. If used as blocks, ceramics have to be shaped to fit the bone defect. This may be difficult and labor intensive and poor tissue to implant contact may result. (Ginebra et al. 2006; Habraken et al. 2007) Drug release from ceramic materials depends strongly on the chemical structure of the ceramic, type of the drug and drug load (Habraken et al. 2007). Drug release patterns from purely ceramic materials may be difficult to control because highly porous ceramic materials are unable to retain the drug for a long time (Mouriño and Boccaccini 2010). For example, linezolid loaded calcium deficient hydroxy apatite blocks were able to release linezolid for a maximum 26 days *in vitro* (Gautier et al. 2012).

Drugs can be incorporated either during the processing of the bioceramic or at the end of the processing. Because the processing of ceramics includes extremely high temperatures, the incorporation of temperature sensitive drugs cannot be made during processing. (Vallet-Regí and Arcos 2013) There are, however, several methods to incorporate drugs after the thermal treatment of ceramics. Wet granulation and impregnation are examples of these methods. (Gautier et al. 2012; Vallet-Regí and Arcos 2013)

Both single antibiotic delivery and simultaneous delivery of two antibiotics have been investigated with ceramic materials. Kundu *et al.* studied the simultaneous release of ceftriaxone and sulbactam from porous β-TCP both *in vitro* and in a rabbit osteomyelitis model. The majority of both of the studied antibiotics was released during first week and comparable results were obtained for both of the antibiotics *in vitro*. The porosity of the ceramic had an effect on the drug release. In the rabbit model, they concluded that infection was eradicated and new bone was formed in the group treated with the ceftriaxone and sulbactam-releasing β-TCP implants. (Kundu et al. 2012) Takigami *et al.* reported a series of 8 patients treated successfully with antibiotic-loaded porous hydroxy apatite blocks in two-stage revision surgery of an infected hip joint prosthesis. The antibiotic loaded to the ceramic was chosen according to the bacteria found in cultures obtained pre-operatively. (Takigami et al. 2010) Vogt *et al.* studied the release of gentamycin and vancomycin from mixed calcium sulphate and calcium carbonate (1 wt-% gentamycin or vancomycin). A high burst for four days and continuous release of small amounts of antibiotic for three weeks was reported. (Vogt et al. 2007)

One approach to achieve both adequate drug release and osteoconductivity provided by calcium phosphate ceramics has been to coat the ceramics with a biodegradable polymer, where the drug has been incorporated. Such an approach was carried out by Luginbuehl *et al.* where β-TCP granules were coated with P(DL-LA) and PLGA containing tetracycline. Good biocompatibility of such materials was found in a sheep model and tailorable drug release properties were reported. (Luginbuehl et al. 2010)

Nanoscale HA, which has been successfully used to repair bone defects, has also been investigated as a drug delivery material in an experimental osteomyelitis animal model (rabbits). In a study by Jiang *et al.*, vancomycin delivery using nano-hydroxy apatite was found to be effective in inhibiting the proliferation of the infection. They suggested that nano-HA is more suitable than conventional HA for drug delivery applications. (Jiang et al. 2012)

Calcium sulphates have also been researched as antibiotic delivery materials for musculoskeletal infections. Parker *et al.* studied two varieties of calcium sulphates (naturally sourced and synthetic) enhanced by the addition of potassium sulphate (K_2SO_4) as a daptomycin-releasing material. The *in vitro* release times were only 2 days in this preliminary study. (Parker et al. 2011)

Silica-based bioactive glasses, which were first developed by Larry Hench, (Hench 1973; Hench and Paschall 1973; Hench 2006), have been used as antibiotic delivery materials (Domingues et al. 2004; Thanyaphoo and Kaewsrichan 2012). Bioactive glasses are able to form a covalent bond with bone tissue and have been applied, for example, as bone replacement in periodontal diseases and maxillofacial reconstructions (Jones 2013; Vallet-Regí and Arcos 2013). Conventional methods for producing bioactive glasses utilize high temperatures, but nowadays they are also produced using sol-gel processing where high temperatures are not required (Habraken et al. 2007). Thus, temperature sensitive drugs can be incorporated in the glass during processing (Vallet-Regí and Arcos 2013). Antibiotics that have been experimentally incorporated in bioactive glasses include vancomycin (Thanyaphoo and Kaewsrichan 2012; Xie et al. 2009), tetracycline (Domingues et al. 2004), and gentamycin (Mouriño and Boccaccini 2010). Because the mechanical properties of bioactive glasses are not good, ceramics have been added to them to produce glass-ceramic composites that have better mechanical properties (Habraken et al. 2007).

The recent development of mesoporous silica matrices composed of ordered porous SiO_2 structures, that have narrow pore size distribution and a large surface area may offer new possibilities for antibiotic delivery for bone applications. These materials have been reviewed by Vallet-Regí and Arcos. (Vallet-Regí and Arcos 2013)

2.3.1.4 Composites

Composites offer a very attractive combination of the bioabsorbability, drug release properties, and good processability of polymers together with the bioactivity of ceramic materials, especially calcium phosphates and bioactive glasses (Habraken et al. 2007; Mouriño and Boccaccini 2010). Neither of these material groups has good mechanical properties, but in composites the brittleness of the ceramics can be avoided by combining them with viscoelastic polymers. Both synthetic and natural polymers have been studied in composite materials. In the case of synthetic polymers, polymer properties can be tailored to meet the required degradation and drug-releasing profiles.

(Habraken et al. 2007) Composite materials that combine controlled antibiotic delivery and also contribute to bone regeneration are the most ideal local antibiotic delivery vehicles in orthopaedics (Hanssen 2005). As some of the antibiotics may, however, affect bone regeneration, especially in high doses, a balance between the antibiotic treatment to eradicate bacteria without compromising bone regeneration must be found (Hanssen 2005).

The composite approach towards drug-releasing materials often includes incorporating the ceramic as particles in a biodegradable polymer matrix (Habraken et al. 2007). Numerous approaches have been reported in the literature. Some antibiotic-releasing composites of bioabsorbabale polymers and ceramics and their release characteristics as well as their production methods are presented in Table 2. The antibiotic release from the composites is often characterized by a large burst in the beginning of the release that typically lasts for one to two days. The release may be as high as 50-60 % of the drug loaded in the system (Baro et al. 2002; Kankilic et al. 2011). If needed, the burst and the following phase of continuous release can be modified, for example, by dip coating the composite with polymer (Fang et al. 2012; Kankilic et al. 2011; Soriano and Évora 2000).

Table 2. Summary of some antibiotic-releasing composites of bioabsorbable polymers and ceramics.

Polymer	Ceramic	Antibiotic	Processing method	Release *in vitro*	Results *in vivo*	Reference
PDLLA[a]	Mixture of HA (25%) and TCP (75%) (crystalline form not specified). Ceramic content of the composites 78.5%.	Gentamycin sulphate (3%)	Main method compressing. Other methods used: emulsification and mixing with solvents, dip coating.	High initial burst of 46-63% of the total gentamycin during the first day. Complete release in 1-3 weeks depending on the composition. When coated with PLGA or PDLLA, two-phase release up to 10 weeks.		(Soriano and Évora 2000)
PDLLA[a]	Mixture HA (25%) and TCP (75%) (crystalline form not specified) Ceramic content of the composites 72%.	Ciprofloxacin (10%)	Mixing and compressing.	80% release in 6 weeks, complete release in 12 weeks.	Rabbit model with *S. aureus*. Successful eradication of the infection. Complete release in 6 weeks.	(Alvarez et al. 2008)
PCL[b]	β-TCP	Gentamycin (Drug embedded in gelatin-β-TCP microspheres)	Gelatin-β-TCP particles with water-in-oil emulsion method. Solvent casting for the composite films.	Continuous release (50-80% of the total gentamycin) up to 96-120 hours. No complete release.		(Sezer et al. 2013)
Gelatin	β-TCP (0-50%)	Vancomycin	Dissolution, foaming, cross-linking and freeze-drying		Rat model. High initial burst (2 days) with sustained release up to 56 days depending on the composition.	(Zhou et al. 2012)
PDLLA[b] (50/50)	Bioactive glass	Ciprofloxacin (7.6%)	Melt-mixing	Small initial burst (2%) during first 6 h followed by continuous release above therapeutical level for 300 days (100% release)	Rabbit model. Successful eradiaction of *S. aureus* from bone.	(Koort et al. 2005; Koort et al. 2008)
PLGA[c]	Bioactive glass (27%)	Ciprofloxacin (8.3%)	Melt-mixing and self-reinforcing	Small initial burst of approximately 3% during the first 6 h followed by continuous release in therapeutical level for 120 days. Complete release in 150 days.	Rabbit model. High local bone concentrations up to 3 months.	(Mäkinen et al. 2005b)

PCL[b] (low MW)	β-TCP	Gatifloxacine	Sintering of a β-TCP scaffold and impregnation with molten PCL mixed with the antibiotic.	Moderate initial burst (6% in 2 days) followed by continuous release for 4 weeks (90% release).	Rabbit model. Successful eradication of the infection.	(Miyai et al. 2008)
PDLLA	Mixture of HA (25%) and TCP (75%) (crystal form not specified)	Gentamycin sulphate (3.5%)	Emulsion of gentamycin and PDLLA, mixed with HA & TCP paste, mixing, drying and granulation.	Large initial burst (50%) during two days. 90% release in two weeks. Longer continuous release up to 12 weeks was achieved by coating the composites with PDLLA.	Rabbit model. Concentrations above MIC of *S. aureus* were found next to the implant for 4 weeks.	(Baro et al. 2002)
PDLLA	Mixture of HA (25%) and TCP (75%) (crystal form not specified). Ceramic content of the composites 40-72%.	Ciprofloxacin (10-40%)	Mixing and compressing.	Small initial burst (appr. 10%) during first couple of days followed by continuous release for 4 to 12 weeks (100% release) depending on the composition and compression parameters.	Rabbit model. 90% release in 6-8 weeks above therapeutic level.	(Castro et al. 2003; Castro et al. 2005)
PLLA	β-TCP	Vancomycin	Vancomycin impregnated in β-TCP, after that mixing with polymer solution, solvent casting, and dip-coating with PLLA.	Large initial burst (63%) during first day followed by continuous release up to 6 weeks (92% release).		(Kankilic et al. 2011)
Chitosan	Borate glass	Teicoplanin (4 or 8%)	Solvent casting	Large initial burst (45-47% of the loaded drug) during the first day followed by continuous release up to 2 weeks (78-83% release).	Rabbit osteomyelitis model. Better effect with implanted composites (with 7.1 mg teicoplanin) than with intravenous administration of teicoplanin (6 mg/kg i.v. once a day for four weeks).	(Jia et al. 2010)
Chitosan, dip-coating with PCL[b]	β-TCP	Vancomycin	Dissolving chitosan and vancomycin, dispersing β-TCP in the solution followed by freeze-drying.	Moderate initial burst (8-40%) during the first three days followed by continuous release up to 10-42 days (70-80% release) depending on the composition.		(Fang et al. 2012)

a: poly(DL-lactide)
b: polycaprolactone
c: poly(lactide-co-glycolide)
d: poly(L-lactide)

2.3.1.5 Allografts and autografts

One approach to deliver antibiotics locally to bone defects is the use of antibiotic impregnated bone grafts (autografts and allografts). In the use of allografts, there is always the risk of transmitting pathogens. Demineralized human bone matrix has been studied *in vitro* as a gentamycin-delivering material and has been found to deliver gentamycin continuously for 13 days (Lewis et al. 2012). There is great variability in the literature concerning antibiotic-impregnated bone grafts and their comparison is very difficult. Anagnostakos and Schröder have reviewed this topic (Anagnostakos and Schröder 2012). The concentrations released from antibiotic impregnated bone grafts are often higher than the concentrations achieved with antibiotic-releasing PMMA cements. The reported elution times of various antibiotics from bone grafts are only three weeks at maximum (Anagnostakos and Schröder 2012), which is considered too short a time period for the treatment of osteomyelitis. Additionally, it has been observed that the elution times are strongly depended on the impregnation time (Witsø et al. 1999). However, antibiotic impregnated bone grafts have been clinically used successfully in the treatment of various orthopaedic infections (Anagnostakos and Schröder 2012).

Antibiotics have been incorporated in bone grafts (autografts or allografts) by e.g. soaking them in antibiotic loaded solutions before insertion, manually mixing, or by using more complex methods such as iontophoresis (Anagnostakos and Schröder 2012; Hanssen 2005). There are, however, very little data available about the antibiotic concentrations reached in this way (Hanssen 2005).

2.3.2 Micro- and nanoparticles

Most recently, interest in micro- and nanoparticles has been growing. Microparticles (microspheres and microcapsules) are spherical particles in the size range of 50 μm – 2 mm and can have drugs either encapsulated or entrapped in them. Nanoparticles (nanospheres and nanocapsules) are particles in the sub-micron (< 1 μm) scale. (Dash and Konkimalla 2012)

Nano-sized particles have been developed to improve the pharmacokinetics and accumulation of antibiotics. At the same time, they may also reduce the side effects of the drugs (Huh and Kwon 2011). There is also the hope that nanostructured drug-delivery systems may offer new tools in the fight against resistant bacteria (Huh and Kwon 2011). Because they can be injected, particles (microspheres, microcapsules, nanocapsules, nanospheres) offer the advantage that they do not require a surgical insertion (Makadia and Siegel 2011). Additionally, they offer a large surface area-tovolume ratio (Dash and Konkimalla 2012). Drug release from the particles may be controlled by diffusion or degradation of the polymer or it may be a combination of both of the phenomena (Dash and Konkimalla 2012; Makadia and Siegel 2011).

The major drawback of micro- and nanoparticles is that the processing methods are often based on organic solvents (Dash and Konkimalla 2012; Ismail et al. 2012; Makadia and Siegel 2011). This may be problematic if solvent residues are left in the particles. Some drugs may also be denatured if in contact with organic solvents. It is also possible to produce particles without harmful solvents using supercritical fluid technology (i.e. supercritical carbon dioxide) in a rapid expansion or anti-solvent precipitation process. (Dash and Konkimalla 2012)

Ismail *et al.* have, for example, developed gentamycin-releasing PLGA microspheres. The gentamycin release from the particles showed a very high burst. The authors proposed a solution for this problem that is a combination of different dosage forms to achieve an ideal release profile. (Ismail et al. 2012) This approach is very interesting. Although slow, continuous release was achieved for only four weeks in the study, this approach could work for other dosage forms for longer times. Balmayor *et al.* recently reported the development of gentamycin-releasing starch/chitosan microparticles for short-term drug delivery. These particles also showed a large burst in the beginning of the release *in vitro*. (Balmayor et al. 2012)

Nanoparticles based on calcium phosphate ceramics have also been developed and studied. Their primary advantage over biodegradable polymer nanoparticles is that their degradation products are Ca^{2+} and PO_3^{-4} ions which are naturally found in the human body and in the blood stream in rather large concentrations (1-5 mM). (Bose and Tarafder 2012)

3 AIMS OF THE WORK

The aims of this thesis work were the following:

- To develop bioabsorbable and antibiotic (either ciprofloxacin or rifampicin) releasing composites which also contain an osteoconductive ceramic component. The ciprofloxacin-containing composites are intended to be used together with rifampicin-containing composites in the local antibiotic treatment of osteomyelitis and other bone related infections. The materials are to be used together so that the surgeon can decide the ratio in which to use them.

- To find out the degradation as well as ciprofloxacin-releasing and rifampicin-releasing properties of the composites and to evaluate their suitability for the treatment of osteomyelitis *in vitro*. The requested length of the release of ciprofloxacin and rifampicin was from three to six months and degradation in a similar time scale.

- To prove the efficiency of the ciprofloxacin and rifampicin-releasing composite materials against osteomyelitis-causing model bacteria *in vitro* and also to study the usability of bioluminescent bacteria in inhibition zone tests.

4 MATERIALS AND METHODS

4.1 Materials

The materials and reagents used in this work are presented in Table 3 along with the suppliers. The molecular structures of the two active agents, ciprofloxacin and rifampicin, are presented in Figure 3 and Figure 4 in the section 2.2.3, respectively. The general copolymer structure of lactide and ε-caprolactone is presented in Figure 5. The copolymer, which was chosen as the polymer matrix based on preliminary experiments, was a commercial medical grade copolymer obtained from Purac Biomaterials and it was a copolymer of L-lactide and ε-caprolactone with the comonomer ratio of 70/30 (L-lactide to ε-caprolactone). The abbreviation PLCL is used in this work to describe the copolymer.

Table 3. Materials and reagents used in this work.

Material/reagent	Supplier	Used in
Ciprofloxacin	Uquifa, Mexico	II, IV
Rifampicin	Orion, Finland	III, IV
β-tricalcium phosphate (granule size < 38 µm)	Plasma Biotal, United Kingdom	I, II, III, IV
Poly(L-lactide-co-ε-caprolactone) M_w 229 000 g/mol and 245 000 g/mol (2 batches)	Purac, Gorinchem, the Netherlands (two batches, one for composites without antibiotics and one for antibiotic containing composites)	I, II, III, IV
Na_2HPO_4	J.T. Baker, the Netherlands	I, II, III, IV
KH_2PO_4	J.T. Baker, the Netherlands	I, II, III, IV
Chloroform	Riedel-de Haën AG, Germany	I, II, III
Chloroform	J.T. Baker, the Netherlands	II, III
Deuterochloroform	Merck, Germany	I, II, III
Glycerol	Sigma-Aldrich, Malaysia	IV
Ampicillin	Sigma-Aldrich, China	IV
Erythromycin	Sigma-Aldrich, China	IV
Gentamycin sulphate	Sigma-Aldrich, China	IV
Glucose	Prolabo, Merck Eurolab, UK	IV
Isopropyl-β-D-thiogalaktopyranoside (IPTG)	Fermentas, Lithuania	IV
Trypton	Lab M Limited, UK	IV
Yeast extract	Lab M Limited, UK	IV
Sodium Chloride	Merck, Germany	IV
Agar	Merck, Germany	IV

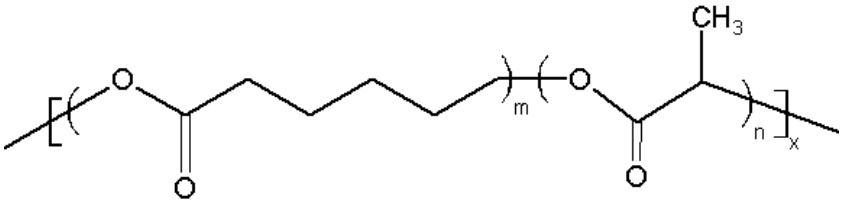

Figure 5. Molecular structure of the poly(lactide-co-ε-caprolactone) polymer.

4.2 Methods

4.2.1 Manufacturing of the composite materials

Composite materials were manufactured as follows: Prior to processing, the materials were dried in vacuum at room temperature for 72 hours. Processing was done using a co-rotating custom-built intermeshing twin-screw extruder (length to diameter (L/D) ratio of the extruder screws 22.5) and the processing was done using nitrogen atmosphere to avoid moisture-induced degradation during processing. The polymer, β-tricalcium phosphate (β-TCP), and active agents were delivered in the process with separate gravimetric screw feeders and the mixing of the materials took place in the extruder. Total feed rate was 200 g/h in all of the cases. A haul-off unit was used to guide the extrudate from the die and the diameter of the billets was fine-tuned by adjusting the speed of the haul-off unit. The materials were processed into rod-shaped billets with a diameter of approximately 2.5 mm. The manufactured composites, their compositions and abbreviations that are used throughout this work are presented in Table 4.

Pellet shaped samples (length approximately 2.5 mm) were cut from the billets. Examples of the manufactured pellets are shown in Figure 6. Before degradation and drug release studies were carried out, the samples were packed and sterilized using gamma irradiation (minimum dose 25 kGy).

Table 4. Compositions in mass percentages of the manufactured composites of PLCL, β-TCP and the antibiotics rifampicin and ciprofloxacin and their abbreviations.

Number	Name	PLCL 70/30	β-TCP	Ciprofloxacin	Rifampicin	Used in
1	**Plain PLCL**	100				I
2	**PLCL+TCP10**	90	10			I
3	**PLCL+TCP20**	80	20			I
4	**PLCL+TCP35**	65	35			I
5	**PLCL+TCP50**	50	50			I, IV
6	**PLCL+C**	92		8		II
7	**PLCL+TCP50+C**	42	50	8		II, IV
8	**PLCL+TCP60+C**	32	60	8		II
9	**PLCL+R**	92			8	III
10	**PLCL+TCP50+R**	42	50		8	III, IV
11	**PLCL+TCP60+R**	32	60		8	III

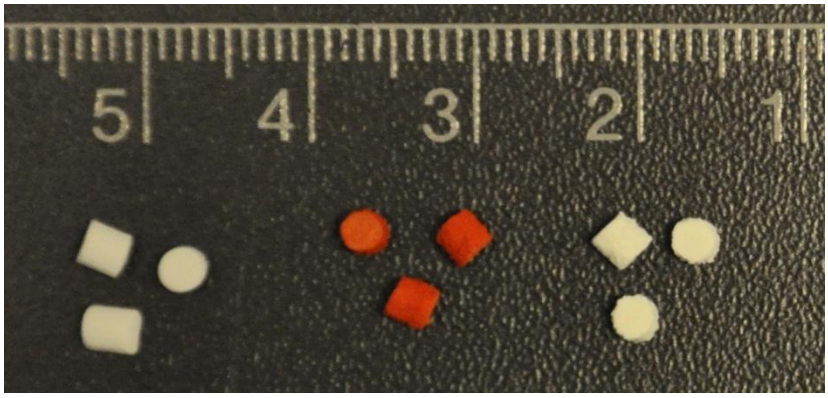

Figure 6. Pellet shaped composite samples. PLCL+TCP50 on the left, PLCL+TCP50+R in the middle and PLCL+TCP50+C on the right.

4.2.2 Residual monomer measurements

The determination of residual L-lactide and ε-caprolactone monomer contents of the PLCL copolymer were performed by Ramboll Analytics Oy (Lahti, Finland). The ε-caprolactone and L-lactide contents were measured after chloroform extraction of the samples using gas chromatography (DC8000, CE Instruments, Rodano, Italy) and an FI-detector after chloroform dilution. The measuring resolution was 0.02%.

4.2.3 *In vitro* degradation of the polymer

The buffer solution used in the *in vitro* testing was Sörensen buffer solution (pH 7.4) and it was prepared according to the standard ISO 15814 (ISO 15814). The chemicals used for the buffer solution were sodium hydrogen phosphate (Na_2HPO_4) and potassium dihydrogen phosphate (KH_2PO_4). Degradation tests were conducted at 37 °C *in vitro* following the standard ISO 15814 (ISO 15814). First, weighed test specimens were placed in brown glass bottles with 20 ml Sörensen buffer solution. A test sample consisted of 15 pellets weighing approximately 300 mg in total and a set of five parallel test samples were tested at each time point separately. The bottles were placed in an incubator shaker (Infors Multitron, Infors Bottmingen, Switzerland) at 37 °C. The pH of the buffer solution was measured once a week with a calibrated pH meter (Mettler Toledo, SevenMulti) and the buffer solutions were changed every two weeks in the beginning of the test series and once a week as the degradation accelerated. Test samples were withdrawn at predetermined time points, which were 2, 4, 6, 8, 10, 12, 16, 20, 26, 39 and 52 weeks.

4.2.4 Measurement of mass loss and, water absorption and pH

After the test samples were withdrawn from the shaking bath, they were rinsed twice with distilled water and the surfaces of the pellets were carefully wiped with tissue paper. The test samples were weighed immediately after wiping. Next, the test samples were dried for at least three days at ambient conditions and for one week in vacuum. After vacuum drying, the test samples were weighed again to obtain the dry masses. Dried test samples were stored in a desiccator for further analysis.

The mass loss was calculated as the difference between the initial mass of the test sample and the mass of the dried test sample divided by the initial mass of the test sample. The water absorption was calculated as the difference between the mass of the wet test sample and the mass of the dried test sample divided by the mass of the dried test sample.

4.2.5 Measurements of molar weights of the polymers

The number average and weight average molecular weights (M_n and M_w respectively) and polydispersity (PD) values of the copolymers were determined at room temperature by size exclusion chromatography (SEC) (Waters Associates system equipped with a Waters 717plus autosampler, a Waters 510 HPLC solvent pump, four linear PL gel columns (10^4, 10^5, 10^3 and 100 Å) connected in series, and a Waters 2414 differential refractometer). Chloroform (Riedel-de Haën AG, stabilized with 1% ethanol) was used as solvent and eluent. The samples were filtered through a 0.5 μm Millex SR filter. The injected volume was 200 μl and the flow rate was 1.0 ml/min. Monodisperse polystyrene standards were used for primary calibration.

4.2.6 Measurement of thermal properties

The thermal properties of the composites were measured using DSC Q1000 differential scanning calorimeter (TA Instruments, Delaware, USA). The samples were heated twice to ensure that their thermal histories were similar during the second heating. Nitrogen was used as a sweeping gas. The heating rate was 20 °C/min, the cooling rate 50 °C/min, and the temperature range was from -60 °C to +200 °C. The results were analyzed using Universal Analysis Software. Second heating cycle was used for the analysis of glass transition temperatures (T_g) and first heating cycle for the analysis of melting temperatures (T_m) and melting enthalpies (heats of fusion, ΔH_f). Five parallel samples were tested for each material and time point. Averages and standard deviations were then calculated.

In order to detect the possible melting peaks of the active agents ciprofloxacin (265-275 °C (Dorofeev et al. 2004)) and rifampicin (approximately 190 °C (Agrawal et al. 2004)) in the composites, samples of 5-7 mg of the composites were heated up to 300 °C at the rate of 20 °C/min using DSC. Additionally, samples of pure rifampicin and ciprofloxacin were studied the same way. The melting peaks in the mentioned ranges, if detected, give information about the active agent being at least partly dispersed in the polymer matrix and not totally dissolved.

4.2.7 Determination of molecular structure

The proton NMR spectra were measured from selected samples of composites without antibiotics and the composites containing rifampicin or ciprofloxacin. The samples were measured using a Varian Mercury 300 MHz NMR Spectrometer (Varian Associates Inc., Palo Alto, California, USA) at room temperature. Tetramethylsilane (TMS) was used as an internal standard, and chemical shifts were measured relative to TMS. The ^{1}H NMR spectra were measured at room temperature in standard 5 mm tubes in deuterochloroform (Merck, Germany). The data were gathered until the quality of the spectrum was sufficient, and the number of scans varied between 190 and 512. The proton NMR spectra of the samples were processed and analyzed using SpinWorks 3.1 and ACD/Spectrus software. Phase correction and baseline correction were applied to all spectra.

4.2.8 Measurement of ceramic content

The β-TCP content of the test samples was measured using thermogravimetric analysis (TGA Q500 (TA Instruments, Delaware, USA)). Approximately 20 mg of a sample was used and the samples were heated starting from room temperature at a rate of 20 °C/min up to 700 °C. Five parallel samples were tested at each time point of each composite, and the results were then analyzed using Universal Analysis Software.

4.2.9 Determination of the microstructure of the samples

The microstructure of the composites was observed using scanning electron microscopy (SEM) (Philips XL-30 SEM equipped with a LaB6 filament with SE and BSE detectors, Philips, the Netherlands) with an acceleration voltage of 12.0 kV. The micrographs were taken both on the surface of the samples and on cryogenically fractured samples that were coated with gold (Edwards S150 Sputter Coater) prior to microstructure examination.

4.2.10 Antibiotic release tests

The drug release tests were conducted at 37 °C *in vitro*. Weighed test samples (each test sample consisted of 15 pellets) were placed in brown glass bottles along with 20 ml Sörensen buffer solution. Five parallel test samples were tested for each composite material. The bottles were placed in an incubator shaker (Infors Multitron, Infors Bottmingen, Switzerland) at 37 °C. At predetermined time intervals, the buffer solution was withdrawn from each of the bottles and replaced with fresh solution. The amount of buffer solution and the periodical change to fresh buffer solution enabled sink conditions to be valid throughout the test series. Sink condition is usually referred as a condition where the concentration of the active agent in the solution does not affect the dissolution of the active agent from the device to the medium. Typically the limit for sink condition is considered as 5% of the saturation concentration (Baker 1987). The solubility of rifampicin in water at 30 °C has been reported to be 1.5-1.7 mg/ml depending on the crystal form of rifampicin (Henwood et al. 2000). Solubility of ciprofloxacin at 37 °C has been reported to be 0.20 mg/ml at pH 7.8 and 0.22 mg/ml at pH 6.9 (Breda et al. 2009). These solubilities were noticed to be adequate in ensuring sink conditions in this method. The amount of released antibiotic (ciprofloxacin or rifampicin) was determined from the buffer solution using a Unicam UV 500 spectrometer (ThermoSpectronic, Cambridge, United Kingdom) at maximum absorption wavelength of 271 nm for ciprofloxacin and 226 nm for rifampicin. A wavelength area from 190 to 400 nm for ciprofloxacin and 190 to 650 nm for rifampicin was scanned in order to detect possible changes in the molecular structures of the antibiotics (ciprofloxacin and rifampicin) that cause deviation in the UV-spectrum. Ciprofloxacin and rifampicin concentrations were calculated using Beer-Lambert law and standard curves prepared with known concentrations of both of the antibiotics.

4.2.11 Statistical testing

Mann-Whitney U test was used to determine if there was a statistical difference in the drug release results between the composites containing 50 wt-% and 60 wt-% of β-TCP. The significance level of $p < 0.05$ was used.

4.2.12 Initial and final antibiotic content measurements

Samples of about 150 mg were weighed from each manufactured composition containing antibiotics. The samples were dissolved in 50 ml of chloroform (J.T. Baker, the Netherlands). The amount of ciprofloxacin or rifampicin in the chloroform solution was determined using a Unicam UV 540 Spectrophotometer (ThermoSpectronic, Cambridge, United Kingdom) at a maximum absorption wavelength of 284 nm for ciprofloxacin and 349 nm for rifampicin. The concentrations of the antibiotics in the solution were calculated using Beer-Lambert law and standard curves prepared with known concentrations of the antibiotics.

4.2.13 Inhibition zone testing using bioluminescence imaging

The effects of the antibiotic-releasing composite materials against common osteomyelitis causing bacteria were tested using bioluminescence imaging based on the ability of genetically engineered bacteria to emit light. This method gives more information of the developing inhibition zones than the conventional inhibition zone method. The antibiotic containing composite materials chosen for this study were the composites containing 50 wt-% of β-TCP based on the drug release results. Composite of PLCL and 50 wt-% of β-TCP was used as control.

Two different engineered bacteria strains were used as biosensor cells: *Pseudomonas aeruginosa* PAO-LAC carrying plasmid pUCP24GW (Moir et al. 2007), and *Staphylococcus epidermidis* ATCC-14990 carrying plasmid pAT19-lux-hlaP-frp. None of the bacteria strains were actually pathogenic.

Bacteria were cultured on antibiotic L-agar plates overnight at 30 °C, and suitable colonies were moved into liquid culturing in Luria-Bertani (LB) medium (5 g/l yeast extract, 10 g/l tryptone, 5 g/l NaCl). The bacteria were cultured overnight at 30 °C and 300 rpm with suitable antibiotics. If the bacteria did not produce luminescence in the morning, 1/50 dilution was made in a culture tube and it was incubated at 37 °C and 300 rpm for three hours. The level of luminescence of the cultures was measured by using Plate Chameleon^{TM} multilabel counter 1.001 (Hidex Ltd., Turku, Finland). At volume of 200 µl, counts of 1.1-2.3×10^6 (*S. epidermidis*), and 1.1-2.3×10^6 (*P. aeruginosa*) were found optimal.

Layers of LB-agar (agar 15 g/l, 2 ml) were cast into 6-well plate, and the controls and antibiotic containing composite pellets were placed on top of them (one pellet per well). Bacteria culture of 350-500 µl per well was mixed with 1 ml of soft LB-agar (agar concentration 7.5 g/l) solution and cast on top of the first layers. The amount of bacterial culture was dependent on the luminescence level. After solidification, the plate was taken to the imaging station of Xenogen VivoVision IVIS® Lumina luminescence camera (Caliper LifeSciences, USA). Images were taken every 20 minutes for 16 hours

with exposure time of 30 seconds. The pictures were analyzed using Living Image® 3.1 program (Caliper LifeSciences, USA). The intensities of the light emitted from the wells were analyzed as well as the development of the inhibition zones around the antibiotic-releasing pellets. The results are presented as false color photos, where dark blue and purple were interpreted as dead bacteria with no bioluminescence. The red and yellow colors were interpreted to indicate situation where the bacteria are in contact with subinhibitory concentrations of the antibiotics and produce strong light emission that is presumably due to the nonspecific activation of central metabolic pathways. These red and yellow zones are called stress zones (SZ). Green color was considered to be unaffected bacteria because this was the usual light intensity in the control wells.

5 RESULTS

5.1 The effects of processing and sterilization on the materials

The processing of the materials with twin-screw extrusion caused only slight decrease in the molar weights of the PLCL copolymer in the composites without antibiotics and the composites containing rifampicin. The M_w of the copolymer seemed to decrease more in the composites containing ciprofloxacin. The results of the M_w determined using SEC are presented in Table 5. Sterilization using gamma-irradiation caused significant degradation in all studied composites. The decrease of molecular weights during gamma-irradiation is a well-known fact with biodegradable polymers e.g. lactide based polymers (Daculsi et al. 2011; Paakinaho et al. 2009). It is based on the random chain scission due to the high-energy irradiation (Plikk et al. 2006). The measured doses of gamma-irradiation were 28.7-34.0 kGy for composites without antibiotics and 29.3-35.0 kGy for the composites with antibiotics. It has also been suggested that gamma-irradiation may cause cross-linking for pure poly-ε-caprolactone (Cottam et al. 2009), but such an effect was not seen in these results. Cross linking would cause decrease in the M_n and increase the M_w of the polymer. Here, a significant decrease in both M_n and M_w was seen.

Table 5. M_w of the polymer matrix of the composites as raw material, after processing and after sterilization.

Composite	M_w (g/mol) · 10^3		
	PLCL raw material	After processing	After γ-irradiation
Plain PLCL	229	227	195
PLCL+TCP10	229	228	187
PLCL+TCP20	229	228	177
PLCL+TCP35	229	226	163
PLCL+TCP50	229	226	166
PLCL+C	245	227	196
PLCL+TCP50+C	245	237	134
PLCL+TCP60+C	245	239	120
PLCL+R	245	241	172
PLCL+TCP50+R	245	244	151
PLCL+TCP60+R	245	245	143

The percentual decrease of the molecular weights (both M_n and M_w) of the composites without antibiotics during gamma irradiation is presented in Figure 7. Gamma irradiation caused more degradation to the composites with higher β-TCP content and the dependency was almost linear (shown with the trend lines). This may be due to that the samples were not stored in totally dry conditions before sterilization and the composites may have absorbed some moisture from air, which causes more degradation during the sterilization step. The composites with high β-TCP contents may absorb more water than the plain copolymer or the composites with low β-TCP contents. This causes more degradation in the composites with high β-TCP contents. Additionally, increased interfacial area between the ceramic particles and polymer may enhance the uptake of water.

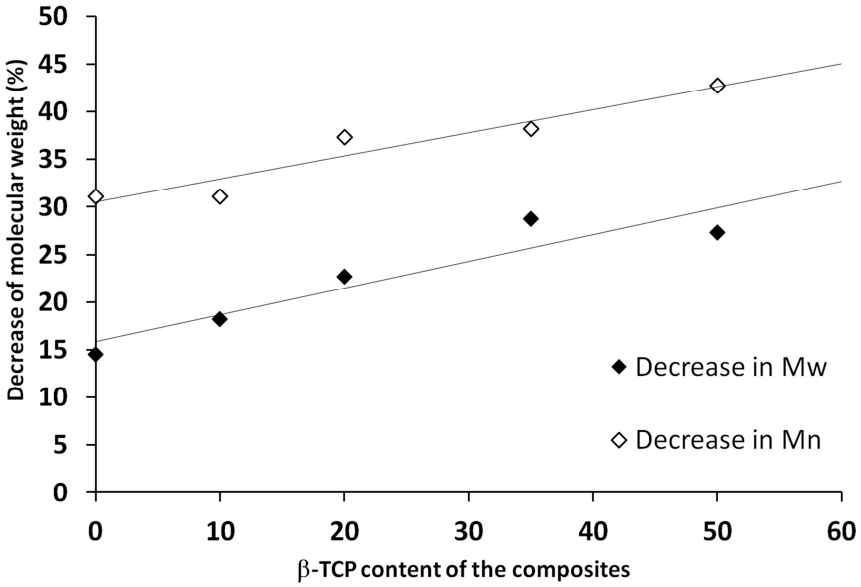

Figure 7. The percentual decrease in the M_w and M_n of the composites of PLCL and β-TCP during sterilization using gamma irradiation (28.7-35.0 kGy).

The residual L-lactide and ε-caprolactone monomer contents were measured from the raw material (plain PLCL) as well as from the processing batches of composites with and without the antibiotics. The results are presented in Table 6 as averages and standard deviations of the measurements. The residual ε-caprolactone monomer contents were below detection limit in all the samples and the residual L-lactide monomer content did not increase during processing.

Table 6. Residual L-lactide and ε-caprolactone monomer contents in the raw material and after the processing of the composites.

	Raw material (n=4)	PLCL+TCP (n=6)	PLCL+TCP+C (n=6)	PLCL+TCP+R (n=4)
L-lactide (wt-%)	0.08 ± 0.02	0.08 ± 0.02	0.05 ± 0.02	0.06 ± 0.02
ε-caprolactone (wt-%)	< 0.02	< 0.02	< 0.02	< 0.02

5.2 Degradation of the materials

5.2.1 pH of the buffer solution

pHs of the buffer solutions were measured and the buffer solutions were changed periodically in all of the degradation test series to ensure that the pH stayed between values 7.2-7.6.

As the hydrolytic degradation of the polymer proceeded, acidic degradation products were released to the surrounding buffer solution. Lower pH values were measured from the time point of 12 weeks onwards, and there was a clear need to change buffer solution more often than in the beginning of the degradation test series. In the degradation test series of the antibiotic containing composites, the buffer was changed in the same rate as the drug release samples were taken, to avoid the effect of accumulating drug on the degradation of the composites. Overall, the pH of the buffer solution retained close to 7.4, which is the initial pH of the Sörensen buffer solution, for the most parts of the test series.

5.2.2 Molecular structure

The molecular structures of the polymer and antibiotic constituents of the composites were analyzed using NMR in order to gain information about the degradation of the polymer and the molecular structure of the antibiotics. Of special interest was the effect of sterilization using gamma irradiation on the molecular structures of the antibiotics. The NMR measurements were done at time points of 0 (after processing and sterilization), 26 and 52 weeks of the *in vitro* test series and the samples measured were: plain PLCL, PLCL+TCP50, PLCL+C, PLCL+TCP50+C, PLCL+R, and PLCL+TCP50+R. Additionally, plain rifampicin sample was measured as well as the raw material PLCL. There were two different raw materials batches used for the manufacturing of the composites. One batch was used for the composites without antibiotics and another batch was used for all antibiotic-containing composites.

Because polymer degradation is dependent not only on the comonomer ratio but also on the microstructure of the polymer, e.g. sequence lengths and randomness of the polymer

structure, a closer look at the molecular structure needed to be taken in order to understand polymer degradation behavior (Fernández et al. 2012; Herbert 1993).

Polymer

The chemical shifts of the protons remained constant in all of the studied samples. The signals of the ^{1}H NMR spectra were assigned to the polymer molecule, as shown in Figure 8. Some signals were overlapping and could not be used for the analysis. The most informative signals of the PLCL copolymer were the signals at δ 5.16 for the –CH group proton of the lactide comonomer, at δ 4.05-4.13 for the α-oxy methylene protons of the ε-caprolactone comonomer, and at δ 2.3-2.4 for the protons of the methylene group of ε-caprolactone that was bonded to the carbonyl group. The signals of the caprolactone protons at δ 4.05-4.13 and at δ 2.3-2.4 were clearly split into two parts according to the position in the polymer chain. The triplet at δ 4.13 indicated the CH_2 group in the ε-caprolactone fragment bonded to an L-lactide unit and the broader multiplet at δ 4.05 indicated the α-oxy methylene group bonded to another ε-caprolactone unit. (Fernández et al. 2012; In Jeong et al. 2004) The signal at δ 2.3-2.4 was split the same way. The triplet at δ 2.4 indicated a group bonded to a L-lactide group and the broader multiplet at δ 2.3 corresponded to a group that is bonded to another ε-caprolactone group (Fernández et al. 2012; In Jeong et al. 2004). This information could be used for the calculation of the average sequence lengths of the L-lactide and ε-caprolactone comonomers. The comonomer ratios of the copolymer were calculated as the ratio of the integral of the signal at δ 5.16 to the average integrals of the caprolactone signals at δ 4.05-4.13 and at δ 2.3-2.4 (Fernández et al. 2012). The results are shown in Table 7.

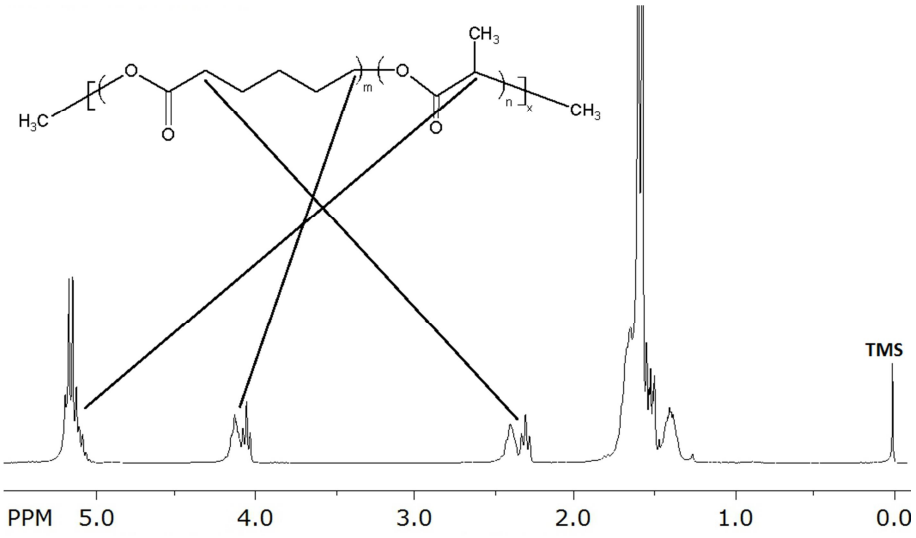

Figure 8. Peak assignment of the ^{1}H NMR spectrum of the PLCL raw material to the molecular structure of the PLCL copolymer.

Table 7. Comonomer molar ratio (L-lactide to ε-caprolactone) of the PLCL copolymer at different time points of the in vitro test series (pH 7.4, 37 °C).

Time (weeks)	Plain PLCL	PLCL+TCP50	PLCL+C	PLCL+TCP50+C	PLCL+R	PLCL+TCP50+R
0	68/32	68/32	68/32	68/32	69/31	69/31
26	75/25	70/30	68/32	68/32	78/22	71/29
52	83/17	79/21	75/25	77/23	84/16	80/20

The L-lactide and ε-caprolactone sequence lengths and randomness were studied from the results of the ^{1}H NMR analysis according to the text by Herbert (Herbert 1993) and Fernández *et al.* (Fernández et al. 2012). The number average sequence lengths, ñ, of the comonomers were calculated using Equations 14 and 15:

$$\tilde{n}_{LA} = \frac{2(LA)}{(LA-CL)} \quad (14)$$

$$\tilde{n}_{CL} = \frac{2(CL)}{(LA-CL)} \quad (15)$$

where (LA) and (CL) are the molar fractions of the L-lactide and ε-caprolactone comonomers in the copolymer and (LA-CL) is the average dyad relative fraction, which can be calculated from the ^{1}H NMR data of the copolymer (Fernández et al. 2012). Additionally, the randomness factor, R, can be calculated using the Equation 16:

$$R = \frac{(LA-CL)}{2(LA)(CL)} \quad (16)$$

If the randomness factor is 1, it means that the polymer has a totally random structure and if it is 0, the copolymer is a block copolymer (Fernández et al. 2012). The results of the average sequence length calculations and the randomness factors for all of the composites are presented in Table 8.

The randomness of all the studied materials decreased as the degradation proceeded. Only the composite of PLCL+C showed behavior that differed from the other composites. In this particular composite, the decrease of randomness was not substantial. The average sequence lengths of the comonomers showed that L-lactide tends to form long blocks and ε-caprolactone blocks were shorter on average, mainly between 6-7 units long. The notable increase in the average sequence length of the L-lactide comonomer as the degradation proceeded showed that the short blocks of L-lactide were removed from the polymer chains, as the copolymer was hydrolytically degraded. There was only a slight increase in the ε-caprolactone sequence length as the degradation proceeded, which indicated that the sequence length was not much affected

by the hydrolytic degradation although the ε-caprolactone comonomer fraction in the copolymer decreased.

The decrease of the randomness factor R supports the interpretation that the random parts of the copolymer were removed from the polymer structure and more blocky structures, consisting mainly of L-lactide units, remained as the hydrolytic degradation proceeded.

Table 8. Number average sequence lengths of L-lactide and ε-caprolactone in the PLCL copolymer and randomness factors (R) for the copolymer at different time points of the in vitro test series (pH 7.4, 37 °C).

Sample name	Time *in vitro* (weeks)	L-lactide sequence length	ε-caprolactone sequence length	Randomness factor, R
Raw material (used for the composites without antibiotics)	0	12.70	5.88	0.25
Raw material (used for the antibiotic containing composites)	0	12.22	5.74	0.26
PLCL	26	16.85	6.32	0.22
PLCL	52	28.85	7.07	0.18
PLCL+TCP50	0	11.92	5.77	0.26
PLCL+TCP50	26	14.10	6.27	0.23
PLCL+TCP50	52	20.61	6.80	0.20
PLCL+C	0	12.94	6.02	0.24
PLCL+C	26	13.02	6.44	0.23
PLCL+C	52	15.15	6.26	0.23
PLCL+TCP50+C	0	12.99	5.99	0.24
PLCL+TCP50+C	26	12.07	6.49	0.23
PLCL+TCP50+C	52	22.77	7.15	0.18
PLCL+R	0	11.41	5.44	0.27
PLCL+R	26	21.23	6.31	0.21
PLCL+R	52	31.28	6.97	0.18
PLCL+TCP50+R	0	11.32	5.57	0.27
PLCL+TCP50+R	26	14.60	6.11	0.23
PLCL+TCP50+R	52	23.25	7.10	0.18

Ciprofloxacin

Signals of ciprofloxacin protons were visible in the ^{1}H NMR only in the 0 week samples. At 26 or 52 weeks, the ciprofloxacin content in the samples was below the limit that could be detected using NMR. Thus, the molecular structure of ciprofloxacin during *in vitro* test series could not be analyzed. The signal assignment of ciprofloxacin molecule to the peaks in the ^{1}H NMR spectrum is shown in Figure 9. Some signals were overlapping with the signals of the polymer and thus could not be used for analysis. The integrals of protons of the quinoline ring at 8.80 and 8.06 ppm (a and b in Figure 9) were in good agreement with the stoichiometric proportion 1:1 in both ciprofloxacin-containing samples where ciprofloxacin signals were detected. Additionally, the signals of cyclopropane proton at 3.55 ppm (c), and the 8 protons in the piperazine ring, which appear as a multiplet at 3.25 ppm (d), show good agreement with the stoichiometric values 1:8. Based on these results, it can be concluded that the ciprofloxacin molecule maintained its original structure throughout the processing and sterilization steps. This result supports the findings of Koort *et al.* and Alvarez *et al.* who concluded that processing and gamma-sterilization do not affect the bactericidal effect of ciprofloxacin (Koort et al. 2005; Koort et al. 2006; Koort et al. 2008; Mäkinen et al. 2005b; Alvarez et al. 2008).

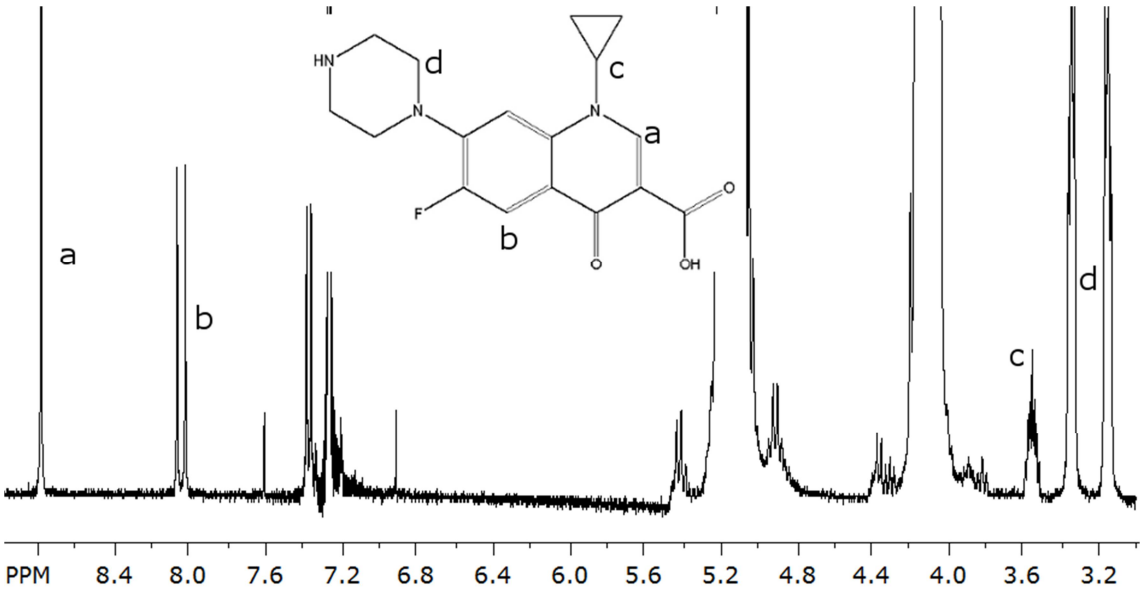

Figure 9. Part of the ^{1}H NMR spectrum of PLCL+C after processing and sterilization and positions of the peaks assigned to the protons in the ciprofloxacin molecule.

Rifampicin

The molecular structure of rifampicin was studied from three samples (pure rifampicin, PLCL+R and PLCL+TCP50+R after processing and sterilization). Rifampicin signals were not seen in other samples due to the rather low sensitivity of NMR and low content of rifampicin in the samples. The ^{1}H spectrum of pure rifampicin was compared to the spectra of the 0 week samples. ^{1}H NMR analysis of rifampicin reported by Cellai *et al.* (Cellai et al. 1982) was also used when the signals were assigned to the protons of the rifampicin molecule. Proton assignment is presented as Figure 10 and spectra as an Appendix.

In the composite samples, some signals of the rifampicin molecules were overlapping with the polymer signals and could not be analyzed accurately. These were some of the protons in the *ansa* chain (protons 16, 18, 20, 21, 22, 24, and 31), protons 32 of the naphtalene ring, and protons 59 of the methyl group attached to the piperazinyl ring. Amide proton and the OH-groups of the naphthalene ring were clearly visible at δ 11.98 ppm 13.11 ppm and 13.41 ppm, respectively. Their chemical shifts were stable and the integrals were in good stoichiometric ratio. The protons of the methylene group located above the plane of the naphthalene ring (protons 45) showed a signal below 0 at δ -0.31 ppm in pure unprocessed rifampicin and processed PLCL+R and PLCL+TCP50+R samples. The fact that this signal is identical in all the samples proves that the *ansa* chain has retained its original configuration. Otherwise, the signal of this group would have appeared elsewhere in the spectrum. The *ansa* bridge protons 13, 14, 15, 17, 19, 23, and 25 were clearly visible, stable when compared between the samples, and were in good stoichiometric agreement with the rifampicin structure. The signals of the protons 37, 39, and 41 of the methyl substituents of the *ansa* chain and the signals of the protons 54 and 56 of the piperazine ring were in the shoulder of a large polymer signal and thus their accurate integration was not possible. Additionally, signals of the equivalent protons 53 and 57 of piperazine ring appeared at δ 3.02 overlapping with signals of the protons 19 and 47 and thus could not be accurately integrated. However, their combined integral showed that there was no change between samples in either the positions of the signals or their integrals.

As a conclusion of the NMR analysis, it can be stated that no deviations of the original rifampicin structure were found after the analysis of the composite samples (PLCL+R and PLCL+TCP50+R) and pure rifampicin sample. Thus, rifampicin maintained its original structure during processing and sterilization steps.

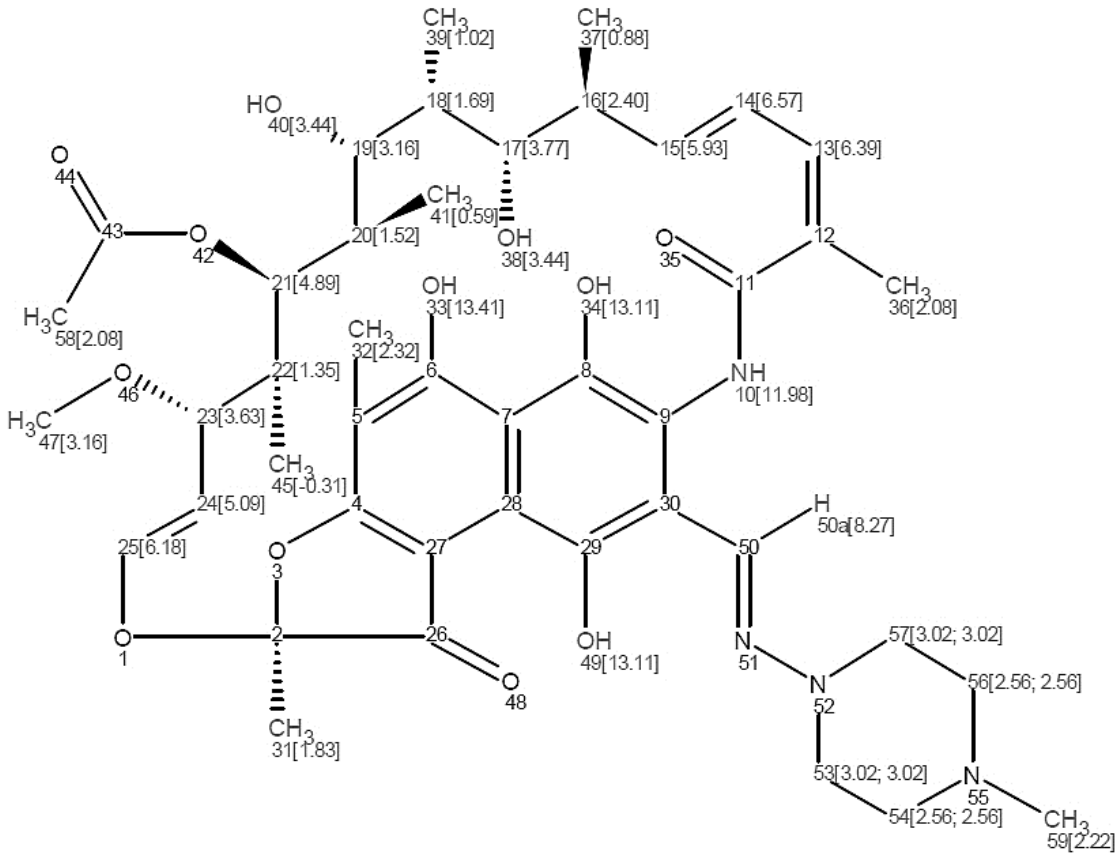

Figure 10. Chemical structure, atom numbering and ^{1}H chemical shifts of rifampicin.

5.2.3 Molecular weights of the PLCL copolymer

The molecular weights (both M_w and M_n) of PLCL in all the studied composites decreased rapidly during the 52-week *in vitro* test period. There were small differences in the initial M_w and M_n, but the degradation proceeded similarly in all the studied composites. Typical degradation results are presented in Figure 11, where the M_ws of the composites containing 50 wt-% of β-TCP are presented. The M_ws of all the antibiotic containing composites are shown as Figure 6 and Figure 4 in publications II and III respectively. The M_ns of the composites without antibiotics are shown as Figure 3 in publication I. The SEC distribution curves showed emerging bimodality from the 20 week time point onwards. An example presenting the bimodality is shown as Figure 4 in the Publication I.

The rapid decrease of the M_w was due to the random chain scission of the ester bonds in the polymer backbone, which occurs first in the amorphous sections of the polymer and proceeds later to the crystalline parts (Li and Vert 1999).

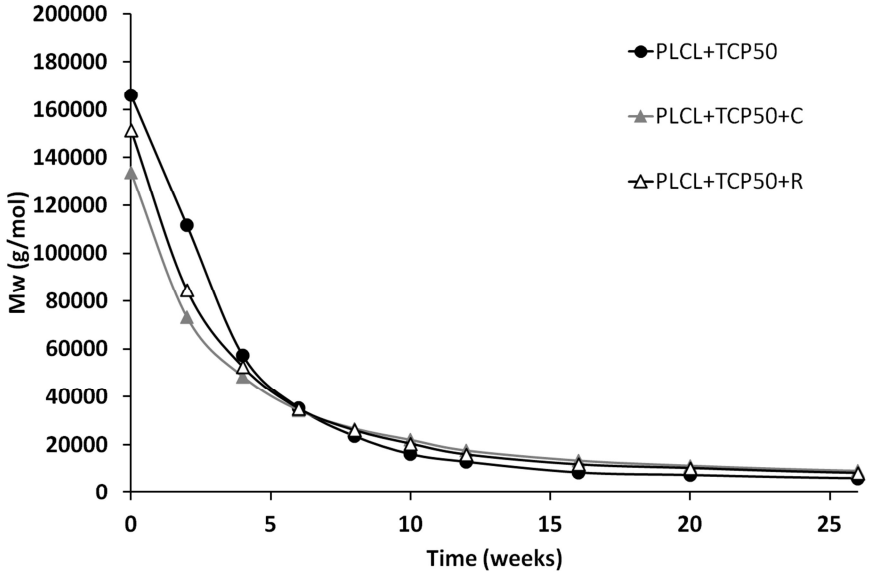

Figure 11. Examples of the decrease in the M_w of the composites of poly(L-lactide-co-ε-caprolactone) (PLCL) and 50 wt-% β-tricalcium phosphate (TCP) with and without antibiotics (ciprofloxacin (C) and rifampicin (R))(8 wt-%) as a function of time in vitro (pH 7.4, 37 °C).

The molecular weights (M_w) decreased according to the first order kinetics (Equation 11 in section 2.1.2.3) (Lao et al. 2011; Li and Vert 1999; Pitt et al. 1981):

$$M_{w,t} = M_{w,0} exp(-kt) \qquad (11)$$

where $M_{w,t}$ is the polymer molecular weight at time t and $M_{w,0}$ is the initial polymer molecular weight and k is the degradation rate constant. When plotted to logarithmic scale the decrease of molecular weight is linear. This is valid until the onset of mass loss (Li and Vert 1999; Pitt et al. 1981).

Fitting the Equation 11 to the experimental results using the t in hours and least squares regression analysis gave the degradation rate constant k values that are presented in Table 9. The values are all reasonably close to each other except the PLCL+C, which has slightly higher degradation rate constant.

Table 9. The rate constants for the molecular weight decrease (k) for the hydrolytic degradation of the PLCL copolymer in the studied composites in vitro (pH 7.4, 37 °C).

Composite	$k \cdot 10^{-3}$ (1/h)
Plain PLCL	1.7
PLCL+TCP10	1.7
PLCL+TCP20	1.6
PLCL+TCP35	1.4
PLCL+TCP50	1.4
PLCL+C	2.1
PLCL+TCP50+C	1.5
PLCL+TCP60+C	1.4
PLCL+R	1.7
PLCL+TCP50+R	1.5
PLCL+TCP60+R	1.4

5.2.4 Water absorption and mass loss of the composites

Water absorption and mass loss were clearly affected by the β-TCP contents of the composites as well as the antibiotics in them. The results of the mass loss and water absorption measurements are presented as Figures 6, 6 and 4 in the publications I, II and III respectively. As a summary, the results from the water absorption and mass loss measurements of the composites without antibiotics are collected in Figure 12 and the results of the composites containing ciprofloxacin or rifampicin are collected in Figure 13. The bars showing standard deviations were omitted for clarity.

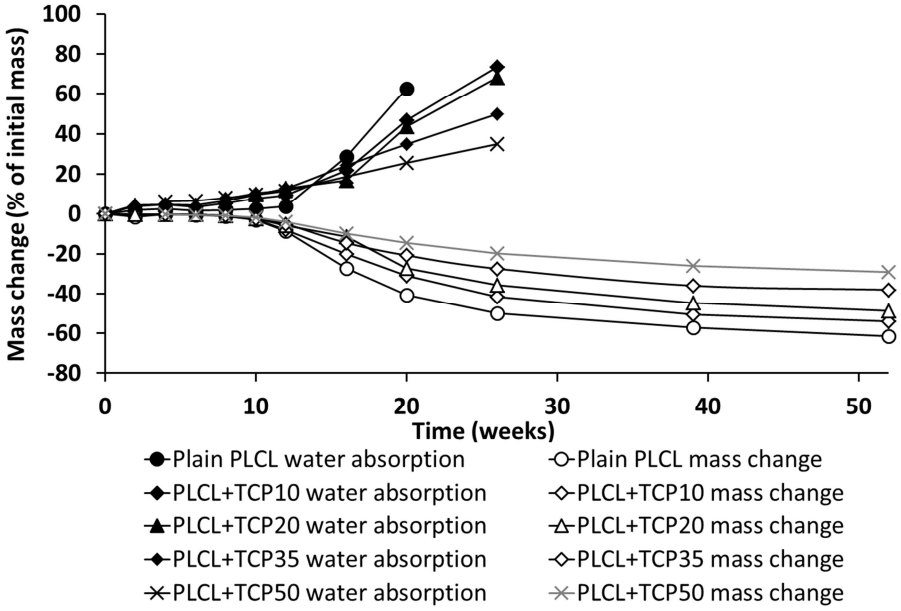

Figure 12. Water absorption and mass loss of the composites of poly(L-lactide-co-ε-caprolactone) (PLCL) and β-tricalcium phosphate (TCP) (presented as mass change as a function of time, pH 7.4, 37 °C). Standard deviations were omitted for clarity (n=5).

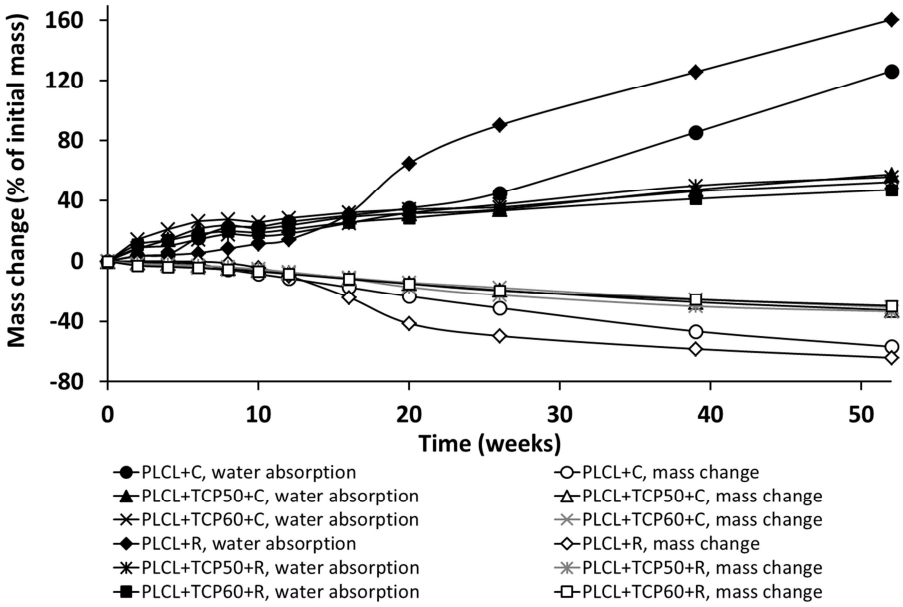

Figure 13. Water absorption and mass loss of composites of poly(L-lactide-co-ε-caprolactone) (PLCL), β-tricalcium phosphate (TCP), and ciprofloxacin (C) or rifampicin (R) (presented as mass change as a function of time, pH 7.4, 37 °C). Standard deviations were omitted for clarity (n=5).

The antibiotic containing composites tended to absorb more water in the beginning of the degradation test series (weeks 0-12) than the composites without antibiotics. Additionally, increasing β-TCP content in the composites caused more water absorption in the same time period, probably caused by the hydrophilicity of β-TCP (Figure 12) (Bernstein et al. 2010). The polymer mass loss was slow during the first ten weeks of the test series. The slight mass loss seen in the experiments during this time period was mainly due to the antibiotic release.

After the time point of 12 weeks, mass loss of the composites increased due to the fact that chain scission caused by hydrolysis had proceeded to the point where short polymer chain fractions were able to diffuse out from the matrix causing mass loss. This behavior was seen more in the plain copolymer samples and in samples where polymer fraction was large. The water absorption behavior of the composites changed so that the composites with low β-TCP contents absorbed more water than the composites with high β-TCP contents (Figure 12). In composites with antibiotics, such behavior was not seen and the water absorption for the antibiotic containing composites with 50 wt-% or 60 wt-% β-TCP proceeded similarly. On the other hand, the antibiotic content had an effect also on the water absorption. The rifampicin containing composite without β-TCP had identical water absorption behavior to the plain copolymer after the time point of 12 weeks. Rifampicin is able to form hydrogen bonds (Agrawal et al. 2004; Freire et al. 2009; Henwood et al. 2000; Henwood et al. 2001) due to its complex structure and thus may affect water absorption of the composites. The water absorptions of the composites without antibiotic were not measurable after 26 weeks (plain copolymer after 20 weeks) due to the degraded structure of the samples.

5.2.5 Ceramic content of the composites

Ceramic contents of the composites, measured using thermogravimetric analysis, increased as the degradation proceeded in all of the composites (Figure 14). Additionally, the results of the β-TCP dissolution test series showed very slow dissolution (results not included in this thesis but are reported in publication I). At 10-12 weeks, polymer degradation had proceeded to a stage when mass loss started and this can be seen as increase in the ceramic content curves shown in Figure 14. There were no differences in the ceramic content behavior of the composites containing 50 wt-% of β-TCP without antibiotic and with antibiotic (triangular symbols in Figure 14). Also the ceramic content curves of the composites containing 60 wt-% of β-TCP and rifampicin or ciprofloxacin showed no difference. The deviations between the five tested samples in all of the cases were very small, thus the standard deviations are not visible in Figure 14. Twin-screw extrusion as a production method produces very homogenous samples and the variation between them was thus very small.

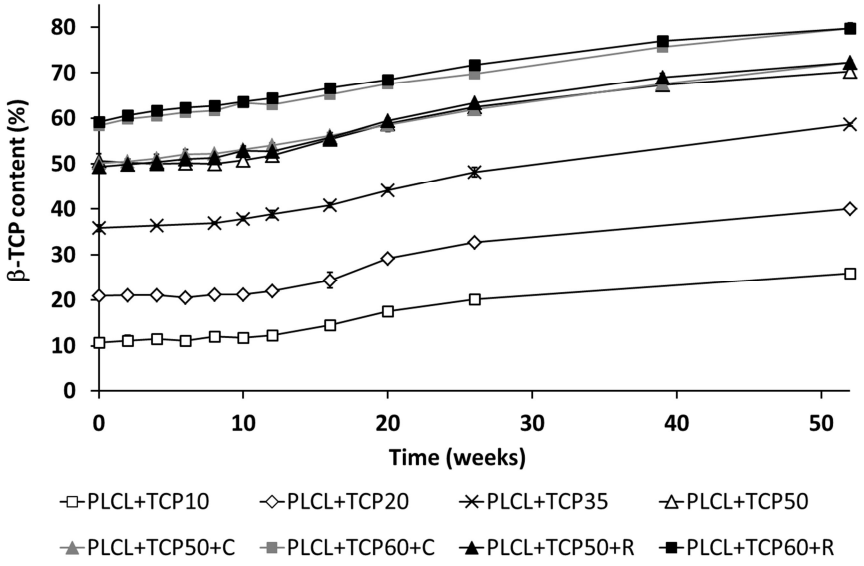

Figure 14. β-TCP contents of the composites of poly(L-lactide-co-ε-caprolactone) (PLCL), β-tricalcium phosphate (TCP), and ciprofloxacin (C) or rifampicin (R). Results presented as averages with standard deviations (n=5).

5.2.6 Thermal properties

Thermal properties of the composites were measured using differential scanning calorimeter with the heating rate of 20 °C/min and with two heating cycles to ensure similar thermal histories of the samples in the second heating cycle. The original T_g data are shown as Figures, 10, 8 and 6 in Publications I, II and III respectively. Representative T_g data are shown as Figure 15. Standard deviations are omitted for clarity. They are, however, seen in the figures in the original publications. There was a clear decrease in the T_g of all of the composites during the first weeks of the degradation test series. The decrease lasted until the time point of 12-20 weeks depending on the composite. The decrease in T_g was most pronounced in composites without antibiotics and PLCL+R and reached the minimum at 12 weeks. In other composites the decrease was less and the minimum was reached at 16-20 weeks.

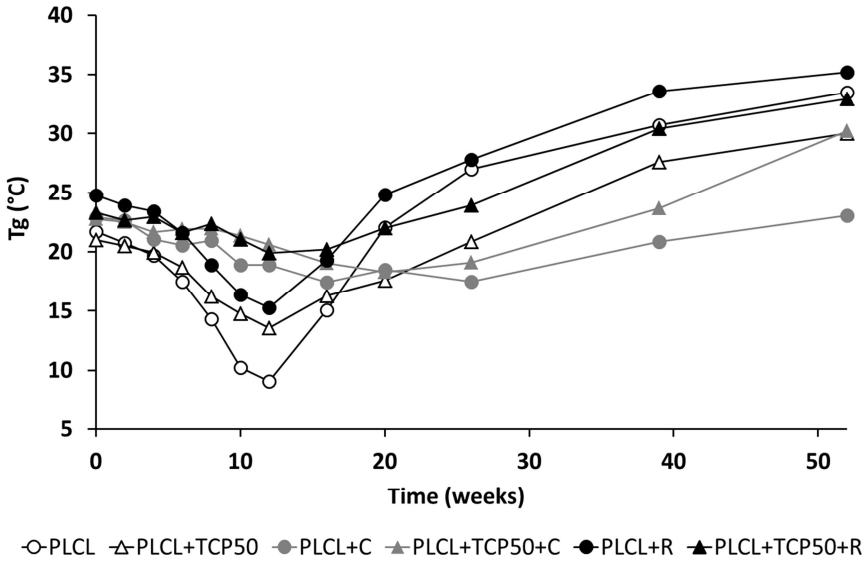

Figure 15. Changes in the T_gs of some of the studied composites of poly(L-lactide-co-ε-caprolactone) (PLCL), β-tricalcium phosphate (TCP), and ciprofloxacin (C) or rifampicin (R) during in vitro degradation test series. Standard deviations are omitted for clarity.

Melting temperatures of the composites were measured from the first heating of the DSC analysis. During second heating, the melting peaks were not visible anymore due to the fast cooling of the samples after the first heating that results an amorphous structure of this copolymer. The melting enthalpies were also analyzed and corrected to correspond to the polymer or polymer + drug part of the composite. There was some tendency for cold crystallization towards the end of the degradation test series. The composites without antibiotics and composites containing rifampicin behaved almost similarly. The melting peaks were mostly bimodal and they were mainly between 110-125 °C throughout the test series.

The heat of fusion (ΔH_f), which describes the crystallinity of a polymer, is presented for representative samples in Figure 16. The original data is shown in Figures 11, 8, and 6 in publications I, II and III respectively. The ΔH_f of the plain PLCL, PLCL+TCP10, PLCL+TCP20, PLCL+TCP35, PLCL+TCP50, PLCL+R, PLCL+TCP50+R, PLCL+TCP60+R and PLCL+C increased steadily throughout the test series. The composites of PLCL+TCP50+C and PLCL+TCP60+C showed a peculiar behavior. There was a dramatic increase in the crystallinity of the samples during the first weeks of the *in vitro* test series until the 8 week time point. After that, the crystallinity started to decrease and from the 16 week time point, followed the behavior of increasing crystallinity until the end of the test series.

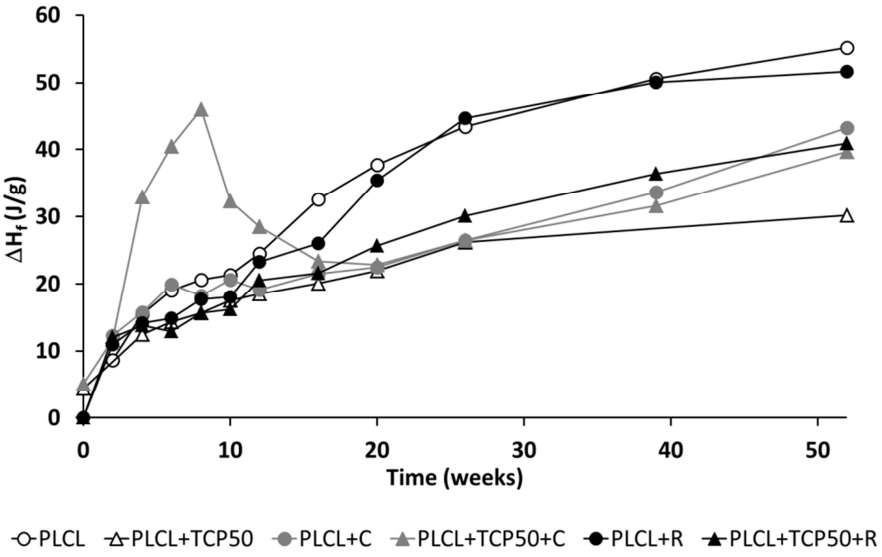

Figure 16. The heats of fusion (ΔH_f) of the polymer component in the composites of poly(L-lactide-co-ε-caprolactone) (PLCL), β-tricalcium phosphate (TCP), and ciprofloxacin (C) or rifampicin (R) during the in vitro degradation test series. Standard deviations are omitted for clarity (n=5).

Melting peaks around 236-245 °C were observed when ciprofloxacin containing composites were heated up to 300 °C using DSC. For pure ciprofloxacin, the melting peak was observed at 272 °C. On the other hand, melting peaks of 265-275 °C and 255-257 °C have been reported in the literature with a comment that the heating rate and the purity of the sample have an effect on the result (Dorofeev et al. 2004). These observations suggest that at least part of the ciprofloxacin antibiotic is dispersed in the composites. If ciprofloxacin would be totally dissolved in the polymer, no melting peak of ciprofloxacin would be seen in the composite samples (Baker 1987).

The DSC study done with pure rifampicin and the rifampicin containing composites showed a clear melting peak at 196 °C for the pure rifampicin sample but not for any of the composites. This suggests that rifampicin is dissolved in the polymer matrix in the composites. Rifampicin molecule has a number of functional groups in the molecular structure and thus may be able to form hydrogen bonds and van der Waals bonds with the polymer (Agrawal et al. 2004; Freire et al. 2009; Henwood et al. 2000; Henwood et al. 2001). The ability of the polymer and active agent to form these secondary bonds affects greatly on the solubility of the active agent in the polymer.

5.2.7 Microstructure

Scanning electron micrographs were taken both on the surfaces of the pellet shaped samples and on cryogenically fractured samples. Extrusion as a manufacturing method does not produce porous materials as such but the incorporation of ceramic component to the process introduces some porosity to the extruded material (Niemelä et al. 2005; Niemelä et al. 2011). Images of the samples showing porosity both on the surfaces and on the fractured surfaces can be seen in the Figures 12, 9 and 7 of the publications I, II, and III respectively. Selected micrographs are gathered to Figure 18. One example of β-TCP particles inducing porosity in the composite material is shown as Figure 17. Similar porosity induced by bioactive glass particles has been also reported earlier (Niemelä et al. 2005).

No porosity was observed in the plain PLCL after processing or during the 52 week *in vitro* test period. In the PLCL+TCP10, there were no significant porosity seen after processing either, but degradation induced some pore formation on the surfaces of the samples. This is shown as Figure 18 A. In Figure 18 B, the fractured surface of PLCL+TCP50 composite after 52 weeks *in vitro* is shown.

Antibiotic containing composites looked somewhat different than the composites without antibiotics. There was some porosity seen throughout the test series. Samples of PLCL+TCP60+C and PLCL+TCP60+R after 52 weeks *in vitro* are shown in Figure 18 C-F. Surfaces of the samples are shown in C and E and fractured surfaces in D and F, respectively. There are pores reaching the size of 100 μm which has been reported to enhance bone ingrowth (Shore and Holmes 1993).

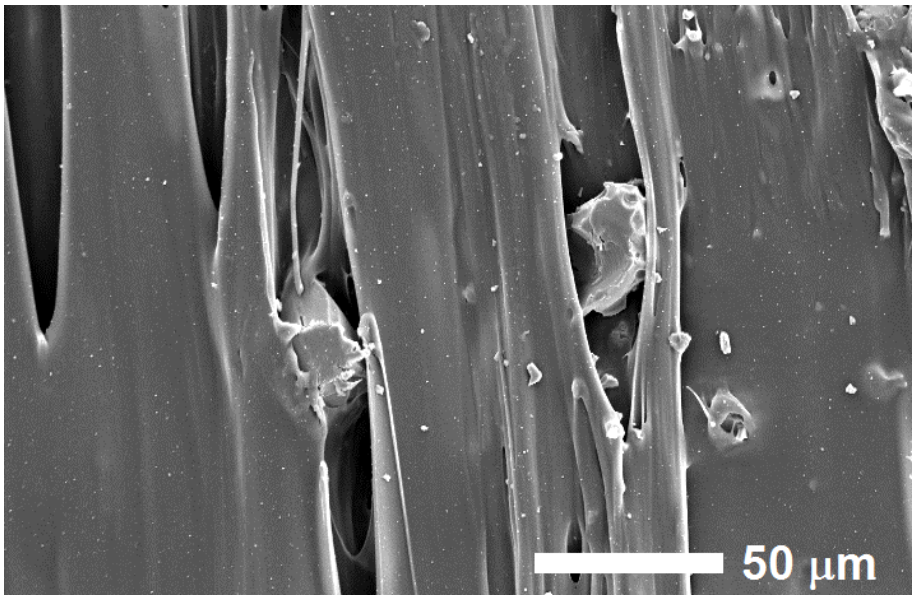

Figure 17. A detail of the surface of the composite of poly(L-lactide-co-ε-caprolactone) with 20 wt-% of β-tricalcium phosphate (TCP) after processing.

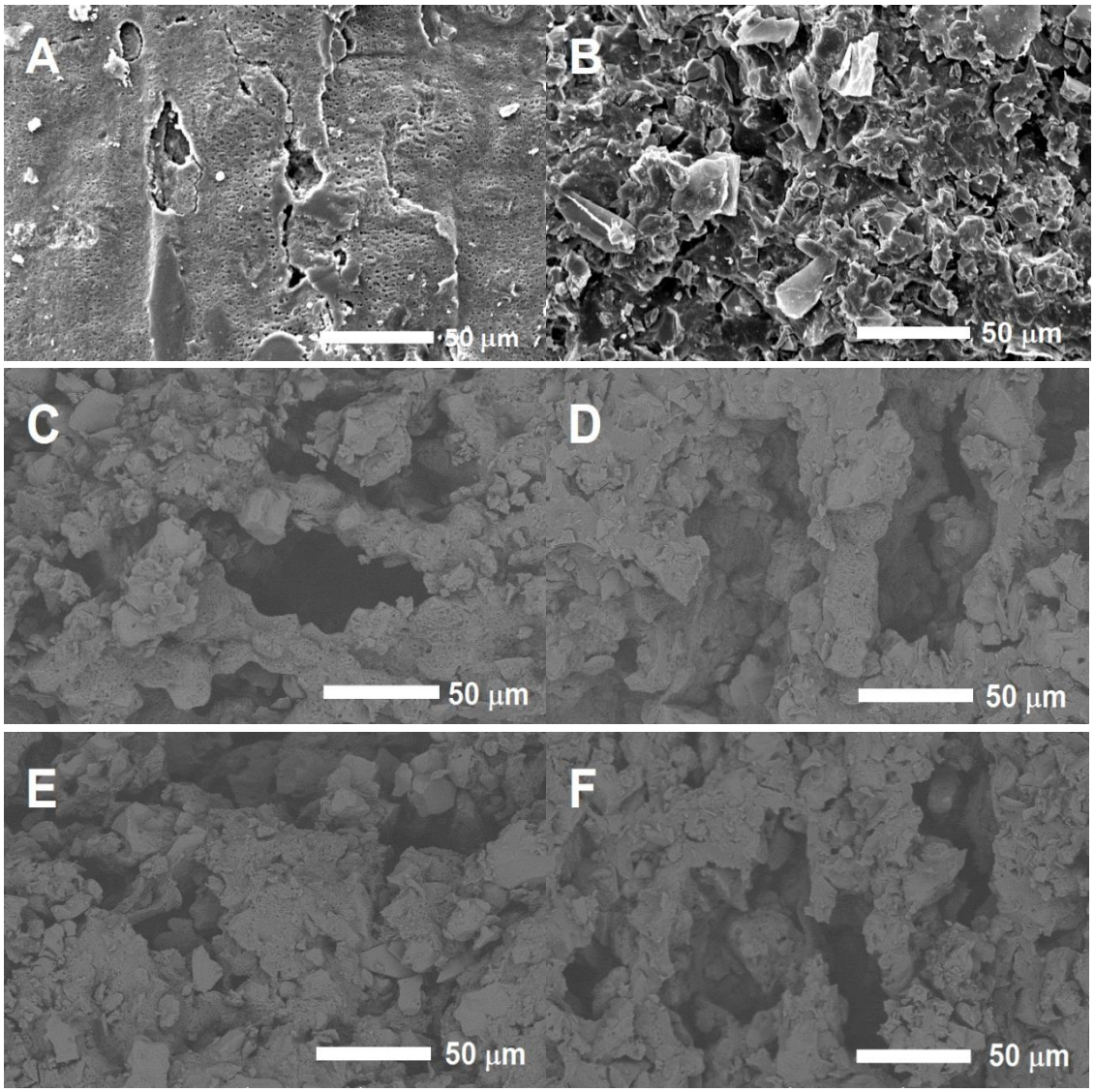

Figure 18. SEM micrographs of the composites. A) surface of PLCL+TCP10 at the time point of 52 weeks in vitro, B) fractured surface of PLCL+TCP50 at 52 weeks in vitro, C) surface of PLCL+TCP60+C 52 at weeks in vitro, D) fractured surface of PLCL+TCP60+C 52 at weeks in vitro, E) surface of PLCL+TCP60+R 52 at weeks in vitro, F) fractured surface of PLCL+TCP60+R at 52 weeks in vitro.

5.3 Antibiotic release

5.3.1 Ciprofloxacin

The initial ciprofloxacin contents of the composites were measured as 7.0 ± 0.4 wt-% for PLCL+C, 8.1 ± 0.1 wt-% for PLCL+TCP50+C, and 7.5 ± 0.2 wt% for PLCL+TCP60+C. Cumulative ciprofloxacin release from the composites is presented as Figure 19 and daily release as Figure 20. The release occurred in three distinct phases. The first phase was the burst in the beginning of the release and it can be seen well in the daily release profile (Figure 20). The burst lasted for one day and the daily release doses started to decrease after that. The burst is normally attributed to the drug molecules on the surface and near the surface of the sample and they are able to be dissolved into the surrounding medium rapidly (Baker 1987; Duvvuri et al. 2006). In these studied materials, the burst was small. The second phase of the release was until the 5-week time point, where there is a clear inflection point seen in the cumulative release curve of PLCL+C and PLCL+TCP50+C. The daily release curve shows a rapid increase in the ciprofloxacin release of PLCL+C and PLCL+TCP50+C around the time-point of 5 weeks. There is a very small peak seen also in the daily release profile of PLCL+TCP60+C. The PLCL+C showed a lag phase in the ciprofloxacin release until the time point of 5 weeks with almost negligible release. The second phase of the release was due to diffusion of the drug molecules through the matrix or through the pores in the composites. At this time period, the mass loss of the polymer was not yet significant (see Figure 13) and thus polymer erosion did not play a role in the antibiotic release. However, due to the hydrolytic degradation, the size of the polymer chains had decreased and enabled higher permeability of the drug in the polymer. Polymers based on ε-caprolactone are known to be well permeable for drug molecules under 400 g/mol of molecular weight (Pitt 1990; Woodruff and Hutmacher 2010). The permeability is also known to be affected by the comonomer ratio in the ε-caprolactone containing copolymers (Pitt et al. 1979). The copolymer used in this work, contained only 30 mol-% of ε-caprolactone comonomer and thus the permeability is considerably less than for pure poly-ε-caprolactone, because the L-lactide comonomer decreased the permeability of the copolymer. As a consequence, PLCL+C shows very slow ciprofloxacin release in the first five weeks of the release test series and differs substantially from the release curves of the PLCL+TCP50+C and PLCL+TCP60+C.

The phase of the release from the beginning to the 5-week time point obeys the first order kinetics for all ciprofloxacin-containing composites, where the release rate of the active agent is dependent on the concentration of the active agent in the test specimen and can be described with the Equation 2 in section 2.1.2.1. The Equation can also be presented as:

$$\ln(M_0 - M_t) = -kt + \ln M_0 \qquad (17)$$

where M_t is the released drug at the time t, M_0 is the initial drug load in the system, and k is the rate constant. When the logarithm of the remaining drug load (M_0-M_t) in the sample is plotted as a function of time, a straight line results. This is shown in Figure 21, where the release kinetics has been studied in two distinct phases. The R^2 was 0.99 for PLCL+TCP50+C and PLCL+TCP60 for the first five weeks of the drug release study and 0.97 for the PLCL+C.

In the third phase of the release, polymer degradation started to affect the drug release. The fitting to the theoretical first order kinetic model is shown in Figure 21. The R^2 was 0.99 for all three composites for the time after five weeks. In the third phase of the release, polymer erosion, degradation, and diffusion through the polymer matrix and through the pores in the composite all have an effect on the release (Baker 1987).

Mann-Whitney U test was performed to the cumulative ciprofloxacin release results of the composites containing 50 wt-% and 60 wt-% of β-TCP throughout all the measured time points. There was a statistically significant difference (Mann-Whitney U test, $P < 0.05$) in the cumulative ciprofloxacin release results of PLCL+TCP50+C and PLCl+TCP60+C until the time point of 26 weeks, where the release had ceased to almost negligible level. When the statistical analysis was done on the daily release of ciprofloxacin (Figure 20), the same kind of result was obtained. There was a statistically significant difference in the daily release of PLCL+TCP50+C and PLCL+TCP60+C until the time point of 27 weeks.

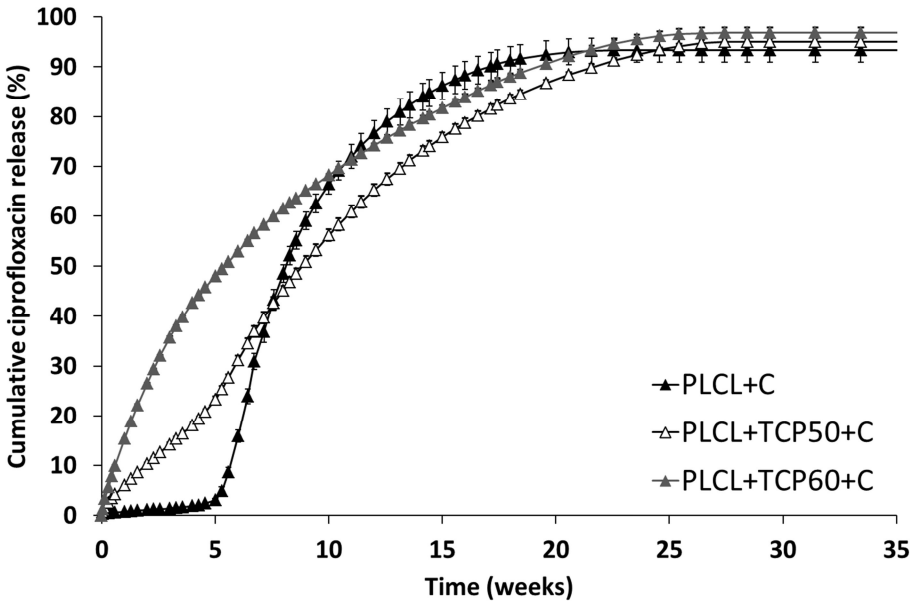

Figure 19. The cumulative release (at 37 °C, pH 7.4) of ciprofloxacin from composites of poly(L-lactide-co-ε-caprolactone) (PLCL) and β-tricalcium phosphate (TCP) with initial TCP contents of 0 wt-%, 50 wt-% and 60 wt-% and initial ciprofloxacin (C) content of 8 wt-%. Results shown as averages with standard deviations (n = 5).

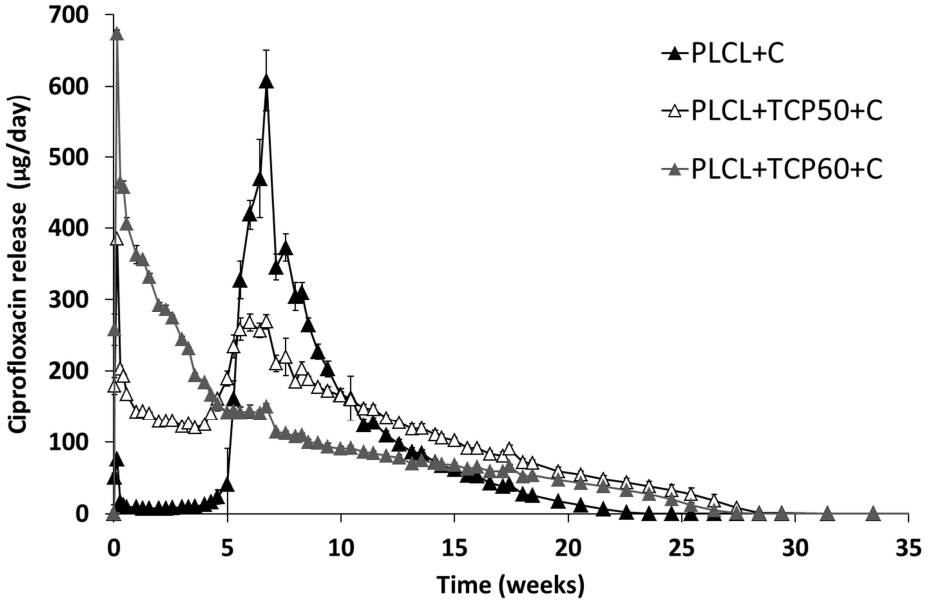

Figure 20. The daily release (at 37 °C, pH 7.4) of ciprofloxacin from composites of poly(L-lactide-co-ε-caprolactone) (PLCL) and β-tricalcium phosphate (TCP) with initial TCP contents of 0 wt%, 50 wt-% and 60 wt-% and initial ciprofloxacin (C) content of 8 wt-%. Results shown as averages with standard deviations (n = 5).

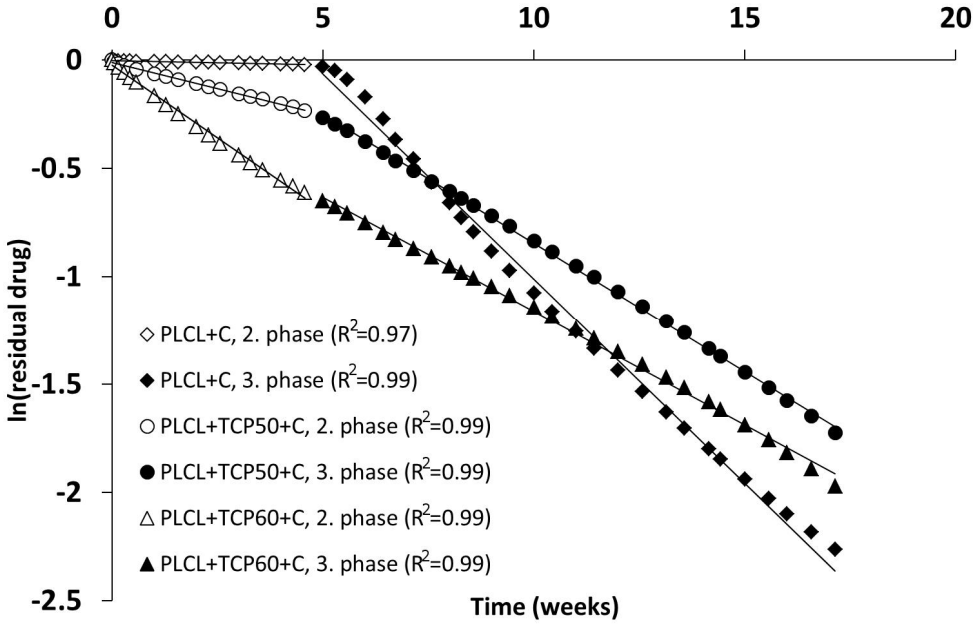

Figure 21. Fitting the ciprofloxacin release results of second and third phase of the release to the first order kinetic model.

5.3.2 Rifampicin

Although rifampicin is known to be very stable in solid form, in mildly alkaline aqueous solutions and in presence of atmospheric oxygen it oxidizes quite readily to rifampicin quinone. This can be seen as a change in the UV-spectrum of a rifampicin solution as well as a change in the color of the solution from reddish orange or yellow to purple. Rifampicin quinone has a partly similar UV-spectrum to rifampicin. The presence of rifampicin quinone interferes with spectrophotometric and also with microbiological techniques, because it also shows antibacterial activity (Bain et al. 1998).

In dissolution studies, ascorbic acid or sodium ascorbate have been used as antioxidants to prevent rifampicin oxidation. The release tests described in the literature have been lasting no more than 36 hours (Sreenivasa Rao 2001; Sreenivasa Rao et al. 2001). In our preliminary tests, we noticed that neither ascorbic acid nor sodium ascorbate can be used in tests lasting more than a few hours due to the decomposition of the antioxidants in conditions used for hydrolytic tests. In addition, a third antioxidant was tested (2-phospho-L-ascorbic acid trisodium salt) but it did not show any activity in preventing rifampicin oxidation.

Another approach that was tested was the utilization of an isosbestic point in the UV-spectrum of rifampicin and rifampicin quinone. Isosbestic point is a specific wavelength at which two (or more) chemical species have the same absorptivity. Several possible points of the UV-spectra of rifampicin were studied. In the literature, an isosbestic point at the wavelength of 330 nm has been reported for rifampicin and rifampicin quinone (Bain et al. 1999). We measured the UV/Vis spectra of rifampicin in Sörensen phosphate buffer solution kept at 37 °C in an incubator shaker at different time points. The results of the changing UV/Vis spectra are shown in Figure 22. There is an isosbestic point seen at the wavelength of 226 nm and it was used in our rifampicin content measurements. At the wavelength of 226 nm, the absorbance remains the same although the rest of the rifampicin spectrum is changed over time. There were also some other possible points, which were at 265 nm, 318 nm, 363 nm, 410 nm, and 517 nm, but the one at 226 nm proved to be the best. At this point we could calculate the rifampicin content of the solution despite that it has partly oxidized to rifampicin quinone. The fact that rifampicin quinone degrades further to other compounds affects the accuracy of this method. The accuracy is at its best if the measurements are made in short intervals, not letting the dissolution medium stay unchanged for long periods. If the measurements are made in two-three day intervals, the accuracy should be sufficient.

At later stages of the release test period, when the polymer degradation had advanced, a broad UV-peak in the beginning of the scanned area was induced. This broad peak, however, did not interfere significantly with the use of the isosbestic point at 226 nm.

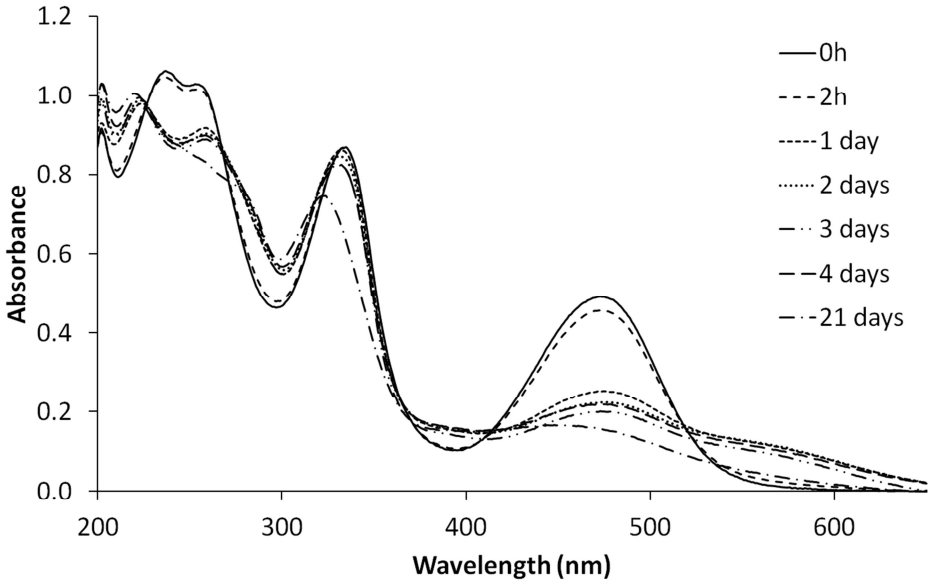

Figure 22. UV/Vis-absorption spectra for rifampicin in Sörensen phosphate buffer solution (pH 7.4) kept at 37 °C and measured at different time points.

The measured initial rifampicin contents were 6.5 wt% for PLCL+R, 7.9 wt% for PLCL+TCP50+R and 7.8 wt% for PLCL+TCP60+R. The low rifampicin content in the PLCL+R was apparently due to the extrusion process and that the antibiotic feeding was not at the desired level.

Cumulative release of rifampicin from the studied composites is presented in Figure 23. The release occurred in four phases, the burst in the beginning of the release being the first one. The inflection points in the release curves around 8 and 17 weeks separate the other three phases. The daily release of rifampicin is presented as Figure 24. In the daily release curves, the accelerations around the time points of 8 and 17 weeks can be seen well.

Rifampicin release was rather complex, due to the different phases in the release. Thus, the release phases had to be considered separately. The first phase was the burst, which lasted for two days. After that, the release rates of PLCL+TCP50+R and PLCL+TCP60+R decreased constantly until the time point of approximately 7 weeks. The release from the PLCL+R was very slow in this time period. During the second phase, the release from the composites fitted well to the square root of time kinetics with correlation factors of 0.99 for PLCL+TCP50+R and PLCL+TCP60+R. The slow release of PLCL+R fitted with R^2 of 0.97.

For comparison, the release results were also fitted to the to the power law kinetics equation (Equation 18) (Baker 1987; Ritger and Peppas 1987):

$$\frac{M_t}{M_\infty} = kt^n \qquad (18)$$

where M_t/M_∞ is the fractional drug release, k is the release rate constant, t is time and n the release exponent. The release exponent n has values of 0.45 for Fickian diffusion and cylindrical geometry (Baker 1987). For Case II diffusion (or anomalous), the n has values of $0.45<n<1$. During the second phase of the release, the rifampicin release from PLCL+TCP50+R and PLCL+TCP60+R had values for n of 0.53 and 0.44 respectively. The result suggests that the rifampicin release occurs by Case II diffusion from the PLCL+TCP50 and by Fickian diffusion from PLCL+TCP60+R during the second phase of the release (Baker 1987).

The third phase of the release started around the 8-week time point, where there is an inflection point seen in the cumulative release curves. In the third phase (between 8 and 17 week time points), the drug release was influenced by the increased permeability of the polymer caused by polymer degradation. Additionally, the polymer erosion started to play a role increasing the release rate. The third phase of the release of PLCL+TCP50+R obeyed again the $t^{1/2}$ kinetics very well (R^2=0.99). The release from PLCL+TCP60+R had at this point reached 60% of the total cumulative release, where the most models are not valid anymore (Lao et al. 2011).

A fourth phase in the release was observed in the release of PLCL+R and PLCL+TCP50+R but not in the PLCL+TCP60+R. The inflection points in the release curves were at the time point of 17 weeks. It coincided well with the increased mass loss from the composites, which was already notable at the time point of 17 weeks and can be seen in Figure 13. The M_w of the polymer had decreased to the level of 9000-14000 g/mol (Figure 11) at this point. From the PLCL+TCP60+R, the available drug for the release was apparently released already at this time point and thus no phase change was seen there.

The drug release decreased to almost negligible level after 35 weeks and at this point 70-85% of the total rifampicin loaded in the composites had been released. There was still some rifampicin left in the samples, which was revealed by the reddish brown color of the samples. However, no further drug release was observed. The tests were terminated at the time point of 56 weeks and the remaining rifampicin in the composites was measured the same way than the initial rifampicin contents in the beginning of the test series. The proportion of the initial rifampicin still in the samples after the termination of the test series was 10.7% for PLCL+R, 5.0% for PLCl+TCP50+R and 3.4% for PLCL+TCP60+R. When combined with the measured released rifampicin, the total rifampicin amount detected did not reach 100% for any of the composites. This was probably because rifampicin oxidized to rifampicin quinone that was further degraded to compounds with no UV-absorbance and explains why part of the rifampicin seems to have disappeared (Bain et al. 1998).

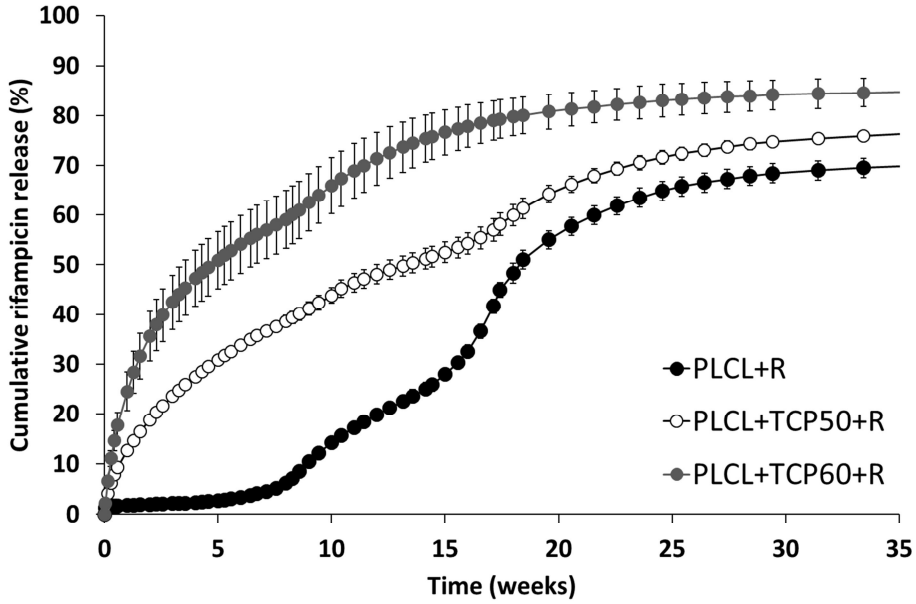

Figure 23. The cumulative release of rifampicin from composites of poly(L-lactide-co-ε-caprolactone) (PLCL) and β-tricalcium phosphate (TCP) with initial TCP contents of 0 wt-%, 50 wt-% and 60 wt-% and initial rifampicin (R) content of 8 wt-%. Results shown as averages with standard deviations (n = 5).

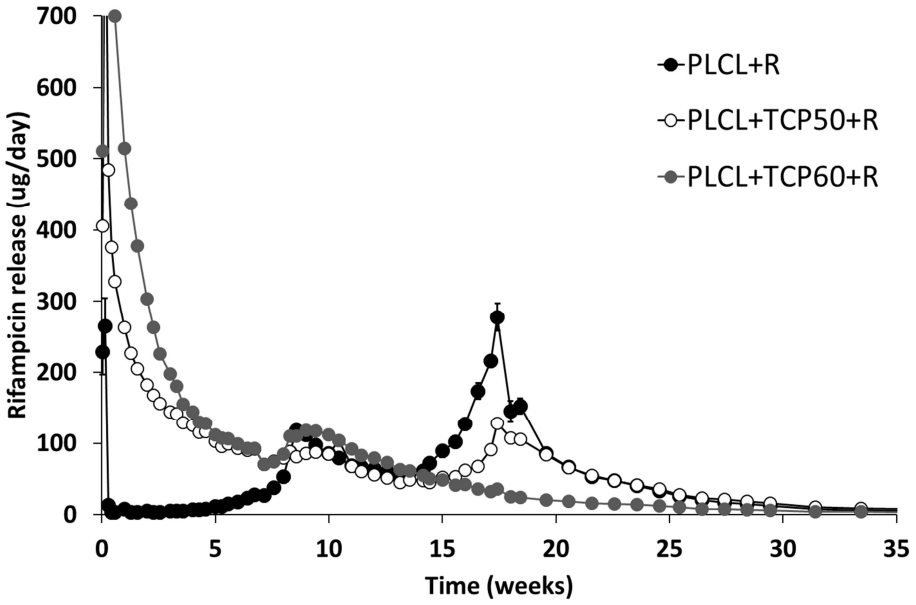

Figure 24. The daily release of rifampicin from composites of poly(L-lactide-co-ε-caprolactone) (PLCL) and β-tricalcium phosphate (TCP) with initial TCP contents of 0 wt-%, 50 wt-% and 60 wt-% and initial rifampicin (R) content of 8 wt-%. Results shown as averages with standard deviations (n = 5).

There was a statistically significant difference (Mann-Whitney U test, $P < 0.05$) in the cumulative rifampicin release results of the composites containing 50 wt-% and 60 wt-% of β-TCP throughout the test series (Figure 23). When similar analysis was done on the daily release of rifampicin (Figure 24) from the composites containing 50 wt-% and 60 wt-% β-TCP, there was a statistically significant difference between the composites excluding the time periods of 5-8 weeks, 13.5-15.5 weeks, from the time point of 44 weeks to the end and the single time point of 10.4 weeks (73 days).

5.4 Inhibition zone measurements

The effect of the antibiotic-releasing composites against the common osteomyelitis causing bacteria, *Staphylococcus epidermidis* and *Pseudomonas aeruginosa,* were tested using bioluminescence imaging. The composites selected for these experiments based on the most promising *in vitro* drug release results, with the most constant release rates, were the ones containing 50 wt-% of β-TCP for both antibiotics. The well plate incubated with bioluminescent *S. epidermidis* and PLCL+TCP50+C pellets is shown in Figure 25 and PLCL+TCP50+R pellets in Figure 26 after 14 hours of incubation. Similar results of bioluminescent *P. aeruginosa* and PLCL+TCP50+C and PLCL+TCP50+R are presented as Figure 27 and Figure 28 respectively after 14 hours of incubation. Additionally, Figure 29 shows how one such plate looks to the naked eye after 16-hour incubation. This illustrates the conventional over-night-grown method in the inhibition zone measurements.

Both of the studied bacteria, *S. epidermidis* and *P. aeruginosa* responded to the antibiotics released from the composite pellets. The formation of the inhibition zones could be seen as growing dark blue areas surrounding the antibiotic-releasing pellets already after four hours. The inhibition zones grew until 12 hours of incubation and after that the changes were detected in the light emission levels. The dark blue color indicated dead bacteria and the bright circles of red and yellow surrounding the inhibition zones indicated bacteria that were in contact with subinhibitory concentrations of the antibiotics. These zones were called stress zones. This refers to the phenomenon where the bacteria are in contact with subinhibitory concentrations of antibiotic and produce strong light emission that is presumably due to the nonspecific activation of central metabolic pathways. As the release of the antibiotics proceeded, the stress zones led the expanding inhibition zones. The green color in Figures 25-28 was considered to be unaffected bacteria because this was the usual color in the control wells. The development of the inhibition zones is illustrated with the Figures 1-4 in the publication IV, where the bioluminescence imaging results of 6-well plates cultured with *S. epidermidis* (Figure 1, IV) and *P. aeruginosa* (Figure 2, IV) exposed to PLCL+TCP50+C, and *S. epidermidis* (Figure 3, IV) and *P. aeruginosa* (Figure 4, IV) exposed to PLCL+TCP50+R are shown. The development of the inhibition zones are shown at 2-hour intervals.

The inhibition zones around the rifampicin-releasing pellets were formed faster than around the ciprofloxacin-releasing pellets, but overall their inhibition zones were smaller than those of the ciprofloxacin-releasing pellets. The initial burst observed in the *in vitro* release tests from the rifampicin-containing composite pellets (Figure 24) was observed to be larger than from the ciprofloxacin-containing pellets (Figure 20). This explains the faster initial formation of the inhibition zones around the rifampicin releasing pellets. Although ciprofloxacin-containing pellets showed a lower initial burst, the final areas of the inhibition zones after 14 hours of incubation were greater. This was probably due to ciprofloxacin molecule being smaller than the rifampicin molecule and thus the diffusion out from the pellet and in the agar may be faster than for rifampicin.

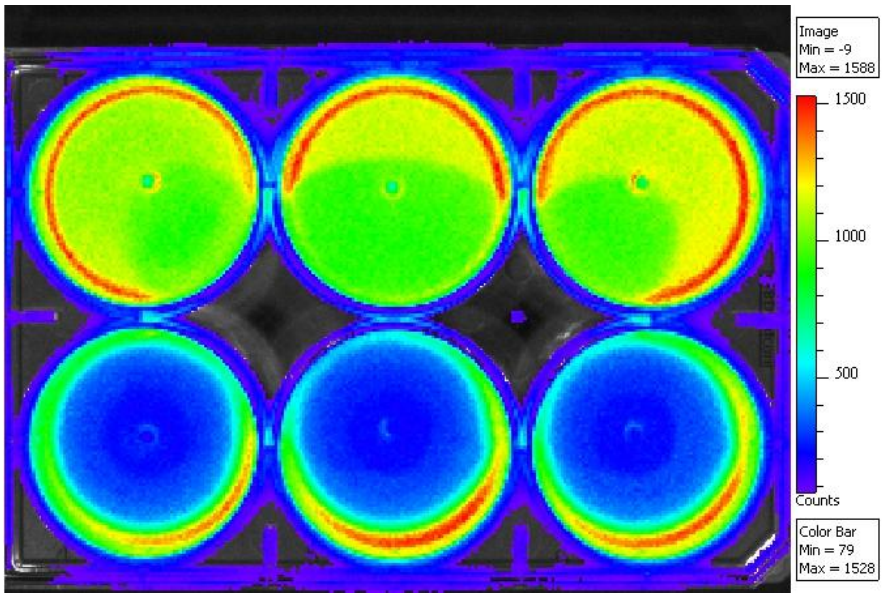

Figure 25. Bioluminescent S. epidermidis and ciprofloxacin containing pellets (PLCL+TCP50+C) on the lower row and controls without antibiotic on the top row after 14 hours of incubation. Dark blue color is interpreted as dead bacteria, green as unaffected bacteria, and red and yellow as bacteria in stress zones.

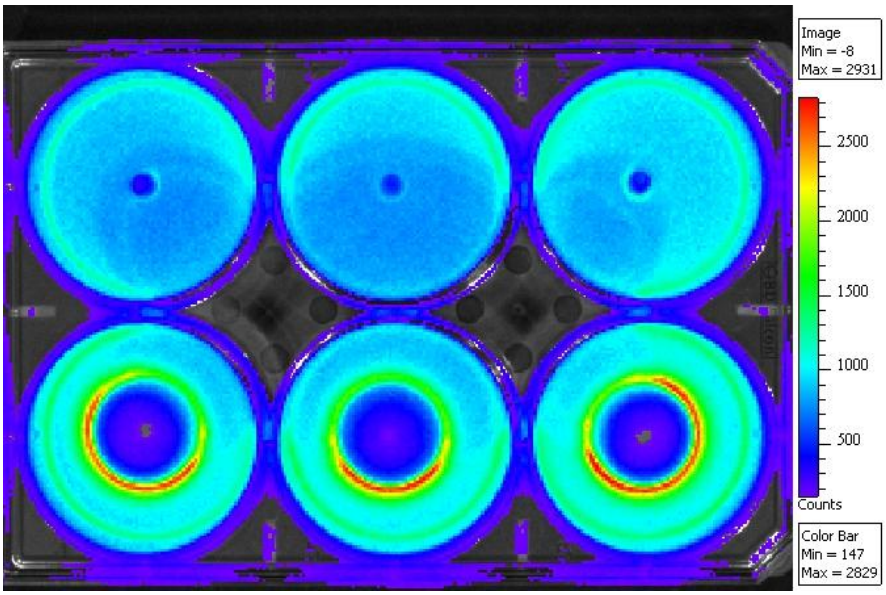

Figure 26. Bioluminescent S. epidermidis and rifampicin containing pellets (PLCL+TCP50+R) on the lower row and controls without antibiotic on the top row after 14 hours of incubation. Dark blue color is interpreted as dead bacteria, green as unaffected bacteria, and red and yellow as bacteria in stress zones.

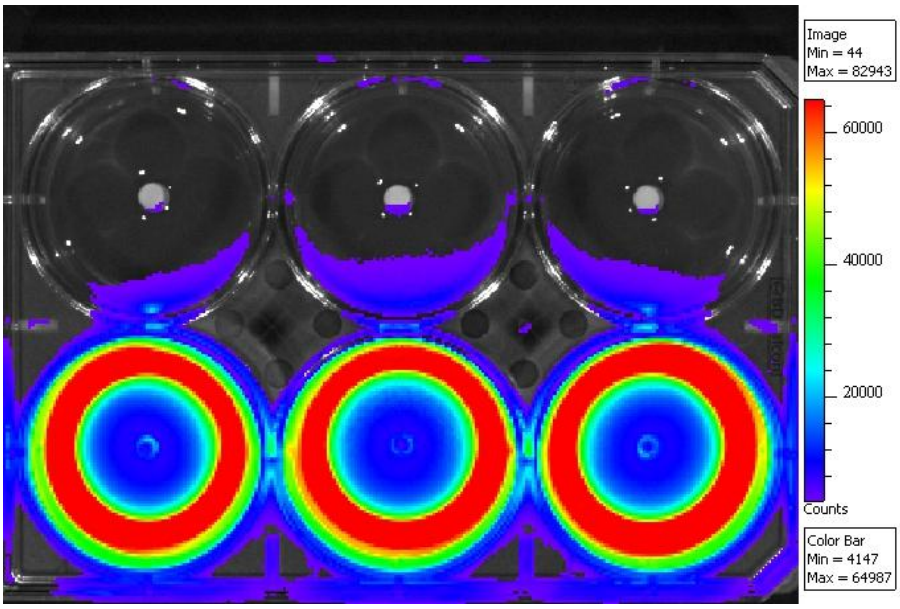

Figure 27. Bioluminescent P. aeruginosa and ciprofloxacin containing pellets (PLCL+TCP50+C) on the lower row and controls without antibiotic on the top row after 14 hours of incubation. Dark blue color is interpreted as dead bacteria, green as unaffected bacteria, and red and yellow as bacteria in stress zones.

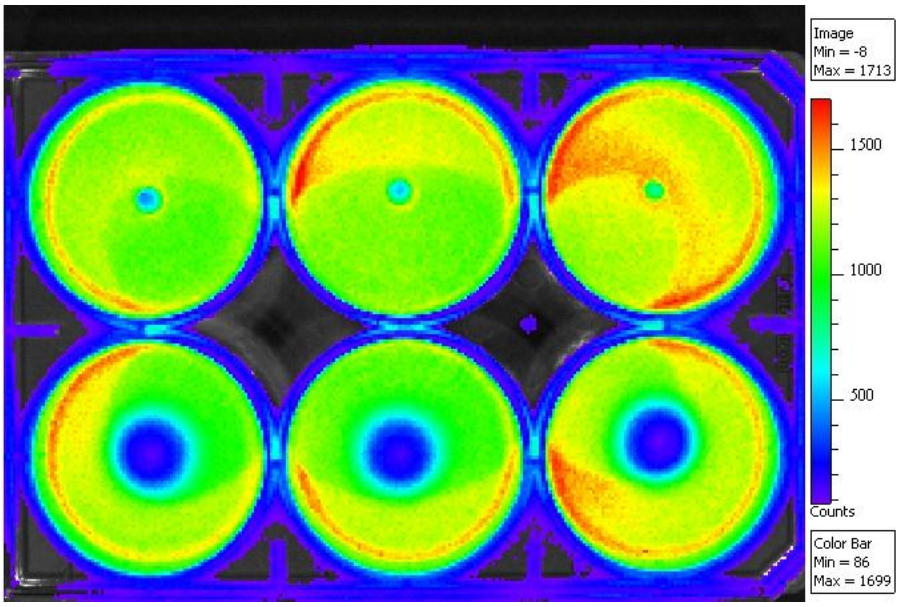

Figure 28. Bioluminescent P. aeruginosa and rifampicin containing pellets (PLCL+TCP50+R) on the lower row and controls without antibiotic on the top row after 14 hours of incubation. Dark blue color is interpreted as dead bacteria, green as unaffected bacteria, and red and yellow as bacteria in stress zones.

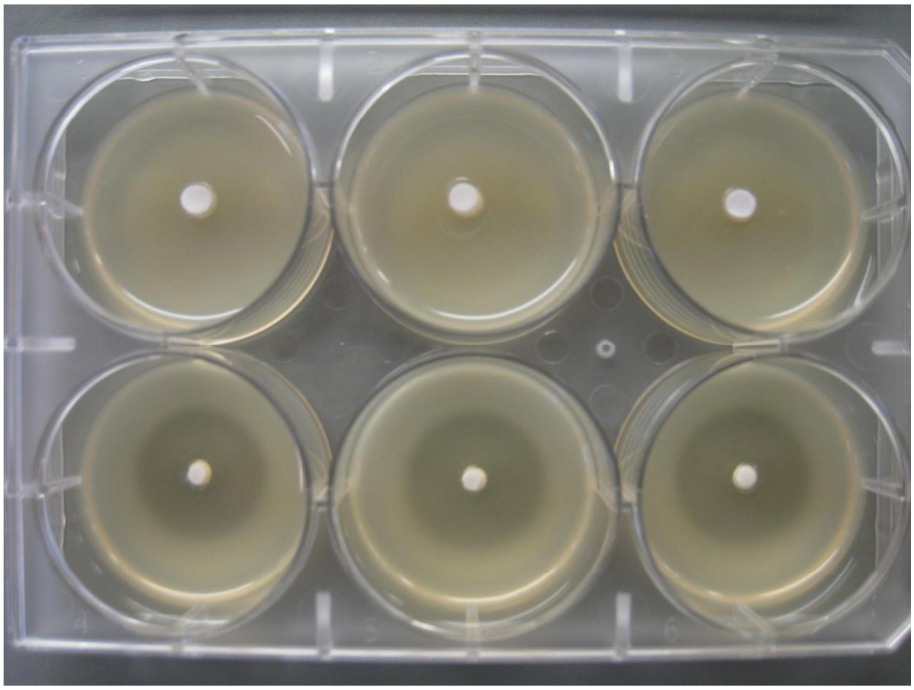

Figure 29. Inhibition zones as seen by naked eye after 16 hour incubation with S. epidermidis and ciprofloxacin containing pellets on the lower row. Controls without antibiotic are on the top row.

6 DISCUSSION

In the treatment of osteomyelitis, long-term antibiotic courses are required. With orally or intravenously administered antibiotics, a concentration adequate to eradicate bacteria in the infection site is often difficult to achieve. Due to the multitude of infection-causing bacteria, there have been suggestions in the literature that it would be advantageous if different drugs could be combined in a way that the decision of the drugs to be used could be made during surgery, just before implantation (Arruebo et al. 2010; Ginebra et al. 2006). The materials developed in this work answer this material need. The materials also provide a platform technology for the development of other drug-releasing materials and combinations of them. As a result of this work, we offer composite materials that are ready for preclinical testing and have potential to be used in the local treatment of osteomyelitis and other bone-related infections alone or together and, at the same time, act as osteoconductive bone filler materials. The surgeon, who is treating a patient with osteomyelitis or other bone-related infections can decide in which ratio to use the antibiotic-releasing materials because they are separate materials and can be mixed in the desired ratios.

The use of combination therapy of two different antibiotics has been justified with synergistic effects of two antibiotics against the causative bacteria. The synergistic effects are an accelerated bacterial count decline, a wider antibacterial spectrum with two antibiotics, and a reduction in the risk of resistant strain development to one of the antibiotics. (Coiffier et al. 2013)

The materials used in this work were commercially available FDA approved materials. The antibiotics, ciprofloxacin and rifampicin, were chosen based on the literature review and experts' opinions. The poly(L-lactide-co-caprolactone) copolymer was chosen based on the good drug-release properties found in preliminary tests. The ceramic component, β-TCP, is known to be osteoconductive and, along with hydroxy apatite, is the most well-known ceramic bone substitute (Neumann and Epple 2006). Due to the brittleness of ceramics, their use is sometimes limited and composites with polymers may improve their mechanical properties. In the following sections, different aspects of the composites materials developed in this work and their behavior *in vitro* are discussed.

6.1 Effect of processing and sterilization on the materials

The processing of degradable polymers by extrusion often causes a significant decrease in the M_w of the polymer (Södergård and Stolt 2002). This decrease is caused by the high temperature and shear forces in the extruder (Crowley et al. 2007; Repka et al. 2007). If moisture is present in the material, the decrease of M_w is ever higher (Li and

Vert 1999; Lim et al. 2008; Södergård and Stolt 2002). The degradation of the materials can be, however, prevented by adjusting the processing parameters and by carefully drying the polymer as well as preventing the moisture of the surrounding air from entering the extruder equipment during processing. In our study, all these measures were taken to prevent the excessive degradation of the polymer matrix of the composites during extrusion. Additionally, care was taken in feeding the polymer, antibiotics, and β-TCP into the extruder. Overall, as a production method, extrusion is fast, continuous, reproducible, and easy to scale up to an industrial scale (Crowley et al. 2007; Repka et al. 2007). The samples produced using extrusion are very homogenous and deviations between them are small (Crowley et al. 2007; Repka et al. 2007; Wilson et al. 2012). An additional advantage is the absence of solvents (Crowley et al. 2007; Repka et al. 2007). Due to the efficient mixing caused by the shear forces in the process, the dissolution rates of poorly soluble drugs can be enhanced because they can be molecularly dispersed in the polymer carrier during the process (Wilson et al. 2012).

In this work, the degradation of the polymer material during processing, seen as the decrease in M_w of the polymer, was very small in the composites without antibiotics. It may be even, that in some cases, the decrease seen could fall into the measurement inaccuracy of the size exclusion chromatography that was used to measure the molecular weights of the polymers. Higher degradation during processing was observed with composites containing the antibiotics (ciprofloxacin or rifampicin), and the composites containing ciprofloxacin degraded more than the composites containing rifampicin. In the antibiotic containing composites, more degradation was seen in the composites without β-TCP than in the ones with β-TCP. One would expect this to be other way round because β-TCP particles are expected to cause shear forces and friction in the polymer melt during extrusion which in turn cause scission of the polymer chains (Crowley et al. 2007; Repka et al. 2007).

Sterilization using gamma irradiation caused significant degradation of the polymer matrix. There was a linear dependency of decrease in the M_w and M_n of the polymer matrix in the composites. The higher the β-TCP content in the composite was, the more degradation gamma irradiation caused. The samples that were sent for gamma irradiation were not packed in nitrogen, and no other measures were taken to keep the samples totally dry. They were stored in desiccator, but during packing and shipping the composites with a higher β-TCP content were likely to absorb more moisture in the material. This would consequently cause more degradation to those composites with a higher moisture content.

Residual lactide monomer has been reported to affect the degradation of lactide-based polymers and accelerate the mass loss and loss of mechanical properties (Paakinaho et al. 2009). In this study, the residual L-lactide monomer content was seen not to change during processing and sterilization, and thus it can be assumed that the monomer content did not have an effect on the polymer degradation. Additionally, the measured

levels of ε-caprolactone monomers were below detection limit in all the samples, and therefore it suggests that ε-caprolactone monomer did not have an effect on the degradation.

6.2 Hydrolytic degradation of the materials

Lactide-based copolymers are known to be hydrolytically unstable and degrade in the presence of water. Water molecules attack the ester bonds in the polymer and thus break the polymer backbone to smaller fractions. This is normally seen as a decrease in the molecular weight of the polymer and it also has an effect on the other properties of the polymer including mechanical, thermal, and water absorption properties as well as the microstructure of the polymer (Fernández et al. 2012; Hiljanen-Vainio et al. 1996; Hiljanen-Vainio et al. 1997; Malin et al. 1996). Mechanical properties were not studied here, but the other properties with regard to the degradation process were investigated using several analytical methods.

The properties of copolymers of ε-caprolactone and lactides as well as the degradation behavior are strongly dependent on the molecular structure, meaning the comonomer ratio, the type of lactide used and how random the copolymer is, the flexibility of the polymer chain, the presence of polar groups, molecular mass, crystallinity, and orientation (Albertsson and Varma 2003; Fernández et al. 2012; Malin et al. 1996). In this study, the ^{1}H NMR analysis showed a clear change in the comonomer ratio (L-lactide / ε-caprolactone) of the copolymer, as hydrolytic degradation proceeded. This effect was accompanied by an increasing average sequence length of L-lactide. This was observed in all the composites and it was supported by the results of thermal analysis where an increase in the T_gs of the copolymer was seen as a function of time *in vitro*. It is well known that the T_gs of copolymers of L-lactide and ε-caprolactone are strongly dependent on the comonomer composition. The T_g increases dramatically even with small increments of the L-lactide content (Pitt 1990). The ^{1}H NMR results clearly showed that the copolymer PLCL was rather blocky. The randomness of the copolymers of lactides and ε-caprolactone is greatly affected by polymerization conditions and depends on the polymerization temperature and time (Albertsson and Varma 2003; Hiljanen-Vainio et al. 1996; Hiljanen-Vainio et al. 1997; Södergård and Stolt 2002). These comonomers tend to form blocks and it is rather challenging to produce a completely random copolymer structure using them (Fernández et al. 2012).

Changes in the comonomer ratio of copolymers of L-lactide and ε-caprolactone during hydrolytic degradation have been reported, for example, by In Jeong *et al.* (In Jeong et al. 2004) and Lemmouchi *et al.* (Lemmouchi et al. 1998). The results of In Jeong *et al.* are similar to ours with a copolymer initially having more L-lactide in the structure than ε-caprolactone. Lemmouchi *et al.* reported increasing ε-caprolactone fraction during hydrolytical degradation of a copolymer having initially more ε-caprolactone in the structure than L-lactide (74/26 ratio of CL/LA). The connection of these results lies in

the ability of the comonomers to crystallize. It has been reported that 14 units are required for L-lactide units to be able to form crystals (Sarasua et al. 1998). Additionally, Lemmouchi *et al.* postulated that in the copolymer of their study, it was the ε-caprolactone units that were able to form crystals (Lemmouchi et al. 1998). This leads to the interpretation that the comonomer with a larger initial fraction, and eventually also with longer sequence lengths, is able to crystallize in the copolymer and is degraded slower than the comonomer with lower initial fraction. Additionally, both In Jeong *et al.* and Lemmouchi *et al.* proposed that the degradation starts in the amorphous regions of the polymer, and this is accepted nowadays in practice in the biomaterial field (Södergård and Stolt 2002; Lemmouchi et al. 1998; In Jeong et al. 2004).

In conclusion, the ^{1}H NMR analysis showed that the PLCL copolymer was blocky having some random parts in the structure. The random parts were removed as the hydrolytic degradation proceeded and the blocky characteristic of the copolymer increased. The bonds between the L-lactide and ε-caprolactone comonomers were most susceptible to hydrolytic degradation in this studied PLCL copolymer.

The hydrolytic degradation of the polymer matrix, i.e. the decrease of the molecular weight, obeyed first order kinetics meaning that the degradation occurred by random scission in the polymer backbone (Lao et al. 2011; Li and Vert 1999). The β-TCP content did not have a notable effect on the degradation and nor did either of the studied antibiotics. There are factors that have been reported in the literature that may affect the degradation of these kinds of composites. Bernstein *et al.* have reported results of composites containing nanosized tricalcium phosphate and polycaprolactone with very high β-TCP contents (85 vol-% and 95 vol-%) (Bernstein et al. 2010). β-TCP was proposed to enhance the hydrolytic degradation of polycaprolactone due to the increased hydrophilicity. On the other hand, a buffering effect of the dissolution products of β-TCP against the acidic degradation products of the polymer has been proposed (Ara et al. 2002; Lin et al. 1999). The buffering effect would lead to slower degradation of the polymer component in the composite. These two factors, increased hydrophilicity and buffering, work in opposite ways and, if simultaneous, their overall effect on the degradation may be evened out.

Water absorption tells about the hydrophilicity of the material. During the *in vitro* degradation test series, changes in the water absorption and differences between the studied materials were observed. These can be explained with the different phases in the polymer degradation as well as the differences in the composition of the materials. Although rifampicin is considered lipophilic, there are groups in the molecule capable of hydrogen bonding and they may have an effect on water absorption. Ciprofloxacin is claimed to be more hydrophilic than rifampicin, which explains well the greater water absorption in the beginning of the test series. Additionally, the interphases between dispersed ciprofloxacin particles and the polymer may act as channels for water absorption. β-TCP is hydrophilic (Lei et al. 2007) and thus may accelerate the water

absorption of the composites. This was seen especially in the first 12 weeks of the test series. After 12 weeks, the water absorption behavior changed, and the composites with the highest polymer content showed the greatest water absorption. The polymer degradation had at this point reached a level where there were more hydrophilic end groups available in the polymer, which in turn increased the water absorption. Also, mass loss of the composites, due to the polymer erosion, started around the 12-week time point. Mass loss of hydrolytically unstable polyesters starts when the molecular chains have been cut to fractions that are small enough, i.e. monomers and oligomers, to be dissolved in the surrounding hydrolysis medium. M_ws of 5000 g/mol for poly-ε-caprolactone and 15000 g/mol for poly-DL-lactide have been reported to enable the start of mass loss (Sawhney and Hubbell 1990). In this study, mass loss started after 10 weeks *in vitro* and, at this point, the M_w of the polymer in the composites without antibiotics had decreased to 12000-15000 g/mol. For ciprofloxacin containing composites, the M_w values were in the range of 19000-22000 g/mol and for rifampicin containing composites 16000-23000 g/mol. During the very first weeks of the test series, some mass loss was observed, but it was mainly due to the drug release from the antibiotic-containing composites.

There was bimodality seen in the SEC curves of the degrading PLCL polymer starting from week 20 *in vitro*. Traditionally, bimodality seen in the SEC distribution curve has been explained by the autocatalytic effect in the inner parts of the polymer (Daculsi et al. 2011; Li et al. 1990; Li 1999; Sawhney and Hubbell 1990). In the composites studied here, this was unlikely because of the porous structure of the composites induced by the β-TCP granules in the structure. The porous structure enabled the short chain degradation products to escape from the inner parts on the samples and thus did not catalyze the degradation reaction further. It was seen in the ^{1}H NMR analysis that the PLCL polymer was rather blocky and the random parts degraded first. This structure was pronounced as the hydrolysis proceeded and might have caused an increase in a certain part of the SEC distribution curve as the blocky parts consisting mainly of L-lactide units remained in the copolymer and the number of the other parts in the copolymer decreased.

pH results fitted well with the mass loss results. At the same time with accelerated mass loss, there was a decrease seen in the pH values of the buffer solution acting as the hydrolysis medium. The medium was changed to keep the pH between 7.2-7.6. The decrease in the pH values was caused by the degradation of the PLCL copolymer, which had proceeded to the level that enabled mass loss of the polymer. The polymer was degraded down to oligomers and monomers that, in this case, were acidic and were released into the surrounding medium.

The results of the T_g measurements supported the results of the ^{1}H NMR analysis that showed a change in the comonomer ratio of the polymer during the *in vitro* test series. This change explained the increase in the T_g towards the end of the test series. The T_gs

of copolymers of lactides and ε-caprolactone are known to be strongly dependent on the comonomer ratio (Pitt 1990). Even very small increments in the lactide content have a noticeable effect on the T_g. Before the increase of the T_g, there was a decrease in the beginning of the degradation test series (0-10 weeks). This was apparently due to the degradation of the polymer by random chain scission that produced shorter polymer chains, as the molecular weight decreased. (Li and Vert 1999; Li et al. 1990)

There was an increase in the measured heats of fusion, i.e. crystallinity, of all the composites throughout the *in vitro* test series. All the composites showed steadily increasing crystallinity with the exeption of the composites of PLCL+TCP50+C and PLCL+TCP60+C. In these two composites, there was a dramatic increase followed by a decrease in the crystallinity, during the first weeks of the *in vitro* test series. This behavior can be attributed to the simultaneous presence of ciprofloxacin and β-TCP in the samples, as this was not observed for any other composites. The increase of crystallinity is normally due to both the degradation of the amorphous parts of the copolymer and to the increased mobility of the polymer chains, as they get shorter due to the degradation. These more mobile chains are able to rearrange themselves and form crystals.

The DSC analysis of the antibiotic containing composites, which were conducted in order to find out if the antibiotics were dissolved or partially dispersed in the polymer matrix, showed interesting results. The ciprofloxacin-containing composites showed clear melting peaks indicating at least partially dispersed ciprofloxacin in the polymer matrix. In the rifampicin-containing composites, no melting peak of rifampicin was observed indicating dissolved antibiotic in the polymer matrix and strong interactions between rifampicin and the copolymer.

In the ceramic content measurements, steadily increasing ceramic contents were observed for all the composites containing β-TCP. This was due to the very slow dissolution of β-TCP and polymer mass loss, as the polymer degraded. This kind of behavior may, however, be beneficial in the bone healing process. As the polymer component degrades and is lost from the composite, the ceramic component stays in the bone defect and can aid the bone healing, due to its bioactive properties.

Microstructure analysis done with scanning electron microscopy showed some porosity in the samples with β-TCP content over 20 wt-%. The addition of β-TCP particles induced porosity in the composites and some of the pores were seen to reach the size of 100-200 μm which has been reported to enhance bone ingrowth (Shore and Holmes 1993).

6.3 Drug release

The two studied antibiotics showed different drug release behavior from the composites. The difference was partially due to the difference in the size of the molecules of ciprofloxacin and rifampicin. Ciprofloxacin is a smaller molecule than rifampicin and is thus able to diffuse easier through the polymer matrix. On the other hand, a rifampicin molecule has many functional groups in the molecular structure and, based on the structure, is able to form hydrogen bonds (Agrawal et al. 2004; Freire et al. 2009; Henwood et al. 2000; Henwood et al. 2001) with the polymer, which in turn may lead to better solubility of the drug in the polymer (Coleman et al. 1991).

At the very beginning of the release tests, both antibiotics showed a 1-2 day burst release. This was the phase where the molecules located on or near the surface of the test specimens were released. Although the rifampicin molecule is larger than ciprofloxacin molecule, the burst of rifampicin was generally stronger than the burst of ciprofloxacin. The poor solubility of ciprofloxacin in water may inhibit the rapid release of ciprofloxacin molecules located on or near the surface of the test specimens. Also, the fact that rifampicin was at least partially dissolved in the polymer matrix and that it is easily dissolved in water may have enhanced the burst.

Initial burst in the drug release has often been claimed as an unwanted phenomenon (Zamoume et al. 2011; Kankilic et al. 2011). It may, however, be beneficial in the cases when the target is to destroy any remaining bacteria after the surgical debridement of infected tissue. If the burst is at least moderate, it may help to achieve the required antibiotic concentration in the tissue and eradicate bacteria or to prevent the attachment of bacteria to the operated bone or implant (Kundu et al. 2012; Luginbuehl et al. 2010; Mouriño and Boccaccini 2010; Zilberman and Elsner 2008). Especially in the case of orthopaedic implant-related infections, the prevention of bacteria adhesion on the surface of the implant during or right after the surgery is extremely important. After surgery, a six-hour “decisive period” has been identified in which the success of the implantation is determined. During this period, the implant is particularly vulnerable to bacterial adhesion. (Hetrick and Schoenfisch 2006; Zilberman and Elsner 2008) Several approaches, often very complex ones, e.g. manipulation of the drug loading in the matrix radially, have been studied in order to avoid the burst phenomenon in the beginning of the release as well as to achieve close to zero order (i.e. linear) drug release (Rothstein and Little 2011; Zamoume et al. 2011). These are often very complicated to produce and thus are not feasible for industrial production. Additionally, they often include the use of harmful organic solvents (Calhoun and Mader 1997; Jones et al. 2011), which can, as residues, be problematic if used *in vivo* (Puga et al. 2012). At least, proving that the solvent residues are totally absent can be a challenging task.

The presence of the inflection points in the cumulative release profiles of both of the antibiotics is characteristic for a release mechanism combining diffusion and erosion

mechanisms (Baker 1987). In this work, the release in the second phase, i.e. after the burst, was due to a combination of diffusion through the polymer matrix, which was in fact almost negligible, and through the pores introduced to the composites by the addition of β-TCP. This was quite evident when the cumulative release profiles of composites without the ceramic and with the ceramic were compared. Additionally, the polymer erosion was not notable in this time period. There was a significant difference in the release profiles of both ciprofloxacin and rifampicin between the composites with 50 wt-% and 60 wt-% of β-TCP, although the difference in the ceramic content was not that large. This was probably because of increased porosity caused by the increased ceramic content between 50 wt-% and 60 wt-% of β-TCP.

When the molecular weight of a polymer decreases, the diffusion properties of the polymer change considerably. As the number of shorter polymer chains in the polymer matrix increases, they are able to move more and permeability increases. Here, this observation was supported by the thermal properties results, where a decrease in T_g was measured in the beginning of the test series showing more flexible polymer chains, as degradation proceeded. On the other hand, crystallinity of the polymer increased during degradation and the amorphous regions, where the diffusion happens, were reduced.

There was a clear acceleration of the antibiotic release both in the ciprofloxacin and rifampicin composites (Figure 20 and Figure 24). This acceleration occurred at around 5 weeks for ciprofloxacin and at around 8 weeks for rifampicin. The three-week difference in the onset of the acceleration was probably due to the difference in the molecular size of the antibiotics, rifampicin being larger than ciprofloxacin. Thus, ciprofloxacin was able to diffuse easier through the polymer matrix and through the pores in the composite structure. The third phase of the release was governed by diffusion accelerated by polymer degradation and increasing permeability as well as polymer erosion, which started to play a role after 10 weeks.

In ciprofloxacin release, no further phase changes were observed after the change at the 5-week time point. In rifampicin release, there was a further phase change seen at the time point of 17 weeks, where the mass loss of the composites also accelerated. The fourth phase of the release was governed by the diffusion and mass loss.

During the time of *in vitro* tests, rifampicin release did not reach 100% cumulative release. The release decreased to a negligible level and part of the rifampicin still remained in the composites. In the literature, there is evidence about rifampicin being incorporated in the crystalline domains of poly-ε-caprolactone (Jones et al. 2011). This may also explain why part of the rifampicin antibiotic seemed to be trapped in the polymer matrix in the experiments carried out in this thesis. If the release test series would have been continued long enough to allow the crystalline domains of the polymer matrix to degrade, the rest of the rifampicin may also have been released.

When the released rifampicin and the amount of the rifampicin remaining in the composites were combined, the total amount of rifampicin did not reach 100% of the initial rifampicin. One reason for this was likely the instability of rifampicin in aqueous solutions and in the presence of atmospheric oxygen, which enables the rifampicin to be oxidized to rifampicin quinone and further to other products that do not have UV-absorbance. Because the release test series was long, part of the rifampicin had time to oxidize to other products even though the measurements were done at short intervals. Additionally, it has been reported that rifampicin degrades more in solutions with a low rifampicin concentration (Jindal et al. 1995). Unfortunately, this affects the accuracy of this method. However, the method can be used to estimate the rifampicin release and compare the composites with each other. This may not, however, be such a problem *in vivo*, because possible *in vivo* stabilization has been reported by Le Guellec *et al.* (Le Guellec et al. 1997). In their study, rifampicin stability was better in rifampicin-containing plasma samples taken from patients than in plasma samples where rifampicin was added in the laboratory. They suggest that rifampicin may be more stable *in vivo* than *in vitro*. This means that the stability problems encountered in laboratory conditions may not be an issue in implanted, rifampicin-delivering materials.

With a non-eroding system, the drug release would slowly decrease as time goes on because the release is often proportional to the drug concentration in the device and to the diffusion path of the drug to the surface. In the case of a bioabsorbable system, the increased permeability and polymer erosion accelerate the release (Baker 1987). In our approach, the decline in the drug release was counterbalanced with the increased permeability of the composite matrix to allow drug release to continue at nearly the same rate as in the beginning of the release. In the beginning of the release, there was a burst, but as already mentioned above, it was moderate and thus is not considered unwanted, but optionally beneficial.

6.4 Inhibition zone testing

Bioluminescence imaging (BLI) has been used widely in research e.g. for stem cell differentiation (De Boer et al. 2006; Vilalta et al. 2009), vascularization (Gafni et al. 2006; Zhang et al. 2004), apoptosis (De Boer et al. 2006), controlled release of genes (Peterson et al. 2009; Shin and Shea 2010), inflammation of tissue (Hanada and Yoshimura 2002), implant-related bacterial infections (Engelsman et al. 2009; Kadurugamuwa et al. 2003), and in osteomyelitis animal model (mouse) (Funao et al. 2012). It can also be used to test the effect of antibiotic-releasing materials against osteomyelitis-causing bacteria *in vitro*. The method, using whole bacteria cells as biosensors, offers several advantages: it is easy to use, it is non-invasive, and it has high throughput and low costs (Close et al. 2011; De Boer et al. 2006). In the case of inhibition zone testing, the method provides more information than the conventional method because information on the bacteria and their reactions can be followed in real

time when exposed to the antibiotics. In this study, the effect of the ciprofloxacin and rifampicin-releasing composites was tested against two different model bacteria strains that were genetically engineered to emit light. The antibiotic-releasing materials for the bioluminescence testing were chosen based on the antibiotic release results. The most promising composites were the ones with 50 wt-% of β-TCP for both of the antibiotics. Composites without antibiotics were used as controls in the bacterial cultures. The controls were noticed not to have any effect on the bacteria and shows that the PLCL copolymer and β-TCP do not have antibacterial effects. Both of the antibiotic-releasing composites had an effect on the bacteria and generally the ciprofloxacin-releasing materials produced larger inhibition zones than the rifampicin-releasing materials. Ciprofloxacin-releasing composites also showed a smaller initial burst in the release and a slower development of the inhibition zone in the beginning of the bacterial culture. These effects correspond well with the *in vitro* antibiotic release results. The first signs of antibiotic activity were seen after four hours of incubation. The inhibition zones and the stress zones, which were shown as bright yellow and orange areas around the inhibition zones, reached maximum during the first twelve hours of incubation. No significant changes were noticed after that. The fast response of the bacteria to the antibiotic was due to the burst, which is very typical for these kinds of drug-releasing materials, and is caused by the release of the antibiotic molecules at or near the surface of the composite pellets.

The results gained using bioluminescent bacteria show that the manufactured composite materials release the two antibiotics, ciprofloxacin and rifampicin, in levels high enough to eradicate common osteomyelitis-causing bacteria.

In this study, the antibiotic-releasing composites were studied separately. It would be, however, important to study their synergistic effect against osteomyelitis-causing bacteria because they are intended to be used together. Rifampicin should never be used alone because of the rapid development of resistant bacterial strains that can result (Bliziotis et al. 2007; Perlroth et al. 2008). Additionally, the simultaneous administration of two or more antibiotics that have synergistic action is often used (Chusri et al. 2009; Mesak and Davies 2009).

The method, using bioluminescent bacteria as sensors in inhibition zone testing, proved to be efficient in assessing the effects of antibiotics against the bacteria. It provides more information than that provided by conventional inhibition zone testing. We suggest that bioluminescent imaging can be used as an efficient tool in the product development phase of controlled antibiotic delivery materials preceding *in vivo* tests.

7 SUMMARY AND CONCLUSIONS

Numerous research groups around the world have addressed the problems of local drug delivery and the local antibiotic treatment of osteomyelitis. However, only a few applications have so far reached the commercial stage. Today, osteomyelitis remains a disease that is problematic and expensive to treat and, additionally, is painful for the patient. A search for the perfect treatment protocol is still going on.

In this study, promising composite materials for the treatment of osteomyelitis and other bone related infections were developed. The composites are bioabsorbable and release antibiotics to eradicate osteomyelitis-causing bacteria. Additionally, the composites include an osteoconductive component, β-tricalcium phosphate. The *in vitro* release behavior of both of the studied antibiotics, ciprofloxacin and rifampicin, from the composites containing 50 wt-% of β-tricalcium phosphate was found to be promising, despite that the behavior did not follow the ideal zero-order release. The release behavior of the two antibiotics was not identical. However, the release occurred in a comparable time scale and at a comparable rate. The release was continuous and ciprofloxacin was released in the time period of approximately 20 week; whereas the continuous rifampicin release lasted almost 25 weeks.

Both antibiotics retained their original molecular structure through the processing and sterilization steps. Polymer was affected by the gamma-irradiation used in the sterilization and the molar weights were decreased, substantially. By utilizing genetically engineered bioluminescent bacteria, the effect of the released antibiotics from the most promising composites against the osteomyelitis-causing bacteria was shown. Moreover, the method of using bioluminescent bacteria in the inhibition zone tests was proven to be an efficient method. The method also gave more information on the reactions of the bacteria than conventional inhibition zone testing.

β-TCP did not have a considerable effect on the hydrolytic degradation behavior of any of the composites and nor did the antibiotics. The hydrolytic degradation of the polymer component proceeded very similarly, following first order kinetics, in all the studied composites, with and without antibiotics.

The materials developed in this work offer great potential to be developed into material for the treatment of osteomyelitis and other bone related infections. The properties of the antibiotic-releasing composites show desirable drug release and degradation behavior and are also effective against osteomyelitis-causing bacteria. With these materials, osteomyelitis patients, who are going through surgical debridement of the infected tissue, could be treated in one stage instead of two stages, which is nowadays the standard method when non-biodegradable gentamycin releasing PMMA beads are used to eradicate the bacteria remaining in the tissue. Because every operation carries a

risk for the patient, reducing the number of surgical operations is beneficial. There is, however, need for the further development of these composite materials and *in vivo* studies to prove the efficacy of the materials also in a living organism.

8 REFERENCES

Achermann Y, Vogt M, Spormann C, Kolling C, Remschmidt C, Wüst J, Simmen B, Trampuz A. 2011. Characteristics and outcome of 27 elbow periprosthetic joint infections: Results from a 14-year cohort study of 358 elbow prostheses. Clin Microbiol Infect 17(3):432-8.

Acocella G. 1978. Clinical pharmacokinetics of rifampicin. Clin Pharmacokinet 3(2):108-27.

Agrawal S, Ashokraj Y, Bharatam PV, Pillai O, Panchagnula R. 2004. Solid-state characterization of rifampicin samples and its biopharmaceutic relevance. Eur J Pharm Sci 22(2-3):127-44.

Ahola N, Rich J, Karjalainen T, Seppala J. 2003. Release of ibuprofen from poly(epsilon-caprolactone-co-D,L-lactide) and simulation of the release. J Appl Polym Sci 88:1279-88.

Albertsson A-C and Varma IK. 2003. Recent developments in ring opening polymerization of lactones for biomedical applications. Biomacromolecules 4(6):1466-86.

Alvarez H, Castro C, Moujir L, Perera A, Delgado A, Soriano I, Évora C, Sánchez E. 2008. Efficacy of ciprofloxacin implants in treating experimental osteomyelitis. J Biomed Mater Res Part B Appl Biomater 85(1):93-104.

Anagnostakos K and Schröder K. 2012. Antibiotic-impregnated bone grafts in orthopaedic and trauma surgery: A systematic review of the literature. Int J Biomater (2012) 538061.

Ara M, Watanabe M, Imai Y. 2002. Effect of blending calcium compounds on hydrolytic degradation of poly(DL-lactic acid-co-glycolic acid). Biomaterials 23(12):2479-83.

Arcieri GM, Becker N, Esposito B, Griffith E, Heyd A, Neumann C, O'Brien B, Schacht P. 1989. Safety of intravenous ciprofloxacin. A review. Am J Med 87(5A):92S-97S.

Arruebo M, Vilaboa N, Santamaria J. 2010. Drug delivery from internally implanted biomedical devices used in traumatology and in orthopedic surgery. Expert Opin Drug Deliv 7(5):589-603.

Bain DF, Munday DL, Smith A. 1999. Modulation of rifampicin release from spray-dried microspheres using combinations of poly-(DL-lactide). J Microencapsulation 16(3):369-85.

Bain DF, Munday DL, Cox PJ. 1998. Evaluation of biodegradable rifampicin-bearing microsphere formulations using a stability-indicating high-performance liquid chromatographic assay. Eur J Pharm Sci 7(1):57-65.

Baker R. 1987. Controlled release of biologically active agents. New York: John Wiley & Sons. 279 p.

Ball P. 1989. Adverse reactions and interactions of fluoroquinolones. Clin Invest Med 12(1):28-34.

Balmayor ER, Baran ET, Azevedo HS, Reis RL. 2012. Injectable biodegradable starch/chitosan delivery system for the sustained release of gentamicin to treat bone infections. Carbohydr Polym 87(1):32-9.

Baro M, Sánchez E, Delgado A, Perera A, Évora C. 2002. In vitro-in vivo characterization of gentamicin bone implants. J Control Release 83(3):353-64.

Bauer S, Bouldouyre M-, Oufella A, Palmari P, Bakir R, Fabreguettes A, Gros H. 2012. Impact of a multidisciplinary staff meeting on the quality of antibiotherapy prescription for bone and joint infections in orthopedic surgery. Med Mal Infect 42(12):603-7.

Bernstein M, Gotman I, Makarov C, Phadke A, Radin S, Ducheyne P, Gutmanas EY. 2010. Low temperature fabrication of β-TCP-PCL nanocomposites for bone implants. Adv Eng Mater 12(8): B341-B347.

Bertino Jr. J and Fish D. 2000. The safety profile of the fluoroquinolones. Clin Ther 22(7):798-817.

Bliziotis IA, Ntziora F, Lawrence KR, Falagas ME. 2007. Rifampin as adjuvant treatment of gram-positive bacterial infections: A systematic review of comparative clinical trials. Eur J Clin Microbiol Infect Dis 26(12):849-56.

Bohner M, Gbureck U, Barralet JE. 2005. Technological issues for the development of more efficient calcium phosphate bone cements: A critical assessment. Biomaterials 26(33):6423-9.

Bohner M, Lemaître J, Van Landuyt P, Zambelli P, Merkle HP, Gander B. 1997. Gentamicin-loaded hydraulic calcium phosphate bone cement as antibiotic delivery system. J Pharm Sci 86(5):565-72.

Bose S and Tarafder S. 2012. Calcium phosphate ceramic systems in growth factor and drug delivery for bone tissue engineering: A review. Acta Biomater 8(4):1401-21.

Bourne RB. 2004. Prophylactic use of antibiotic bone cement: An emerging standard - in the affirmative. J Arthroplasty 19(4 Suppl. 1):69-72.

Breda SA, Jimenez-Kairuz AF, Manzo RH, Olivera ME. 2009. Solubility behavior and biopharmaceutical classification of novel high-solubility ciprofloxacin and norfloxacin pharmaceutical derivatives. Int J Pharm 371(1-2):106-13.

Buchholz HW and Engelbrecht H. 1970. Depot effects of various antibiotics mixed with palacos resins. Chirurg 41(11):511-5.

Calhoun JH and Mader JT. 1997. Treatment of osteomyelitis with a biodegradable antibiotic implant. Clin Orthop Relat Res (341):206-14.

Cao H, Chen L-, Liu Y-, Xiu H, Wang H. 2012. Poly-D, L-lactide and levofloxacin-blended beads: A sustained local releasing system to treat osteomyelitis. J Appl Polym Sci 124(5):3678-84.

Castro C, Évora C, Baro M, Soriano I, Sánchez E. 2005. Two-month ciprofloxacin implants for multibacterial bone infections. Eur J Pharm Biopharm 60(3):401-6.

Castro C, Sánchez E, Delgado A, Soriano I, Núñez P, Baro M, Perera A, Évora C. 2003. Ciprofloxacin implants for bone infection. in vitro-in vivo characterization. J Control Release 93(3):341-54.

Cellai L, Cerrini S, Segre A, Brufani M, Fedeli W, Vaciago A. 1982. Comparative study of the conformations of rifamycins in solution and in the solid state by proton nuclear magnetic resonance and X-rays. J Org Chem 47(13):2652-61.

Chang Y, Chen W, Hsieh P, Chen DW, Lee MS, Shih H, Ueng SWN. 2011. In vitro activities of daptomycin-, vancomycin-, and teicoplanin-loaded polymethylmethacrylate against methicillin-susceptible, methicillin-resistant, and vancomycin-intermediate strains of staphylococcus aureus. Antimicrob Agents Chemother 55(12):5480-4.

Charlier A, Leclerc B, Couarraze G. 2000. Release of mifepristone from biodegradable matrices: Experimental and theoretical evaluations. Int J Pharm 200(1):115-20.

Chen W-, Lin J-C, Ju C-. 2003. Transmission electron microscopic study on setting mechanism of tetracalcium phosphate/dicalcium phosphate anhydrous-based calcium phosphate cement. J Biomed Mater Res Part A 64(4):664-71.

Chihara S and Segreti J. 2010. Osteomyelitis. Dis Mon 56(1):6-31.

Chin NX and Neu HC. 1984. Ciprofloxacin, a quinolone carboxylic acid compound active against aerobic and anaerobic bacteria. Antimicrob Agents Chemother 25(3):319-26.

Chiu Li L, Deng J, Stephens D. 2002. Polyanhydride implant for antibiotic delivery - from the bench to the clinic. Adv Drug Deliv Rev 54(7):963-86.

Chusri S, Villanueva I, Voravuthikunchai SP, Davies J. 2009. Enhancing antibiotic activity: A strategy to control acinetobacter infections. J Antimicrob Chemother 64(6):1203-11.

Cierny 3rd. G, Mader JT, Penninck JJ. 2003. A clinical staging system for adult osteomyelitis. Clin Orthop (414):7-24.

Close DM, Xu T, Sayler GS, Ripp S. 2011. In vivo bioluminescent imaging (BLI): Noninvasive visualization and interrogation of biological processes in living animals. Sensors 11(1):180-206.

Coiffier G, Albert J-, Arvieux C, Guggenbuhl P. 2013. Optimizing combination rifampin therapy for staphylococcal osteoarticular infections. Jt Bone Spine 80(1):11-7.

Coleman MM, Graf JF, Painter PC. 1991. Specific interactions and the miscibility of polymer blends. Technomic Publishing Company.

Cottam E, Hukins DWL, Lee K, Hewitt C, Jenkins MJ. 2009. Effect of sterilisation by gamma irradiation on the ability of polycaprolactone (PCL) to act as a scaffold material. Med Eng Phys 31(2):221-6.

Crank J. 1975. The mathematics of diffusion. 2nd edition ed. Oxford: Clarendon Press.

Crowley MM, Zhang F, Repka MA, Thumma S, Upadhye SB, Battu SK, McGinity JW, Martin C. 2007. Pharmaceutical applications of hot-melt extrusion: Part I. Drug Dev Ind Pharm 33(9):909-26.

Cussler EL. 2008. Diffusion: Mass transfer in fluid systems. 3rd edition ed. Cambridge: Cambridge University Press.

Daculsi G, Goyenvalle E, Cognet R, Aguado E, Suokas EO. 2011. Osteoconductive properties of poly(96L/4D-lactide)/beta-tricalcium phosphate in long term animal model. Biomaterials 32(12):3166-77.

Darouiche RO. 2001. Device-associated infections: A macroproblem that starts with microadherence. Clin Infect Dis 33(9):1567-72.

Dash TK and Konkimalla VB. 2012. Polymeric modification and its implication in drug delivery: Poly-ε-caprolactone (PCL) as a model polymer. Mol Pharm 9(9):2365-79.

De Boer J, Van Blitterswijk C, Löwik C. 2006. Bioluminescent imaging: Emerging technology for non-invasive imaging of bone tissue engineering. Biomaterials 27(9):1851-8.

Domingues ZR, Cortés ME, Gomes TA, Diniz HF, Freitas CS, Gomes JB, Faria AMC, Sinisterra RD. 2004. Bioactive glass as a drug delivery system of tetracycline and tetracycline associated with β-cyclodextrin. Biomaterials 25(2):327-33.

Dorofeev VL, Arzamastsev AP, Veselova OM. 2004. Melting point determination for the analysis of drugs of the fluoroquinolone group. Pharm Chem J 38(6):333-5.

Drancourt M, Stein A, Argenson JN, Zannier A, Curvale G, Raoult D. 1993. Oral rifampin plus ofloxacin for treatment of staphylococcus-infected orthopedic implants. Antimicrob Agents Chemother 37(6):1214-8.

Duvvuri S, Gaurav Janoria K, Mitra AK. 2006. Effect of polymer blending on the release of ganciclovir from PLGA microspheres. Pharm Res 23(1):215-23.

Efstathopoulos N, Giamarellos-Bourboulis E, Kanellakopoulou K, Lazarettos I, Giannoudis P, Frangia K, Magnissalis E, Papadaki M, Nikolaou VS. 2008. Treatment of experimental osteomyelitis by methicillin resistant staphylococcus aureus with bone cement system releasing grepafloxacin. Injury 39(12):1384-90.

Engelsman AF, Van Der Mei HC, Francis KP, Busscher HJ, Ploeg RJ, Van Dam GM. 2009. Real time noninvasive monitoring of contaminating bacteria in a soft tissue implant infection model. J Biomed Mater Res Part B Appl Biomater 88(1):123-9.

Esposito S and Leone S. 2008. Prosthetic joint infections: Microbiology, diagnosis, management and prevention. Int J Antimicrob Agents 32(4):287-93.

Fang T, Wen J, Zhou J, Shao Z, Dong J. 2012. Poly (ε-caprolactone) coating delays vancomycin delivery from porous chitosan/β-tricalcium phosphate composites. J Biomed Mater Res Part B Appl Biomater 100 B(7):1803-11.

Fernández J, Etxeberria A, Sarasua J-. 2012. Synthesis, structure and properties of poly(L-lactide-co-ε-caprolactone) statistical copolymers. J Mech Behav Biomed Mater 9:100-12.

Fong IW, Ledbetter WH, Vandenbroucke AC, Simbul M, Rahm V. 1986. Ciprofloxacin concentrations in bone and muscle after oral dosing. Antimicrob Agents Chemother 29(3):405-8.

Frank A, Rath SK, Venkatraman SS. 2005. Controlled release from bioerodible polymers: Effect of drug type and polymer composition. J Control Release 102(2):333-44.

Freire FD, Aragão CFS, De Lima E Moura TFA, Raffin FN. 2009. Thermal studies of isoniazid and mixtures with rifampicin. J Therm Anal Calor 97(1):333-6.

Funao H, Ishii K, Nagai S, Sasaki A, Hoshikawa T, Aizawa M, Okada Y, Chiba K, Koyasu S, Toyama Y, and others. 2012. Establishment of a real-time, quantitative, and reproducible mouse model of staphylococcus osteomyelitis using bioluminescence imaging. Infect Immun 80(2):733-41.

Gafni Y, Zilberman Y, Ophir Z, Abramovitch R, Jaffe M, Gazit Z, Domb Jr. A, Gazit D. 2006. Design of a filamentous polymeric scaffold for in vivo guided angiogenesis. Tissue Eng 12(11):3021-34.

Garvin KL, Miyano JA, Robinson D, Giger D, Novak J, Radio S. 1994. Polylactide/polyglycolide antibiotic implants in the treatment of osteomyelitis. A canine model. Journal of Bone and Joint Surgery - Series A 76(10):1500-6.

Gautier H, Plumecocq A, Amador G, Weiss P, Merle C, Bouler J-. 2012. In vitro characterization of calcium phosphate biomaterial loaded with linezolid for osseous bone defect implantation. J Biomater Appl 26(7):811-28.

Ger E, Dall D, Miles T, Forder A. 1977. Bone cement and antibiotics. S Afr Med J 51(9):276-9.

Ginebra MP, Traykova T, Planell JA. 2006. Calcium phosphate cements as bone drug delivery systems: A review. J Control Release 113(2):102-10.

Ginebra M, Canal C, Espanol M, Pastorino D, Montufar EB. 2012. Calcium phosphate cements as drug delivery materials. Adv Drug Deliv Rev 64(12):1090-110.

Guillaume M, Garraffo R, Bensalem M, Janssen C, Bland S, Gaillat J, Bru J-. 2012. Pharmacokinetic and dynamic study of levofloxacin and rifampicin in bone and joint infections. Med Mal Infect 42(9):414-20.

Gursel I, Yagmurlu F, Korkusuz F, Hasirci V. 2002. In vitro antibiotic release from poly(3-hydroxybutyrate-co-3-hydroxyvalerate) rods. J Microencapsulation 19(2):153-64.

Gürsel I, Korkusuz F, Türesin F, Gürdal Alaeddinoğlu N, Hasirci V. 2001. In vivo application of biodegradable controlled antibiotic release systems for the treatment of implant-related osteomyelitis. Biomaterials 22(1):73-80.

Habraken WJEM, Wolke JGC, Jansen JA. 2007. Ceramic composites as matrices and scaffolds for drug delivery in tissue engineering. Adv Drug Deliv Rev 59(4-5):234-48.

Haidar R, Boghossian AD, Atiyeh B. 2010. Duration of post-surgical antibiotics in chronic osteomyelitis: Empiric or evidence-based? Int J Infect Dis 14(9):e752-e758.

Hamanishi C, Kitamoto K, Tanaka S, Otsuka M, Doi Y, Kitahashi T. 1996. A self-setting TTCP-DCPD apatite cement for release of vancomycin. J Biomed Mater Res 33(3):139-43.

Hanada T and Yoshimura A. 2002. Regulation of cytokine signaling and inflammation. Cytokine Growth Factor Rev 13(4-5):413-21.

Hanssen AD. 2005. Local antibiotic delivery vehicles in the treatment of musculoskeletal infection. Clin Orthop Relat Res (437):91-6.

Harris LG and Richards RG. 2006. Staphylococci and implant surfaces: A review. Injury 37(2 Suppl):S3-S14.

Heller J. 1996. Drug delivery systems. Ratner BD, Hoffman AS, Schoen FJ, and others, editors. In: Biomaterials science: An introduction to materials in medicine. San Diego: Academic Press. 346 p.

Hench LL. 2006. The story of bioglass®. J Mater Sci Mater Med 17(11):967-78.

Hench LL. 1973. Ceramics, glasses, and composites in medicine. Med Instrum 7(2):136-44.

Hench LL and Polak JM. 2002. Third-generation biomedical materials. Science 295(5557):1014+1016-1017.

Hench LL and Paschall HA. 1973. Direct chemical bond of bioactive glass ceramic materials to bone and muscle. J Biomed Mater Res 7(3):25-42.

Henwood S, de Villiers M, Liebenberg W, Lotter A. 2000. Solubility and dissolution properties of generic rifampicin raw materials. Drug Dev Ind Pharm 26:403-8.

Henwood S, Liebenberg W, Tiedt L, Lotter A, de Villiers M. 2001. Characterization of the solubility and dissolution properties of several new rifampicin polymorphs, solvates, and hydrates. Drug Dev Ind Pharm 27(1):1017-30.

Herbert IR. 1993. Statistical analysis of copolymer sequence distribution. Ibbet RN, editor. In: NMR spectroscopy of polymers. London: Blackie Academic & Professional. 50 p.

Herbold BA, Brendler-Schwaab SY, Ahr HJ. 2001. Ciprofloxacin: In vivo genotoxicity studies. Mutat Res Genet Toxicol Environ Mutagen 498(1-2):193-205.

Hetrick EM and Schoenfisch MH. 2006. Reducing implant-related infections: Active release strategies. Chem Soc Rev 35(9):780-9.

Higuchi T. 1963. Mechanism of sustained-action medication. theoretical analysis of rate. J Pharm Sci 52:1145-9.

Hiljanen-Vainio M, Karjalainen T, Seppälä J. 1996. Biodegradable lactone copolymers. I. characterization and mechanical behavior of ε-caprolactone and lactide copolymers. J Appl Polym Sci 59(8):1281-8.

Hiljanen-Vainio MP, Orava PA, Seppala JV. 1997. Properties of ε-caprolactone/DL-lactide (ε-CL/DL-LA) copolymers with a minor ε-CL content. J Biomed Mater Res 34(1):39-46.

Holtom PD, Pavkovic SA, Bravos PD, Patzakis MJ, Shepherd LE, Frenkel B. 2000. Inhibitory effects of the quinolone antibiotics trovafloxacin, ciprofloxacin, and levofloxacin on osteoblastic cells in vitro. Journal of Orthopaedic Research 18:721-727.

Huh AJ and Kwon YJ. 2011. "Nanoantibiotics": A new paradigm for treating infectious diseases using nanomaterials in the antibiotics resistant era. J Control Release 156(2):128-45.

Hurrell S and Cameron RE. 2002. The effect of initial polymer morphology on the degradation and drug release from polyglycolide. Biomaterials 23(11):2401-9.

In Jeong S, Kim B-, Lee YM, Ihn KJ, Kim SH, Kim YH. 2004. Morphology of elastic poly(L-lactide-co-ε-caprolactone) copolymers and in vitro and in vivo degradation behavior of their scaffolds. Biomacromolecules 5(4):1303-9.

Ipsen T, Jorgensen PS, Damholt V, Torholm C. 1991. Gentamicin-collagen sponge for local applications: 10 cases of chronic osteomyelitis followed for 1 year. Acta Orthop Scand 62(6):592-4.

Ismail AF, Abdalmonemdoolaanea, Awang M, Mohamed F. 2012. High initial burst release of gentamicin formulated as PLGA microspheres implant for treating orthopaedic infection. Int J Pharmcy Pharm Sci 4(Suppl. 4):685-91.

ISO 15814. Implants for surgery – copolymers and blends based in polylactide – *in vitro* degradation testing.

Jackson J, Leung F, Duncan C, Mugabe C, Burt H. 2011. The use of bone cement for the localized, controlled release of the antibiotics vancomycin, linezolid, or fusidic acid: Effect of additives on drug release rates and mechanical strength. Drug Deliv Transl Res 1(2):121-31.

Jain A, Gupta Y, Agrawal R, Khare P, Jain SK. 2007. Biofilms - A microbial life perspective: A critical review. Crit Rev Ther Drug Carrier Syst 24(5):393-443.

Jain JP, Modi S, Domb AJ, Kumar N. 2005. Role of polyanhydrides as localized drug carriers. J Control Release 103(3):541-63.

Jia W, Zhang X, Luo S, Liu X, Huang W, Rahaman MN, Day DE, Zhang C, Xie Z, Wang J. 2010. Novel borate glass/chitosan composite as a delivery vehicle for teicoplanin in the treatment of chronic osteomyelitis. Acta Biomater 6(3):812-9.

Jiang J, Li Y, Fang T, Zhou J, Li X, Wang Y, Dong J. 2012. Vancomycin-loaded nano-hydroxyapatite pellets to treat MRSA-induced chronic osteomyelitis with bone defect in rabbits. Inflamm Res 61(3):207-15.

Jindal KC, Chaudhary RS, Singla AK, Gangwal SS, Khanna S. 1995. Effects of buffers and pH on rifampicin stability. Pharm Ind 57(5):420-2.

Jones DS, McCoy CP, Andrews GP. 2011. Physicochemical and drug diffusion analysis of rifampicin containing polyethylene glycol-poly(ε-caprolactone) networks designed for medical device applications. Chem Eng J 172(2-3):1088-95.

Jones JR. 2013. Review of bioactive glass: From Hench to hybrids. Acta Biomater 9(1):4457-86.

Jones ME, Karlowsky JA, Draghi DC, Thornsberry C, Sahm DF, Nathwani D. 2004. Antibiotic susceptibility of bacteria most commonly isolated from bone related infections: The role of cephalosporins in antimicrobial therapy. Int J Antimicrob Agents 23(3):240-6.

Kadurugamuwa JL, Sin L, Albert E, Yu J, Francis K, DeBoer M, Rubin M, Bellinger-Kawahara C, Parr Jr. TR, Contag PR. 2003. Direct continuous method for monitoring biofilm infection in a mouse model. Infect Immun 71(2):882-90.

Kankilic B, Bayramli E, Kilic E, Dağdeviren S, Korkusuz F. 2011. Vancomycin containing PLLA/β-TCP controls MRSA in vitro. Clin Orthop Relat Res 469(11):3222-8.

Kaunisto E, Tajarobi F, Abrahmsen-Alami S, Larsson A, Nilsson B, Axelsson A. 2013. Mechanistic modelling of drug release from a polymer matrix using magnetic resonance microimaging. Eur J Pharm Sci 48(4-5):698-708.

Kettunen K, editor. 2004. Pharmaca fennica 2004. Helsinki: Lääketietokeskus Oy.

Khanlari B, Elzi L, Estermann L, Weisser M, Brett W, Grapow M, Battegay M, Widmer AF, Flückiger U. 2010. A rifampicin-containing antibiotic treatment improves outcome of staphylococcal deep sternal wound infections. J Antimicrob Chemother 65(8):1799-806.

Kiedrowski MR and Horswill AR. 2011. New approaches for treating staphylococcal biofilm infections. Ann New York Acad Sci 1241(1):104-21.

Kim H and Fassihi R. 1997. Application of binary polymer system in drug release rate modulation. 2. influence of formulation variables and hydrodynamic conditions on release kinetics. J Pharm Sci 86(3):323-8.

Kim Y, Park MR, Kim MS, Kwon OH. 2012. Polyphenol-loaded polycaprolactone nanofibers for effective growth inhibition of human cancer cells. Mater Chem Phys 133(2-3):674-80.

Kluin OS, van der Mei HC, Busscher HJ, Neut D. 2009. A surface-eroding antibiotic delivery system based on poly(trimethylene carbonate). Biomaterials 30(27):4738-42.

Knaepler H. 2012. Local application of gentamicin-collagen implant in the prophylaxis and treatment of surgical site infection in orthopaedic surgery: A review of clinical experience. Int J Surg 10(Suppl.1):S15-S20.

Kolk A, Handschel J, Drescher W, Rothamel D, Kloss F, Blessmann M, Heiland M, Wolff K, Smeets R. 2012. Current trends and future perspectives of bone substitute materials - from space holders to innovative biomaterials. J Cranio-Maxillofac Surg 40(8):706-18.

Koort JK, Mäkinen TJ, Knuuti J, Jalava J, Aro HT. 2004. Comparative 18F-FDG PET of experimental staphylococcus aureus osteomyelitis and normal bone healing. J Nucl Med 45(8):1406-11.

Koort JK, Mäkinen TJ, Suokas E, Veiranto M, Jalava J, Törmälä P, Aro HT. 2008. Sustained release of ciprofloxacin from an osteoconductive poly(DL)-lactide implant. Acta Orthop 79(2):295-301.

Koort JK, Suokas E, Veiranto M, Mäkinen TJ, Jalava J, Törmälä P, Aro HT. 2006. In vitro and in vivo testing of bioabsorbable antibiotic containing bone filler for osteomyelitis treatment. J Biomed Mater Res Part A 78(3):532-40.

Koort JK, Mäkinen TJ, Suokas E, Veiranto M, Jalava J, Knuuti J, Törmälä P, Aro HT. 2005. Efficacy of ciprofloxacin-releasing bioabsorbable osteoconductive bone defect filler for treatment of experimental osteomyelitis due to staphylococcus aureus. Antimicrob Agents Chemother 49(4):1502-8.

Korkusuz F, Korkusuz P, Ekşioğlu F, Gürsel I, Hasirci V. 2001. In vivo response to biodegradable controlled antibiotic release systems. J Biomed Mater Res 55(2):217-28.

Kundu B, Nandi SK, Roy S, Dandapat N, Soundrapandian C, Datta S, Mukherjee P, Mandal TK, Dasgupta S, Basu D. 2012. Systematic approach to treat chronic osteomyelitis through ceftriaxone-sulbactam impregnated porous β-tricalcium phosphate localized delivery system. Ceram Int 38(2):1533-48.

Kwok CS, Wan C, Hendricks S, Bryers JD, Horbett TA, Ratner BD. 1999. Design of infection-resistant antibiotic-releasing polymers: I. fabrication and formulation. J Control Release 62(3):289-99.

Langer R. 1990. New methods of drug delivery. Science 249(4976):1527-33.

Lao LL, Peppas NA, Boey FYC, Venkatraman SS. 2011. Modeling of drug release from bulk-degrading polymers. Int J Pharm 418(1):28-41.

Laycock PA, Brayford M, Cooper JJ. 2011. Effects of antibiotic addition on the setting time of calcium sulphate bone cement. Eur Cells and Mater 21(Suppl.2):58.

Lazzarini L, Lipsky BA, Mader JT. 2005. Antibiotic treatment of osteomyelitis: What have we learned from 30 years of clinical trials? Int J Infect Dis 9(3):127-38.

Le Guellec C, Gaudet M-, Lamanetre S, Breteau M. 1997. Stability of rifampin in plasma: Consequences for therapeutic monitoring and pharmacokinetic studies. Ther Drug Monit 19(6):669-74.

LeBel M. 1988. Ciprofloxacin: Chemistry, mechanism of action, resistance, antimicrobial spectrum, pharmacokinetics, clinical trials, and adverse reactions. Pharmacotherapy 8(1):3-33.

Lei Y, Rai B, Ho KH, Teoh SH. 2007. In vitro degradation of novel bioactive polycaprolactone-20% tricalcium phosphate composite scaffolds for bone engineering. Mater.Sci.Eng.C 27(2):293-8.

Leite B, Gomes F, Teixeira P, Souza C, Pizzolitto E, Oliveira R. 2011. In vitro activity of daptomycin, linezolid and rifampicin on staphylococcus epidermidis biofilms. Curr Microbiol 63(3):313-7.

Lemmouchi Y, Schacht E, Lootens C. 1998. In vitro release of trypanocidal drugs from biodegradable implants based on poly(ε-caprolactone) and poly(D,L-lactide). J Control Release 55(1):79-85.

Levine AM and DiBona JR. 2002. Fluoroquinolones. J Am Acad Orthop Surg 10(1):1-4.

Lewis CS, Supronowicz PR, Zhukauskas RM, Gill E, Cobb RR. 2012. Local antibiotic delivery with demineralized bone matrix. Cell Tissue Bank 13(1):119-27.

Li B, Brown KV, Wenke JC, Guelcher SA. 2010. Sustained release of vancomycin from polyurethane scaffolds inhibits infection of bone wounds in a rat femoral segmental defect model. J Control Release 145(3):221-30.

Li P, Cheng N-, Chen B-, Wang Y-. 2004. In vivo and in vitro chondrotoxicity of ciprofloxacin in juvenile rats. Acta Pharmacol Sin 25(10):1262-6.

Li S. 1999. Hydrolytic degradation characteristics of aliphatic polyesters derived from lactic and glycolic acids. J Biomed Mater Res 48(3):342-53.

Li S, Girod-Holland S, Vert M. 1996. Hydrolytic degradation of poly(DL-lactic acid) in the presence of caffeine base. J Control Release 40(1-2):41-53.

Li S, Garreau H, Vert M. 1990. Structure-property relationships in the case of the degradation of massive poly(α-hydroxy acids) in aqueous media - part 3 influence of the morphology of poly(l-lactic acid). J Mater Sci: Mater Med 1(4):198-206.

Li S and Vert M. 1999. Biodegradable polymers: Polyesters. Mathiowtz E, editor. In: Encyclopedia of controlled drug delivery. New York: John Wiley & Sons Inc.

Lim L, Auras R, Rubino M. 2008. Processing technologies for poly(lactic acid). Prog Polym Sci (Oxford) 33(8):820-52.

Lin F, Chen T, Lin C, Lee C. 1999. The merit of sintered PDLLA/TCP composites in management of bone fracture internal fixation. Artif Organs 23(2):186-94.

Lucke M, Wildemann B, Sadoni S, Surke C, Schiller R, Stemberger A, Raschke M, Haas NP, Schmidmaier G. 2005. Systemic versus local application of gentamicin in prophylaxis of implant-related osteomyelitis in a rat model. Bone 36(5):770-8.

Luginbuehl V, Ruffieux K, Hess C, Reichardt D, Von Rechenberg B, Nuss K. 2010. Controlled release of tetracycline from biodegradable β-tricalcium phosphate composites. J Biomed Mater Res Part B Appl Biomater 92(2):341-52.

Luukkainen T. 1991. Levonorgestrel-releasing intrauterine device. Ann New York Acad Sci 626:43-9.

MacGowan AP, Wootton M, Holt HA. 1999. The antibacterial efficacy of levofloxacin and ciprofloxacin against pseudomonas aeruginosa assessed by combining antibiotic exposure and bacterial susceptibility. Journal of Antimicrobial Chemotherapy 43(3):345-9.

Makadia HK and Siegel SJ. 2011. Poly lactic-co-glycolic acid (PLGA) as biodegradable controlled drug delivery carrier. Polym 3(3):1377-97.

Mäkinen T. 2005. Osteomyelitis and orthopedic implant infections, Doctoral dissertation, University of Turku.

Mäkinen TJ, Veiranto M, Knuuti J, Jalava J, Törmälä P, Aro HT. 2005a. Efficacy of bioabsorbable antibiotic containing bone screw in the prevention of biomaterial-related infection due to staphylococcus aureus. Bone 36(2):292-9.

Mäkinen TJ, Veiranto M, Lankinen P, Moritz N, Jalava J, Törmälä P, Aro HT. 2005b. In vitro and in vivo release of ciprofloxacin from osteoconductive bone defect filler. J Antimicrob Chemother 56(6):1063-8.

Malin M, Hiljanen-Vainio M, Karjalainen T, Seppälä J. 1996. Biodegradable lactone copolymers. II. hydrolytic study of ε-caprolactone and lactide copolymers. J Appl Polym Sci 59(8):1289-98.

Manzano M, Lamberti G, Galdi I, Vallet-Regí M. 2011. Anti-osteoporotic drug release from ordered mesoporous bioceramics: Experiments and modeling. AAPS PharmSciTech 12(4):1193-9.

Marchidanu D, Raducanu N, Miron DS, Radulescu FSR, Anuta V, Mircioiu I, Prasacu I. 2013. Comparative pharmacokinetics of rifampicin and 25-desacetyl rifampicin in healthy volunteers after single oral dose administration. Farmacia 61(2):398-410.

Marschall J, Lane MA, Beekmann SE, Polgreen PM, Babcock HM. 2013. Current management of prosthetic joint infections in adults: Results of an emerging infections network survey. Int J Antimicrob Agents 41(3):272-7.

McLaren AC. 2004. Alternative materials to acrylic bone cement for delivery of depot antibiotics in orthopaedic infections. Clin Orthop Relat Res (427):101-6.

Menschik M, Neumüller J, Steiner C, Erlacher L, Köller M, Ullrich R, Graninger W, Graninger WB. 1997. Effects of ciprofloxacin and ofloxacin on adult human cartilage in vitro. Antimicrob Agents Chemother 41(11):2562-5.

Mesak LR and Davies J. 2009. Phenotypic changes in ciprofloxacin-resistant staphylococcus aureus. Res Microbiol 160(10):785-91.

Miclau T, Edin ML, Lester GE, Lindsey RW, Dahners LE. 1998. Effect of ciprofloxacin on the proliferation of osteoblast-like MG-63 human osteosarcoma cells in vitro. Journal of Orthopaedic Research 16(4):509-512.

Mitscher LA. 2005. Bacterial topoisomerase inhibitors: Quinolone and pyridone antibacterial agents. Chem Rev 105(2):559-92.

Miyai T, Ito A, Tamazawa G, Matsuno T, Sogo Y, Nakamura C, Yamazaki A, Satoh T. 2008. Antibiotic-loaded poly-ε-caprolactone and porous β-tricalcium phosphate composite for treating osteomyelitis. Biomaterials 29(3):350-8.

Moir DT, Di M, Opperman T, Schweizer HP, Bowlin TL. 2007. A high-throughput, homogeneous, bioluminescent assay for pseudomonas aeruginosa gyrase inhibitors and other DNA-damaging agents. J Biomol Screen 12(6):855-64.

Mönkäre J, Hakala RA, Kovalainen M, Korhonen H, Herzig K, Seppälä JV, Järvinen K. 2012. Photocrosslinked poly(ester anhydride)s for peptide delivery: Effect of oligomer hydrophobicity on PYY3-36 delivery. Eur J Pharm Biopharm 80(1):33-8.

Mönkäre J, Hakala RA, Vlasova MA, Huotari A, Kilpeläinen M, Kiviniemi A, Meretoja V, Herzig KH, Korhonen H, Seppälä JV, and others. 2010. Biocompatible photocrosslinked poly(ester anhydride) based on functionalized poly(ε-caprolactone) prepolymer shows surface erosion controlled drug release in vitro and in vivo. J Control Release 146(3):349-55.

Mont MA, Mathur SK, Frondoza CG, Hungerford DS. 1996. The effects of ciprofloxacin on human chondrocytes in cell culture. Infection 24(2):151-5.

Moscicka-Studzinska A and Ciach T. 2012. Mathematical modelling of buccal iontophoretic drug delivery system. Chem Eng Sci 80:182-7.

Mouriño V and Boccaccini AR. 2010. Bone tissue engineering therapeutics: Controlled drug delivery in three-dimensional scaffolds. J R Soc Interface 7(43):209-27.

Mouzopoulos G, Kanakaris NK, Kontakis G, Obakponovwe O, Townsend R, Giannoudis PV. 2011. Management of bone infections in adults: The surgeon's and microbiologist's perspectives. Injury 42(Suppl. 5):S18-23.

Muñoz-Bonilla A and Fernández-García M. 2012. Polymeric materials with antimicrobial activity. Prog Polym Sci (Oxford) 37(2):281-339.

Nair LS and Laurencin CT. 2007. Biodegradable polymers as biomaterials. Prog Polym Sci (Oxford) 32(8-9):762-98.

Nandi SK, Roy S, Mukherjee P, Kundu B, De DK, Basu D. 2010. Orthopaedic applications of bone graft & graft substitutes: A review. Indian J Med Res 132(7):15-30.

Narasimhan B and Peppas NA. 1997. The role of modeling studies in the development of future controlled-release devices. Park K, editor. In: Controlled drug delivery, challenges and strategies. Washington D.C.: American Chemical Society.

Narasimhan B, Mallapragada SK, Peppas NA. 1999. Release kinetics, data interpretation. Mathiowtz E, editor. In: Controlled drug delivery. New York: John Wiley & sons.

Näslund J, Hedman JE, Agestrand C. 2008. Effects of the antibiotic ciprofloxacin on the bacterial community structure and degradation of pyrene in marine sediment. Aquatic Toxicol 90(3):223-7.

Neumann M and Epple M. 2006. Composites of calcium phosphate and polymers as bone substitution materials. Eur J Trauma 32(2):125-31.

Neut D, Kluin OS, Crielaard BJ, Van Der Mei HC, Busscher HJ, Grijpma DW. 2009. A biodegradable antibiotic delivery system based on poly-(trimethylene carbonate) for the treatment of osteomyelitis. Acta Orthop 80(5):514-9.

Neut D, Van De Belt H, Stokroos I, Van Horn JR, Van Der Mei HC, Busscher HJ. 2001. Biomaterial-associated infection of gentamicin-loaded PMMA beads in orthopaedic revision surgery. J Antimicrob Chemother 47(6):885-91.

Niemelä T, Niiranen H, Kellomäki M, Törmälä P. 2005. Self-reinforced composites of bioabsorbable polymer and bioactive glass with different bioactive glass contents. part I: Initial mechanical properties and bioactivity. Acta Biomater 1(2):235-42.

Niemelä T, Aydogan DB, Hannula M, Hyttinen J, Kellomäki M. 2011. Determination of bioceramic filler distribution and porosity of self-reinforced bioabsorbable composites using micro-computed tomography. Compos Part A Appl Sci Manuf 42(5):534-42.

Nikkola L, Vapalahti K, Huolman R, Seppälä J, Harlin A, Ashammakhi N. 2008. Multilayer implant with triple drug releasing properties. J.Biomed.Nanotechnol. 4(3):331-8.

Otsuka M. 1994. A novel skeletal drug delivery system using self-setting bioactive glass bone cement. III: The in vitro drug release from bone cement containing indomethacin and its physicochemical properties. J Control Release 31(2):111-9.

Otsuka M, Matsuda Y, Suwa Y, Fox JL, Higuchi WI. 1994. A novel skeletal drug-delivery system using self-setting calcium phosphate cement. 3. physicochemical properties and drug-release rate of bovine insulin and bovine albumin. J Pharm Sci 83(2):255-8.

Otsuka M, Nakahigashi Y, Matsuda Y, Fox JL, Higuchi WI, Sugiyama Y. 1997. A novel skeletal drug delivery system using self-setting calcium phosphate cement VIII: The relationship between in vitro and in vivo drug release from indomethacin-containing cement. J Control Release 43(2-3):115-22.

Otsuka M, Matsuda Y, Kokubo T, Yoshihara S, Nakamura T, Yamamuro T. 1992. New skeletal drug delivery system containing antibiotics using self-setting bioactive glass cement. Chem Pharm Bull 40(12):3346-8.

Overbeck JP, Winckler ST, Meffert R, Törmälä P, Spiegel HU, Brug E. 1995. Penetration of ciprofloxacin into bone: A new bioabsorbable implant. J Invest Surg 8(3):155-62.

Paakinaho K, Ellä V, Syrjälä S, Kellomäki M. 2009. Melt spinning of poly(l/d)lactide 96/4: Effects of molecular weight and melt processing on hydrolytic degradation. Polym Degradation Stab 94(3):438-42.

Pääkkönen M and Peltola H. 2011. Antibiotic treatment for acute haematogenous osteomyelitis of childhood: Moving towards shorter courses and oral administration. Int J Antimicrob Agents 38(4):273-80.

Pargal A and Rani S. 2001. Non-linear pharmacokinetics of rifampicin in healthy asian indian volunteers. Int J Tuberc Lung Dis 5(1):70-9.

Parker AC, Smith JK, Courtney HS, Haggard WO. 2011. Evaluation of two sources of calcium sulfate for a local drug delivery system: A pilot study. Clin Orthop Relat Res 469(11):3008-15.

Parsons B and Strauss E. 2004. Surgical management of chronic osteomyelitis. Am J Surg 188(1 Suppl. 1):57-66.

Pavithra D and Doble M. 2008. Biofilm formation, bacterial adhesion and host response on polymeric implants - issues and prevention. Biomed Mater (Bristol) 3(3) 034003.

Perlroth J, Kuo M, Tan J, Bayer AS, Miller LG. 2008. Adjunctive use of rifampin for the treatment of staphylococcus aureus infections: A systematic review of the literature. Arch Intern Med 168(8):805-19.

Peterson CY, Shaterian A, Borboa AK, Gonzalez AM, Potenza BM, Coimbra R, Eliceiri BP, Baird A. 2009. The noninvasive, quantitative, in vivo assessment of adenoviral-mediated gene delivery in skin wound biomaterials. Biomaterials 30(35):6788-93.

Pitt CG. 1990. Poly-ε-caprolactone and its copolymers Chasin M and Langer R, editors. In: Biodegradable polymers as drug delivery systems. New York: Marcel Dekker Inc. 71 p.

Pitt CG, Gratzl MM, Kimmel GL. 1981. Aliphatic polyesters II. the degradation of poly (DL-lactide), poly (ε-caprolactone), and their copolymers in vivo. Biomaterials 2(4):215-20.

Pitt CG, Jeffcoat R, Zweidinger RA, Schindler A. 1979. Sustained drug delivery systems. I. the permeability of poly(ε-caprolactone), poly(DL-lactic acid), and their copolymers. J Biomed Mater Res 13(3):497-507.

Plikk P, Odelius K, Hakkarainen M, Albertsson AC. 2006. Finalizing the properties of porous scaffolds of aliphatic polyesters through radiation sterilization. Biomaterials 27(31):5335-47.

Puga AM, Rey-Rico A, Magariños B, Alvarez-Lorenzo C, Concheiro A. 2012. Hot melt poly-ε-caprolactone/poloxamine implantable matrices for sustained delivery of ciprofloxacin. Acta Biomater 8(4):1507-18.

Pulkkinen M, Malin M, Tarvainen T, Saarimäki T, Seppälä J, Järvinen K. 2007. Effects of block length on the enzymatic degradation and erosion of oxazoline linked poly-ε-caprolactone. Eur J Pharm Sci 31(2):119-28.

Ramchandani M and Robinson D. 1998. In vitro and in vivo release of ciprofloxacin from PLGA 50:50 implants. J Control Release 54(2):167-75.

Repka MA, Battu SK, Upadhye SB, Thumma S, Crowley MM, Zhang F, Martin C, McGinity JW. 2007. Pharmaceutical applications of hot-melt extrusion: Part II. Drug Dev Ind Pharm 33(10):1043-57.

Ritger PL and Peppas NA. 1987. A simple equation for desciption of solute release I. fickian and non-fickian release from non-swellable devices in the form of slabs, spheres, cylinders or discs. J Control Release 5(1):23-36.

Rod-Fleury T, Dunkel N, Assal M, Rohner P, Tahintzi P, Bernard L, Hoffmeyer P, Lew D, Uçkay I. 2011. Duration of post-surgical antibiotic therapy for adult chronic osteomyelitis: A single-centre experience. Int Orthop 35(11):1725-31.

Roth B. 1984. Penetration of parenterally administered rifampicin into bone tissue. Chemotherapy 30(6):358-65.

Rothstein SN and Little SR. 2011. A "tool box" for rational design of degradable controlled release formulations. J Mater Chem 21(1):29-39.

Sarasua J, Prud'homme RE, Wisniewski M, Le Borgne A, Spassky N. 1998. Crystallization and melting behavior of polylactides. Macromolecules 31(12):3895-905.

Sawhney AS and Hubbell JA. 1990. Rapidly degraded terpolymers of dl-lactide, glycolide, and ε-caprolactone with increased hydrophilicity by copolymerization with polyethers. J Biomed Mater Res 24(10):1397-411.

Schmidmaier G, Lucke M, Wildemann B, Haas NP, Raschke M. 2006. Prophylaxis and treatment of implant-related infections by antibiotic-coated implants: A review. Injury 37(2 SUPPL.):S105-S112.

Schnieders J, Gbureck U, Vorndran E, Schossig M, Kissel T. 2011. The effect of porosity on drug release kinetics from vancomycin microsphere/calcium phosphate cement composites. J Biomed Mater Res Part B Appl Biomater 99 B(2):391-8.

Sendi P and Zimmerli W. 2012. Antimicrobial treatment concepts for orthopaedic device-related infection. Clin Microbiol Infect 18(12):1176-84.

Sendi P and Zimmerli W. 2011. Challenges in periprosthetic knee-joint infection. Int J Artif Organs 34(9):947-56.

Senneville E, Joulie D, Legout L, Valette M, Dezèque H, Beltrand E, Roselé B, D'Escrivan T, Loïez C, Caillaux M, and others. 2011. Outcome and predictors of treatment failure in total hip/knee prosthetic joint infections due to staphylococcus aureus. Clin Infect Dis 53(4):334-40.

Sezer UA, Aksoy EA, Hasirci V, Hasirci N. 2013. Poly(ε-caprolactone) composites containing gentamicin-loaded β-tricalcium phosphate/gelatin microspheres as bone tissue supports. J Appl Polym Sci 127(3):2132-9.

Shen, SI, Bhaskara, RJ, Li, X. 2003. Design of controlled-release drug delivery systems. Kutz M, editor. In: Standard handbook of biomedical engineering & design. New York: McGraw-Hill.

Shin S and Shea LD. 2010. Lentivirus immobilization to nanoparticles for enhanced and localized delivery from hydrogels. Mol Ther 18(4):700-6.

Shore EC and Holmes E. 1993. Porous hydroxyapatite. Hench LL and Wilson J, editors. In: An introduction to bioceramics. Singapore: World Scientific Publishing. 181 p.

Sia IG and Berbari EF. 2006. Osteomyelitis. Best Pract Res Clin Rheumatol 20(6):1065-81.

Siepmann J and Peppas NA. 2011. Higuchi equation: Derivation, applications, use and misuse. Int J Pharm 418(1):6-12.

Södergård A and Stolt M. 2002. Properties of lactic acid based polymers and their correlation with composition. Prog Polym Sci (Oxford) 27(6):1123-63.

Soriano I and Évora C. 2000. Formulation of calcium phosphates/poly (d,l-lactide) blends containing gentamicin for bone implantation. J Control Release 68(1):121-34.

Soundrapandian C, Datta S, Sa B. 2007. Drug-eluting implants for osteomyelitis. Crit Rev Ther Drug Carrier Syst 24(6):493-545.

Spellberg B and Lipsky BA. 2012. Systemic antibiotic therapy for chronic osteomyelitis in adults. Clin Infect Dis 54(3):393-407.

Sreenivasa Rao B. 2001. Development of dissolution medium for rifampicin sustained release formulations. Indian J Pharm Sci 63(3):258-60.

Sreenivasa Rao B, Seshasayana A, Pardha Saradhi SV, Ravi Kumar N, Narayan CPS, Ramana Murthy KV. 2001. Correlation of 'in vitro' release and 'in vivo' absorption characteristics of rifampicin from ethylcellulose coated nonpareil beads. Int J Pharm 230(1-2):1-9.

Stahlmann R, Kühner S, Shakibaei M, Schwabe R, Flores J, Evander SA, Van Sickle DC. 2000. Chondrotoxicity of ciprofloxacin in immature beagle dogs: Immunohistochemistry, electron microscopy and drug plasma concentrations. Arch Toxicol 73(10-11):564-72.

Stephens D, Li L, Robinson D, Chen S, Chang H, Liu RM, Tian Y, Ginsburg EJ, Gao X, Stultz T. 2000. Investigation of the in vitro release of gentamicin from a polyanhydride matrix. J Controlled Release 63(3):305-17.

Takacs-Novak K, Jozan M, Hermecz I, Szasz G. 1992. Lipophilicity of antibacterial fluoroquinolones. Int J Pharm 79(2-3):89-96.

Takigami I, Ito Y, Ishimaru D, Ogawa H, Mori N, Shimizu T, Terabayashi N, Shimizu K. 2010. Two-stage revision surgery for hip prosthesis infection using antibiotic-loaded porous hydroxyapatite blocks. Arch Orthop Trauma Surg 130(10):1221-6.

Tan H, Guo S, Yang S, Xu X, Tang T. 2012. Physical characterization and osteogenic activity of the quaternized chitosan-loaded PMMA bone cement. Acta Biomater 8(6):2166-74.

Thakhiew W, Waisayawan P, Devahastin S. 2011. Comparative evaluation of mathematical models for release of antioxidant from chitosan films prepared by different drying methods. Dry Technol 29(12):1396-403.

Thanyaphoo S and Kaewsrichan J. 2012. Synthesis and evaluation of novel glass ceramics as drug delivery systems in osteomyelitis. J Pharm Sci 101(8):2870-82.

Tiainen J, Knuutila K, Veiranto M, Suokas E, Törmälä P, Kaarela O, Länsman S, Ashammakhi N. 2009. Pull-out strength of multifunctional bioabsorbable ciprofloxacin-releasing polylactide-polyglycolide 80/20 tacks: An experimental study allograft cranial bone. J Craniofac Surg 20(1):58-61.

Tiainen J, Veiranto M, Koort JK, Suokas E, Kaarela O, Törmälä P, Waris T, Ashammakhi N. 2012. Bone tissue concentrations of ciprofloxacin released from biodegradable screws implanted in rabbits skull. Eur J Plast Surg 35(2):171-175.

Timurkaynak F, Can F, Azap ÖK, Demirbilek M, Arslan H, Karaman SÖ. 2006. In vitro activities of non-traditional antimicrobials alone or in combination against multidrug-resistant strains of pseudomonas aeruginosa and acinetobacter baumannii isolated from intensive care units. Int J Antimicrob Agents 27(3):224-8.

Türesin F, Gürsel I, Hasirci V. 2001. Biodegradable polyhydroxyalkanoate implants for osteomyelitis therapy: In vitro antibiotic release. J Biomater Sci Polym Ed 12(2):195-207.

Uckay I, Jugun K, Gamulin A, Wagener J, Hoffmeyer P, Lew D. 2012. Chronic osteomyelitis. Curr Infect Dis Rep 14(5):566-75.

Vallet CM, Marquez B, Ngabirano E, Lemaire S, Mingeot-Leclercq M, Tulkens PM, Van Bambeke F. 2011. Cellular accumulation of fluoroquinolones is not predictive of their intracellular activity: Studies with gemifloxacin, moxifloxacin and ciprofloxacin in a pharmacokinetic/pharmacodynamic model of uninfected and infected macrophages. Int J Antimicrob Agents 38(3):249-56.

Vallet-Regí M and Arcos D. 2013. Bioceramics for drug delivery. Acta Mater 61(3):890-911.

Vallet-Regí M and Ruiz-Hernández E. 2011. Bioceramics: From bone regeneration to cancer nanomedicine. Adv Mater 23(44):5177-218.

Van Bambeke F, Michot J, Van Eldere J, Tulkens PM. 2005. Quinolones in 2005: An update. Clin Microbiol Infect 11(4):256-80.

Veiranto M, Törmälä P, Suokas E. 2002. In vitro mechanical and drug release properties of bioabsorbable ciprofloxacin containing and neat self-reinforced P(L/DL)LA 70/30 fixation screws. J Mater Sci Mater Med 13(12):1259-63.

Veiranto M, Suokas E, Ashammakhi N, Törmälä P. 2004a. Novel bioabsorbable antibiotic releasing bone fracture fixation implants. Adv Exp Med Biol 553:197-208.

Veiranto M, Tiainen J, Niemelä S, Suokas E, Ikäheimo I, Koskela M, Syrjälä H, Ashammakhi N, Törmälä P. 2004b. Novel ciprofloxacin releasing SR-PLGA miniscrews. Trans World Biomater Congr :173.

Vilalta M, Jorgensen C, Dégano IR, Chernajovsky Y, Gould D, Noël D, Andrades JA, Becerra J, Rubio N, Blanco J. 2009. Dual luciferase labelling for non-invasive bioluminescence imaging of mesenchymal stromal cell chondrogenic differentiation in demineralized bone matrix scaffolds. Biomaterials 30(28):4986-95.

Vogt S, Schnabelrauch M, Weisser J, Kautz AR, Büchner H, Kühn K. 2007. Design of an antibiotic delivery system based on a bioresorbable bone substitute. Adv Eng Mater 9(12):1135-40.

Von Keutz E, Rühl-Fehlert C, Drommer W, Rosenbruch M. 2004. Effects of ciprofloxacin on joint cartilage in immature dogs immediately after dosing and after a 5-month treatment-free period. Arch Toxicol 78(7):418-24.

Waknis V and Jonnalagadda S. 2011. Novel poly-DL-lactide-polycaprolactone copolymer based flexible drug delivery system for sustained release of ciprofloxacin. Drug Deliv 18(4):236-45.

Waldvogel FA, Medoff G, Swartz MN. 1970. Osteomyelitis: A review of clinical features, therapeutic considerations and unusual aspects. N Engl J Med 282(4):198-206.

Walter G, Kemmerer M, Kappler C, Hoffmann R. 2012. Treatment algorithms for chronic osteomyelitis. Dtsch Arztebl 109(14):254-64.

Wesselingh JA. 1993. Controlling diffusion. J Control Release 24(1-3):47-60.

Williams DL, Haymond BS, Woodbury KL, Beck JP, Moore DE, Epperson RT, Bloebaum RD. 2012. Experimental model of biofilm implant-related osteomyelitis to test combination biomaterials using biofilms as initial inocula. J Biomed Mater Res Part A 100 A(7):1888-900.

Wilson M, Williams MA, Jones DS, Andrews GP. 2012. Hot-melt extrusion technology and pharmaceutical application. Ther Deliv 3(6):787-97.

Witsø E, Persen L, Løseth K, Bergh K. 1999. Adsorption and release of antibiotics from morselized cancellous bone. Acta Orthop Scand 70(3):298-304.

Woodruff MA and Hutmacher DW. 2010. The return of a forgotten polymer - polycaprolactone in the 21st century. Prog Polym Sci (Oxford) 35(10):1217-56.

Xie Z, Liu X, Jia W, Zhang C, Huang W, Wang J. 2009. Treatment of osteomyelitis and repair of bone defect by degradable bioactive borate glass releasing vancomycin. J Control Release 139(2):118-26.

Yee YC, Kisslinger B, Yu VL, Jin DJ. 1996. A mechanism of rifamycin inhibition and resistance in pseudomonas aeruginosa. J Antimicrob Chemother 38(1):133-7.

Zamoume O, Thibault S, Regnié G, Mecherri MO, Fiallo M, Sharrock P. 2011. Macroporous calcium phosphate ceramic implants for sustained drug delivery. Mater Sci Eng C 31(7):1352-6.

Zhang N, Fang Z, Contag PR, Purchio AF, West DB. 2004. Tracking angiogenesis induced by skin wounding and contact hypersensitivity using a Vegfr2-luciferase transgenic mouse. Blood 103(2):617-26.

Zhou J, Fang T, Wang Y, Dong J. 2012. The controlled release of vancomycin in gelatin/β-TCP composite scaffolds. J Biomed Mater Res Part A 100 A(9):2295-301.

Zilberman M and Elsner JJ. 2008. Antibiotic-eluting medical devices for various applications. J Control Release 130(3):202-15.

Zimmerli W. 2006. Prosthetic-joint-associated infections. Best Pract Res Clin Rheumatol 20(6):1045-63.

Zimmerli W and Sendi P. 2011. Pathogenesis of implant-associated infection: The role of the host. Semin Immunopathol 33(3):295-306.

Zimmerli W and Ochsner PE. 2003. Management of infection associated with prosthetic joints. Infection 31(2):99-108.

Zimmerli W, Trampuz A, Ochsner PE. 2004. Current concepts: Prosthetic-joint infections. New Engl J Med 351(16):1645-54.

Zimmerli W, Widmer AF, Blatter M, Frei R, Ochsner PE. 1998. Role of rifampin for treatment of orthopedic implant-related staphylococcal infections: A randomized controlled trial. J Am Med Assoc 279(19):1537-41.

Zoubos AB, Galanakos SP, Soucacos PN. 2012. Orthopedics and biofilm - what do we know? a review. Med Sci Monit 18(6):RA89-96.

9 APPENDIX

^{1}H NMR spectrum of pure rifampicin and PLCL+R

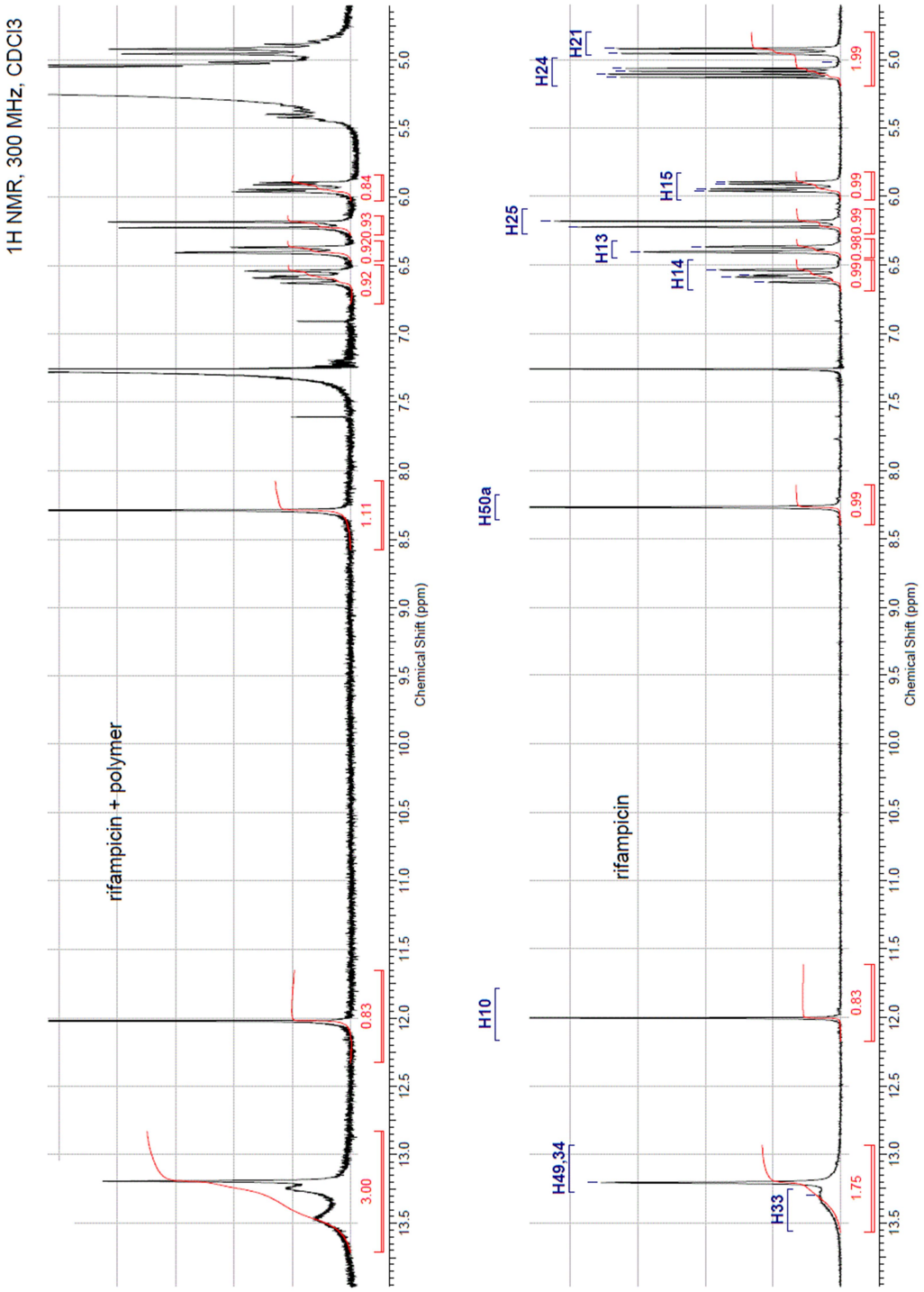

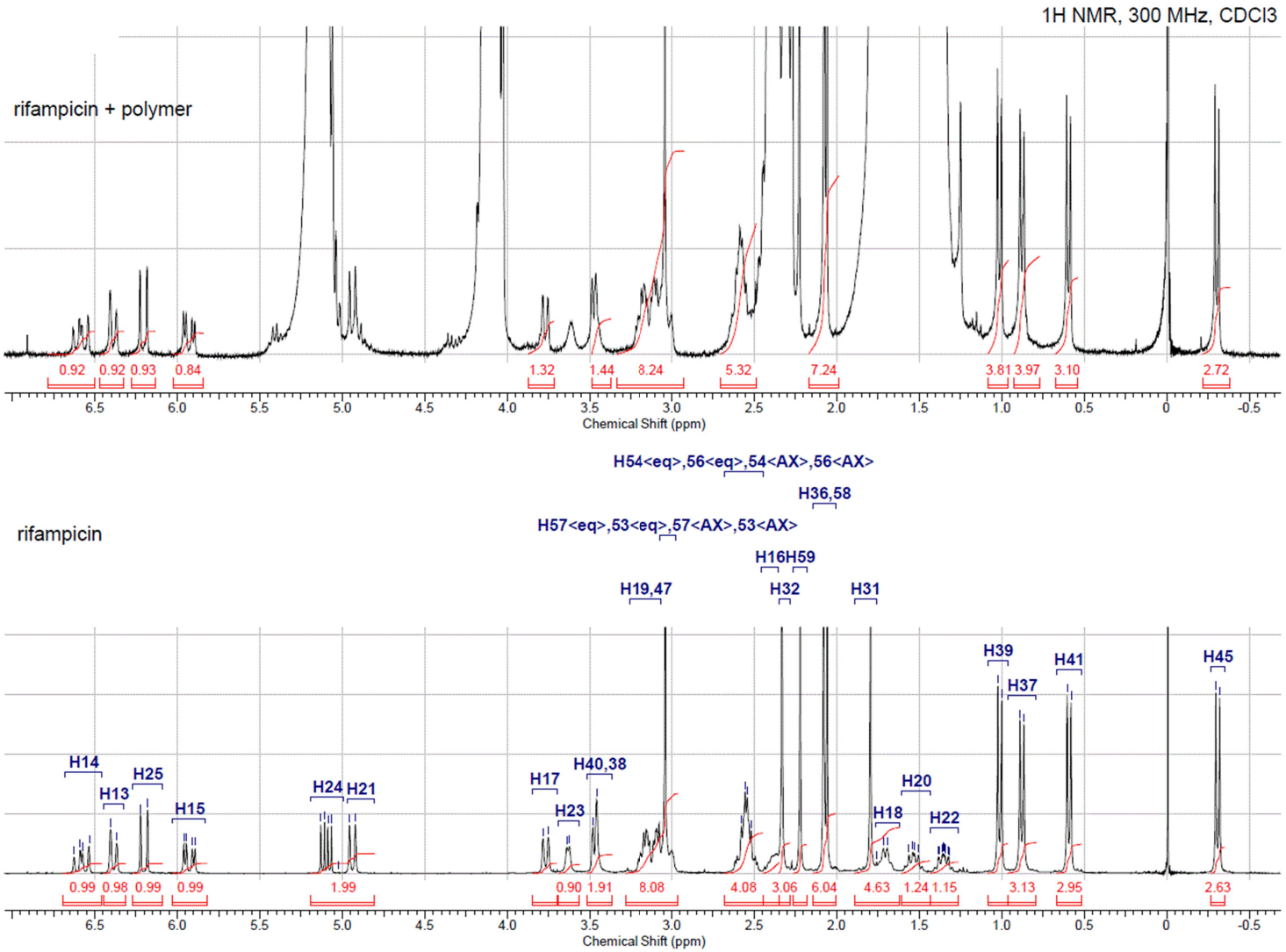
1H NMR, 300 MHz, CDCl3
rifampicin + polymer
0.92 0.92 0.93 0.84 1.32 1.44 8.24 5.32 7.24 3.81 3.97 3.10 2.72
Chemical Shift (ppm)
rifampicin
H54<eq>,56<eq>,54<AX>,56<AX>
H36,58
H57<eq>,53<eq>,57<AX>,53<AX>
H16H59
H19,47
H32
H31
H14
H13
H25
H15
H24
H21
H17
H23
H40,38
H20
H18
H22
H39
H37
H41
H45
0.99 0.98 0.99 0.99 1.99 0.90 1.91 8.08 4.08 3.06 6.04 4.63 1.24 1.15 3.13 2.95 2.63
Chemical Shift (ppm)

ORIGINAL PUBLICATIONS

Publication I

Ahola, N., Veiranto, M., Rich, J., Efimov, A., Hannula, M., Seppälä, J.,
and Kellomäki, M.

Hydrolytic degradation of composites of poly(L-lactide-co-ε-caprolactone) 70/30 and β-tricalcium phosphate

Journal of Biomaterials Applications, 28 (2013), 529-543

Hydrolytic Degradation of Composites of Poly(L-lactide-co-ε-Caprolactone) 70/30 and β-Tricalcium Phosphate

Niina Ahola[1,2,*], Minna Veiranto[1,3], Jaana Rich[4], Alexander Efimov[5], Markus Hannula[1], Jukka Seppälä[4] and Minna Kellomäki[1,2]

[1]Tampere University of Technology, Department of Biomedical Engineering, Hermiankatu 12, 33720 Tampere, Finland

[2]BioMediTech, Tampere, Finland

[3]Bioretec Ltd, Hermiankatu 22, 33720 Tampere, Finland

[4]Aalto University, School of Chemical Technology, Department of Biotechnology and Chemical Technology, Kemistintie 1, 02015 Espoo Finland

[5]Tampere University of Technology, Department of Chemistry and Bioengineering, Korkeakoulunkatu 8, 33720 Tampere, Finland

* To whom correspondence should be addressed
e-mail: niina.ahola@tut.fi
tel. +358-40-7049390
fax +358-3-3115 2250

Abstract

There is an increasing need for synthetic bone substitute materials that decrease the need for allografts and autografts. In this study, composites of β-TCP and a biodegradable poly(L-lactide-co-ε-caprolactone) were manufactured using extrusion to form biodegradable composites with high β-TCP contents for osteoconductivity. The hydrolytic degradation of the composites containing 0, 10, 20, 35 and 50% of β-TCP was studied *in vitro* for 52 weeks. During the study, it was observed that β-TCP did not have an effect on the degradation rate of the polymer matrix. However, the crystallinity of the materials increased throughout the test series and changes in Tgs were also observed as the comonomer ratio of the polymer matrix changed as the degradation proceeded. The results show that the materials have desirable degradation properties and, thus, possess great potential as bioabsorbable and osteoconductive bone filling materials.

Introduction

Due to the problems associated with autografts and allografts, there is an obvious need in orthopaedics for synthetic bone substitute materials that are easy to handle in surgical conditions and do not carry the risk of infection or suffer from limited availability (1). An optimal material that is biodegradable, bioactive, and easy to handle has not been found as yet. The currently available polymers or ceramics alone do not provide a sufficient solution to this problem. Numerous studies have been published where the properties of biodegradable polymers and bioceramics have been combined to form composites (2-5). Such composites have promising properties for use in the fabrication of scaffolds for bone tissue engineering applications (6,7).

In order to overcome the problems of autografts and allografts, β-tricalcium phosphate (β-TCP), a bioresorbable ceramic, is used as a bone graft substitute due to its osteoconductive properties (1,8). This material is clinically used, for example, as granules and blocks (9). β-TCP has the same Ca/P ratio as the amorphous inorganic phase of bone (7) and does not dissolve as quickly as α-TCP (9). According to Aunoble *et al.* (10), 60 wt-% of β-TCP in poly-L-lactide is as active as plain β-TCP with regard to osteogenesis. This fact supports the idea that composites combine the advantageous properties of biodegradable polymers and bioceramics.

The mechanical and hydrolytic degradation properties of poly-ε-caprolactone and poly-L-lactide are very different as homopolymers. Both polymers have proven biocompatibility and are Food and Drug Administration (FDA) approved for a wide range of applications in the biomedical field (11). Via the copolymerization of the monomers, lactide (D, L or DL), and ε-caprolactone, interesting properties can be

achieved that combine the elasticity, good processability and drug releasing properties of poly-ε-caprolactone as well as mechanical properties and faster degradability via the hydrolysis of polylactides (11-18).

Many groups have studied the composites of poly-ε-caprolactone or polylactide and various bioceramics (19-25). However, the reported research results of *in vitro* testing have usually concentrated on relatively short periods of time, often less than a month (22,26) or less than 26 weeks (4,21). Reports of the studies performed on copolymers of lactide and ε-caprolactone can be found, but the majority of them concentrate on copolymers of D,L-lactide and ε-caprolactone or different comonomer ratios than the one reported in this study.

In this study, various ratios of a filler, β-tricalcium phosphate, and a bioabsorbable polymer, poly(L-lactide-co-ε-caprolactone) with the comonomer ratio of 70/30, were extrusion compounded in order to create a material that is biodegradable, osteoconductive and easy to handle. The properties as well as the potential of the composites for use as bone graft substitutes were examined in a long term *in vitro* test lasting for 52 weeks. Despite the fact that some of the composites had high β-TCP content, they showed good processability and handling properties as well as promising degradation behaviour. Special attention will be paid in the report to the effect of various β-TCP contents on the degradation of the composites.

Materials and Methods

Materials

Medical grade poly(L-lactide-co-ε-caprolactone) with the comonomer ratio of 70/30 and initial M_w of 229 000 g/mol was purchased from Purac Biomaterials (the

Netherlands), and β-tricalcium phosphate (granule size < 38 μm) was purchased from Plasma Biotal Ltd (United Kingdom). Sörensen buffer solution was prepared according to the standard ISO 15814 (27). The chemicals used for the buffer solution (Na_2HPO_4 and KH_2PO_4) were purchased from J.T. Baker (the Netherlands). For the phosphate dissolution testing, Tris buffer solution was used and it was prepared using Tris Base Ultra Pure ($C_4H_{11}NO_3$) (ICN Biomedicals, USA) and Trizma HCl ($C_4H_{11}NO_3 \times HCl$) (Sigma-Aldrich, Germany). Other chemicals used for the determination of phosphate release from the composites were ammoniumheptamolybdate (Merck, Germany), L(+)-ascorbic acid (Merck, Germany), acetic acid (J.T. Baker, the Netherlands), sodium acetate (Merck, Germany) and sulphuric acid (J.T. Baker, the Netherlands).

Processing

Dried (72 h in vacuum at room temperature) polymer and β-TCP powder were processed into rod-shaped billets with a diameter of approximately 2.5 mm with a co-rotating custom-built intermeshing twin-screw extruder (L/D ratio = 22.5) in a nitrogen atmosphere. Temperature range in the extruder was 25-130 °C. PLCL copolymer and β-TCP were delivered in the process with separate gravimetric screw feeders and the mixing of the components took place in the extruder. Total feed rate of the components was 200g/h in all of the cases. A haul-off unit was used to guide the extrudate from the die and the diameter of the billets was fine-tuned adjusting the speed of the haul-off unit. Four different composites and a plain copolymer were processed. The β-TCP-contents of the composites were 10, 20, 35 and 50 wt-% and the composites are denoted as PLCL + 10% TCP, PLCL + 20% TCP, PLCL + 35% TCP, and PLCL + 50% TCP, respectively. Pellet shaped samples (length approximately 2.5 mm) were cut from the

billets. Before degradation studies were carried out, the samples were packed and sterilized using gamma irradiation (minimum dose 25 kGy).

In vitro procedure

Degradation tests were conducted at 37°C *in vitro* following the standard ISO 15814 (27). First, weighed test samples were placed in brown glass bottles with 20 ml Sörensen buffer solution. A test sample consisted of 15 pellets weighing approximately 300 mg in total and five parallel test samples were tested at each time point. Then the bottles were placed in a shaking bath at 37°C. The pH of the buffer solution was measured periodically with a calibrated pH meter and the buffer solutions were changed every two weeks in the beginning of the test series and once a week as the degradation accelerated. Test samples were withdrawn at predetermined time points of 2, 4, 6, 8, 10, 12, 16, 20, 26, 39 and 52 weeks.

Methods of analysis

Residual monomer

The determination of residual L-lactide and ε-caprolactone monomer contents was performed by Ramboll Analytics Oy (Lahti, Finland). The ε-caprolactone and L-lactide contents were measured after chloroform extraction of the samples using gas chromatography (DC8000, CE Instruments, Rodano, Italy) and an FI-detector after chloroform dilution. The measuring resolution was 0.02%. The monomer contents of the processed samples were analyzed from three time points in the processing batch. Two parallel samples were taken from the beginning, middle and the end of the processing batch. Additionally, the monomer content of the raw material was measured.

Molecular weights

The molecular weights (number average, M_n, and weight average, M_w, molecular weights) and polydispersity values of the copolymer were determined at room temperature by size exclusion chromatography (SEC) (Waters Associates system equipped with a Waters 717plus autosampler, a Waters 510 HPLC solvent pump, four linear PL gel columns (10^4, 10^5, 10^3 and 100 Å) connected in series, and a Waters 2414 differential refractometer). Chloroform (Riedel-de Haën AG, stabilized with 1% ethanol) was used as solvent and eluent. The samples were filtered through a 0.5 μm Millex SR filter. The injected volume was 200 μl and the flow rate was 1.0 ml/min. Monodisperse polystyrene standards were used for primary calibration. Two parallel samples were analyzed at each time point.

Mass loss and water absorption

After the test samples were withdrawn from the shaking bath, they were rinsed twice with distilled water and the surfaces of the pellets were carefully wiped with tissue paper. The test samples were weighed immediately after wiping. The test samples were dried for at least three days at ambient conditions and for one week in vacuum. After vacuum drying, the test samples were weighed again to obtain the dry masses. Dried test samples were stored in a desiccator for further analysis.

The mass loss was calculated as the difference between the mass of the initial test sample and the mass of the dried test sample divided by the initial mass of the test sample. The water absorption was calculated as the difference between the mass of the wet test sample and the mass of the dried test sample divided by the mass of the dried test sample.

Thermal properties

Thermal analysis was performed using DSC Q1000 differential scanning calorimeter (TA Instruments, Delaware, USA). To ensure similar thermal histories of the samples, they were heated twice and cooled rapidly in between. The heating rate was 20 °C/min, the cooling rate 50 °C/min, and the temperature range was -60 °C to +200 °C. Nitrogen was used as the sweeping gas. The results were analyzed using Universal Analysis Software. Second heating cycle was used for the analysis of glass transition temperatures (T_g) and first heating cycle for the analysis of melting temperatures (T_m) and enthalpies (ΔH_f). Five parallel samples were tested for each material and time point. Averages and standard deviations were then calculated.

Ceramic content and dissolution

The β-TCP content of the test samples was measured using thermogravimetric analysis (TGA Q500 (TA Instruments, Delaware, USA)). Approximately 20 mg of a sample was used and the samples were heated at a rate of 20°C/min up to 700°C. Five parallel samples were tested at each time point, and the results were then analyzed using Universal Analysis Software.

The dissolution of phosphate ions from the composites was measured using a method described in ISO 6878 (28). In this method, the orthophosphate ions that have been dissolved in the buffer solution form an ammonium phosphomolybdate complex in acidic solution. This complex is then reduced by ascorbic acid into a blue complex. The absorbance of the complex was measured using a Unicam UV 500 spectometer (ThermoSpectronic, Cambridge, United Kingdom) at the wavelength of 700 nm. Five parallel samples of each composite weighing about 250-300 mg were tested once a week up to 48 weeks. Plain PLCL was used as a negative control and plain β-TCP

samples weighing about 160 mg were tested as positive controls. Concentrations of the released phosphate ions were calculated with the help of a standard curve prepared with known concentrations of phosphate ions.

Molecular structure

The proton spectra of the samples were measured using a Varian Mercury 300 MHz NMR Spectrometer (Varian Associates Inc., Palo Alto, California, USA) at room temperature. Tetramethylsilane (TMS) was used as an internal standard, and chemical shifts were measured relative to TMS. The ^{1}H NMR spectra were measured at room temperature in standard 5 mm tubes in deuterochloroform. The data were gathered until the quality of the spectrum was sufficient, and the number of scans was 190-300. The proton NMR spectra of the samples were processed and analyzed using SpinWorks 3.1 software. Phase correction and baseline correction were applied to all spectra. Information on the molecular composition and the comonomer ratio of the copolymer was obtained.

Microstructure of the samples

The microstructure of the composites was observed using scanning electron microscopy (Philips XL-30 SEM equipped with a LaB6 filament with SE and BSE detectors, Philips, the Netherlands) with an acceleration voltage of 12.0 kV. The micrographs were taken both on the surface of the samples and on cryogenically fractured samples that were coated with gold (Edwards S150 Sputter Coater) prior to microstructure examination. An Energy Dispersive X-ray Spectrometer (Edax DX4 and eDXi software) was used to analyze the composition of the surfaces of the samples.

The structure of the materials was also studied using micro-computed tomography (µ-CT), which is an efficient way to do non-destructive analysis of the structure. In this study, µ-CT imaging was employed to analyse pores inside the material. All the imagings were done by MicroXCT-400 (Xradia, Pleasanton, CA, USA) and the same imaging parameters were applied for every sample. 40 kV as source voltage was used and 150 µA as source current. The isometric voxel size was 2.2 µm. No filters were utilized. Reconstruction was done by using Xradia's XMReconstructor software. Images were segmented by manual thresholding using ImageJ (U.S. National Institutes of Health, Bethesda, Maryland, U.S.A). The same software was used for the analysis.

Results and discussion

The effects of processing and sterilization on the materials

Processing using the twin-screw extruder degraded the matrix polymer only slightly. The average weight average molecular weight (M_w) of the raw material was 229 000 g/mol and after processing the M_w was 227 000 g/mol. However, the sterilization using gamma irradiation with the measured dose of 28.7-34.0 kGy, caused significant degradation. The M_w of the plain, processed polymer decreased 14% and the M_n decreased 29% during sterilization. The M_w of the composites decreased 18-29% and M_n 31-43% with a tendency that gamma irradiation caused more degradation to those composites with higher β-TCP contents There is almost linear dependency of the percentual decrease in the molecular weights versus the β-TCP content in the samples, which is shown Figure 1. This may be attributed to the hydrophilicity of the β-TCP which may have caused slight water absorption to the material as it was not stored in totally dry conditions before sterilization. As a result, the composites with higher β-TCP content may have absorbed more water and thus were more degraded during

sterilization. It has also been suggested that gamma irradiation may cause not only chain scission in the polymer chains but also cross-linking for pure poly-ε-caprolactone (29). This would have been seen as a drop in the M_n and an increase in the M_w of the polymer. This kind of effect was not observed in this study. Gamma-irradiation caused a significant decrease both in number average and weight average molecular weights. This effect is well known on biodegradable polymers and is caused by the chain-scission of the polymer chain due to high energy gamma irradiation (30) It has been reported by other authors as well (31,32).

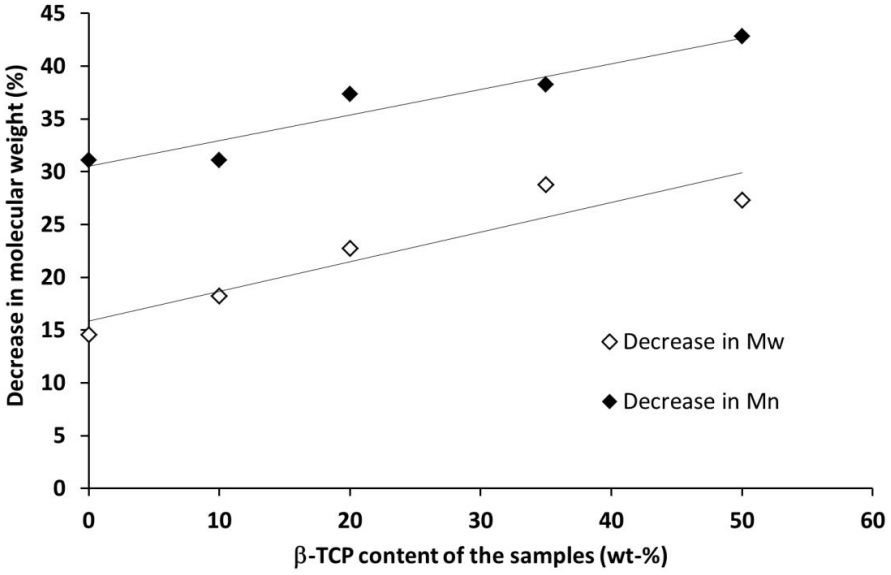

Figure 1. Decrease in weight average molecular weight (M_w) and number average molecular weight (M_n) during the sterilization step.

For the raw material, the residual monomer contents were 0.08 wt-% for the L-lactide monomer and below detection limit (<0.02 wt%) for the ε-caprolactone monomer. No increase was seen in the content of either monomer during the processing event which indicates that the polymer did not decrease during processing and thus no monomers were generated during processing. Because there were no differences in the monomer

contents of any of the manufactured materials, it can be assumed that the monomers did not cause differences in the hydrolytic degradation behaviour of the studied composites. (32).

In vitro degradation of the materials

Molecular structure

^{1}H NMR spectra were measured from five samples (PLCL raw material, PLCL 26 weeks *in vitro*, PLCL 52 weeks *in vitro*, PLCL + 50% TCP 26 weeks *in vitro* and PLCL + 50% TCP 52 weeks *in vitro*). The ^{1}H NMR spectrum of plain PLCL raw material and the assignment of the signals is presented in Figure 2. The signal of the -CH group proton of the lactide comonomer appeared at δ 5.16 as a multiplet. The signals of methyl protons of lactide and the aliphatic protons of caprolactone units (δ 0.5-1.8) were overlapping with each other and accurate integration of the peaks was not possible, and they were not included in the calculations. The most informative signals were the signals of the α-oxy methylene protons of the ε-caprolactone comonomer that appeared at δ 4.05-4.13 and were clearly split into two signals according to the position in the polymer chain. The triplet at δ 4.13 indicated the CH_2 group in the ε-caprolactone fragment bonded to an L-lactide unit and the broader multiplet at δ 4.05 indicates the α-oxy methylene group bonded to another ε-caprolactone unit. (33, 34) Additionally, the signal at δ 2.3-2.4 that corresponds to the signal of the methylene proton of the ε-caprolactone that is bonded to the carbonyl group was split the same way. The triplet at δ 2.4 indicates a group bonded to a L-lactide group and the broader multiplet at δ 2.3 corresponds to a group that is bonded to another ε-caprolactone group (33, 34).

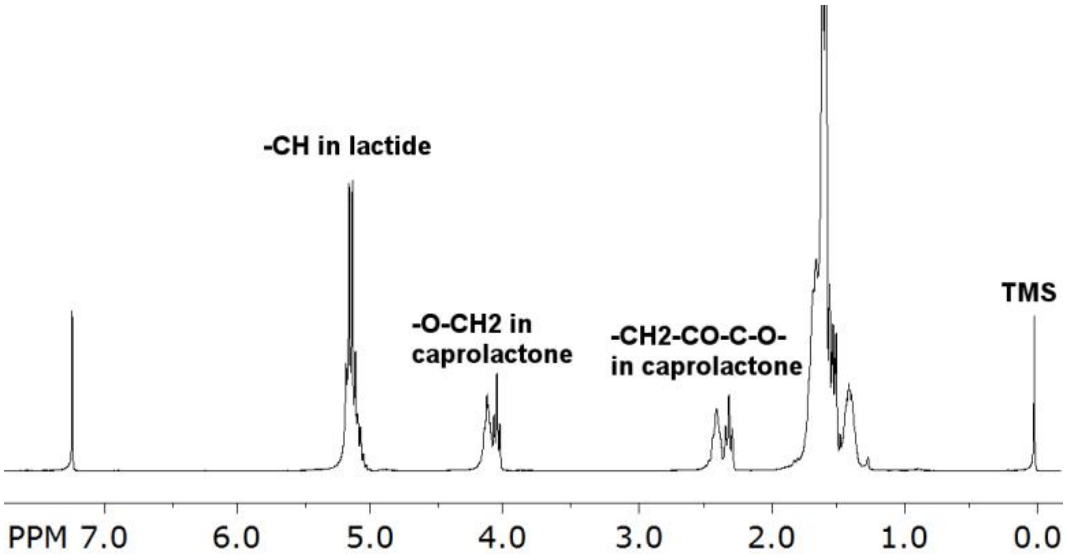

Figure 2. ^{1}H NMR spectrum of the raw material poly(L-lactide-co-ε-caprolactone).

The NMR results showed that the ratio of integrals for these two signals, and therefore the comonomer ratio, changed as the hydrolysis proceeded. The ratio of lactide to caprolactone (LA/CL) was increased from the initial proportion of the raw material 68/32 to 80/20 for the plain copolymer at 52 weeks and 75/25 for the composite containing 50% β-TCP at 52 weeks of hydrolysis. The comonomer ratios are presented in Table 1. The results of NMR measurements also demonstrated that the presence of β-TCP in the composite slowed down the change in the comonomer ratio. The change in the comonomer ratio of a copolymer of L-lactide and ε-caprolactone has also been observed by Jeong *et al.* (33). They suggested that the amorphous regions of the copolymer contain more caprolactone and are more easily attacked by water as water diffuses first into the amorphous regions of the polymer. Additionally, they found that the degradation and increase in the comonomer ratio LA/CL were slightly accelerated *in vivo*. The results of our studies indicate that although β-TCP does not affect the

degradation of the copolymer in a way that could be seen in the SEC measurements, it has an effect on which ester bonds the breaking of the polymer chain preferably occurs.

Table 1. Results of the ^{1}H NMR analysis.

Sample	Comonomer ratio (LA/CL)	Average sequence lengths		
		$\tilde{n}_{LA}$	$\tilde{n}_{CL}$	R
PLCL raw material	68/32	12.2	5.7	0.26
PLCL 26 wk hydrolysis	73/27	16.8	6.3	0.22
PLCL 52 wk hydrolysis	80/20	28.9	7.1	0.18
PLCL + 50% TCP 26 wk	69/31	14.1	6.3	0.23
PLCL + 50% TCP 52 wk	75/25	20.6	6.8	0.20

Because the properties of copolymers do not only depend on the comonomer composition but also on the distribution of the comonomers in the polymer chains, analysis of the microstructure of the polymer was also needed (35, 34). According to the text by Herbert (35), the number average sequence lengths of the comonomers can be calculated using Equations 1 and 2

$$\tilde{n}_{LA} = \frac{2(LA)}{(LA-CL)} \qquad (1)$$

$$\tilde{n}_{CL} = \frac{2(CL)}{(LA-CL)} \qquad (2)$$

where (LA) and (CL) are the molar fractions of the L-lactide and ε-caprolactone comonomers in the copolymer and (LA-CL) is the average dyad relative fraction, which can be calculated from the ^{1}H NMR data of the copolymer. The calculation is well explained in an article by Fernández (34). Additionally the randomness factor, R, can be calculated using the Equation 3

$$R = \frac{(LA-CL)}{2(LA)(CL)} \qquad (3)$$

The randomness factor is 1 for a random copolymer and 0 for a block copolymer (34). The results of the average sequence length calculations and the randomness factor are presented in Table 1.

First of all, the results show that the copolymer is rather blocky, having R values between 0.18-0.26, whereas the totally random copolymer would show the R value of 1. Randomness of the copolymers of lactides and ε-caprolactone are greatly affected by the polymerization conditions and depends on the polymerization temperature and time (13,15,30).

The randomness of the studied copolymer samples is decreased as the degradation proceeds. The average sequence lengths of the comonomers show that L-lactide tends to form long blocks. The notable increase in the average sequence length of the L-lactide comonomer as the degradation proceeds shows that the shorter blocks of the L-lactide are removed from the polymer chains as the copolymer is hydrolytically degraded. There is also a slight increase in the ε-caprolactone sequence length as the degradation proceeds, which indicates that the sequence length is not much affected by the hydrolytic degradation although the ε-caprolactone comonomer fraction in the copolymer is decreased.

The decrease of the randomness factor also supports the conclusion that the random parts of the copolymer are removed from the structure and more blocky structures remain as the degradation proceeds. In conclusion, the ^{1}H NMR analysis shows that the copolymer is blocky having some random parts in the structure but the random parts are removed as the hydrolytic degradation proceeds and the blocky characteristic of the

copolymer is increased. The bonds between the L-lactide and ε-caprolactone comonomers are most susceptible to hydrolytic degradation in this studied copolymer.

Molecular weights

The degradation of the composites was tested in Sörensen buffer solution, *in vitro* at 37°C and pH 7.4. The decrease of the molecular weights (both M_w and M_n) of the polymer matrix was rapid for the plain copolymer and for all the composites and obeys the first order kinetics with the degradation rate constants of $1.4 \cdot 10^{-3}$-$1.7 \cdot 10^{-3}$ 1/h. Although there were small differences in the molecular weights of the polymer matrix at the beginning of the hydrolysis test series, the degradation proceeded in all the composites following the same trend. There were no significant differences in the degradation behaviour during the 52-week test series between the different composites. The same kind of result was recently reported by Daculsi et al. (31) who studied composites of poly(96L/4D)lactide and β-TCP with β-TCP contents of 0, 10, and 24 wt-%. In our study, the M_n of all the composites had already decreased approximately 96% of the initial value of the raw material after 20 weeks of hydrolysis at 37°C in pH 7.4. After 52 weeks, the decrease was 99%. The M_n values of the samples as a function of time *in vitro* up to 20 weeks are presented in Figure 3. The rapid decrease of molecular weights is typically caused by random scission of the hydrolytically labile ester bonds of the polymer backbone. This happens first in the amorphous parts of the polymer. (36)

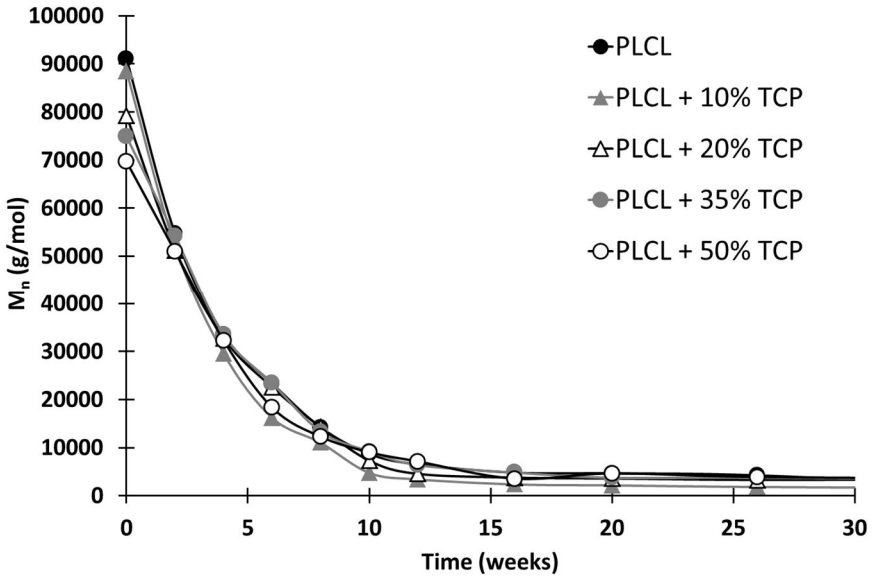

Figure 3. The number average molecular weight (M_n) of the composites of poly(L-lactide-co-e-caprolactone) (PLCL) 70/30 and β-tricalcium phosphate (β-TCP) as a function of time *in vitro* (n=2).

The SEC distribution plots showed bimodality after 20 weeks for all the composites and the plain copolymer except for the samples with 10 wt-% of initial β-TCP content that showed emerging bimodality at the time point of 39 weeks. An example of the emerging bimodality is shown in Figure 4, where 20, 26 and 39-week SEC results of PLCL + TCP 20% are shown.

Bimodality in the SEC distribution curve can be explained with the blocky structure of the copolymer, which is pronounced as the hydrolysis proceeds. The ^{1}H NMR analysis of the plain copolymer and PLCL + 50% TCP showed that the copolymer is rather blocky and the random parts are degrading first. This might cause an increase in a certain part of the SEC distribution curve as the blocky parts consisting mainly of L-lactide monomers remain in the copolymer and the amount of other parts in the copolymer is decreased.

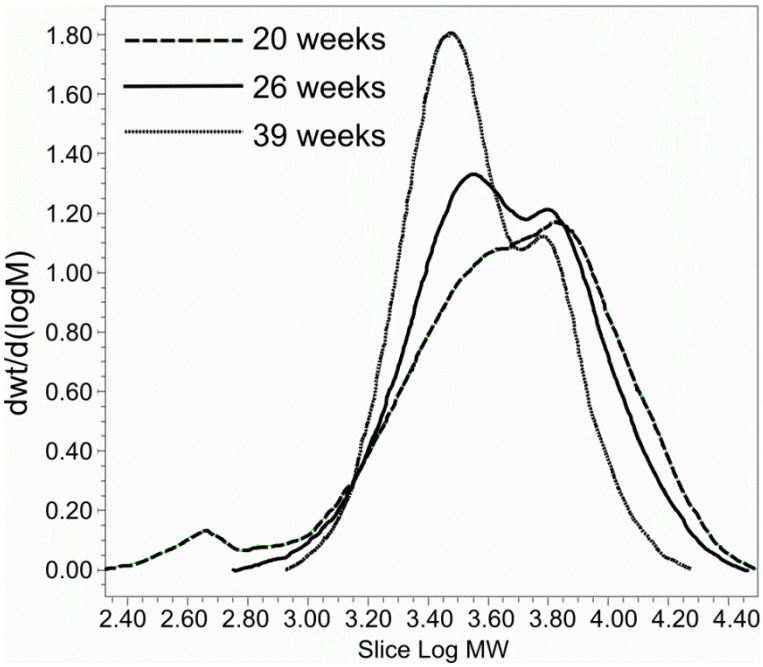

Figure 4. An example of the development of the bimodality in the size exclusion chromatography curves. The samples were poly(L-lactide-co-ε-caprolactone) (PLCL) + 20% tricalcium phosphate (TCP) at 20, 26 and 39 weeks.

Bimodality is often explained by the autocatalytic effect in the inner parts of the polymer (31,36-38), but it is not likely in this case because of the porous structure of the composites induced by the β-TCP granules in the structure, which enables the short chain degradation products to escape from the inner parts on the samples and thus do not catalyse the degradation reaction.

The polydispersity of the polymer matrix changed as the hydrolytic degradation proceeded (Figure 5). These changes are typical in the hydrolysis of biodegradable polymers. First, the molecular weight distribution was narrowed because chain scission reduced the number of long polymer chains. After reaching the lowest values at the 8-week time point, the molecular weight distribution widened because of the introduction of short polymer chains resulting from the chain scission. PD reached the highest value

at the time point of 12 weeks (1.8-2.7) and started to decrease again as the short molecular chains were short enough to be dissolved into the surrounding fluid.

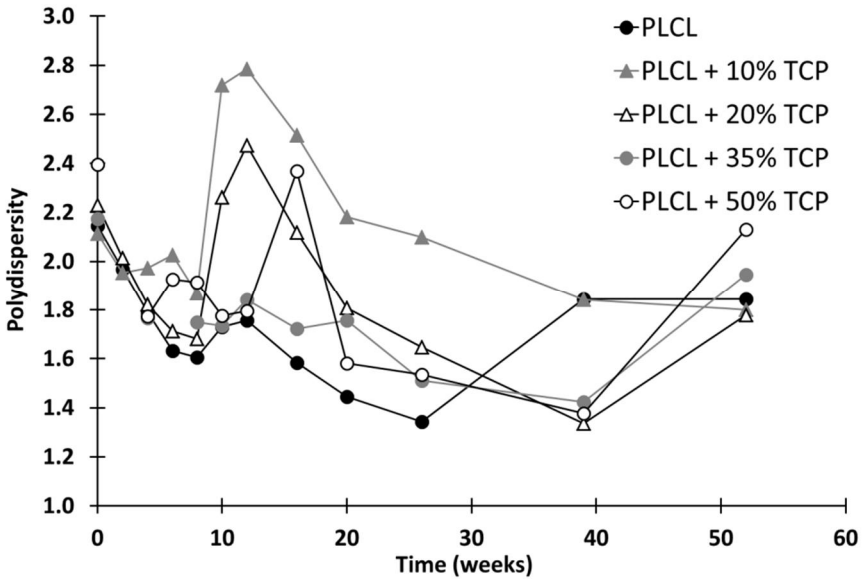

Figure 5. Development of the polydispersity of the poly(L-lactide-co-ε-caprolactone) (PLCL) during hydrolytic degradation of composites of PLCL and β-tricalcium phosphate (TCP).

Mass loss, water absorption and β-TCP content of the materials

The mass loss of the tested materials as a function of time *in vitro* is presented in Figure 6 along with the water absorption results. The mass loss of the plain copolymer was fastest and the mass loss of the composite containing 50% of β-TCP was slowest. This is because the polymer degrades and disappears from the composites and β-TCP dissolves slower than the polymer phase. This result is also supported by the phosphate dissolution test series, where very slow dissolution of β-TCP was observed. The results are shown in Figure 7 as cumulative dissolution of the phosphate ions. The maximum values of 1000-2500 μg of β-TCP at 52 weeks correspond to less than 10 wt-% of the total amount of β-TCP in the samples.

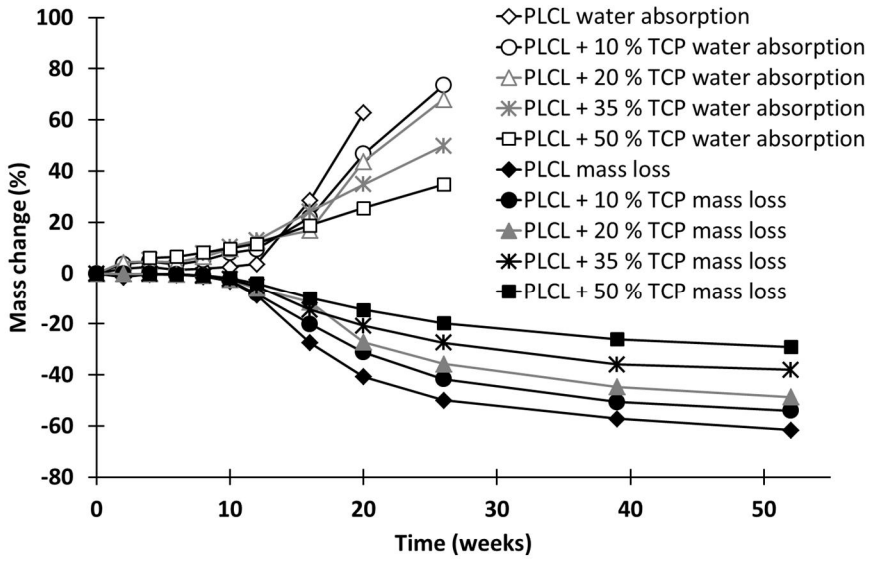

Figure 6. Mass loss and water absorption of the composites of poly(L-lactide-co-ε-caprolactone) (PLCL) and β-tricalcium phosphate (TCP) seen as gained weight as a function of time *in vitro*.

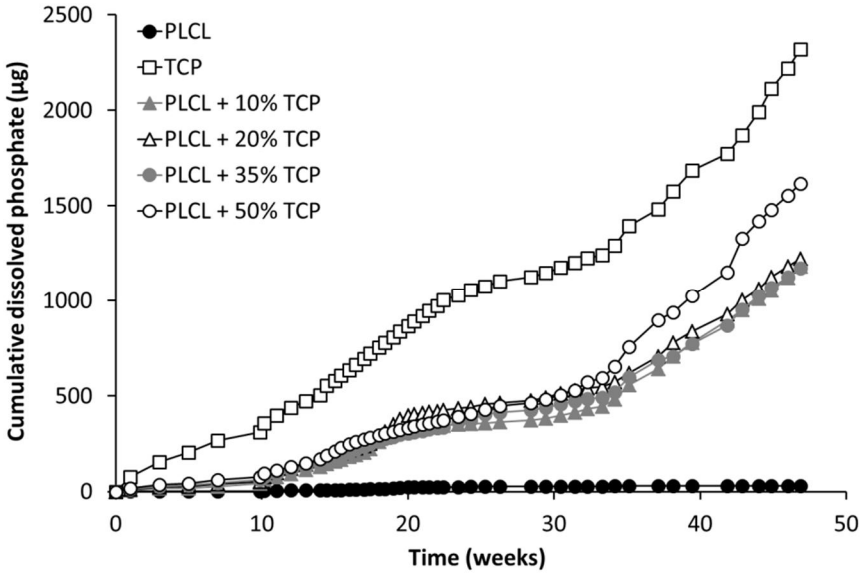

Figure 7. Dissolution of β-tricalcium phosphate (TCP) from the composites of poly(L-lactide-co-ε-caprolactone) (PLCL) and TCP. Plain PLCL was used as a negative and plain TCP as a positive control.

From the β-TCP content analysis, it can be seen that the increase in the β-TCP-content of the test samples started at the same time as the mass loss of the samples (i.e. after 10 weeks in hydrolysis) (Figure 8). At this time point, the M_w of the polymer had decreased to a level of 12000-15000 g/mol and the M_n to a level of 4000-9000 g/mol, which apparently enabled the start of mass loss. In earlier studies, (37) the mass loss of pure poly-ε-caprolactone had begun when the M_w had decreased to a level of 5000 g/mol and for pure poly-DL-lactide to a level of 15 000 g/mol.

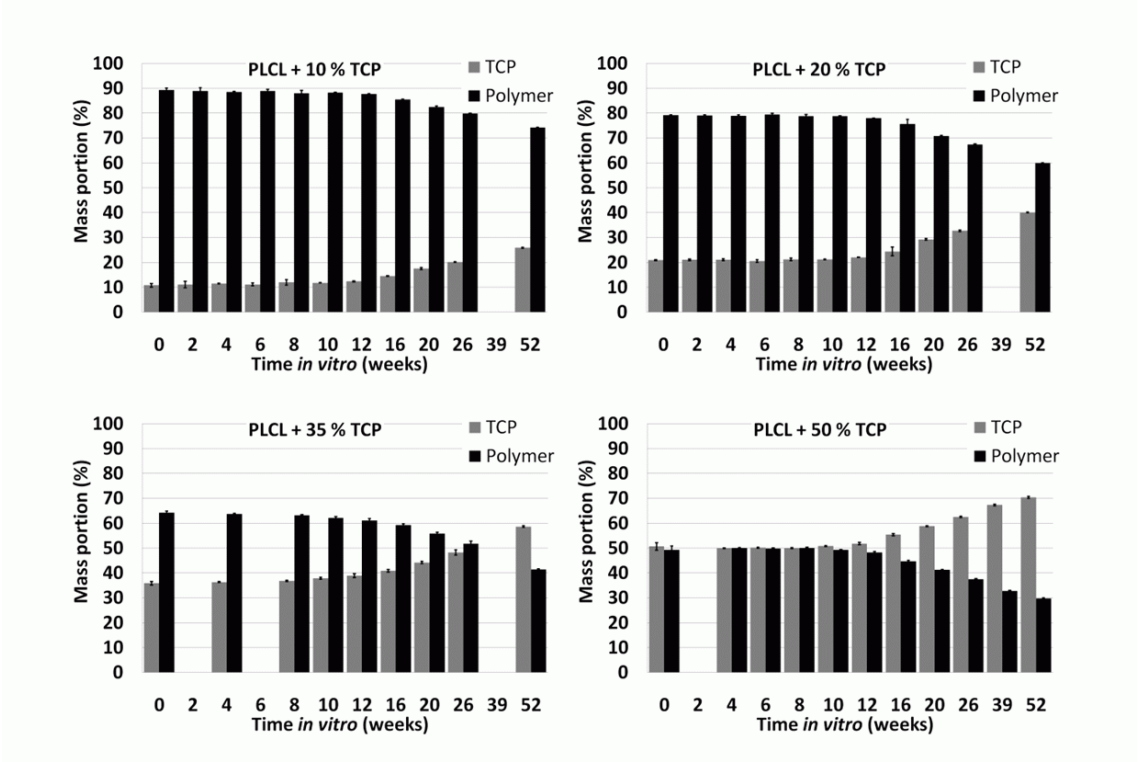

Figure 8. β-tricalcium phosphate (TCP)-contents of the composites of poly(L-lactide-co-ε-caprolactone) (PLCL) and TCP as a function of time *in vitro*. Results shown as averages with standard deviations (n=5).

The increase in β-TCP content of the composites was very clear and the fact that polymer degraded and was lost from the composites may be beneficial in the desired end application of this kind of composite material. β-TCP is left in the bone cavity and as it is known to be an osteoconductive material (1), it may enhance bone ingrowth and healing.

When only the polymer component in the composites was considered, the mass loss was slightly decelerated by increasing β-TCP content. At the time point of 52 weeks, the mass loss of the polymer component of the composites was 62% for plain PLCL and 57% for the composite containing 50 % β-TCP. The mass losses of the polymer composites containing 10-35% of β-TCP fell between these values.

Water absorption, which indicates the hydrophilicity of the material, of all the tested samples was small during the first ten weeks *in vitro* (Figure 6). It is well known that water diffuses first into the amorphous parts of the polymer and causes degradation. (30). The composites containing β-TCP showed greater water absorption than the pure copolymer in the first 12 weeks of the test series, after which the behaviour was changed. The water absorption of the plain polymer increased rapidly and at 20 weeks the water absorption of the plain polymer was already over 60 wt-%. After this time point, the wet masses of the plain polymer test samples were not measurable anymore. From the 12-week time point on, the water absorption of the composites with high β-TCP contents was less than for the composites with low β-TCP contents. The wet masses of the composites were measurable up to 26 weeks. Since TCP is hydrophilic, the composites with high β-TCP contents absorbed more water in the beginning of the *in vitro* time than pure polymer or the composites with less β-TCP. When the polymer

degradation had proceeded to a certain level i.e. the polymer chain scission had reached the point when mass loss is possible and there were more hydrophilic end groups of the polymer, the water absorption behaviour changed and the composites with no or little β-TCP absorbed more water.

Changes in pH of the buffer solution

The pH-values of the buffer solution in the *in vitro* test series were measured periodically and the buffer solution was changed (20 ml) every two weeks at the beginning of the test series. once a week after 10 weeks, and twice a week after the time point of 16 weeks. The pH mainly retained values between 7.2-7.5 and the pH was very stable in the first weeks of the test series. The results of the pH measurements are presented in Figure 9. A significant decrease in the pH-values was observed from the 10^{th} week to the 19^{th} week of the test series. At the 10-week time point, the M_w had decreased to a level of 12 000 - 15 000 g/mol for all the composites and the plain copolymer and mass loss started. This was seen as the decrease in the pH values because the acidic degradation products of the polymer degradation were released to the hydrolysis medium. Throughout the *in vitro* test series, a tendency of increasing pH-value towards the composites with higher β-TCP contents was observed. This is likely due to the buffering effect of the β-TCP that has also been observed earlier by other authors (39,40).

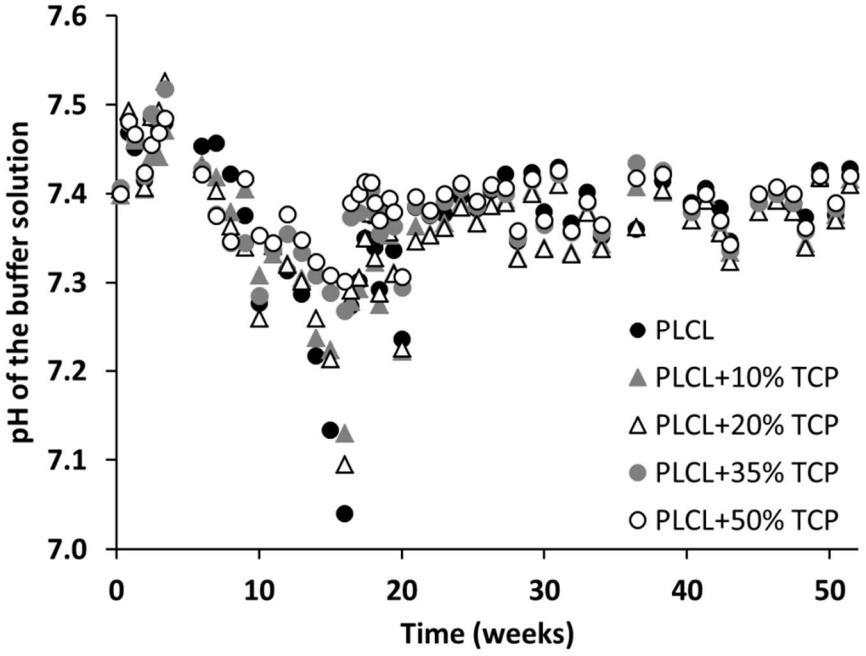

Figure 9. Results of the pH measurements in the *in vitro* degradation test series of composites of poly(L-lactide-co-ε-caprolactone) (PLCL) and β-tricalcium phosphate (TCP).

Bernstein *et al.* (3) reported results where composites of nanosized tricalcium phosphate and polycaprolactone with very high β-TCP contents (85 vol-% and 95 vol-%) showed the same kind of dissolution behaviour as pure β-TCP. They also proposed that β-TCP may enhance the hydrolytic degradation of polycaprolactone due to the increased hydrophilicity. On the other hand, a buffering effect of the dissolution products of β-TCP against the acidic degradation products of the polymer has been proposed (39,40). This would lead to the slower degradation of the polymer component in the composite. These two factors work in opposite ways and, if simultaneous, their overall effect on the degradation may be evened out. In this study, no significant differences in the hydrolytic degradation behaviour of the studied composites compared with the plain poly(L-lactide-co-caprolactone) copolymer were observed.

Thermal properties

T_g, T_m and ΔH_f were measured using a differential scanning calorimeter (DSC) at a temperature range from -60°C to 200°C with a 20°C/min heating rate. The T_gs of the raw material determined during the first and second heating were 15°C and 23°C respectively. This corresponds quite well with the results of Ragaert *et al.* for the same commercial polymer (41). After processing, the T_gs (obtained from the second heating) of all the composites and the pure copolymer were between 21°C and 22°C. DSC analysis revealed changes in the T_g as the hydrolysis proceeded. This can be seen in Figure 10, where the values from the second heating cycle are presented. The T_g started to decrease in the beginning of the *in vitro* test series and reached the lowest values at the 12-week time point (9°C – 14°C). During the same time period, the molecular weights of the samples decreased rapidly and this had a decreasing effect on the T_g. After 12 weeks, the T_gs started to increase and ended up at 34°C for the pure copolymer and at around 30-33°C for the composites at the 52-week time point. The T_gs of the samples were detectable only on the second heating scan from the 16-week time point on. At this point, the degradation of the polymers had proceeded to M_ws of less than 10 000 g/mol. The ^{1}H NMR results showed that the caprolactone monomers disappeared from the copolymer as the hydrolysis went on and, therefore, L-lactide content increased. It is well known that the T_g is dependent on the comonomer composition of the copolymer. In the case of copolymers of lactide and ε-caprolactone, the T_g increases as the lactide content in the copolymer increases (42). The change in the T_g is significant even in small increments in the lactide content.

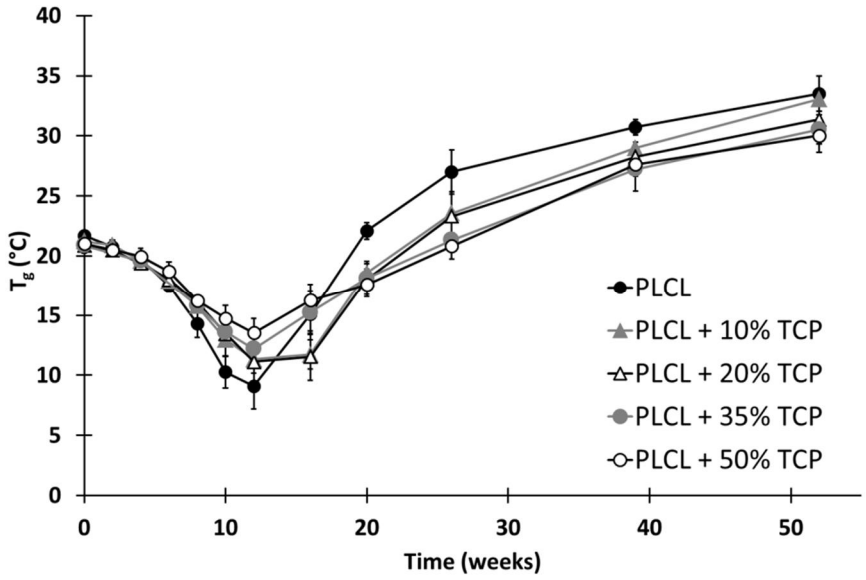

Figure 10. Glass transition temperatures (T_g) of composites of poly(L-lactide-co-ε-caprolactone) (PLCL) and β-tricalcium phosphate (TCP) as a function of time *in vitro*. Results shown as averages with standard deviations (n=5).

T_ms and ΔH_fs were analyzed from the first heating of the samples. This was done because during the second heating the melting peaks did not appear anymore due to the fast cooling in the DSC analysis in which the polymer solidifies to an amorphous structure. The samples showed bimodality in the melting peaks from the 6-week time point on and the bimodality was seen especially clearly in the samples from the 16-week time point on until the 39-week time point. This can be due to two different kinds of crystals in the sample (43). More probable reason for this according to Sarasua *et al.* (43) is the annealing during DSC scan, where imperfect crystals might have time to melt and recrystallize and then melt again in a few degrees higher temperature. It was observed that the melting temperatures increased from the 111-113°C at the 2-week time point to 116-120°C at the 16-week time point. After this, the melting temperatures decreased constantly and they were 107-110°C at the 52-week time point.

Increasing melting enthalpies were recorded throughout the test series (Figure 11). The values were corrected to correspond to the polymer portion of the samples. They indicated increasing crystallinity as the amorphous parts of the polymer are the first to degrade. Also, the fact that shorter polymer chains can more easily rearrange themselves into crystals has an effect on the increasing crystallinity. The increase in crystallinity was largest in the plain copolymer and lowest in the composite containing 50 % of β-TCP. Absolute crystallinity values were not calculated because the theoretical value of 100% crystalline poly(L-lactide-co-ε-caprolactone) 70/30 was not available. It has been reported that the sequence length of 14 is required for lactides to be able to crystallize (43). Additionally, it has also been suggested that in a copolymer of L-lactide and ε-caprolactone, only the L-lactide is able to form crystals. These factors also explain the increasing crystallinity as the L-lactide fraction in the copolymer is increased during *in vitro* degradation.

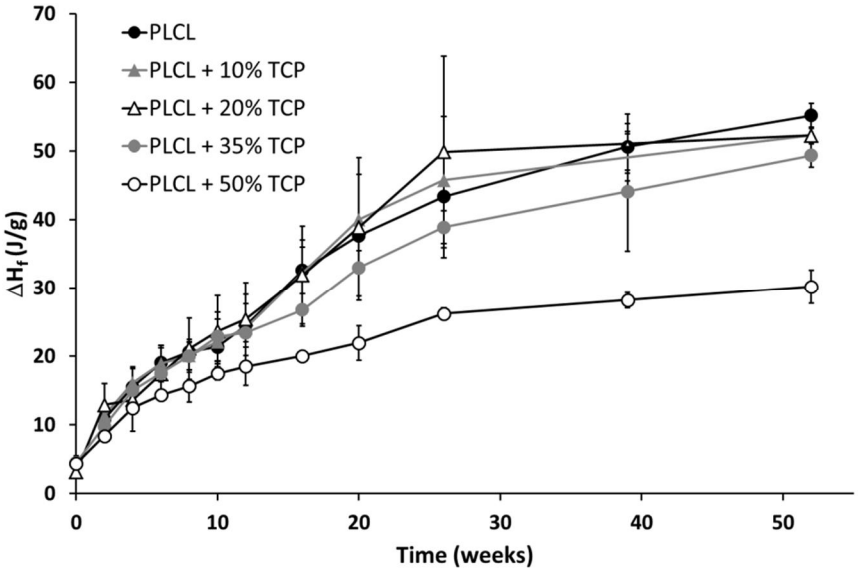

Figure 11. Melting enthalpies (ΔH_f) of the composites of poly(L-lactide-co-ε-caprolactone) (PLCL) and β-tricalcium phosphate (TCP) as a function of time *in vitro*. Results shown as averages with standard deviations (n=5).

Microstucture

SEM micrographs, which were taken both on the surface of the samples and on cryogenically fractured samples, showed some porosity in all the samples. The micrographs of the surface and cross section of composites containing 50% β-TCP are shown in Figure 12. The appearance of the composites changed when the hydrolysis proceeded and the formation of smaller pores was observed. The majority of the pores were however smaller than 100 μm, and according to the literature, this is not enough to enhance bone ingrowth (44).

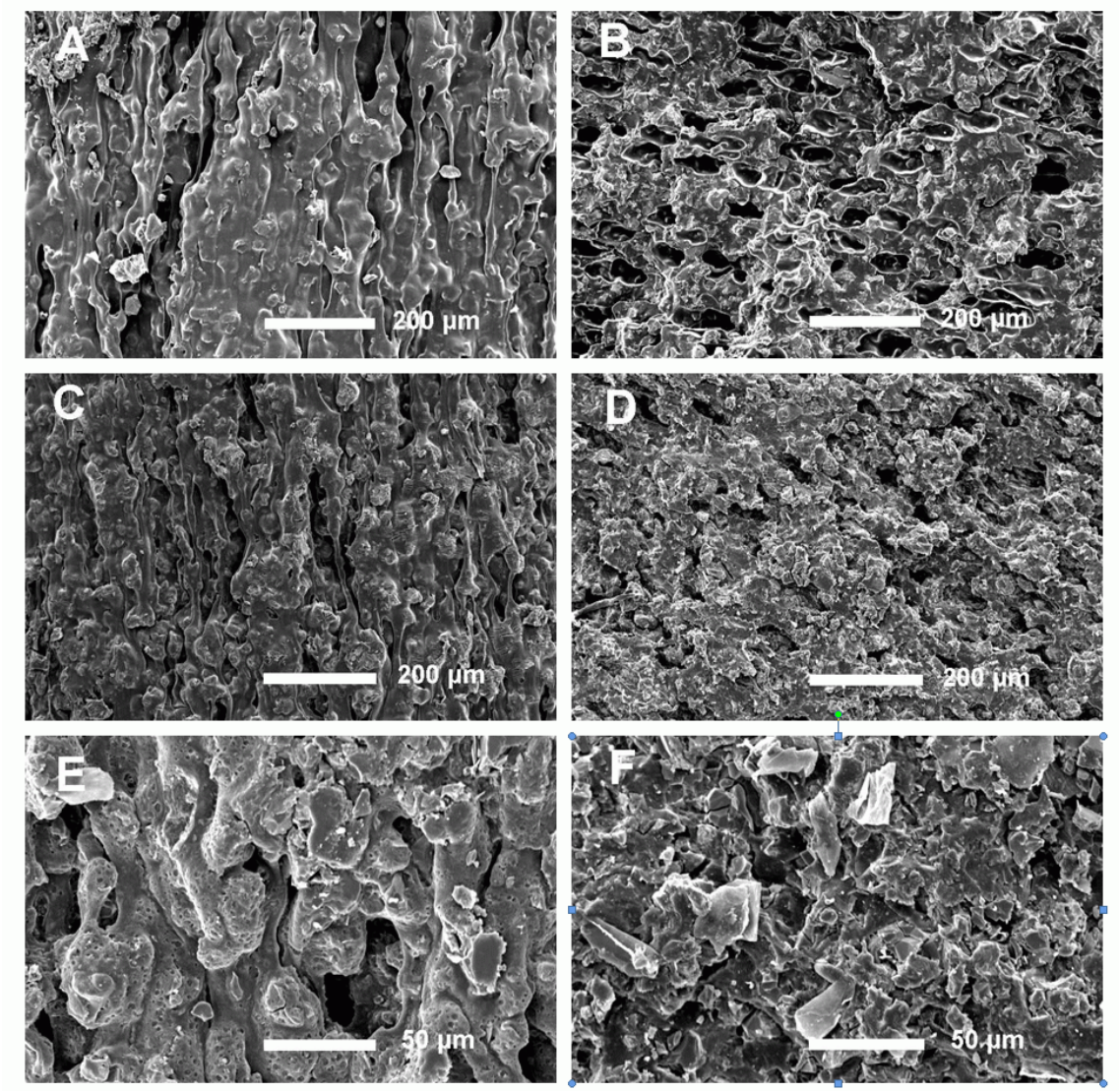

Figure 12. Scanning electron microscopy (SEM) micrographs of the composites of poly(L-lactide-co-ε-caprolactone) (PLCL) and β-tricalcium phosphate (TCP) containing 50 wt-% of TCP. (A) surface at 0 weeks, (B) cross section at 0 weeks, (C) surface at 26 weeks, (D) cross section at 26 weeks, (E) surface at 52 weeks and (F) cross section at 52 weeks (E and F are at higher magnification).

The porosity of the samples containing 50 % of β-TCP (at 0, 26 and 52 weeks) was additionally imaged using µ-CT. Examples of the imaging are shown as Figure 13. The analysis showed surprisingly that the porosity decreased in the samples during

hydrolysis test series. The porosity analysis results are presented as Table 2. Overall, the pore sizes and the porosity values were very small. Additionally, the pores were generally not interconnected. There may however reside an artefact in this analysis, because the samples were imaged dry. If the imaging would have been done wet, right after the samples were withdrawn from the incubator shaker, the results might have been different, because the samples may shrink during drying.

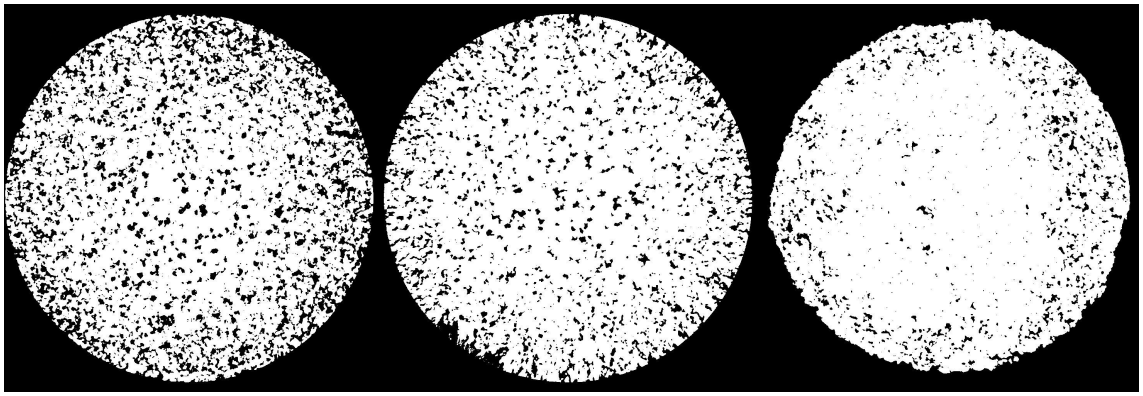

Figure 13. Micro-computed tomography (μ-CT) imaging of samples of poly(L-lactide-co-ε-caprolactone) (PLCL) and β-tricalcium phosphate (TCP) containing 50% of TCP at 0 weeks (left), 26 weeks (middle), and 52 weeks (right).

Table 2. Results of the porosity analysis

Sample name	Porosity (%)	Mean pore size (μm)
PLCL + 50% TCP 0 weeks	10.5	16.10
PLCL + 50% TCP 26 weeks	7.6	13.16
PLCL + 50% TCP 52 weeks	2.6	9.82

The EDS analysis was performed both on the outer surfaces of the samples and the cryogenically fractured surfaces of the samples. It showed that there were no significant differences in the Ca/P ratio of the β-TCP. If β-TCP was dissolved and precipitated again as hydroxyapatite, the Ca/P molar ratio would have increased (it is initially 1.67 for hydroxyapatite and 1.5 for β-TCP) (1). However, this was not seen in the results of the EDS analysis. It should be noted that Sörensen phosphate buffer solution was used in our study, and bioactivity studies are usually performed using simulated body fluid as the buffer solution (26). Similar kinds of composites comprising poly-α-hydroxy acids and β-TCP have been reported to show bioactivity that has been observed as the formation of hydroxyapatite on the surface of the composites when simulated body fluid has been used in *in vitro* studies as the buffer solution (2,3,26).

There were also very small amounts of sodium and potassium present in the samples that had been in hydrolysis for over 26 weeks. Na and K ions are present in the Sörensen phosphate buffer solution and have most likely not been totally washed from the samples during the rinsing of the samples with distilled water before drying.

Conclusions

Composites of poly(L-lactide-co-ε-caprolactone) with an initial comonomer ratio of 70/30 and β-tricalcium phosphate were studied in a long-term *in vitro* test series for up to 52 weeks. The degradation was studied and the effect of β-TCP on the degradation of the composites was evaluated using various analysis methods.

β-TCP had only a slight effect on the degradation properties of the composites studied and the effect on the degradation properties was mainly seen in the water absorption behaviour, as β-TCP dissolution was very slow in comparison with the copolymer

degradation. Mass loss and water absorption behaviour were significantly changed at 12 weeks *in vitro*. At this point, the molecular weight of the polymer had decreased to a level that enables mass loss.

Although the degradation of the tested composites proceeded similarly, there was a slight buffering effect of β-TCP seen throughout the *in vitro* test series in the pH values of the hydrolysis medium. The effect of β-TCP on the degradation was also seen in ^{1}H NMR analysis. It showed that the presence of β-TCP in the composites decelerated the change in the comonomer ratio as the hydrolysis proceeded. Additionally, the copolymer was noticed to have rather blocky structure, where the more amorphous parts degraded first leaving crystalline parts consisting mainly of L-lactide blocks in the structure.

For the end use in bone applications, it is desirable that the polymer degrades relatively quickly, leaving the β-TCP-particles behind to promote bone healing. The results presented here show that the β-TCP content of the tested materials was constantly increased throughout the *in vitro* test series. Additionally, it was shown that even high β-TCP contents can be compounded in the poly(L-lactide-co-ε-caprolactone) 70/30 copolymer without significant effect on the degradation of the polymer. These composite materials show good processability, handling properties, and potential to be used as bone filling materials. In addition, the processing method is easy to scale up to commercial scale.

Acknowledgements

Research collaboration with Bioretec Ltd. and financial support from the Finnish Funding Agency for Technology and Innovation and National Graduate School of Musculoskeletal Disorders and Biomaterials (N.A and M.V) are gratefully appreciated. Mrs. Raija Reinikainen, Ms. Eija Ahonen, M.Sc. Vuokko Heino, M.Sc. Noora Männistö, M.Sc. Kalle Räsänen and Ms. Inari Lyyra are warmly thanked for their technical assistance.

References

(1) Kamitakahara M, Ohtsuki C, Miyazaki T. Review paper: Behavior of ceramic biomaterials derived from tricalcium phosphate in physiological condition. J Biomater Appl 2008;23(3):197-212.

(2) Huttunen M, Ashammakhi N, Törmälä P, Kellomäki M. Fibre reinforced bioresorbable composites for spinal surgery. Acta Biomater 2006;2(5):575-587.

(3) Bernstein M, Gotman I, Makarov C, Phadke A, Radin S, Ducheyne P, et al. Low temperature fabrication of β-TCP-PCL nanocomposites for bone implants. Adv Eng Mater 2010;12(8).

(4) Neumann M, Epple M. Composites of calcium phosphate and polymers as bone substitution materials. Eur J Trauma 2006;32(2):125-131.

(5) Niemelä T, Kellomäki M, Törmälä P. In vitro Degradation of Osteoconductive Poly-L/DL-lactide/β-TCP composites. Key Eng Mat 2004 6 November 2003 through 9 November 2003;254-256:509-512.

(6) Ignjatovic N, Uskokovic D. Synthesis and application of hydroxyapatite/polylactide composite biomaterial. Appl Surf Sci 2004 13 October 2003 through 18 October 2003;238(1-4 SPEC. ISS.):314-319.

(7) Lam CXF, Teoh SH, Hutmacher DW. Comparison of the degradation of polycaprolactone and polycaprolactone-(β-tricalcium phosphate) scaffolds in alkaline medium. Polym Int 2007;56(6):718-728.

(8) Ogose A, Kondo N, Umezu H, Hotta T, Kawashima H, Tokunaga K, et al. Histological assessment in grafts of highly purified beta-tricalcium phosphate (OSferion®) in human bones. Biomaterials 2006;27(8):1542-1549.

(9) Bohner M. Calcium orthophosphates in medicine: From ceramics to calcium phosphate cements. Injury 2000;31(SUPPL. 4):D37-D47.

(10) Aunoble S, Clément D, Frayssinet P, Harmand MF, Le Huec JC. Biological performance of a new β-TCP/PLLA composite material for applications in spine surgery: In vitro and in vivo studies. J Biomed Mater Res Part A 2006;78(2):416-422.

(11) Puppi D, Chiellini F, Piras AM, Chiellini E. Polymeric materials for bone and cartilage repair. Prog Polym Sci (Oxford) 2010;35(4):403-440.

(12) Malin M, Hiljanen-Vainio M, Karjalainen T, Seppälä J. Biodegradable lactone copolymers. II. Hydrolytic study of ε-caprolactone and lactide copolymers. J Appl Polym Sci 1996;59(8):1289-1298.

(13) Hiljanen-Vainio M, Karjalainen T, Seppälä J. Biodegradable lactone copolymers. I. Characterization and mechanical behavior of ε-caprolactone and lactide copolymers. J Appl Polym Sci 1996;59(8):1281-1288.

(14) Karjalainen T, Hiljanen-Vainio M, Malin M, Seppälä J. Biodegradable lactone copolymers. III. Mechanical properties of ε-caprolactone and lactide copolymers after hydrolysis in vitro. J Appl Polym Sci 1996;59(8):1299-1304.

(15) Hiljanen-Vainio MP, Orava PA, Seppala JV. Properties of ε-caprolactone/DL-lactide (ε-CL/DL-LA) copolymers with a minor ε-CL content. J Biomed Mater Res 1997;34(1):39-46.

(16) Woodruff MA, Hutmacher DW. The return of a forgotten polymer - Polycaprolactone in the 21st century. Prog Polym Sci (Oxford) 2010;35(10):1217-1256.

(17) Ahola N, Rich J, Karjalainen T, Seppala J. Release of ibuprofen from poly(epsilon-caprolactone-co-D,L-lactide) and simulation of the release. J Appl Polym Sci 2003;88:1279-1288.

(18) Rich J, Karjalainen T, Ahjopalo L, Seppala J. Model compound release from DL-lactide/epsilon-caprolactone copolymers and evaluation of specific interactions by molecular modeling. J Appl Polym Sci 2002;86:1-9.

(19) Guarino V, Ambrosio L. The synergic effect of polylactide fiber and calcium phosphate particle reinforcement in poly ε-caprolactone-based composite scaffolds. Acta Biomater 2008;4(6):1778-1787.

(20) Fabbri P, Cannillo V, Sola A, Dorigato A, Chiellini F. Highly porous polycaprolactone-45S5 Bioglass® scaffolds for bone tissue engineering. Compos Sci Technol 2010;70(13):1869-1878.

(21) Erdemli O, Çaptug O, Bilgili H, Orhan D, Tezcaner A, Keskin D. In vitro and in vivo evaluation of the effects of demineralized bone matrix or calcium sulfate addition to polycaprolactone-bioglass composites. J Mater Sci Mater Med 2010;21(1):295-308.

(22) Deng C, Yao N, Lu X, Qu S, Feng B, Weng J, et al. Comparison of Ca/P mineralization on the surfaces of poly (ε-caprolactone) composites filled with silane-modified nano-apatite. J Mater Sci 2009;44(16):4394-4398.

(23) Song H-, Van Quang D, Min Y, Lee B. Effect of the addition of t-ZrO2 on the material properties of β-TCP/PCL composites. J Mater Sci 2008;43(13):4450-4454.

(24) Xiao X, Liu R, Huang Q, Ding X. Preparation and characterization of hydroxyapatite/polycaprolactone- chitosan composites. J Mater Sci Mater Med 2009;20(12):2375-2383.

(25) Yeo A, Rai B, Sju E, Cheong JJ, Teoh SH. The degradation profile of novel, bioresorbable PCL-TCP scaffolds: An in vitro and in vivo study. J Biomed Mater Res Part A 2008;84(1):208-218.

(26) Lei Y, Rai B, Ho KH, Teoh SH. In vitro degradation of novel bioactive polycaprolactone-20% tricalcium phosphate composite scaffolds for bone engineering. Mater.Sci.Eng.C 2007;27(2):293-298.

(27) ISO 15814. Implants for surgery – Copolymers and blends based in polylactide – *In vitro* degradation testing.

(28) ISO 6878. Water quality - Determination of phosphorus - Ammonium molybdate spectrometric method.

(29) Cottam E, Hukins DWL, Lee K, Hewitt C, Jenkins MJ. Effect of sterilisation by gamma irradiation on the ability of polycaprolactone (PCL) to act as a scaffold material. Med Eng Phys 2009;31(2):221-226.

(30) Södergård A, Stolt M. Properties of lactic acid based polymers and their correlation with composition. Prog Polym Sci (Oxford) 2002;27(6):1123-1163.

(31) Daculsi G, Goyenvalle E, Cognet R, Aguado E, Suokas EO. Osteoconductive properties of poly(96L/4D-lactide)/beta-tricalcium phosphate in long term animal model. Biomaterials 2011;32(12):3166-3177.

(32) Paakinaho K, Ellä V, Syrjälä S, Kellomäki M. Melt spinning of poly(l/d)lactide 96/4: Effects of molecular weight and melt processing on hydrolytic degradation. Polym Degradation Stab 2009;94(3):438-442.

(33) In Jeong S, Kim B, Lee YM, Ihn KJ, Kim SH, Kim YH. Morphology of elastic poly(L-lactide-co-ε-caprolactone) copolymers and in vitro and in vivo degradation behavior of their scaffolds. Biomacromolecules 2004;5(4):1303-1309.

(34) Fernández J, Etxeberria A, Sarasua J-. Synthesis, structure and properties of poly(L-lactide-co-ε-caprolactone) statistical copolymers. J Mech Behav Biomed Mater 2012;9:100-112.

(35) Herbert IR. Statistical analysis of copolymer sequence distribution. In: Ibbet RN, editor. NMR Spectroscopy of Polymers London: Blackie Academic & Professional; 1993. p. 50-79.

(36) Li S. Hydrolytic degradation characteristics of aliphatic polyesters derived from lactic and glycolic acids. J Biomed Mater Res 1999;48(3):342-353.

(37) Sawhney AS, Hubbell JA. Rapidly degraded terpolymers of dl-lactide, glycolide, and ε-caprolactone with increased hydrophilicity by copolymerization with polyethers. J Biomed Mater Res 1990;24(10):1397-1411.

(38) Li S, Garreau H, Vert M. Structure-property relationships in the case of the degradation of massive poly(α-hydroxy acids) in aqueous media - Part 3 Influence of the morphology of poly(l-lactic acid). J Mater Sci: Mater Med 1990;1(4):198-206.

(39) Lin F, Chen T, Lin C, Lee C. The merit of sintered PDLLA/TCP composites in management of bone fracture internal fixation. Artif Organs 1999;23(2):186-194.

(40) Ara M, Watanabe M, Imai Y. Effect of blending calcium compounds on hydrolytic degradation of poly(DL-lactic acid-co-glycolic acid). Biomaterials 2002;23(12):2479-2483.

(41) Ragaert K, Dekeyser A, Cardon L, Degrieck J. Quantification of thermal material degradation during the processing of biomedical thermoplastics. J Appl Polym Sci 2011;120(5):2872-2880.

(42) Pitt CG. Poly- ε-caprolactone and its copolymers In: Chasin M, Langer R, editors. Biodegradable Polymers as Drug Delivery Systems New York: Marcel Dekker Inc.; 1990. p. 71-120.

(43) Sarasua J, Prud'homme RE, Wisniewski M, Le Borgne A, Spassky N. Crystallization and melting behavior of polylactides. Macromolecules 1998;31(12):3895-3905.

(44) Shore EC, Holmes E. Porous Hydroxyapatite. In: Hench LL, Wilson J, editors. An Introduction to Bioceramics Singapore: World Scientific Publishing; 1993. p. 181-198.

Publication II

Ahola, N., Männistö, N., Veiranto, M., Karp, M., Rich, J., Efimov, A., Seppälä, J. and Kellomäki, M.

An in vitro study of composites of poly(L-lactide-co-ε-caprolactone), β-tricalcium phosphate and ciprofloxacin intended for local treatment of osteomyelitis

Biomatter, 3 (2013), e23162

RESEARCH PAPER

Biomatter 3:2, e23162; April/May/June 2013; © 2013 Landes Bioscience

An in vitro study of composites of poly(L-lactide-co-ε-caprolactone), β-tricalcium phosphate and ciprofloxacin intended for local treatment of osteomyelitis

Niina Ahola,[1,2,*] Noora Männistö,[1] Minna Veiranto,[1,3] Matti Karp,[4] Jaana Rich,[5] Alexander Efimov,[4] Jukka Seppälä[5] and Minna Kellomäki[1,2]

[1]Department of Biomedical Engineering; Tampere University of Technology; Tampere, Finland; [2]BioMediTech; Tampere, Finland; [3]Bioretec Ltd.; Tampere, Finland; [4]Department of Chemistry and Bioengineering Tampere; University of Technology; Tampere, Finland; [5]Department of Biotechnology and Chemical Technology; School of Chemical Technology; Aalto University; Espoo, Finland

Keywords: controlled drug delivery, ciprofloxacin, antibiotic, biodegradable, composite, poly(L-lactide-co-caprolactone)

Osteomyelitis is a bacterial disease that can become chronic, and treatment often includes a surgical operation to remove infected bone. The aim of this study was to develop and investigate in vitro bone filling composite materials that release ciprofloxacin to kill any remaining bacteria and contain bioceramic to help the bone to heal. Three composites of poly(L-lactide-co-ε-caprolactone), β-tricalcium phosphate and ciprofloxacin were compounded using twin-screw extrusion and sterilized by gamma irradiation. Drug release and degradation of the composites were investigated in vitro for 52 weeks. The composite with 50 wt% of β-TCP had the most promising ciprofloxacin release profile. The ceramic component accelerated the drug release that occurred in three phases obeying first-order kinetics. Inhibition zone testing using bioluminescence showed that the released ciprofloxacin had effect in eradicating a common osteomyelitis causing bacteria *Pseudomonas aeruginosa*. During the in vitro degradation test series, molar weight of the polymer matrix of the composites decreased rapidly. Additionally, ^{1}H-NMR analysis showed that the polymer had blocky structure and the comonomer ratio changed during hydrolysis. The tested composites showed great potential to be developed into bone filler materials for the treatment of osteomyelitis or other bone related infections.

Introduction

The objective of this work was to develop ciprofloxacin releasing and bioabsorbable bone defect filler material that also contains a ceramic component to aid bone healing. In this study, the in vitro drug release and degradation behavior of biodegradable ciprofloxacin releasing bone filling material, which has high β-TCP content of up to 60 wt%, for enhanced osteoconductivity, was investigated. Additionally, the effect of the released antibiotic against a common osteomyelitis causing bacteria *Pseudomonas aeruginosa* was tested using the bioluminescence method. The required length of the controlled antibiotic delivery is from three to six months. This length of time is considered adequate in the treatment of osteomyelitis.[1] Furthermore, the degradation of the fillers should occur within a similar time frame.

Osteomyelitis is a severe complication that is challenging to treat. It is caused by bacteria, commonly *Staphylococcus aureus*, *Pseudomonas aeruginosa* or *Staphylococcus epidermidis* and leads to bone destruction.[2] Traditionally, osteomyelitis is treated by surgical debridement of the infected tissues followed by a long course of intravenous or parenteral antibiotics.[3-6] Fractures, especially open ones, implant surfaces, and external fracture fixations are examples of situations that are known to enhance bacterial adhesion. These conditions, if left untreated, may lead to a biofilm formation and osteomyelitis. These problems have been addressed in numerous reviews.[7-9]

The surgical debridement of the infected bone in the treating of osteomyelitis creates a defect in the bone called a dead space. Because bacteria may remain in the surrounding tissues, antibiotics are also needed in the treatment. Adequate concentrations of the antibiotic on the site of the dead space are difficult to achieve due to the poor circulation of blood in the infected bone tissue. Local delivery of the antibiotics provides an efficient way of delivering the drug in situ and achieving therapeutic levels of the drug. One of the greatest advantages in local drug therapy is that systemic adverse effects are avoided.[10,11] The challenge is to keep the drug concentration at the therapeutic level and not to exceed toxic levels. Previous studies have shown that with local treatment, the

*Correspondence to: Niina Ahola; Email: niina.ahola@tut.fi
Submitted: 08/08/12; Revised: 11/21/12; Accepted: 12/07/12
Citation: Ahola N, Männistö N, Veiranto M, Karp M, Rich J, Efimov A, et al. An in vitro study of composites of poly(L-lactide-co-ε-caprolactone), β-tricalcium phosphate and ciprofloxacin intended for local treatment of osteomyelitis. Biomatter 2013; 3:23162; http://dx.doi.org/10.4161/biom.23162

systemic drug concentrations in the blood or other tissues are significantly lower than in the surrounding local tissues.[11-17]

Local biodegradable and antibiotic releasing systems have been studied both in vitro and in vivo[11,12,15,16,18-22] and reviewed by many research groups.[10] Koort et al. have studied ciprofloxacin releasing bone defect fillers with osteoconductive ceramic component in a localized osteomyelitis rabbit model and the results have been promising. Ciprofloxacin was found to penetrate bone well and higher local concentrations of ciprofloxacin could be achieved than by using systemic administration.[10,13,14,23]

Mäkinen[24] has proposed a new clinical treatment algorithm in the treatment of osteomyelitis based on osteoconductive materials that release antibiotics locally. In this algorithm, the surgical debridement and the antibiotic treatment of the resulting dead space in the bone are performed in one operation. After treatment, no surgical removal of the antibiotic releasing implants or bone grafting is required due to the bioabsorbable and osteoconductive nature of the implants. The fillers developed in the current study may provide the osteoconductive and antibiotic releasing materials that Mäkinen has proposed. However, there is need to test the most promising composites further in vivo to prove their efficacy in living tissues.

Results and Discussion

The effect of processing and sterilization on the materials. The composite materials were manufactured using twin-screw extrusion and the resulting composites had ceramic particles and ciprofloxacin antibiotic evenly distributed in the polymer matrix due to the efficient mixing in the extrusion process. The composites are denoted PLCL + C [Poly(L-lactide-co-ε-caprolactone) (PLCL) with 8 wt% of ciprofloxacin in feed], PLCL + TCP50 + C [PLCL with 50 wt% of β-tricalcium phosphate (β-TCP) and 8 wt% of ciprofloxacin in feed] and PLCL + TCP60 + C (PLCL with 50 wt% β-TCP and 8 wt% of ciprofloxacin in feed). Processing caused only minor degradation in the composites. The weight average molecular weight (M_w) of the raw material was measured as 245,000 g/mol and the number average molecular weight (M_n) 150,000 g/mol. The processing of the composites caused a slight decrease both in the M_w and M_n. The decrease in the M_w was 8% for PLCL + C and 4% and 3% for the PLCL + TCP50 + C and the PLCL + TCP60 + C respectively and the decrease in the M_n was 12% for the PLCL + C and negligible (below 1%) for both PLCL + TCP50 + C and the PLCL + TCP60 + C. Polydispersity (PD) was slightly increased for PLCL + C (from 1.6 to 1.7) but no change was observed for PLCL + TCP50 + C and PLCL + TCP60 + C. As was expected, the sterilization using gamma irradiation with the measured dose of 29–35 kGy caused considerable degradation to all the composites. Gamma irradiation is known to affect polymers and cause degradation.[25,26] The decrease was 20%, 45% and 50% for the PLCL + C, the PLCL + TCP50 + C, and the PLCL + TCP60 + C respectively, when compared with the initial M_w of the raw material.

The residual monomer content of the raw material was 0.08 wt% for the L-lactide monomer and below detection limit (< 0.02 wt%) for the ε-caprolactone monomer. The L-lactide and ε-caprolactone monomer contents of the processed samples were analyzed from two parallel samples of each manufactured composite and the amounts of both monomers were very low. The average L-lactide monomer content after processing was 0.05-mol% and caprolactone monomer content below 0.02-mol%. This indicates that no monomers were generated during processing in any of the studied composites. Because there were no differences in the monomer contents of the manufactured materials, it can be assumed that the monomers did not cause differences in the hydrolytic degradation behavior of the studied composites.[25]

Drug release from the materials. The initial ciprofloxacin contents of the composites were measured as 7.0 ± 0.4 wt% for PLCL + C, 8.1 ± 0.1 wt% for PLCL + TCP50 + C, and 7.5 ± 0.2 wt% for PLCL + TCP60 + C. The cumulative ciprofloxacin release from the studied materials is presented as **Figure 1A**, where the release occurring in three phases can be noticed. The first phase was the burst in the beginning of the drug release that lasted for one day. This is the phase when the drug molecules at the surface or near the surface are released.[27,31] Although initial burst, which is typical for drug releasing polymeric materials, has been claimed as unwanted phenomenon,[28,29] it may be beneficial when the target is to destroy remaining bacteria after the surgical debridement of infected tissue. If the burst is moderate, it may help to achieve the required antibiotic concentration in the tissue and eradicate bacteria or to prevent the attachment of bacteria to the operated bone or implant.[10,30]

The second phase was from the day 1 until day 32, when the ciprofloxacin release from PLCL + C was very slow and the release from the composites with 50 and 60 wt% of β-TCP occurred steadily. The second phase was diffusion controlled[31] and obeyed the first-order kinetics (R^2 values 0.99 for both of the composites containing 50 wt% and 60 wt% of β-TCP). In first order kinetics, the release rate of the drug is dependent on the concentration and obeys **Equation 1**:

$$\ln A = -kt + \ln A_0 \quad (1)$$

where A is the drug load at the time t, A_0 is the initial drug load, and k is the rate constant. This equation results in a straight line when the logarithm of the remaining drug in the sample is plotted against time.

The third phase of the ciprofloxacin release started around day 32 of the release tests, where the release from PLCL + C and PLCL + TCP50 + C accelerated. This can be seen as a change in the release profile at 32 d in **Figure 1A**. There was, however, no notable change in the release profile at this point for the composite with 60-wt% of β-TCP. This was probably due to the porous structure of the composite caused by the high β-TCP content that enabled a high diffusion rate of ciprofloxacin out of the polymer matrix. In this case, the polymer degradation did not seem to have much of an effect on the ciprofloxacin release. After the phase change at 32 d, all the materials obeyed first-order kinetics (R^2 values 0.99 for all the tested materials) but with different slopes than seen in the second phase.

It was noticed that the β-TCP content of the composites had a considerable effect on the ciprofloxacin release (**Fig. 1A**).

β-TCP introduces porosity to the test samples and therefore enables accelerated diffusion of the drug out of the polymer matrix. The processing of the PLCL copolymer with β-TCP particles produces voids at the interfaces of the materials. In addition to the increased diffusion, β-TCP also increases the roughness of the surface; thus, it increases the surface area of the pellets and provides more area for the diffusion to happen. Other research groups have had rather similar results in studies concerning composites of bioceramics and biodegradable polymers containing antibiotics.[16,18,22]

Plain poly-ε-caprolactone is known to have good diffusion properties for low molecular weight substances (MW below 400 g/mol).[32] However, the permeability falls when the ε-caprolactone content decreases in copolymers, e.g., in copolymer of DL-lactide and ε-caprolactone.[33] The polymer studied here contains only 30% of the ε-caprolactone monomer and, therefore, the ciprofloxacin molecules that have a molar mass of 331 g/mol were not able to diffuse very well through the plain copolymer during the first 32 d.

At the time point of 32 d, the polymer degradation had apparently reached a level that enables accelerated diffusion for the plain copolymer as well as the composite with 50 wt% of β-TCP. At this point, the M_w of the polymer had decreased to the level of 30,000–34,000 g/mol and the M_n to the level of 17,000–20,000 g/mol. The mass loss of the test samples accelerated in a later stage of the test series, so in conclusion, the change in the diffusion properties due to the degradation of the polymer was most probably the reason for the acceleration of the drug release around 32 d.

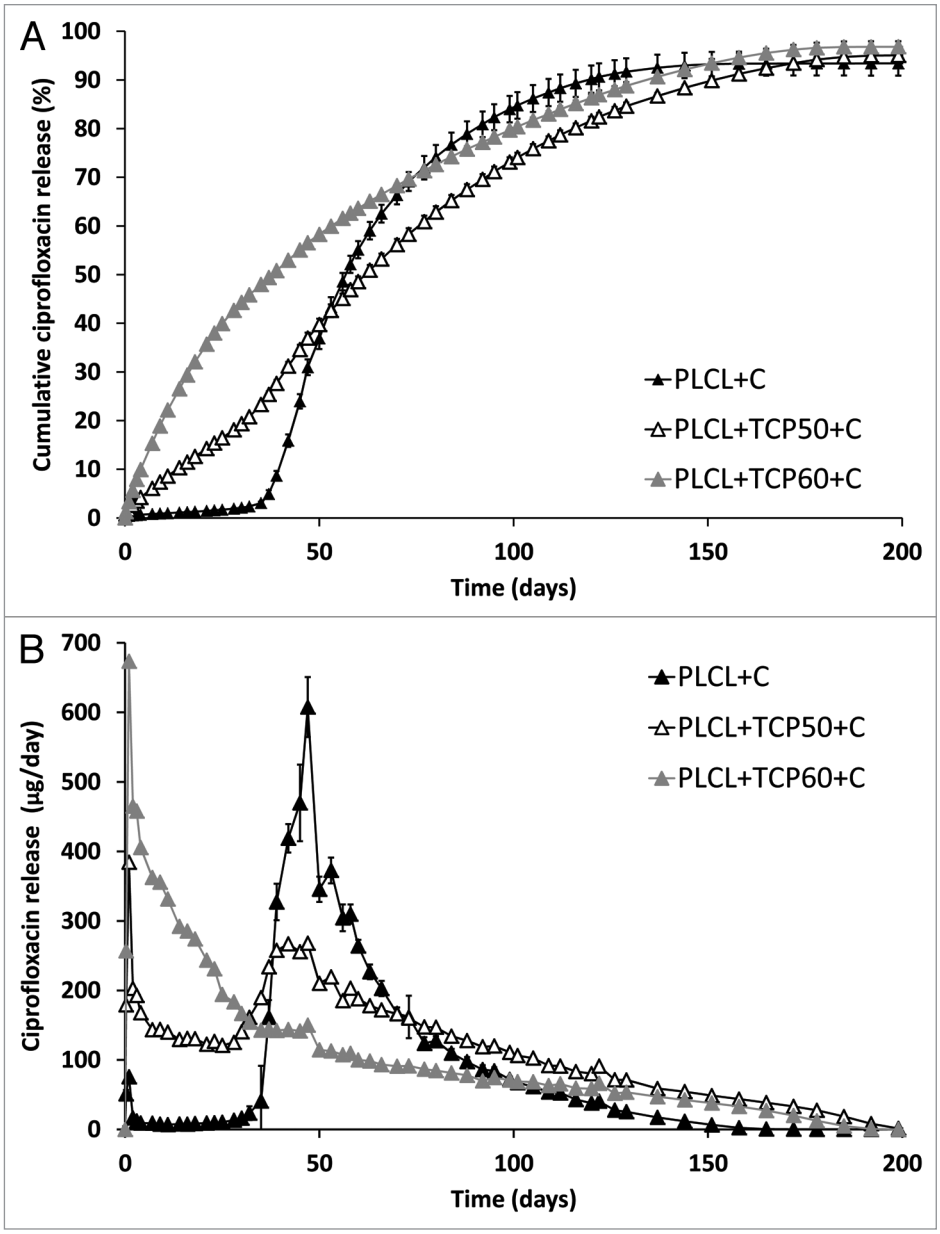

Figure 1. The cumulative (**A**) and daily (**B**) release of ciprofloxacin from composites of poly(L-lactide-co-ε-caprolactone) (PLCL) and β-tricalcium phosphate (TCP) with initial TCP contents of 0 wt%, 50 wt% and 60 wt% and initial ciprofloxacin (**C**) content of 8 wt%. Results shown as averages with standard deviations (n = 5).

The acceleration of the drug release can be easily seen in **Figure 1B** where the daily release of ciprofloxacin is presented. The release rate reached a peak at the time point of 50 d for all the tested materials, but the peak was most notable for the PLCL + C. A very small acceleration peak could also be observed at the time point of 120 d. At this point, most of the drug had diffused out from the tested materials and, therefore, the degradation degree of PLCL did not cause a larger peak to the daily release of ciprofloxacin.

As the steady zero order release is the ideal release profile in this case, the composite with 50% of β-TCP shows the most promising drug release properties for the treatment of osteomyelitis. The drug release of this composite continued up to 160 d with daily released concentrations above 2 μg/ml, which has been reported to be above the minimum inhibitory concentration (MIC) of the most common osteomyelitis pathogen *Staphylococcus aureus*.[34,35] The slow release period after 160 d when the daily release of ciprofloxacin was decreased below 2 μg/ml is of concern because it may allow the development of resistant bacteria.[10] However, the

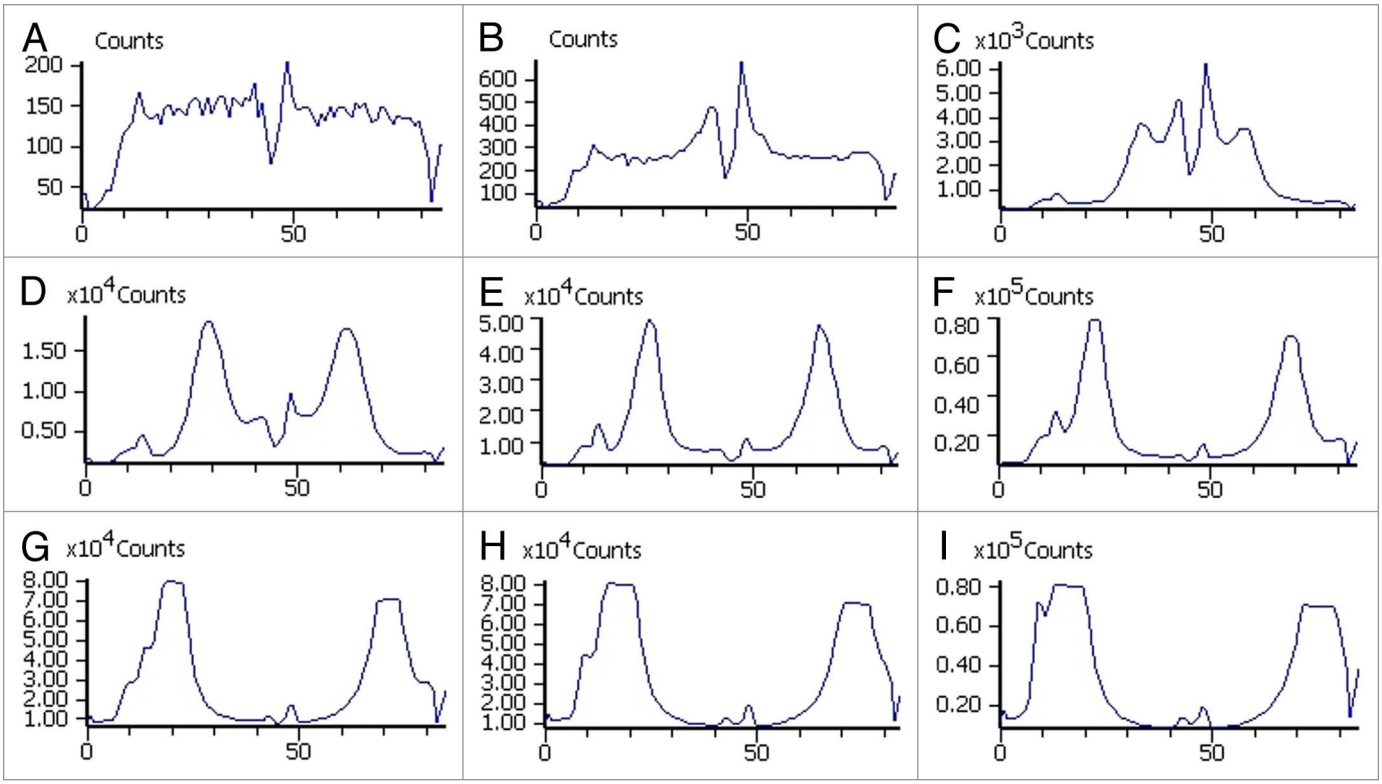

Figure 2. Light intensity level as photon counts of *Pseudomonas aeruginosa* exposed to one ciprofloxacin releasing pellet in the middle of a well. The results are presented at different time points of incubation. **A** is at the time point of 0 h, **B** at 2 h, **C** at 4 h, **D** at 6 h, **E** at 8 h, **F** at 10 h, **G** at 12 h, **H** at 14 h and **I** at 16 h. Note the different scales of the y-axes.

drug release rate and behavior in vivo may be different from what has been observed in vitro.

At the time point of 180 d, the drug release had decreased to a negligible level and 93–97% of the total ciprofloxacin loaded in the composites had been released. The test series was continued up to 392 d, but no further release of ciprofloxacin was detected.

The effect of the released ciprofloxacin against *Pseudomonas aeruginosa*. We studied the effect of the released ciprofloxacin against a common osteomyelitis causing bacteria *Pseudomonas aeruginosa*. The composite for this experiment contained 50 wt% of β-TCP and was chosen based on the most promising ciprofloxacin release results. A bacterial strain of *P. aeruginosa* engineered to emit light was used in the bacterial culture. The results of our bioluminescence measurements are shown in **Figure 2** as light intensity levels (photon counts). The measurements were taken in one well at different time points (0, 2, 4, 6, 8, 10, 12, 14 and 16 h) of incubation. To illustrate the results, a 6-well plate cultured with *P. aeruginosa* and ciprofloxacin-releasing pellets on the lower row and with control pellets without antibiotic on the top row after 16 h of incubation is shown in **Figure 3**, as a false color picture. The light intensity levels of the control wells are not shown in **Figure 2** because there were no significant changes observed in light intensity levels when compared with the results of antibiotic releasing pellets. All the light production in the control wells shut down at the time point of 6 h. This may have been due to quorum sensing mechanism[36] where the bacteria react to possible stress by turning off the light production. The light seen in the top row wells of **Figure 3** is not actual light production from the bacteria, but a reflection from the wells in the lower row. The first signs of the antibacterial activity were already seen after two hours of incubation both visually (false color picture) and in the light intensity levels (photon counting). The formation of the inhibition zone can be seen in **Figure 2** as a developing valley in the middle of the graphs with lower light intensity that gradually spreads toward the edge of the well. A region with very high light intensity can be seen surrounding the developing valley. The inhibition zone can also be seen in **Figure 3** as the dark blue zone in the middle of the wells that indicates dead bacteria. The effectiveness of ciprofloxacin released from the pellets in eradicating the bacteria and forming clear inhibition zones around the pellets in the wells was clearly seen. Bright yellow and red in the areas around the inhibition zones indicated increased light production. This increased light production preceded total decay in the light production. The reason for the decay in the light production was probably that when the bacteria came in contact with ciprofloxacin, the bacteria tried to survive by shutting down the non-vital systems consuming Adenosine triphosphate (ATP). As a result, more ATP was available for the bioluminescence pathway, and the light production increased.

In vitro degradation of the materials. *Molecular structure.* The ^{1}H NMR spectra were measured from seven samples (raw material PLCL, PLCL + C at 0, 26 and 52 weeks in vitro and PLCL + TCP50 + C at 0, 26 and 52 weeks in vitro). Some signals

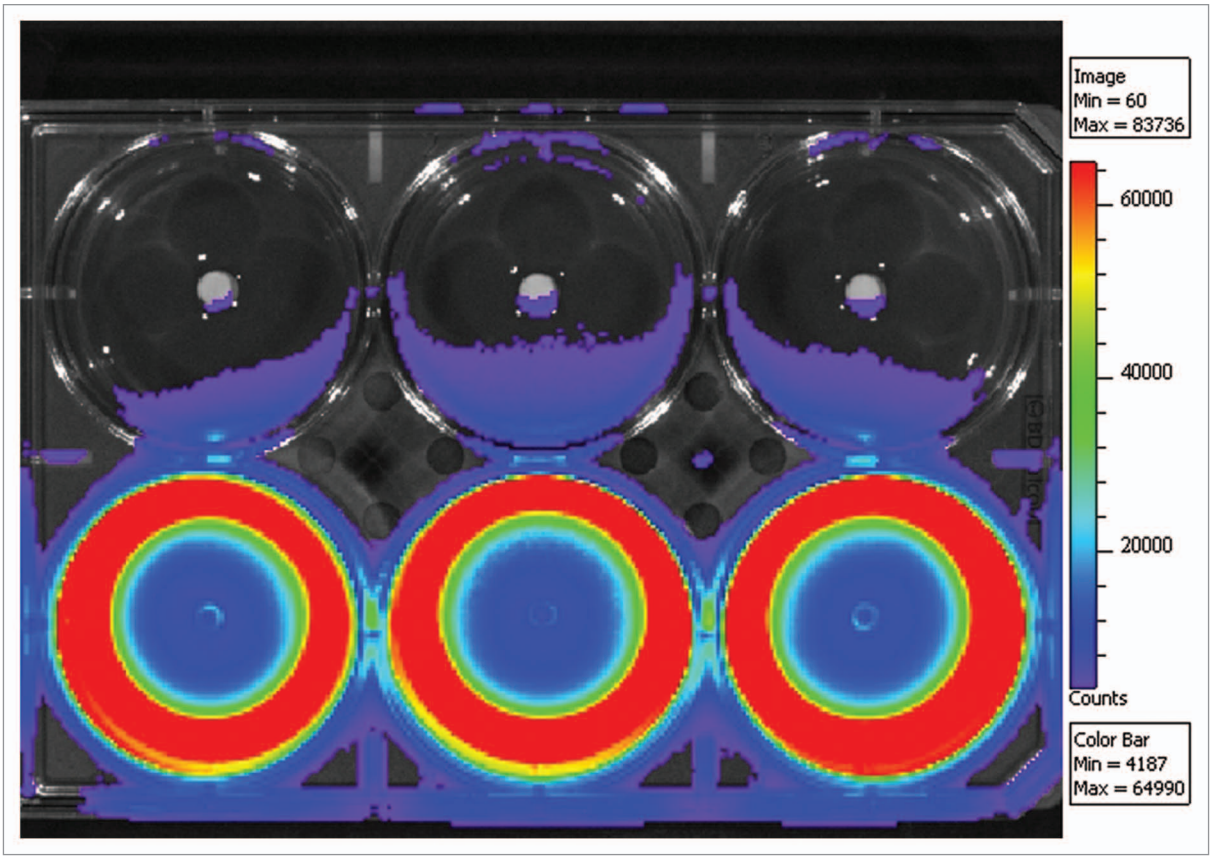

Figure 3. Bioluminescence results of the ciprofloxacin containing (8 wt%) composites of poly(L-lactide-co-ε-caprolactone) and 50 wt% of β-tricalcium phosphate on a bacterial culture of light emitting *Pseudomonas aeruginosa*. Pellets containing ciprofloxacin are on the lower row and corresponding composites without ciprofloxacin are on the top row and act as negative controls.

were overlapping and could not be used for the analysis. The most informative signals of the polymer are shown in **Figure 4** where a part of the PLCL raw material ^{1}H NMR spectrum is seen. The polymer showed signals at δ 5.16 for the –CH group proton of the lactide comonomer, at δ 4.05–4.13 for the α-oxy methylene protons of the ε-caprolactone comonomer and at δ 2.3–2.4 for the protons of the methylene group of ε-caprolactone that is bonded to the carbonyl group. The signals of the caprolactone protons at δ 4.05–4.13 and at δ 2.3–2.4 were clearly split into two signals according to the position in the polymer chain. The triplet at δ 4.13 indicated the CH_2 group in the ε-caprolactone fragment bonded to an L-lactide unit and the broader multiplet at δ 4.05 indicated the α-oxy methylene group bonded to another ε-caprolactone unit.[37,38] The signal at δ 2.3–2.4 was split the same way. The triplet at δ 2.4 indicated a group bonded to a L-lactide group and the broader multiplet at δ 2.3 corresponded to a group that is bonded to another ε-caprolactone group.[37,38] The comonomer ratios of the copolymer were calculated as the ratio of the integral of the signal at δ 5.16 to the average integrals of the caprolactone signals at δ 4.05–4.13 and at δ 2.3–2.4.[38] The ^{1}H NMR analysis showed that the L-lactide to ε-caprolactone ratio was increased from 68/32 of the raw material and the samples of 0 weeks to 76/24 of the PLCL + TCP50 + C at 52 weeks and 71/29 of the PLCL + C at 52 weeks. The results showed a similar effect of the changing of the comonomer ratio of the copolymer as the hydrolysis proceeds, as was seen in our earlier study with similar composites without ciprofloxacin (Ahola et al. Accepted to Journal of Biomaterials Applications). Jeong et al. have also reported this effect.[37]

Because the copolymer properties depend not only on the comonomer composition but also on the distribution of the comonomers in the polymer chains, analysis of the microstructure of the polymer was also needed.[38,39] The number average sequence lengths of L-lactide and ε-caprolactone were calculated according to Herbert[39] and Fernández[38] using **Equations 2 and 3**:

$$\tilde{n}_{LA} = \frac{2\,(LA)}{(LA - CL)} \quad (2)$$

$$\tilde{n}_{CL} = \frac{2\,(CL)}{(LA - CL)} \quad (3)$$

where (LA) and (CL) are the molar fractions of the L-lactide and ε-caprolactone comonomers in the copolymer and (LA - CL) is the average dyad relative fraction, which can be calculated from the ^{1}H NMR data of the copolymer. The calculation is well explained in an article by Fernández.[38] Additionally, the randomness factor, R, was calculated using **Equation 4**.

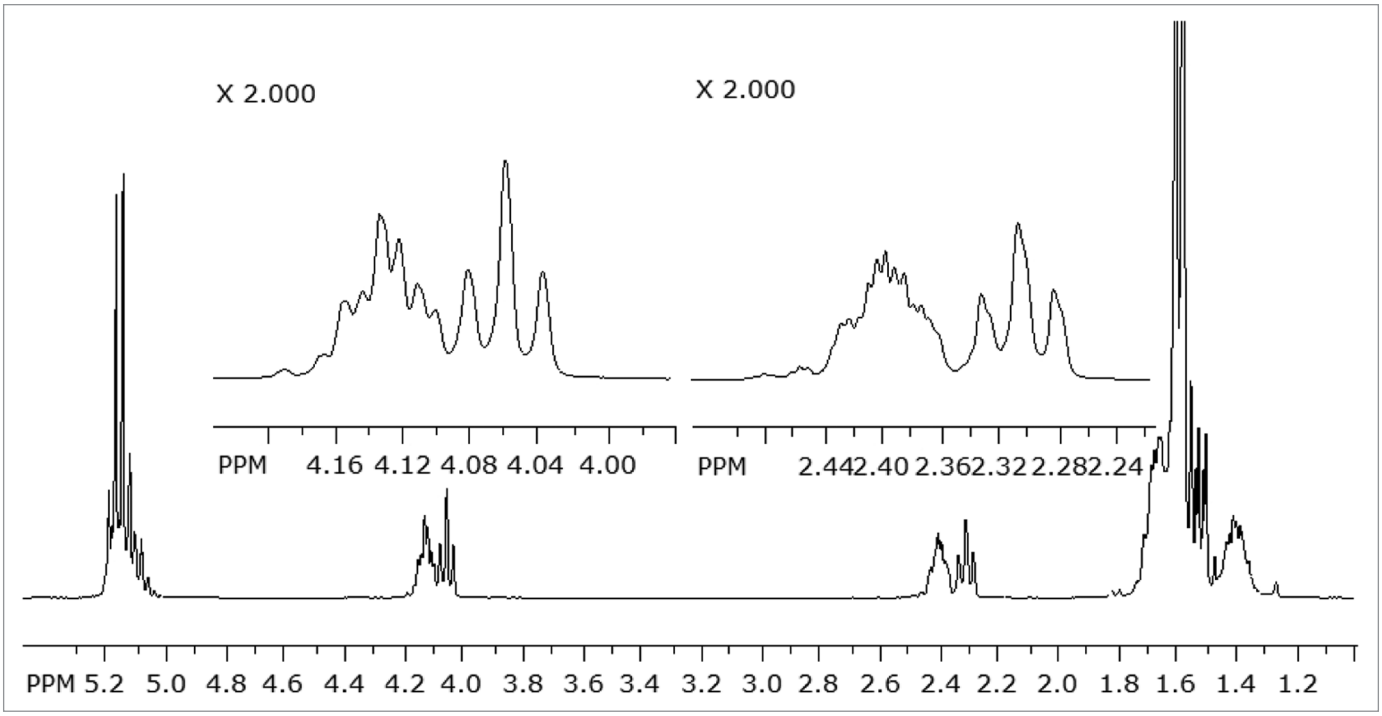

Figure 4. Part of the ^{1}H NMR spectrum of the poly(L-lactide-co-ε-caprolactone) raw material.

$$R = \frac{(LA - CL)}{2\,(LA)(CL)} \qquad (4)$$

The randomness factor is 1 for a random copolymer and 0 for a block copolymer.[38] The results of the average sequence length calculations showed that the polymer is rather blocky, R having values of 0.25 for the raw material and the samples prior to in vitro testing. The R factor decreased during degradation of the polymer to 0.18 for PLCL + TCP50 + C to 0.23 for the PLCL + C at 52 weeks indicating that the more random parts of the copolymer degrade first. The average sequence lengths of L-lactide were 13 in the beginning of the test series and increased to 22 and 15 for PLCL + TCP50 + C and PLCL + C respectively at 52 weeks. This also supports the fact that random parts of the copolymer having short blocks of the comonomers degraded first and thus the average sequence length was increased. The average sequence length of ε-caprolactone was not changed during hydrolysis and had values of 6–7 for all the analyzed samples.

Lemmouchi et al.[40] have reported degradation results of ε-caprolactone and L-lactide having a comonomer ratio of 74/26 (caprolactone to lactide) before hydrolysis, changed so that the amount of ε-caprolactone comonomer in the polymer increased and L-lactide decreased. This supports the interpretation that polymer degradation depends largely on the microstructure of the polymer and the amorphous parts degrade first despite the comonomer ratio.[40]

Signals of ciprofloxacin were visible only in the samples of 0 weeks. At 26 or 52 weeks the ciprofloxacin content in the samples was low and under the limit that could be detected in NMR. The integrals of protons of the quinoline ring at 8.80 and 8.06 ppm (**Fig. 5**) were in good agreement with the stoichiometric proportion 1:1 in both ciprofloxacin containing samples. Additionally, the signals of cyclopropane proton at 3.55 ppm, and the 8 protons in the piperazine ring, which appeared as a multiplet at 3.25 ppm showed good agreement with the stoichiometric values 1:8. Based on these results, it can be concluded that the ciprofloxacin molecule has maintained its original structure throughout the processing and sterilization steps. This result supports the findings of Koort et al. who concluded that processing and sterilization do not affect the bactericidal effect of ciprofloxacin.[12-14,23]

Molecular weights, mass loss and water absorption. At the start of the hydrolysis test series, the molecular weights of PLCL + TCP50 + C (M_w = 134,000 g/mol and M_n = 69,000 g/mol), and PLCL + TCP60 + C (M_w = 120,000 g/mol and M_n = 70,000 g/mol) were considerably lower than of PLCL + C (M_w = 196,000 g/mol and M_n = 90,000 g/mol). Despite the differences, the degradation proceeded rapidly in all three composites and the differences were leveled out during the hydrolysis test series (**Fig. 6A**). There were no differences observed in the degradation behavior between the studied materials. We noticed the same kind of effect in our earlier study with composites without antibiotics (Ahola et al. Accepted to the Journal of Biomaterials Applications), as did Daculsi et al.[26] At the time point of 4 weeks, the M_w values of the samples were already between 43,000 g/mol and 50,000 g/mol. The decrease of the molecular weight from this time point on was very similar for all the tested composites. After 52 weeks of hydrolysis at 37°C and pH 7.4, the molecular weights (both M_w and M_n) of all the composites had decreased by 97–98% to 2–3% of the initial value of the raw material. Polydispersity of the polymer decreased slightly and steadily throughout the test series, from

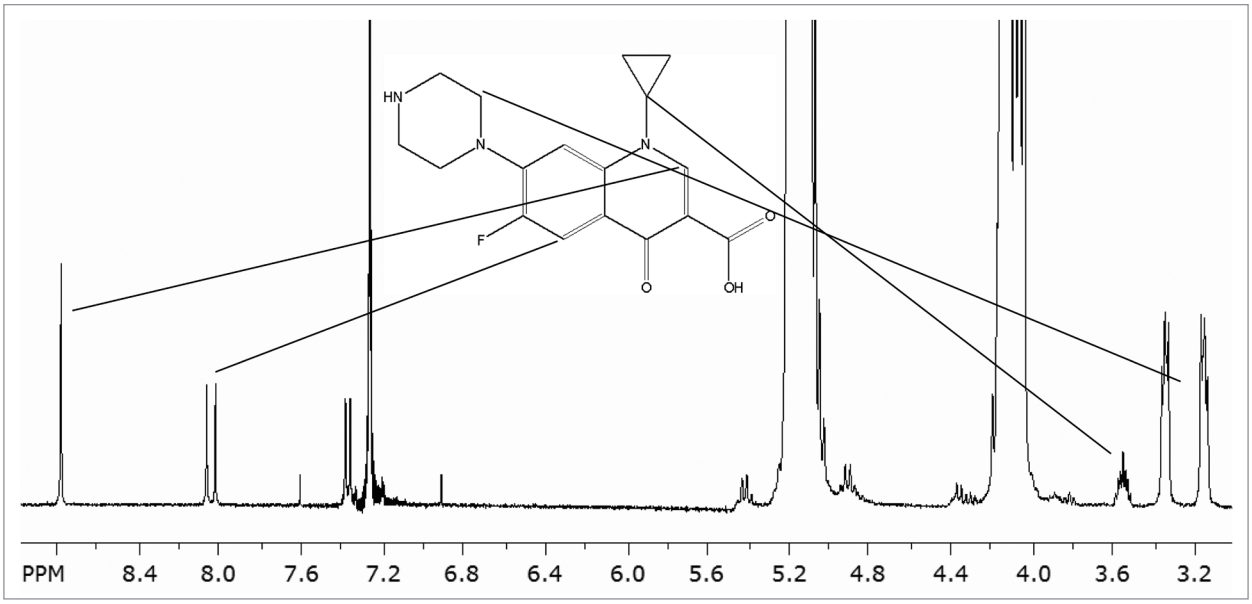

Figure 5. Part of the ^{1}H NMR spectrum of poly(L-lactide-co-ε-caprolactone) and ciprofloxacin after processing and positions of the peaks assigned to the protons in the ciprofloxacin molecule.

1.7–2.2 at 0 weeks to 1.2–1.3 at 52 weeks. The decrease indicated that M_w decreased more rapidly than M_n and that the molecular mass distribution was narrowed. The degradation of the aliphatic polyesters is known to occur first in the amorphous sections of the polymer and via random chain scission.[41] The random chain scission caused the molecular weight of the polymer to decrease rapidly following first order kinetics with k having values of 2.0 × 10^{-3} 1/h for the plain copolymer and 1.3 × 10^{-3} 1/h for PLCL + TCP50 + C and 1.2 × 10^{-3} 1/h for PLCL + TCP60 + C.

The SEC distribution plots showed emerging bimodality at 16 weeks for all the tested materials. In our earlier studies, the same kind of bimodality was present in composites without ciprofloxacin antibiotic (Ahola et al. Accepted to the Journal of Biomaterials Applications) beginning from the 20th week of the test series. Bimodality in the SEC distribution curve can be explained with the blocky structure of the copolymer, which was shown by the ^{1}H NMR analysis. The random parts of the copolymer degrade first, which might cause an increase in a certain part of the SEC distribution curve as the blocky parts consisting mainly of L-lactide monomers remain in the copolymer.

The mass loss of the test samples was steady and started from the very beginning of the test series (**Fig. 6B**). The first part of the mass loss was due to the drug release as ciprofloxacin was released from the composites. When the mass loss caused by the ciprofloxacin release was taken into account, it could be concluded that the mass loss caused by the polymer erosion started after 6 weeks for PLCL + TCP50 + C and PLCL + TCP60 + C and after 4 weeks for PLCL + C. The mass loss in the very beginning of the test series was greater for PLCL + TCP50 + C and PLCL + TCP60 + C than for PLCL + C, which correlated well with the drug release data. The dissolution of β-TCP was very slow as was also noted in our earlier study (Ahola et al. Accepted to the Journal of Biomaterials Applications) and it was not significant in the time scale of this study. The mass loss of the composites was almost linear during the whole 52-week test period (R^2 values 0.98).

Water absorption in PLCL + TCP50 + C and PLCL + TCP60 + C was greater than in PLCL + C during the first 10 weeks (**Fig. 6B**). After 20 weeks, this behavior changed as the water absorption of PLCL + C accelerated and it absorbed more water than the other tested composites. The polymer content in this composition was greater than in PLCL + TCP50 + C and PLCL + TCP60 + C, and this naturally affected the total water absorption of the samples. As the degradation proceeded, there were more hydrophilic end groups in the polymer to absorb water. There was no notable difference in the water absorption between the composites with 50 wt% and 60 wt% of β-TCP. This might be due to the fact that the difference in the ceramic content in these composites was not enough to cause notable differences in the water absorption behavior.

β-TCP content of the materials. The relative amount of β-TCP, determined by thermogravimetric analysis, in the composites increased throughout the test series (**Fig. 7A and B**). This is because β-TCP dissolves very slowly compared with the polymer degradation (Ahola et al. Accepted to the Journal of Biomaterials Applications). This kind of behavior might be beneficial regarding bone healing, as the polymer disappears from the site and the osteoconductive β-TCP particles remain to help bone ingrowth. Additionally, the voids at the interfaces between the ceramic particles and polymer matrix may also enable bone ingrowth.

Thermal properties. Compared with the similar composites without the ciprofloxacin antibiotic (Ahola et al. Accepted to the Journal of Biomaterials Applications), slightly higher T_gs were measured after processing and sterilization. T_gs were about 20°C for the composites without ciprofloxacin and 23°C for the composites containing ciprofloxacin. The changes in the T_gs of the

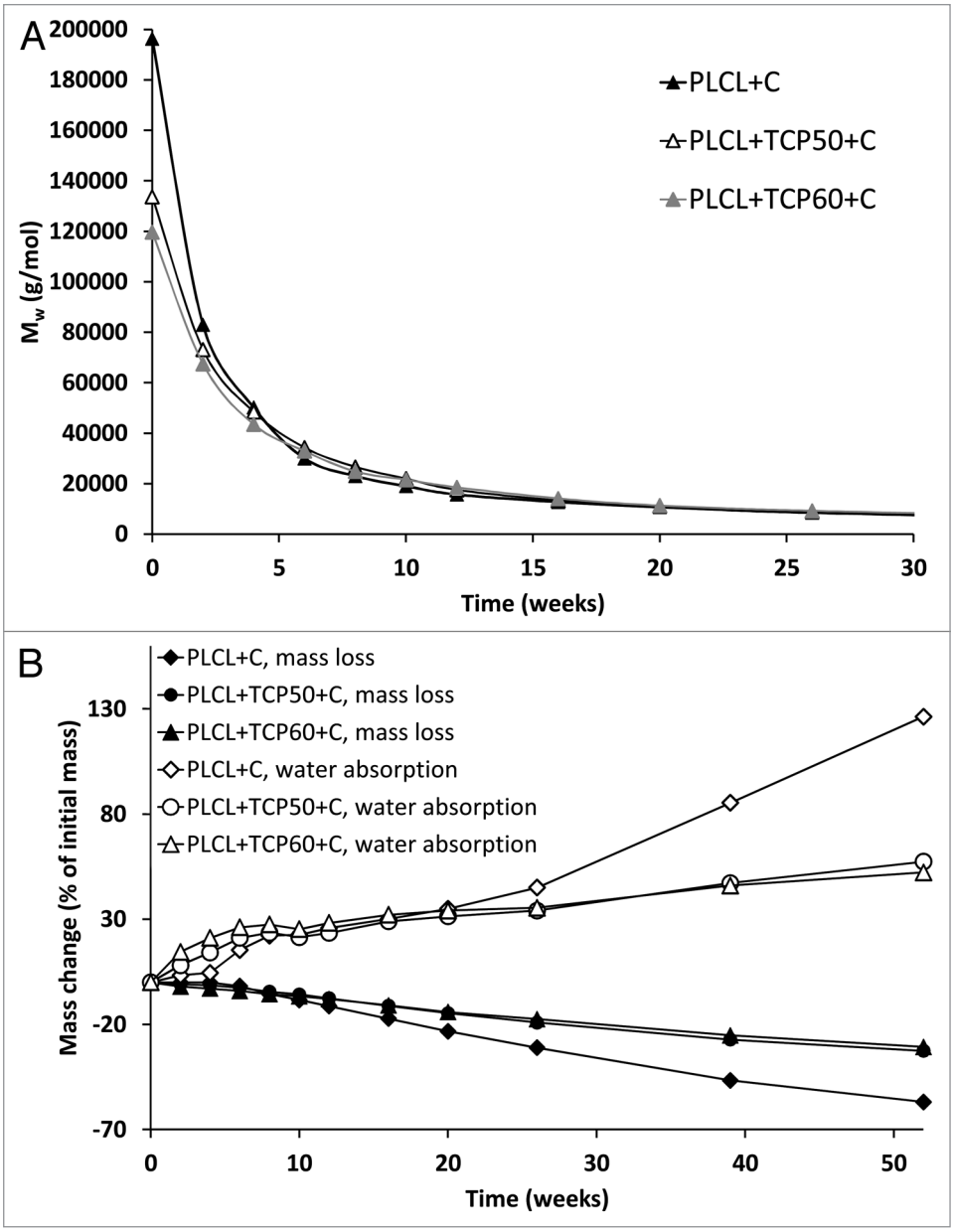

Figure 6. The weight average molar weight (M_w) (**A**), and mass loss and water absorption (**B**) of the studied composites as a function of time in vitro. The composites comprised of poly(L-lactide-co-ε-caprolactone) (PLCL), β-tricalcium phosphate (TCP) and ciprofloxacin (**C**) with initial TCP contents of 0 wt%, 50 wt%, and 60 wt% and ciprofloxacin content of 8 wt%. Error bars in part B are not visible due to the small values of standard deviations (n = 5).

materials during the in vitro test series are shown in **Figure 8A**. During the in vitro test series, there was a slow decrease in the T_g:s of the composites with ciprofloxacin until week 20 when the T_gs gradually decreased to 18°C. At the same time, the M_ws of the polymers decreased dramatically affecting also the T_g. This behavior is well known with biodegradable polymers.[42,43] After the time point of 20 weeks, the T_g:s began to increase ending up at 30°C for PLCL + TCP50 + C and PLCL + TCP60 + C and 23°C for PLCL + C at 52 weeks. At this time period, the loss of the short polymer chains has an increasing effect on the T_g[42] as well as the fact that the ratio of the comonomers in the copolymer changed as the degradation proceeded. This change was seen in the ^{1}H NMR analysis as an increase in the L-lactide content and decrease in ε-caprolactone content. The same kind of trend in T_g:s was observed with composites without ciprofloxacin, but it was more noticeable and the T_g:s decreased to 12–15°C during the first 12 weeks of the test series and started to increase after that (Ahola et al. Accepted to the Journal of Biomaterials Applications). T_gs of copolymers of L-lactide and ε-caprolactone are known to be strongly dependent on the comonomer composition. The T_g increases dramatically even with small increments of the L-lactide content.[32] The melting temperatures and melting enthalpies were analyzed from the first heating of the samples because during the second heating, the melting peaks did not appear anymore due to the fast cooling in the DSC analysis. Most of the samples showed clear bimodality in the melting peaks indicating two kinds of crystals in the polymer. The reason for the bimodality may be imperfect crystals in the polymer which may be annealed during DSC scan. As a result, they melt, recrystallize and melt again in higher temperature, which shows a bimodal melting peak in the DSC scan.[44] There were no clear trends in the melting temperatures of the composites. The bimodal melting peaks appeared mainly between 80°C and 120°C. There was a small decrease in the values between weeks 4 and 20 and a tendency to cold-crystallization at the 26th week.

Melting enthalpies, which describe the crystallinity of the polymer, were analyzed and corrected to correspond to the combined polymer and ciprofloxacin part of the composites. There was a dramatic increase in the crystallinity of the composites from the beginning of the test series until the time point of 6 weeks. After this, the crystallinity started to decrease until the 20 weeks time point and then started to increase again (**Fig. 8B**). With the composite without β-TCP, the same behavior was observed, but it was considerably weaker. When compared with similar composites without ciprofloxacin, there was a considerable difference in the changes in melting enthalpies. The melting enthalpy of the composites without ciprofloxacin increased steadily until the time point of

26 weeks (Ahola et al., accepted to the *Journal of Biomaterials Applications*). In conclusion, the dramatic increase and decrease in melting enthalpies during weeks 0–20 is attributed to the presence of ciprofloxacin in the composites. The overall increase in the crystallinity of the polymer as hydrolysis proceeds is probably due to the increased proportion of L-lactide blocks in the copolymer as the amorphous and more random parts of the copolymer degrade first, which was shown by the ^{1}H-NMR analysis. The L-lactide blocks are able to rearrange and form crystals due to the increased mobility of the polymer chains.

Microstructure. SEM micrographs showed pores of different sizes in the samples containing β-TCP. No notable differences were seen in the structures of composites with 50 wt% and 60 wt% of β-TCP. In the samples without β-TCP, no pores were seen after processing of the material, but some very small pores were formed during the in vitro study. In the **Figure 9**, SEM micrographs of composites with 60 wt% of β-TCP are shown. In the inner parts of the samples, porosity was seen throughout the hydrolysis test series (**Fig. 9A–C**). Pores reaching the size of 100–200 μm were observed as well as smaller pores. Additionally, the surfaces of the pellet-shaped samples were porous (**Fig. 9D–F**). The pores were created around the ceramic particles in the process when the composite in melt phase was drawn from the die of the extruder because there was practically no adhesion between the ceramic particles and the polymer.

Pores of a size over 100 μm have been reported to enhance bone ingrowth[45] and would, therefore, be beneficial in the healing phase of the bone after the infection causing bacteria have been eradicated. Smaller pores are critical because they enable liquid, nutrition, and waste to flow in the material to and from the cells.

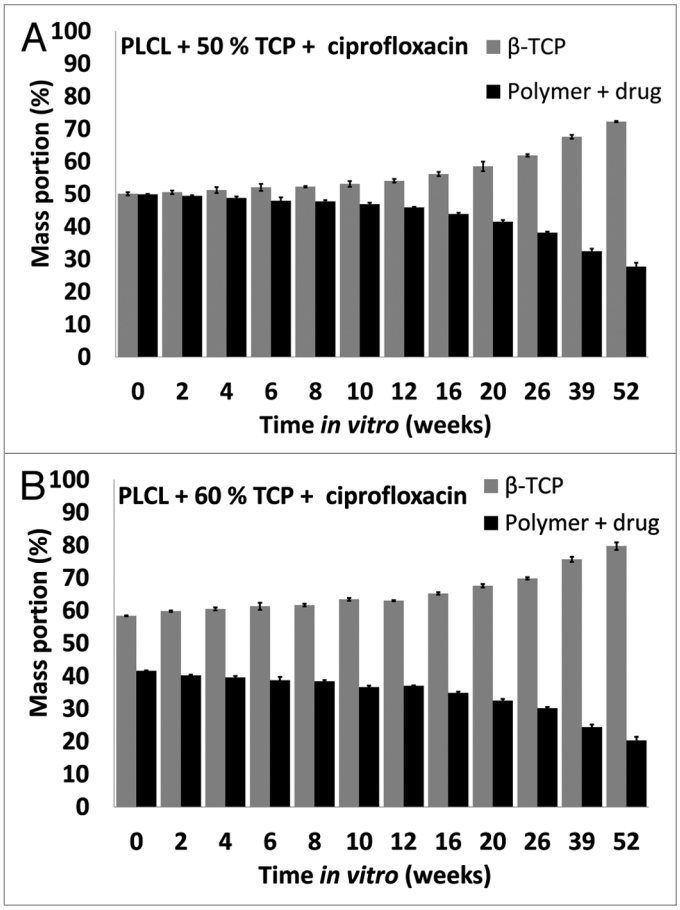

Figure 7. β-tricalcium phosphate (TCP) contents of the studied composites as a function of time in vitro. The composites comprised of poly(L-lactide-co-ε-caprolactone) (PLCL) and β-tricalcium phosphate (TCP) with initial TCP contents of 50 wt% and 60 wt% and ciprofloxacin (C) content of 8 wt%. Results shown as averages with standard deviations (n = 5).

Materials and Methods

Materials. The copolymer that was used as the matrix in the composites was medical grade poly(L-lactide-co-ε-caprolactone) (PLCL, Purac Biomaterials) with the comonomer ratio of 70/30 and M_w of 246,000 g/mol. β-Tricalcium phosphate (β-TCP) (granule size < 38 μm) was used as the ceramic component and it was purchased from Plasma Biotal Ltd. Ciprofloxacin antibiotic (M = 331.4 g/mol) was purchased from Uquifa. Sörensen phosphate buffer solution was prepared according to the standard ISO 15814[46] and the chemicals used for the buffer solution (Na_2HPO_4 and KH_2PO_4) were purchased from J.T. Baker. The chemicals used for the bioluminescence bacterial cultures were: Gentamicin sulfate (Sigma-Aldrich), Isopropyl-β-D-thiogalaktopyranoside (IPTG) (Fermentas, Lithuania), Trypton (Lab M Limited), Yeast extract (Lab M Limited), Sodium Chloride (Merck), Agar (Merck).

Processing. The components of the composite materials, that are PLCL polymer, β-TCP, and ciprofloxacin antibiotic, were dried for 72 h in vacuum at room temperature before processing. The materials were processed into rod-shaped billets with a diameter of approximately 2.5 mm with a co-rotating, custom-built intermeshing twin-screw extruder (L/D ratio 22.5) in a nitrogen atmosphere. PLCL copolymer, β-TCP and rifampicin antibiotic were delivered to the process with separate gravimetric screw feeders. The mixing of the components took place in the extruder. A haul-off unit was used to guide the extrudate from the die and the diameter of the billets was fine-tuned adjusting the speed of the haul-off unit. Three different composites were processed. Each composite had 8 wt% ciprofloxacin antibiotic in feed and different β-TCP contents (0, 50 and 60 wt%). These composites are denoted PLCL + C, PLCL + TCP50 + C and PLCL + TCP60 + C respectively. The billets were cut into approximately 2.5 mm long pellet-shaped samples. Before degradation and drug release tests were performed, the samples were packed and sterilized using gamma irradiation (minimum dose 25 kGy).

Drug release study. The drug release tests were conducted at 37°C in vitro. Weighed test samples (each test sample consisted of 15 pellets) were placed in brown glass bottles along with 20 ml Sörensen buffer solution. Five parallel test samples were tested for each composite material. The bottles were placed in an incubator shaker at 37°C. At predetermined time intervals, the buffer solution was withdrawn from each of the bottles and replaced with fresh solution. The amount of buffer solution and the periodical

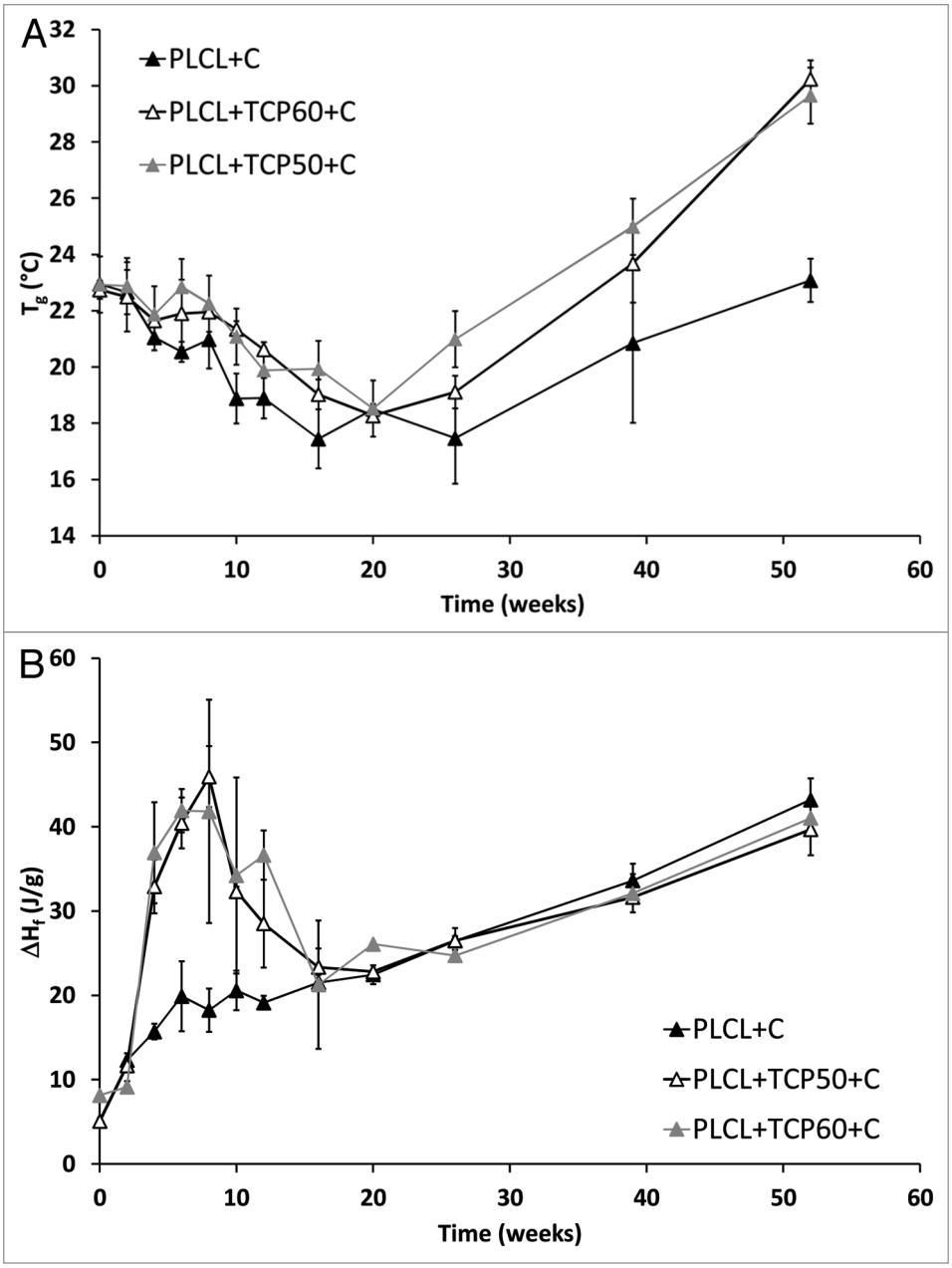

Figure 8. Glass transition temperatures (T_g) (**A**) and melting enthalpies (ΔH_f) (**B**) of the studied composites as a function of time in vitro. The composites comprised of poly(L-lactide-co-ε-caprolactone) (PLCL) and β-tricalcium phosphate (TCP) with initial TCP contents of 0 wt%, 50 wt% and 60 wt% and ciprofloxacin (**C**) content of 8 wt%. Results are shown as averages with standard deviations (n = 2–5).

change to fresh buffer solution enabled sink conditions to be valid throughout the test series. The amount of released ciprofloxacin was determined from the buffer solution using a Unicam UV 500 spectrometer (ThermoSpectronic, Cambridge, United Kingdom) at maximum absorption wavelength of 271 nm. A wavelength area from 190 to 400 nm was scanned in order to detect possible changes in the ciprofloxacin molecular structure that cause deviation in the UV-spectrum. Ciprofloxacin concentrations were calculated using Beer-Lambert law and with the help of a standard curve prepared with known concentrations of ciprofloxacin.

Inhibition zone testing using bioluminescence imaging. The effect of a ciprofloxacin releasing composite material against a common osteomyelitis causing bacteria *Pseudomonas aeruginosa* was tested using bioluminescence imaging based on the ability of genetically engineered bacteria to emit light.[47,48] In the bioluminescence method, the luminescence and the changes in it emitted by living microorganisms are measured. The changes in the luminescence are caused by *lux* gene-coded luciferase, which respond to the target analyte in a dose-dependent manner.[47,48]

The antibiotic containing composite material chosen for this study was the composite containing 50 wt% of β-TCP (PLCL + TCP50 + C) based on the most promising drug release results. Composite of PLCL and 50 wt% β-TCP without antibiotics was used as control.

An engineered bacteria strain of *Pseudomonas aeruginosa* PAO-LAC carrying plasmid pUCP24GW[49] was used as the biosensor. The *P. aeruginosa* here had been engineered to act as a SOS-response sensor, thereby providing information of the agents that influence chromosomal DNA homeostasis, among others. The bacteria were cultured on antibiotic plates overnight at 30°C and 300 rpm (1 mM IPTG, 10 μg/ml gentamycin), and suitable colonies were moved into liquid culturing in LB (5 g/l yeast extract, 10 g/l tryptone and 5 g/l NaCl). If the bacteria did not produce luminescence as wished in the morning, 1/50 dilution was made in a culture tube and it was incubated at 37°C and 300 rpm for three hours. The level of luminescence of the cultures was measured by using Plate Chameleon™ multilabel counter 1.001 (Hidex Ltd.), and at volume of 200 μl. Counts of 1.1–2.3 × 10^6 were found satisfying.

Layers of LB-agar (agar 15 g/l, 2 ml) were cast into 6-well plate, and the controls and antibiotic containing composite pellets were placed on top of them (one pellet per well). Bacteria were mixed with soft LB-agar (7.5 g/l) solution and cast on top of the first layers. The amount of bacterial culture was dependent on the luminescence level. After solidification, the plate was taken to the imaging station of Xenogen VivoVision IVIS® Lumina luminescence camera (Caliper LifeSciences). Pictures were taken every 20

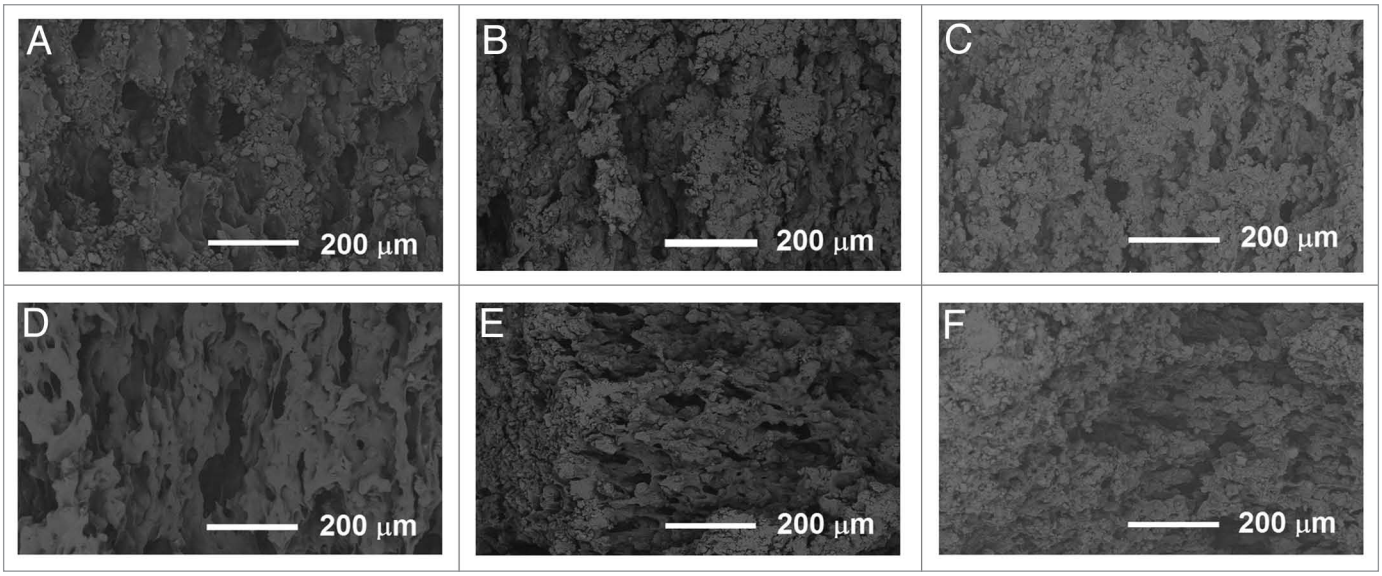

Figure 9. SEM micrographs of the composites of poly(L-lactide-co-ε-caprolactone), 60 wt% β-tricalcium phosphate and ciprofloxacin. (**A–C**) fractured surfaces after 0 weeks, 26 weeks, and 52 weeks in vitro, respectively. (**D–F**) specimen surfaces after 0 weeks, 26 weeks and 52 weeks in vitro, respectively.

min for 16 h with exposure time of 30 sec. The pictures were analyzed using Living Image® 3.1 program (Caliper LifeSciences).

In vitro degradation study. Degradation tests were conducted according to the standard ISO 15814[46] at 37°C in vitro. Five parallel test samples, each consisting of 15 pellets, of each composite material were tested at each time point. First, weighed test samples were placed in brown glass bottles with 20 ml Sörensen buffer solution. Then, the bottles were placed in an incubator shaker at 37°C. The pH of the buffer solution was measured periodically with a calibrated pH meter and the buffer solutions were changed every two days at the beginning of the test series, due to fast drug release and the fact that we wanted to avoid drug accumulation in the buffer solution. After five weeks, the buffer solution was changed twice a week and after ten weeks, once a week. Test samples were withdrawn at predetermined time points, which were 2, 4, 6, 8, 12, 16, 20, 26, 30 and 52 weeks.

Methods of analysis. *Residual monomer.* Ramboll Analytics Oy performed the determination of residual L-lactide and ε-caprolactone monomer contents. The ε-caprolactone and L-lactide contents were measured after chloroform extraction of the samples using gas chromatography (DC8000, CE Instruments) and an FI-detector after chloroform dilution. The measuring resolution was 0.02%.

Initial drug content. Five samples of about 150 mg were weighed from each manufactured composition and dissolved in 50 ml of chloroform (J.T. Baker). The amount of ciprofloxacin in the chloroform solution was determined using a Unicam UV 540 Spectrophotometer (ThermoSpectronic) at a maximum absorption wavelength of 284 nm. The concentrations of ciprofloxacin in the solutions were calculated with the help of a standard curve prepared with known concentrations of ciprofloxacin.

Molecular structure. The molecular structures of the PLCL copolymer and ciprofloxacin antibiotic during degradation test series were studied measuring and analyzing the proton NMR spectra of the samples. The NMR equipment used was a Varian Mercury 300 MHz NMR Spectrometer (Varian Associates Inc.) and the measurements were done at room temperature in standard 5 mm tubes in deuterochloroform. Tetramethylsilane (TMS) was used as an internal standard, and chemical shifts were measured relative to TMS. The data were acquired until the quality of the spectrum was sufficient and the number of scans was about 400. The proton NMR spectra of the samples were processed and analyzed using SpinWorks 3.1 software. Phase correction and baseline correction were applied to all spectra.

Molecular weights. The molecular weights (number average, M_n, and weight average, M_w, molecular weights) and polydispersity (PD) of the copolymer during the in vitro degradation test series were determined at room temperature by size exclusion chromatography (SEC) (Waters Associates system was equipped with a Waters 717plus autosampler, a Waters 510 HPLC solvent pump, four linear PL gel columns (10^4, 10^5, 10^3 and 100 Å) connected in series, and a Waters 2414 differential refractometer). Chloroform (Riedel-de Haën Ag, stabilized with 1% ethanol) was used as a solvent and eluent. Before injection, the samples were filtered through a 0.5 μm Millex SR filter. The injected volume was 200 μl and the flow rate was 1.0 ml/min. Monodisperse polystyrene standards were used for primary calibration. One to two parallel samples were measured at each time point for each composite.

Mass loss and water absorption. For the water absorption analysis, the test samples were withdrawn from the incubator shaker and rinsed twice with distilled water. The surfaces of the test samples were then wiped carefully with tissue paper and the test samples were weighed immediately after wiping. The weighed test samples were dried for at least three days at ambient conditions

and for one week in vacuum. After vacuum drying, the test samples were weighed again to obtain the dry masses for the mass loss calculations. The dried test samples were stored in a desiccator for further analysis.

The mass loss was calculated as the difference between the initial mass of the test sample and the mass of the dried test sample divided by the initial mass of the test sample. The water absorption was calculated as the difference between the mass of the wet test sample and the mass of the dried test sample divided by the mass of the dried test sample

Ceramic content. The β-TCP content of the test samples was measured using thermogravimetric analysis (TGA Q500, TA Instruments). Samples of approximately 20 mg were used and they were heated at a rate of 20°C/min up to 700°C. Universal Analysis Software was used for the analysis of the results. Five parallel samples of each composition were analyzed at each time point and the results were calculated as averages and standard deviations.

Thermal properties. Thermal analysis was performed using a differential scanning calorimeter DSC Q1000 (TA Instruments). Nitrogen was used as the sweeping gas. To ensure the samples had a similar thermal history, they were heated twice and cooled rapidly in between. The heating rate was 20°C/min, the cooling rate was 50°C/min and the temperature range was -60°C to +200°C. Glass transition temperatures (T_g) were obtained from the second heating and melting temperatures and enthalpies (T_m and ΔH_f respectively) were obtained from the first heating cycle. Although absolute crystallinity values could not be calculated because the theoretical value of 100% crystalline poly(L-lactide-co-ε-caprolactone) 70/30 was not available, relative changes in the crystallinity were observed. Two to five parallel samples were tested for each composite material and time point. The results were analyzed using Universal Analysis Software and averages and standard deviations were calculated.

Microstructure of the samples. The microstructure of the composites was observed using scanning electron microscopy (Philips XL-30 SEM equipped with a LaB6 filament, Philips) with an acceleration voltage of 12.0 kV. The micrographs were taken both on the surface of the samples and on cryogenically fractured samples, which were coated with gold (Edwards S150 Sputter Coater) prior to microstructure examination.

Conclusions

The tested composites with high β-TCP contents show desirable ciprofloxacin releasing properties as ciprofloxacin was steadily released during 160 d in concentrations above the MIC of *Staphylococcus aureus*. This is within the desired range when the objective is the treatment of osteomyelitis. The release obeyed first-order kinetics having a phase change at 32 d of the release test period. The increased porosity, introduced by β-TCP particles, enhanced the release of ciprofloxacin and removed the long lag phase in the ciprofloxacin release of the plain copolymer. ^{1}H-NMR analysis showed that processing and sterilization did not affect the ciprofloxacin molecular structure. Additionally, the effect against a common osteomyelitis causing bacteria *Pseudomonas aeruginosa* was shown in cell culture study utilizing bioluminescence.

The polymer matrix of the composites, poly(L-lactide-co-ε-caprolactone) copolymer, was found to have very blocky structure where the L-lactide comonomers formed long blocks in the polymer structure. This also influenced the increase in crystallinity as the polymer degradation proceeded. The decrease in the molecular weight of the copolymer matrix followed the first-order kinetics. The composites with high β-TCP contents, especially the composite with 50 wt% of β-TCP, show great potential to be developed into a product for the treatment of osteomyelitis and other bone related infections. However, in vivo studies as well as clinical studies are needed to establish the effect of these materials when they are implanted in living tissue.

Disclosure of Potential Conflicts of Interest

No potential conflicts of interest were disclosed.

Acknowledgments

Research collaboration with Bioretec Ltd. and financial support from the Finnish Funding Agency for Technology and Innovation (TEKES) and the National Graduate School of Musculoskeletal Disorders and Biomaterials (N.A and M.V) are gratefully appreciated. Raija Reinikainen, Kaija Honkavaara, Eija Ahonen and Vuokko Heino are warmly thanked for their technical assistance. Peter Heath is thanked for checking the language of the manuscript.

References

1. Galanakis N, Giamarellou H, Moussas T, Dounis E. Chronic osteomyelitis caused by multi-resistant Gram-negative bacteria: evaluation of treatment with newer quinolones after prolonged follow-up. J Antimicrob Chemother 1997; 39:241-6; PMID:9069546; http://dx.doi.org/10.1093/jac/39.2.241.
2. Chihara S, Segreti J. Osteomyelitis. Dis Mon 2010; 56:6-31; http://dx.doi.org/10.1016/j.disamonth.2009.07.001.
3. Parsons B, Strauss E. Surgical management of chronic osteomyelitis. Am J Surg 2004; 188(Suppl):57-66; PMID:15223504; http://dx.doi.org/10.1016/S0002-9610(03)00292-7.
4. Soundrapandian C, Datta S, Sa B. Drug-eluting implants for osteomyelitis. Crit Rev Ther Drug Carrier Syst 2007; 24:493-545; PMID:18298388; http://dx.doi.org/10.1615/CritRevTherDrugCarrierSyst.v24.i6.10.
5. Farhad R, Roger PM, Albert C, Pélligri C, Touati C, Dellamonica P, et al. Six weeks antibiotic therapy for all bone infections: results of a cohort study. Eur J Clin Microbiol Infect Dis 2010; 29:217-22; PMID:20012334; http://dx.doi.org/10.1007/s10096-009-0842-1.
6. Haidar R, Der Boghossian A, Atiyeh B. Duration of post-surgical antibiotics in chronic osteomyelitis: empiric or evidence-based? Int J Infect Dis 2010; 14:e752-8; PMID:20471296; http://dx.doi.org/10.1016/j.ijid.2010.01.005.
7. Jain A, Gupta Y, Agrawal R, Khare P, Jain SK. Biofilms--a microbial life perspective: a critical review. Crit Rev Ther Drug Carrier Syst 2007; 24:393-443; PMID:18197780; http://dx.doi.org/10.1615/CritRevTherDrugCarrierSyst.v24.i5.10.
8. Harris LG, Richards RG. Staphylococci and implant surfaces: a review. Injury 2006; 37(Suppl 2):S3-14; PMID:16651069; http://dx.doi.org/10.1016/j.injury.2006.04.003.
9. Esposito S, Leone S. Prosthetic joint infections: microbiology, diagnosis, management and prevention. Int J Antimicrob Agents 2008; 32:287-93; PMID:18617373; http://dx.doi.org/10.1016/j.ijantimicag.2008.03.010.
10. Zilberman M, Elsner JJ. Antibiotic-eluting medical devices for various applications. J Control Release 2008; 130:202-15; PMID:18687500; http://dx.doi.org/10.1016/j.jconrel.2008.05.020.
11. Garvin KL, Miyano JA, Robinson D, Giger D, Novak J, Radio S. Polylactide/polyglycolide antibiotic implants in the treatment of osteomyelitis. A canine model. J Bone Joint Surg Am 1994; 76:1500-6; PMID:7929497.
12. Mäkinen TJ, Veiranto M, Lankinen P, Moritz N, Jalava J, Törmälä P, et al. In vitro and in vivo release of ciprofloxacin from osteoconductive bone defect filler. J Antimicrob Chemother 2005; 56:1063-8; PMID:16234335; http://dx.doi.org/10.1093/jac/dki366.

13. Koort JK, Suokas E, Veiranto M, Mäkinen TJ, Jalava J, Törmälä P, et al. In vitro and in vivo testing of bioabsorbable antibiotic containing bone filler for osteomyelitis treatment. J Biomed Mater Res A 2006; 78:532-40; PMID:16736479; http://dx.doi.org/10.1002/jbm.a.30766.
14. Koort JK, Makinen TJ, Suokas E, Veiranto M, Jalava J, Tormala P, et al. Sustained release of ciprofloxacin from an osteoconductive poly(DL)-lactide implant. Acta Orthop 2008; 79:295-301; PMID:18484258; http://dx.doi.org/10.1080/17453670710015111.
15. Mäkinen TJ, Veiranto M, Knuuti J, Jalava J, Törmälä P, Aro HT. Efficacy of bioabsorbable antibiotic containing bone screw in the prevention of biomaterial-related infection due to Staphylococcus aureus. Bone 2005; 36:292-9; PMID:15780955; http://dx.doi.org/10.1016/j.bone.2004.11.009.
16. Miyai T, Ito A, Tamazawa G, Matsuno T, Sogo Y, Nakamura C, et al. Antibiotic-loaded poly-ε-caprolactone and porous β-tricalcium phosphate composite for treating osteomyelitis. Biomaterials 2008; 29:350-8; PMID:17977596; http://dx.doi.org/10.1016/j.biomaterials.2007.09.040.
17. Lucke M, Wildemann B, Sadoni S, Surke C, Schiller R, Stemberger A, et al. Systemic versus local application of gentamicin in prophylaxis of implant-related osteomyelitis in a rat model. Bone 2005; 36:770-8; PMID:15794930; http://dx.doi.org/10.1016/j.bone.2005.01.008.
18. Alvarez H, Castro C, Moujir L, Perera A, Delgado A, Soriano I, et al. Efficacy of ciprofloxacin implants in treating experimental osteomyelitis. J Biomed Mater Res B Appl Biomater 2008; 85:93-104; PMID:17696153; http://dx.doi.org/10.1002/jbm.b.30921.
19. Tiainen J, Knuutila K, Veiranto M, Suokas E, Törmälä P, Kaarela O, et al. Pull-out strength of multifunctional bioabsorbable ciprofloxacin-releasing polylactide-polyglycolide 80/20 tacks: an experimental study allograft cranial bone. J Craniofac Surg 2009; 20:58-61; PMID:19164990; http://dx.doi.org/10.1097/SCS.0b013e318190df48.
20. Waknis V, Jonnalagadda S. Novel poly-DL-lactide-polycaprolactone copolymer based flexible drug delivery system for sustained release of ciprofloxacin. Drug Deliv 2011; 18:236-45; PMID:21189060; http://dx.doi.org/10.3109/10717544.2010.528070.
21. Castro C, Évora C, Baro M, Soriano I, Sánchez E. Two-month ciprofloxacin implants for multibacterial bone infections. Eur J Pharm Biopharm 2005; 60:401-6; PMID:15996581; http://dx.doi.org/10.1016/j.ejpb.2005.02.005.
22. Castro C, Sánchez E, Delgado A, Soriano I, Núñez P, Baro M, et al. Ciprofloxacin implants for bone infection. In vitro-in vivo characterization. J Control Release 2003; 93:341-54; PMID:14644584; http://dx.doi.org/10.1016/j.jconrel.2003.09.004.
23. Koort JK, Mäkinen TJ, Suokas E, Veiranto M, Jalava J, Knuuti J, et al. Efficacy of ciprofloxacin-releasing bioabsorbable osteoconductive bone defect filler for treatment of experimental osteomyelitis due to Staphylococcus aureus. Antimicrob Agents Chemother 2005; 49:1502-8; PMID:15793132; http://dx.doi.org/10.1128/AAC.49.4.1502-1508.2005.
24. Mäkinen T. Osteomyelitis and orthopedic implant infections, PhD thesis, University of Turku, 2005.
25. Paakinaho K, Ellä V, Syrjälä S, Kellomäki M. Melt spinning of poly(l/d)lactide 96/4: Effects of molecular weight and melt processing on hydrolytic degradation. Polym Degrad Stabil 2009; 94:438-42; http://dx.doi.org/10.1016/j.polymdegradstab.2008.11.010.
26. Daculsi G, Goyenvalle E, Cognet R, Aguado E, Suokas EO. Osteoconductive properties of poly(96L/4D-lactide)/beta-tricalcium phosphate in long term animal model. Biomaterials 2011; 32:3166-77; PMID:21315446; http://dx.doi.org/10.1016/j.biomaterials.2011.01.033.
27. Duvvuri S, Gaurav Janoria K, Mitra AK. Effect of polymer blending on the release of ganciclovir from PLGA microspheres. Pharm Res 2006; 23:215-23; PMID:16320000; http://dx.doi.org/10.1007/s11095-005-9042-6.
28. Zamoume O, Thibault S, Regnié G, Mecherri MO, Fiallo M, Sharrock P. Macroporous calcium phosphate ceramic implants for sustained drug delivery. Mater Sci Eng C 2011; 31:1352-6; http://dx.doi.org/10.1016/j.msec.2011.04.020.
29. Kankilic B, Bayramli E, Kilic E, Dağdeviren S, Korkusuz F. Vancomycin containing PLLA/β-TCP controls MRSA in vitro. Clin Orthop Relat Res 2011; 469:3222-8; PMID:21918801; http://dx.doi.org/10.1007/s11999-011-2082-9.
30. Luginbuehl V, Ruffieux K, Hess C, Reichardt D, von Rechenberg B, Nuss K. Controlled release of tetracycline from biodegradable β-tricalcium phosphate composites. J Biomed Mater Res B Appl Biomater 2010; 92:341-52; PMID:19904817.
31. Baker R. Controlled Release of Biologically Active Agents. New York: John Wiley & Sons, 1987.
32. Pitt CG. Poly-ε-caprolactone and its copolymers In: Chasin M, Langer R, eds. Biodegradable Polymers as Drug Delivery Systems. New York: Marcel Dekker Inc., 1990:71-120.
33. Pitt CG, Jeffcoat AR, Zweidinger RA, Schindler A. Sustained drug delivery systems. I. The permeability of poly(ε-caprolactone), poly(DL-lactic acid), and their copolymers. J Biomed Mater Res 1979; 13:497-507; PMID:438232; http://dx.doi.org/10.1002/jbm.820130313.
34. Bowker KE, Wootton M, Rogers CA, Lewis R, Holt HA, MacGowan AP. Comparison of in-vitro pharmacodynamics of once and twice daily ciprofloxacin. J Antimicrob Chemother 1999; 44:661-7; PMID:10552983; http://dx.doi.org/10.1093/jac/44.5.661.
35. Mouriño V, Boccaccini AR. Bone tissue engineering therapeutics: controlled drug delivery in three-dimensional scaffolds. J R Soc Interface 2010; 7:209-27; PMID:19864265; http://dx.doi.org/10.1098/rsif.2009.0379.
36. Holden MTG, Ram Chhabra S, de Nys R, Stead P, Bainton NJ, Hill PJ, et al. Quorum-sensing cross talk: isolation and chemical characterization of cyclic dipeptides from Pseudomonas aeruginosa and other gram-negative bacteria. Mol Microbiol 1999; 33:1254-66; PMID:10510239; http://dx.doi.org/10.1046/j.1365-2958.1999.01577.x.
37. Jeong SI, Kim BS, Lee YM, Ihn KJ, Kim SH, Kim YH. Morphology of elastic poly(L-lactide-co-ε-caprolactone) copolymers and in vitro and in vivo degradation behavior of their scaffolds. Biomacromolecules 2004; 5:1303-9; PMID:15244444; http://dx.doi.org/10.1021/bm049921i.
38. Fernández J, Etxeberria A, Sarasua JR. Synthesis, structure and properties of poly(L-lactide-co-ε-caprolactone) statistical copolymers. J Mech Behav Biomed Mater 2012; 9:100-12; PMID:22498288; http://dx.doi.org/10.1016/j.jmbbm.2012.01.003.
39. Herbert IR. Statistical analysis of copolymer sequence distribution. In: Ibbet RN, ed. NMR Spectroscopy of Polymers. London: Blackie Academic & Professional, 1993:50-79.
40. Lemmouchi Y, Schacht E, Lootens C. In vitro release of trypanocidal drugs from biodegradable implants based on poly(ε-caprolactone) and poly(D,L-lactide). J Control Release 1998; 55:79-85; PMID:9795018; http://dx.doi.org/10.1016/S0168-3659(98)00021-2.
41. Li S. Hydrolytic degradation characteristics of aliphatic polyesters derived from lactic and glycolic acids. J Biomed Mater Res 1999; 48:342-53; PMID:10398040; http://dx.doi.org/10.1002/(SICI)1097-4636(1999)48:3<342::AID-JBM20>3.0.CO;2-7.
42. Ahmed J, Zhang J, Song Z, Varshney SK. Thermal properties of polylactides - effect of molecular mass and nature of lactide isomer. J Therm Anal Calor 2008:1-8.
43. Li S, Garreau H, Vert M. Structure-property relationships in the case of the degradation of massive poly(α-hydroxy acids) in aqueous media - part 3 influence of the morphology of poly(l-lactic acid). J Mater Sci Mater Med 1990; 1:198-206; http://dx.doi.org/10.1007/BF00701077.
44. Sarasua J, Prud'homme RE, Wisniewski M, Le Borgne A, Spassky N. Crystallization and melting behavior of polylactides. Macromolecules 1998; 31:3895-905; http://dx.doi.org/10.1021/ma971545p.
45. Shore EC, Holmes E. Porous hydroxyapatite. In: Hench LL, Wilson J, eds. An Introduction to Bioceramics. Singapore: World Scientific Publishing, 1993:181-198.
46. ISO 15814. Implants for surgery – copolymers and blends based in polylactide – *in vitro* degradation testing.
47. Su L, Jia W, Hou C, Lei Y. Microbial biosensors: a review. Biosens Bioelectron 2011; 26:1788-99; PMID:20951023; http://dx.doi.org/10.1016/j.bios.2010.09.005.
48. Galluzzi L, Karp M. Whole cell strategies based on lux genes for high throughput applications toward new antimicrobials. Comb Chem High Throughput Screen 2006; 9:501-14; PMID:16925511; http://dx.doi.org/10.2174/138620706777935351.
49. Moir DT, Ming Di, Opperman T, Schweizer HP, Bowlin TL. A high-throughput, homogeneous, bioluminescent assay for Pseudomonas aeruginosa gyrase inhibitors and other DNA-damaging agents. J Biomol Screen 2007; 12:855-64; PMID:17644773; http://dx.doi.org/10.1177/1087057107304729.

Publication III

Ahola, N., Veiranto., M., Männistö, N., Karp, M., Rich, J., Efimov, A., Seppälä, J. and Kellomäki, M.

Processing and sustained in vitro release of rifampicin containing composites to enhance the treatment of osteomyelitis

Biomatter, 2 (2012), 213-225

Biomatter 2:4, 213–225; October/November/December 2012; © 2012 Landes Bioscience

Processing and sustained in vitro release of rifampicin containing composites to enhance the treatment of osteomyelitis

Niina Ahola,[1,2,*] Minna Veiranto,[1,3] Noora Männistö,[1] Matti Karp,[4] Jaana Rich,[5] Alexander Efimov,[4] Jukka Seppälä[5] and Minna Kellomäki[1,2]

[1]Department of Biomedical Engineering; Tampere University of Technology; Tampere, Finland; [2]BioMediTech; Tampere, Finland; [3]Bioretec Ltd; Tampere, Finland; [4]Department of Chemistry and Bioengineering; Tampere University of Technology; Tampere, Finland; [5]Department of Biotechnology and Chemical Technology; School of Chemical Technology; Aalto University; Espoo, Finland

Keywords: drug release, antibiotic, rifampicin, biodegradable, poly(L-lactide-co-caprolactone), polylactide

The objective in this study was to develop an osteoconductive, biodegradable and rifampicin releasing bone filling composite material for the treatment of osteomyelitis, a bacterial infection of bone that is very difficult and expensive to treat. The composite material will be used together with a ciprofloxacin releasing composite, because of the rapid development of resistant bacteria when rifampicin is used alone. Three composites were manufactured by twin-screw extrusion. The polymer matrix for the composites was poly(L-lactide-co-ε-caprolactone) 70/30 and all the composites contained 8 wt% (weight percent) of rifampicin antibiotic. The β-TCP contents of the composites were 0 wt%, 50 wt% and 60 wt%. The composites were sterilized by gamma irradiation before in vitro degradation and drug release tests. The hydrolytical degradation of the studied composites proceeded quickly and the molecular weight of the polymer component of the composites decreased rapidly. Rifampicin release occurred in four phases in which the high β-TCP content of the samples, polymer degradation and mass loss all played a role in determining the phases. The ceramic component was seen to have a positive effect on the drug release. The composite with 50 wt% of β-TCP showed the most promising rifampicin release profile and it also showed activity against a common osteomyelitis causing bacteria *Pseudomonas aeruginosa*. A clear inhibition zone was formed in 16 h incubation. Overall, the tested materials showed great potential to be developed into a bone filler material for the treatment of osteomyelitis or other bone related infections in combination with the ciprofloxacin releasing materials.

Introduction

This paper presents the in vitro degradation and drug release results of three rifampicin releasing composite materials as well as the effect of the most promising rifampicin releasing composite against a common osteomyelitis causing bacteria *Pseudomonas aeruginosa*. The materials are intended for use in the treatment of osteomyelitis or other bone related infections together with the ciprofloxacin releasing composite materials presented in our accompanying study.[1] The composites are bioabsorbable and osteoconductive due to the degradation ability of the polymer matrix (poly-L-lactide-co-ε-caprolactone) (PLCL) and the osteoconductive properties of the ceramic filler, β-tricalcium phosphate (β-TCP). It is envisaged that these materials will enable the simultaneous use of bone fillers that contain different antibiotics. The surgeon applying the fillers will be able to decide which antibiotics and in which ratio to use based on the condition of the patient and the pathogen in question. Such materials have also been requested in the literature.[2]

Osteomyelitis, which is very challenging and expensive to treat, is a bone infection that is caused by bacteria, commonly *Staphylococcus aureus*, *Pseudomonas aeruginosa* or *Staphylococcus epidermidis*.[3] Traditional treatment includes surgical debridement of the infected tissue followed by long courses intravenously or orally administered antibiotics.[4] Poor blood circulation in the infected bone tissue can prevent adequate antibiotic concentrations in the infection site being achieved. To overcome this problem, local antibiotic delivery has been applied with commercially available gentamycin releasing Septopal® beads. The problem with this method of antibiotic delivery is that the beads are not biodegradable and require surgical removal followed by bone grafting.[5,6]

Rifampicin has been used together with ciprofloxacin and other fluoroquinolones in the treatment of osteomyelitis or other bone related infections. The use of rifampicin together with other antibiotics in the treatment of *Staphylococcus aureus* infections has been reviewed by Perlroth et al.[7] In general, in in vivo and human studies, the combination of ciprofloxacin with rifampicin was

*Correspondence to: Niina Ahola; Email: niina.ahola@tut.fi
Submitted: 08/08/12; Revised: 10/13/12; Accepted: 11/06/12
http://dx.doi.org/10.4161/biom.22793

more effective than monotherapy especially in prosthetic device infections and osteomyelitis.[8] Rifampicin has also been studied together with fluoroquinolones in the treatment of deep sternal wound infections and studies have shown that using rifampicin together with fluoroquinolones improves the outcome.[9] The fact that rifampicin is effective against bacterial biofilms encourages the use of rifampicin together with other antibiotics.[7,10] Rifampicin should never be used alone because resistant bacterial strains develop quite rapidly as a result.[7,10]

In most of the studies reported about the combination therapy of rifampicin with other antibiotics, the delivery route of the antibiotics has been either intravenous or oral. With local antibiotic treatment, bone tissue that lacks adequate blood circulation can be effectively treated and the pathogens eradicated.[11-19] Previous studies have also shown that with local treatment, the drug concentrations in the blood or other tissues are low, at least a decade lower than in the surrounding tissues,[20-22] which naturally leads to decreased side effects like nausea which has been reported often as the cause for discontinuation of the therapy or continuing the therapy with lower dose.[8,10]

In this study, the potential of the materials to release rifampicin in adequate concentrations and the degradation were only tested in vitro. There is still a need for in vivo and clinical testing of the materials. The materials do, however, show great potential for use in the treatment of osteomyelitis and other bone related infections and are now ready to be tested further in vivo.

Results and Discussion

The effect of processing and sterilization on the materials. The processing method used for the composite materials was twin-screw extrusion and it can be assumed that the ceramic and drug particles were evenly distributed due to the efficient mixing in the extrusion process. The composites are denoted PLCL + R [poly (L-lactide-co-ε-caprolactone) (PLCL) with 8 wt% of rifampicin in feed], PLCL + TCP50 + R [PLCL with 50 wt% of β-tricalcium phosphate (β-TCP) and 8 wt% of rifampicin in feed] and PLCL + TCP60 + R (PLCL with 50 wt% β-TCP and 8 wt% of rifampicin in feed). Processing did not cause degradation detectable with SEC measurements. However, sterilization using gamma irradiation with a measured dose of 29–35 kGy caused significant degradation, as was expected.[23] The average molecular weight (M_w) of the raw material was measured as 246,000 g/mol and the number average molecular weight (M_n) 150,000 g/mol. The M_w of the PLCL + R decreased 30% during the sterilization stage and the M_w of the PLCL + TCP50 + R and PLCL + TCP60 + R decreased 40% and 30%, respectively. The M_n decreased 40% for all the composites during the sterilization stage. The polydispersity of PLCL + R did not change during processing but increased from 1.6 to 2.0 during sterilization. For PLCL + TCP50 + R and PLCL + TCP60 + R, the PD decreased from 1.6 to 1.5 during processing and increased slightly to 1.8 for PLCL + TCP50 + R and 1.6 for PLCL + TCP60 + R.

The residual monomer content of the raw material measured by gas chromatography was 0.08 wt% for L-lactide monomer and below detection limit (< 0.02 wt%) for ε-caprolactone monomer. The L-lactide and ε-caprolactone monomer contents of the processed samples were analyzed from two points in the processing batch and there were two parallel samples in both. The L-lactide monomer content decreased slightly during processing. It was 0.04–0.07 mol% and the caprolactone monomer content was below 0.02 mol% for all tested samples. Because there were no significant differences in the monomer contents of the manufactured materials, it can be assumed that the monomers did not cause differences in the hydrolytic degradation behavior of the studied composites.[24]

UV measurements utilizing the isosbestic point. The UV-measurements of rifampicin proved challenging due to the oxidation of rifampicin to rifampicin quinone in aqueous solutions and in the presence of atmospheric oxygen. This can be seen as a change in the UV-spectrum of a rifampicin solution as well as a change in the color of the solution.[25] Rifampicin quinone has a UV-spectrum partly similar to rifampicin and also has antibacterial properties.[25] The fact that rifampicin quinone degrades further to other compounds that do not have absorbance in the UV/V is area naturally affects the accuracy of this method. Part of the rifampicin is undetected if it has already degraded. The accuracy is highest when the measurements are made at short intervals, not letting the dissolution medium stay unchanged for long periods. However, as the release test period in this study was long, part of the rifampicin that had oxidized to rifampicin quinone, had time to degrade to other compounds that do not have absorptivity in the UV/V is area, even if the measurements were performed in short intervals. It has also been reported that rifampicin degrades more in solutions with low rifampicin concentration.[26] On the other hand, Le Guellec et al. suggest possible in vivo stabilization of the molecule.[27]

In the later stages of the release test period, it was noticed that the degradation products of the polymer matrix induce a broad UV-peak at the beginning of the scanned area (200–220 nm). This broad peak, however, did not significantly interfere with the use of the isosbestic point at 226 nm.

Rifampicin release from the materials. The measured initial rifampicin contents were 6.5 wt% for PLCL + R, 7.9 wt% for PLCL + TCP50 + R and 7.8 wt% for PLCL + TCP60 + R.

The cumulative release of rifampicin from the studied materials is presented in **Figure 1A**. It can be seen that the release occurred in four phases and that the β-TCP content of the composites had a significant effect on the rifampicin release. Rifampicin release from the PLCL + TCP60 + R was faster than from the PLCL + TCP50 + R and reached 80% in 130 d. Rifampicin release from the PLCL + TCP50 + R was slower but closer to zero order release that is the desirable release profile in this case. After 150 d, the release slowed down. The rifampicin release from PLCL + R showed a lag phase at the beginning of the test series that lasted about 50 d, during which time the release of the drug was very slow. When compared with the ciprofloxacin release,[1] the lag phase lasted longer. This is likely due to the fact that the rifampicin molecule is larger than ciprofloxacin, and this causes slower diffusion through the polymer matrix and the polymer degradation and mass loss have a stronger effect on the release.

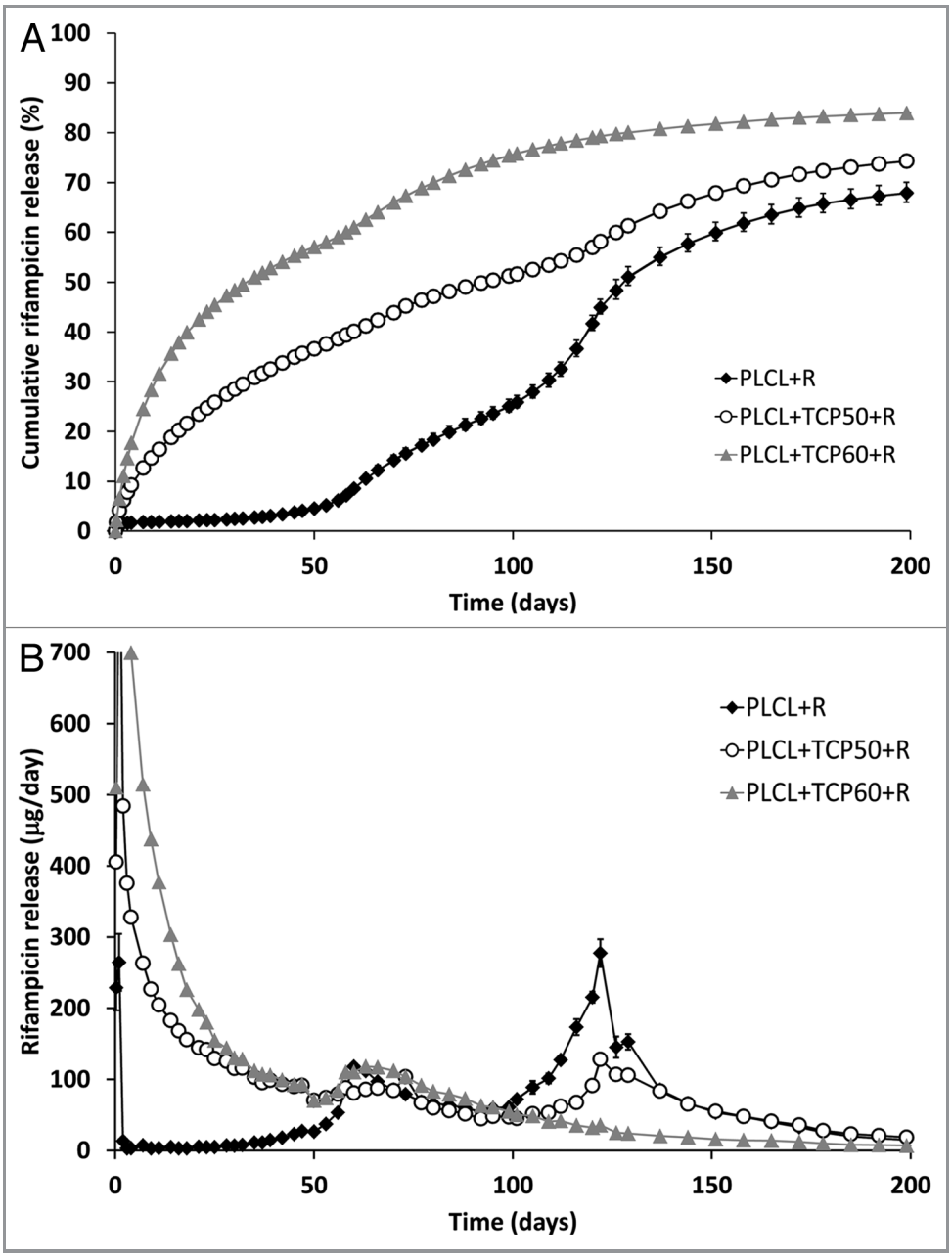

Figure 1. The cumulative (**A**) and daily (**B**) release of rifampicin (R) from composites of poly(L-lactide-co-ε-caprolactone) (PLCL) and β-tricalcium phosphate (TCP) with initial TCP contents of 0 wt%, 50 wt% and 60 wt% and rifampicin content of 8 wt%. Results shown as averages with standard deviations (n = 5).

Because of the complex nature of the rifampicin release, the phases of the release should be considered separately. There are several factors affecting the drug release in this case including: the geometry of the device (cylindrical with a rough surface), high β-TCP content that introduces porosity to the matrix, the properties of the polymer change as it degrades and mass loss. The acceleration of the drug release around the inflection points in the cumulative release curves (**Fig. 1A**) can be easily seen in **Figure 1B**, where the daily release of rifampicin is presented. The presence of the inflection points in the cumulative release profile is characteristic for a release mechanism that is a combination of diffusion and erosion mechanisms.[28]

The first phase of the release was the burst at the beginning of the release. It was during this phase that the rifampicin molecules near the surface were released. The burst in the release was larger than what was observed for ciprofloxacin releasing pellets.[1] Rifampicin is more soluble in water than ciprofloxacin which may be the reason for the larger burst. The second phase of the release lasted approximately until the time point of 53 d. During this phase, the release was mainly governed by diffusion and the release from PLCL + R showed a lag phase with almost negligible

release. From these observations, it can be concluded that the release of rifampicin could not occur solely by diffusion through the plain polymer matrix. The addition of β-TCP to the polymer matrix accelerated the release markedly. β-TCP was likely to introduce porosity to the composite, and thus the rifampicin release could occur via pore diffusion in the time period up to 53 d. The composites containing both rifampicin and β-TCP can be classified as complex monolithic dispersions because of the high amount of filler in the composite. In these cases, the release of the drug is often proportional to the square root of time, but the rate of the release is higher than what is predicted by the Higuchi model.[28] The second phase of the rifampicin release from the composites was proportional to $t^{1/2}$ with R^2 having values of 0.99 for PLCL + TCP50 + R, and 0.98 for PLCL + TCP60 + R. The results were also fitted to the to the power law kinetics equation (**Eqn. 1**):[28,29]

$$\frac{M_t}{M_\infty} = kt^n$$

where M_t/M_∞ is the fractional drug release, k is the release rate constant, t is time and n the release exponent. The rifampicin release from PLCL + TCP50 + R and PLCL + TCP60 + R had n values of 0.53 and 0.44 respectively. For cylindrical geometry and Fickian diffusion, the diffusion release exponent n would have a value of 0.45. For Case II diffusion (or anomalous diffusion), the n has values of $0.45 < n < 1$. The result suggests that the rifampicin release occurs by Case II diffusion[28] from the PLCL + TCP50 and by Fickian diffusion from PLCL + TCP60 + R during the second phase of the release.

In the third phase, the drug release was accelerated due to the increased permeability of the polymer caused by degradation. Additionally, the polymer erosion started to play a role in increasing the release rate. With a non-eroding system, the drug release would slowly decrease because it is often proportional to the drug concentration in the device. In the case of a biodegradable system, the increased permeability and polymer erosion accelerate the release.[28] Here, the third phase of the release of PLCL + TCP50 + R obeyed again the $t^{1/2}$ kinetics very well ($R^2 = 0.99$). The release from PLCL + TCP60 + R had at this point reached 60% of the total cumulative release.

There was also a fourth phase to be seen in the release of PLCL + R and PLCL + TCP50 + R but not in the PLCL + TCP60 + R. The fourth phase of the release was also not seen in the ciprofloxacin release results.[1] The inflection point in the release curves was at the time point of 116 d. It coincided well with the acceleration of mass loss from the composites. The mass loss was already notable at that time and the M_w of the polymer had decreased to the level of 9,000–14,000 g/mol. From the PLCL + TCP60 + R, the available drug for release had apparently been released already at this time point and thus no phase change was seen there.

Rifampicin remaining in the samples after the in vitro test series. At the time point of 250 d, the drug release had decreased to an almost negligible level and 70–85% of the total rifampicin loaded in the composites had been released. The test series was continued for 392 d but no notable rifampicin release was detected. The remaining rifampicin in the composites was measured after the drug release test had been terminated. The measurement was done in a similar way to the initial rifampicin content measurements. The brownish red color of the pellet-shaped samples indicated that some rifampicin remained in the samples even though drug release had ceased. There has been evidence about rifampicin being incorporated within the crystalline parts of a polycaprolactone polymer and this might be the case here although the crystals may be formed of L-lactide units.[30] The remaining portion of the initial rifampicin that was measured after the termination of the test series was 10.7% for PLCL + R, 5.0% for PLCL + TCP50 + R and 3.4% for PLCL + TCP60 + R. When combined with the measured released rifampicin, the total rifampicin amount detected did not reach 100%. The fact that rifampicin oxidizes to rifampicin quinone which is further degraded to compounds with no UV-absorbance, explains why part of the rifampicin seems to have disappeared.[25] Unfortunately, this affects the accuracy of this method in analyzing the released rifampicin. However, the method can be used to estimate the rifampicin release and compare the composites with each other. In in vivo conditions, the situation may be different. Le Guellec et al.[27] found that rifampicin stability was better in rifampicin containing plasma samples taken from patients treated with rifampicin than in plasma samples where rifampicin was added in the laboratory. This improved stability suggests that rifampicin may be more stable in vivo than in vitro.

Inhibition zone testing. The effect of the rifampicin releasing composite containing 50 wt% of β-TCP against the common osteomyelitis causing bacteria *Pseudomonas aeruginosa* was tested using bioluminescence imaging. The results are illustrated with **Figure 2**, where the bioluminescence imaging results (16 h incubation) of a 6-well plate cultured with *Pseudomonas aeruginosa* and rifampicin containing composite pellets are shown. The antibiotic containing composite pellets are on the lower row and control pellets without antibiotics are on the top row. The results show that the composite material releases rifampicin in levels high enough to eradicate *Pseudomonas aeruginosa*. The inhibition zone can be seen as a dark blue area surrounding the antibiotic releasing pellets in **Figure 2**. The blue area indicates dead bacteria whereas the other colors indicate still living bacteria. First signs of the forming inhibition zone were observed already after two hours of incubation. If compared with the bioluminescence results of ciprofloxacin releasing pellets[1] the inhibition zone was smaller with rifampicin. The larger molecular weight of rifampicin may affect the diffusion of the antibiotic in agar and make it rather slow, which is seen as the slow growth of the inhibition zone. However, as seen in the drug release results, the initial burst was larger with rifampicin releasing pellets than with ciprofloxacin pellets and this is probably due to the better solubility of rifampicin.

In vitro degradation of the composites. *Molecular structure.* The ^{1}H NMR spectra were measured from eight samples (raw material PLCL, plain rifampicin, PLCL + R at 0, 26 and 52 weeks and PLCL + TCP50 + R at 0, 26 and 52 weeks in vitro). The ^{1}H NMR signals of the polymer were assigned and the data were analyzed in the same way as in our accompanying study.[1] The

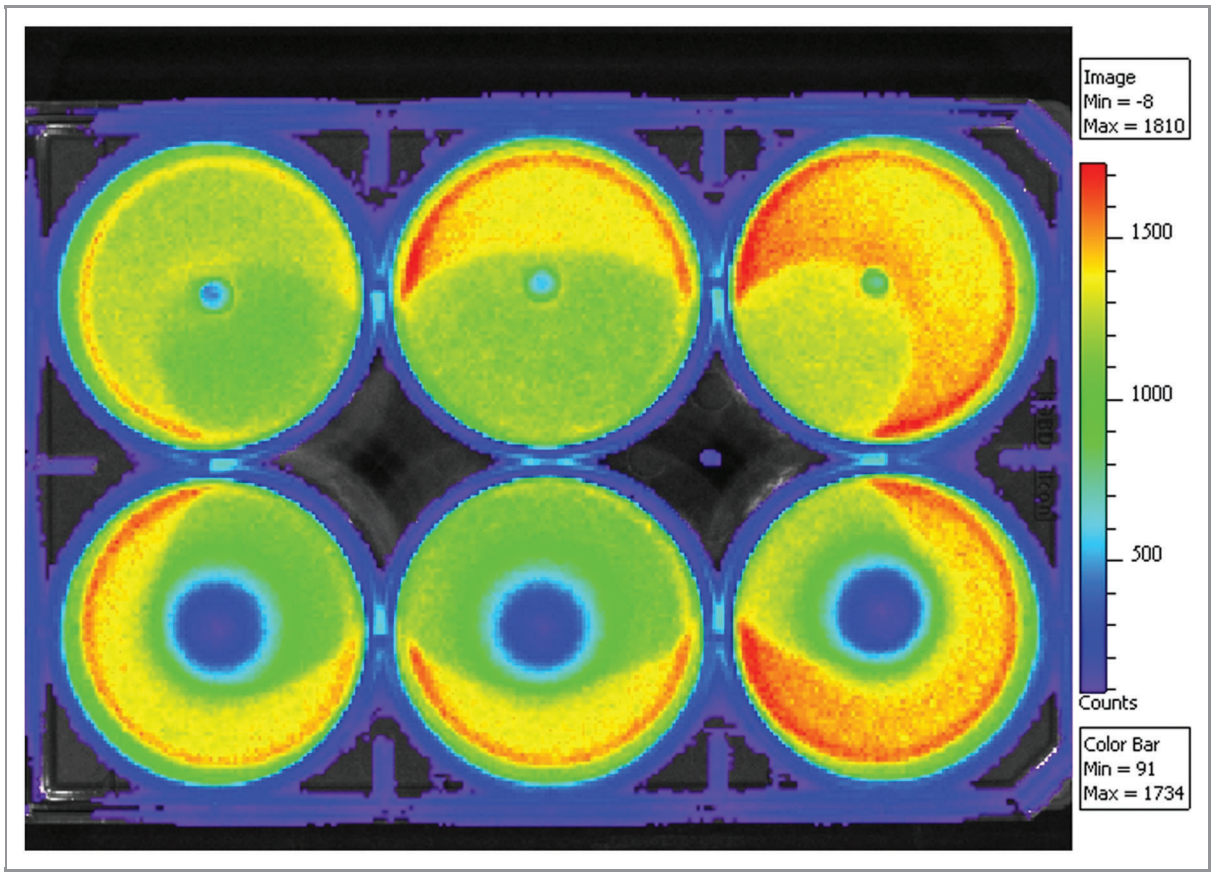

Figure 2. Bioluminescence results of the rifampicin containing (8 wt%) composites of poly(L-lactide-co-ε-caprolactone) and 50 wt% of β-tricalcium phosphate on a bacterial culture of light emitting *Pseudomonas aeruginosa*. Pellets containing rifampicin are on the lower row and corresponding composites without rifampicin are on the top row and act as controls.

results show a similar effect of change in the comonomer ratio of the copolymer as the hydrolysis proceeded that was seen with ciprofloxacin antibiotic containing composites.[1] The L-lactide to ε-caprolactone molar ratio was increased from 68/32 of the raw material and the samples at 0 weeks to 77/23 of the PLCL + TCP50 + C and 82/18 of the PLCL + C at 52 weeks. A similar effect has also been reported by In Jeong et al.[31]

The microstructure of the copolymer was also studied similarly to what was presented in our accompanying study.[1] It was done according to Herbert[32] and Fernández.[33] The results of the average sequence length calculations showed the expected results based on the findings of the ciprofloxacin containing materials.[1] The PLCL copolymer had a block structure with more random parts in between. The randomness factor R had a value of 0.25 for the raw material and close to that for the samples prior to in vitro testing. The R factor decreased dramatically during the degradation of the polymer to 0.18 for both PLCL + TCP50 + R and PLCL + R at 52 weeks. This decrease indicates that the more random parts of the copolymer degrade first and the blocky structures that comprise long L-lactide blocks remain in the structure. At the beginning of the test series, the sequence lengths of L-lactide were 13 and increased to 23 and 31 for PLCL + TCP50 + R and PLCL + R at 52 weeks respectively. This supports the general interpretation that random parts of the copolymer degrade first, and thus the average sequence length is increased. The average sequence length of ε-caprolactone was not significantly changed during hydrolysis for any of the tested samples and had values of 5.5–7 for all the analyzed samples.

Signals of rifampicin were visible in the plain rifampicin sample and for the composite samples only in the 0 week (after processing and sterilization) samples. Due to the rather low sensitivity of NMR, the low contents of rifampicin in the samples from the 26- and 52-week time points were not seen in the NMR spectra. The ^{1}H spectrum of plain rifampicin was compared with the spectra of the 0 week samples. ^{1}H NMR analysis reported by Cellai et al. was also used when the signals were assigned to the protons of the rifampicin molecule.[34]

Some of the rifampicin signals overlapped with the polymer signal in the composite samples and could not be analyzed. These were some of the protons in the ansa chain (protons 16, 18, 20, 21, 22, 2 and 31), protons 32 of the naphtalene ring, and protons 59 of the methyl group attached to the piperazinyl ring. The signal assignment is presented as **Figure 3** and the spectra can be found as supplementary data.

The amide proton and the OH-groups of the naphthalene ring were clearly visible at δ 11.98 ppm, 13.11 ppm and 13.41 ppm,

respectively. Their chemical shifts were stable and the integrals were in good stoichiometric ratio. The protons of the methylene group located above the plane of the naphthalene ring (protons 45) showed a signal below 0 at δ -0.31 ppm in plain unprocessed rifampicin and processed PLCL + R and PLCL + TCP50 + R samples. The fact that this signal is identical in all the samples proves that the ansa chain has retained its original configuration. If not, the signal of this group would have appeared elsewhere in the spectrum. The ansa bridge protons 13, 14, 15, 17, 19, 23 and 25 were clearly visible, stable when compared between the samples, and were in good stoichimetric agreement with the rifampicin structure. The signals of the protons 37, 39 and 41 of the methyl substituents of the ansa chain and the signals of the protons 54 and 56 of the piperazine ring were in the shoulder of a large polymer signal, and thus their accurate integration was not possible. Additionally, signals of the equivalent protons 53 and 57 of piperazine ring appeared at δ 3.02 overlapping with signals of the protons 19 and 47 and thus could not be accurately integrated. However, their combined integral showed that there was no change between samples in either the positions of the signals or their integrals.

As a conclusion of the NMR analysis of rifampicin, it can be stated that no deviations of the original rifampicin structure were found after the analysis of the composite samples and plain rifampicin sample. Thus, rifampicin had maintained its original structure during the processing and sterilization stages.

Molecular weights, mass loss and water absorption. The decrease of the molecular weights (both M_w and M_n) was rapid (**Fig. 4A**), and when compared with the composites with ciprofloxacin antibiotic reported in the accompanying study,[1] there were no significant differences in the degradation behavior. At the beginning of the hydrolysis test series, the molecular weight of the composites containing antibiotics degraded more rapidly than composites without antibiotics,[40] but the differences rapidly leveled out. Overall, the degradation obeyed first order kinetics with k values of 1.6×10^{-3} 1/h for PLCL + R, 1.4×10^{-3} 1/h for PLCL + TCP50 + R, and 1.4×10^{-3} 1/h for PLCL + TCP60 + R. The values are very similar to those calculated for ciprofloxacin containing composites.[1] After 52 weeks of hydrolysis at 37°C and pH 7.4, the molecular weights of all the composites had decreased by 98% to 2% of the initial value of the raw material.

The SEC distribution plots showed emerging bimodality at 20 weeks for PLCL + R and clear bimodality at 39 weeks for PLCL + TCP50 + R and PLCL + TCP60 + R. The same kind of bimodality is present in composites with ciprofloxacin antibiotic[1] beginning from the 20th week of the test series. Bimodality in the SEC distribution suggest that the blocky structure of the copolymer, shown by the ^{1}H NMR analysis, causes the random parts of the copolymer to degrade first and this might cause an

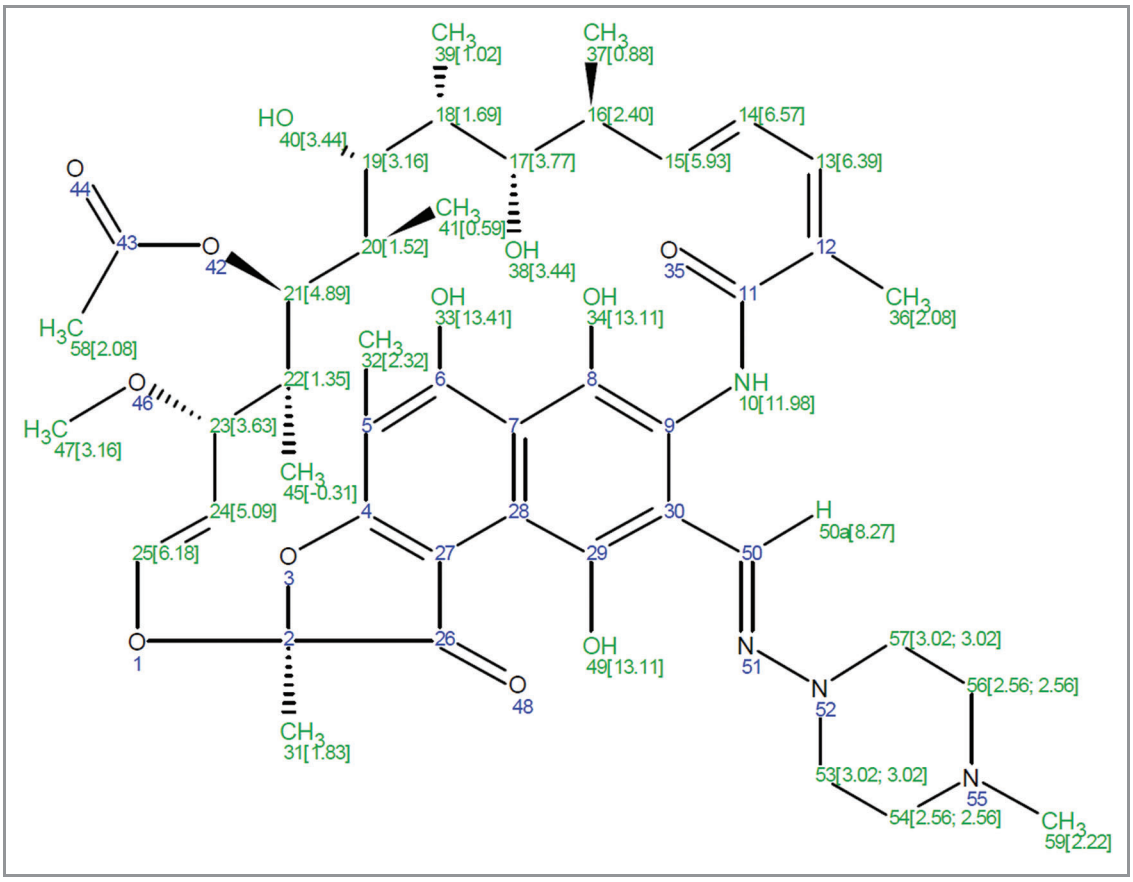

Figure 3. Chemical structure, atom numbering and the ^{1}H chemical shifts of rifampicin.

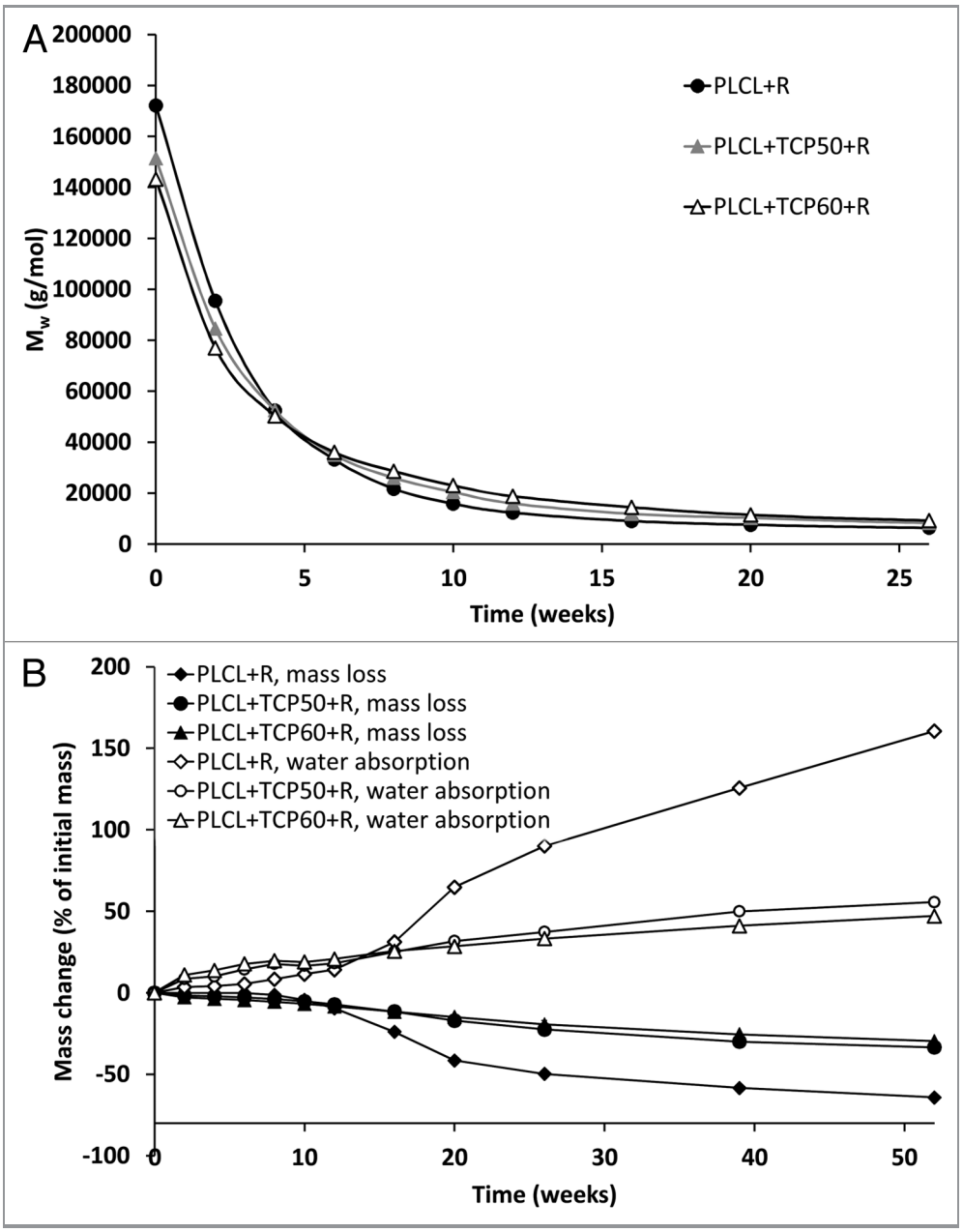

Figure 4. Weight average molar weight (M_w) (**A**), and mass loss and water absorption (**B**) of the studied composites as a function of time in vitro. The composites comprised of poly(L-lactide-co-ε-caprolactone) (PLCL) and β-tricalcium phosphate (TCP) and rifampicin (R) with initial TCP contents of 0 wt%, 50 wt% and 60 wt% and rifampicin content of 8 wt%. Error bars in part **B** are not visible due to the small values of standard deviations.

increase in a certain part of the SEC distribution curve as the blocky parts comprising mainly L-lactide monomers remain in the polymer structure.

The mass loss of the tested materials was small and steady during the first ten weeks. (**Fig. 4B**) During the first six weeks, the mass loss was caused by the rifampicin release from the polymer matrix. After this time point, the mass loss of the polymer started. At the time point of 10 weeks, the mass loss of PLCL + R accelerated and had already reached 50% at 26 weeks. The mass losses of PLCL + TCP50 + R and PLCL + TCP60 + R were steady and proceeded similarly for both of the composites. The same kind of behavior was seen in the water absorption of the tested materials. The PLCL + R showed accelerated water absorption after 10 weeks. When compared with the results of ciprofloxacin containing composites,[1] the acceleration of the water absorption and mass loss started earlier. Rifampicin is likely to be more hydrophilic due to its molecular structure, and thus increases the water absorption of the material.

β-TCP contents of the materials. The proportion of β-TCP in the composites was seen to increase as polymer degradation proceeded, as shown in **Figure 5**. The increase in the proportion of β-TCP accelerated after 10 weeks in vitro which correlates well

with the acceleration of the mass loss of the polymer matrix. β-TCP remained in the samples due to the very slow dissolution of β-TCP.[40]

Thermal properties. The changes in the glass transition temperatures (T_g) of the materials during the in vitro test series are shown in **Figure 6A**. The T_g values presented in **Figure 6A** were taken from the second heating to ensure comparable values of the samples as their thermal histories were similar. T_gs of 23–25°C were measured after processing and sterilization of the composites. This is in agreement with the literature.[35] During the degradation test series, the T_gs of the rifampicin containing composites decreased until week 12. The same kind of decrease was observed with composites with ciprofloxacin but the decrease time period was longer, up to the 20th week.[1] During the first 12 weeks, the M_w of the polymer decreased dramatically, which is known to affect the T_g of a polymer.[36] Additionally, the solubility of the drug in the polymer may play a role in the glass transition of the polymers and may plasticize the polymer causing a decrease in T_g. An increase in the T_g after 12 weeks in vitro was due to the change in the comonomer ratio, seen in the ^{1}H-NMR analysis of the copolymer. The proportion of ε-caprolactone comonomer in the polymer decreased and the L-lactide increased.

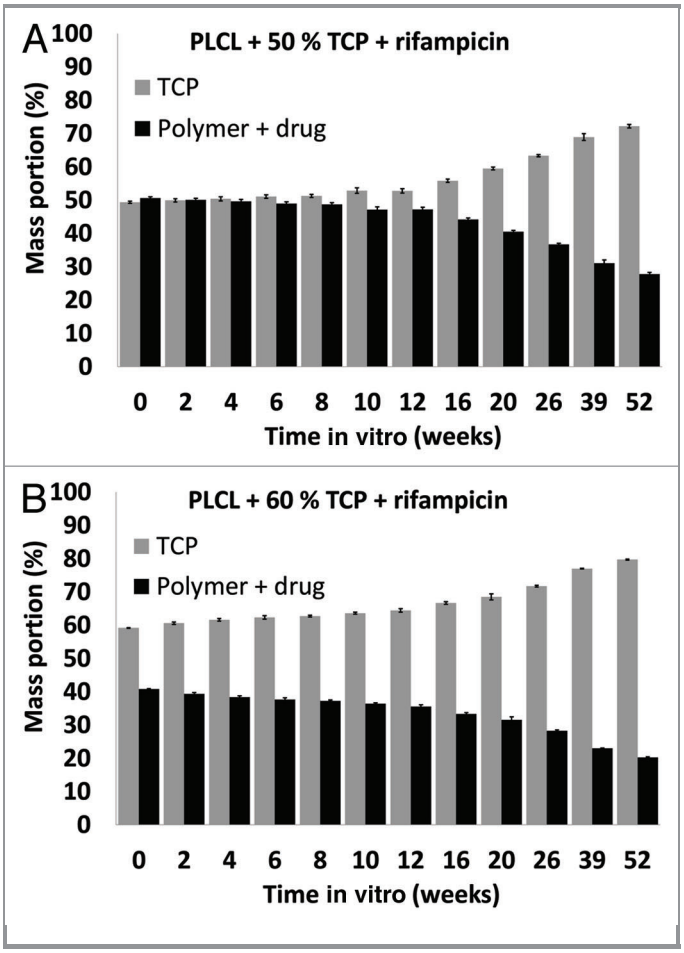

Figure 5. β-tricalcium phosphate (TCP) contents of the studied composites as a function of time in vitro. The composites comprised of poly(L-lactide-co-ε-caprolactone) (PLCL), TCP, and rifampicin (R) with initial TCP contents of 50 wt% (TCP50), and 60 wt% (TCP60) and rifampicin content of 8 wt%. Results shown as averages with standard deviations (n = 5). (**A**) PLC + 50% TCP + rifampcin and (**B**) PLC + 60% TCP + rifampcin.

Melting temperatures and melting enthalpies were analyzed from the first heating of the samples because during the second heating, the melting peaks no longer appeared due to fast cooling in the DSC analysis. Most of the samples showed clear bimodality in the melting peaks the same way which was observed for ciprofloxacin containing composites.[1] Melting temperatures in general showed a clear increase up to the 20th week in the test series (data not shown). They increased from the initial value of 115°C to 120–126°C at 20 weeks. After that the melting temperatures started to decrease again and ended up at 106–109°C at 52 weeks.

Melting enthalpies, which describe the crystallinity of the polymer, were analyzed and corrected to correspond to the combined polymer and rifampicin part of the composites. Although absolute crystallinity values could not be calculated because the theoretical value of 100% crystalline poly(L-lactide-co-ε-caprolactone) 70/30 was not available, relative changes in the crystallinity were observed. There was a steady increase in the crystallinity of the composites throughout the test series (**Fig. 6B**). This indicates an increase in crystallinity as the amorphous parts of the polymer degrade first. Furthermore, the fact that shorter polymer chains are more easily able to rearrange themselves into crystals has an effect on the increasing crystallinity.[37] The ^{1}H NMR study showed that there were rather long L-lactide blocks in the copolymer and their proportion increased as the more amorphous random parts of the copolymer degraded. As the polymer chains were broken into shorter fragments, these blocks formed crystals when they were more able to rearrange themselves. Additionally, it was observed that the composite without β-TCP showed higher melting enthalpies than the composites with β-TCP, especially from the 20-week time point on. This observation suggests that the presence of β-TCP in the composites may have an inhibiting effect on the crystallization.

Microstructure. Some porosity was seen in the composites containing β-TCP throughout the degradation test series. The material without β-TCP did not show significant porosity. The differences between composites containing 50 wt% or 60 wt% of β-TCP were not notable. SEM micrographs showed pores of different sizes in the samples throughout the hydrolysis test series (**Fig. 7A–C**). Pores up to the size of 100–200 μm were observed as well as smaller pores. Additionally, the surfaces of the pellet-shaped samples were porous. (**Fig. 7D–F**).

Rifampicin antibiotic, or ciprofloxacin antibiotic in the accompanying article[1] were not observed to affect the porosity in any way.

Conclusion

The tested composites showed rifampicin release profile with four phases. The composite containing 50 wt% of β-TCP had the most promising steady release profile. The β-TCP was observed to accelerate the rifampicin release. The release from the composite

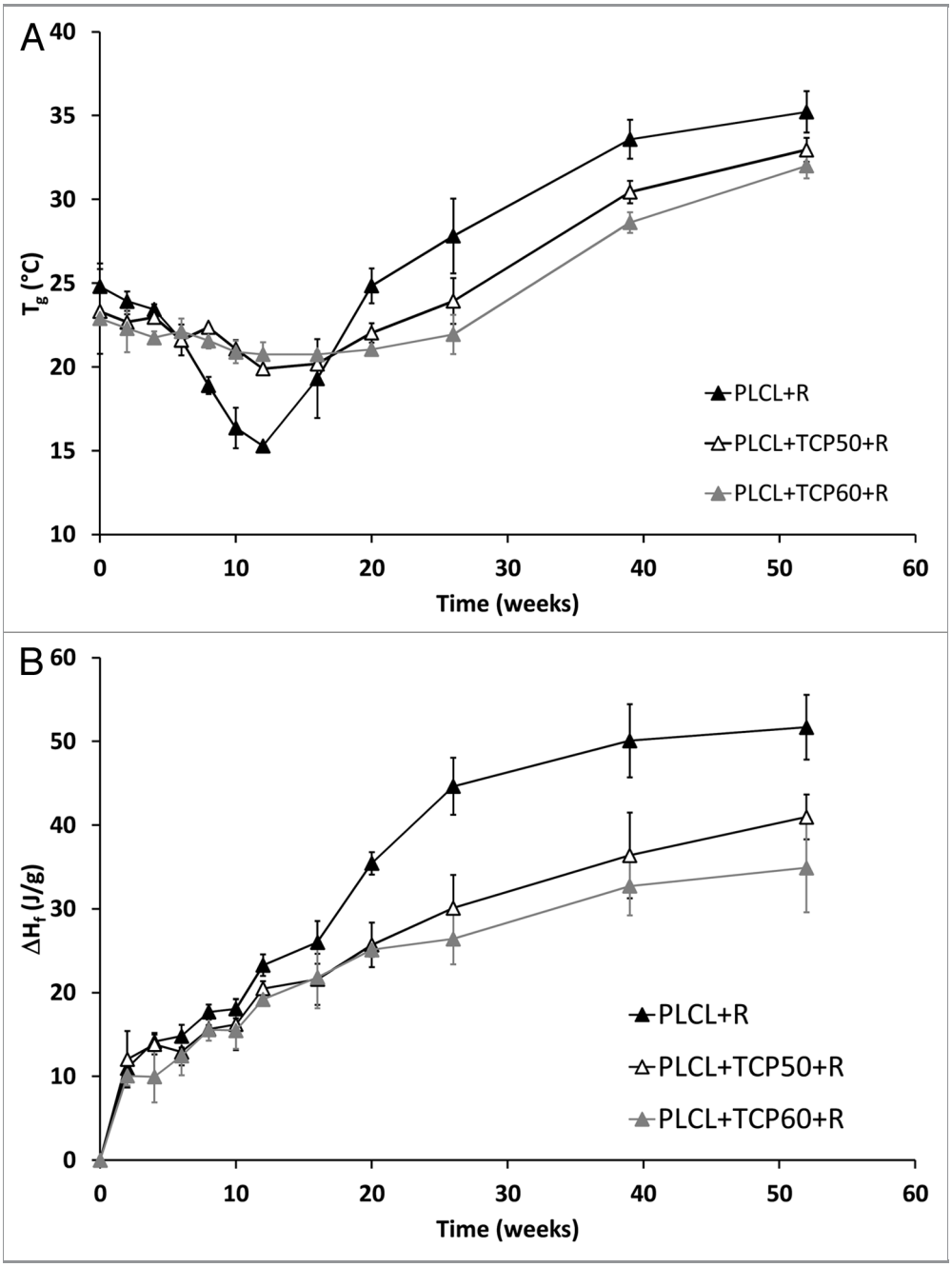

Figure 6. Glass transition temperatures (T_g) (**A**) and melting enthalpies (ΔH_f) (**B**) of the copolymer in the studied composites as a function of time in vitro. The composites comprised of poly(L-lactide-co-ε-caprolactone) (PLCL) and β-tricalcium phosphate (TCP) and rifampicin (R) with initial TCP contents of 0 wt%, 50 wt% and 60 wt%. Results shown as averages with standard deviations (n = 2–5).

without β-TCP showed a long lag phase that was probably due to the large size of the rifampicin molecule and low diffusivity of the drug in the polymer. As the polymer degradation proceeded and the permeability of the polymer increased, the rifampicin release also accelerated. The decrease of the molecular weights was rapid as was expected and the ^{1}H NMR results showed a change in the comonomer ratio toward an increasing lactide comonomer content as degradation proceeded. Additionally, the polymer was observed to have a rather blocky structure, having long L-lactide blocks in the structure. The composite that contained 50 wt% of β-TCP showed activity in eradicating common osteomyelitis causing bacteria *Pseudomonas aeruginosa* which was seen as development of an inhibition zone in bacterial cultures utilizing bioluminescence.

Because rifampicin should not be used alone, a ciprofloxacin releasing composite material was developed in the accompanying study[1] for use with the rifampicin-releasing composite material reported here. Both of the reported composite materials show

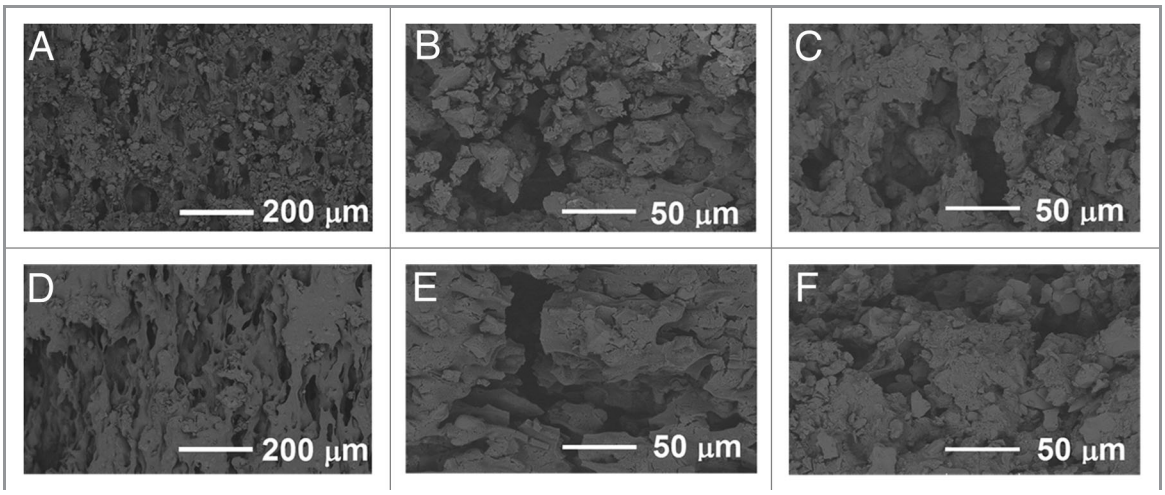

Figure 7. SEM micrographs of the composites of poly(L-lactide-co-ε-caprolactone) (PLCL), 60 wt% of β-tricalcium phosphate (TCP) and rifampicin. (**A–C**) fractured surfaces after 0 weeks, 26 weeks and 52 weeks in vitro respectively. (**D–F**) Outer surfaces after 0 weeks, 26 weeks and 52 weeks in vitro, respectively.

potential to be developed into biodegradable, antibiotic releasing and osteoconductive bone-grafting materials that can be used together in the treatment of osteomyelitis and other bone related infections. In vitro tests are always needed to select the optimal composition of the materials for further studies and according to the results reported here, the choice is the composite with 50 wt% of β-TCP. However, preclinical followed by clinical studies are needed to establish the effect of these materials when they are implanted in living tissue both alone and together.

Materials and Methods

The processing and characterization methods, except UV-analysis, follow the same principles as in our article concerning ciprofloxacin releasing materials.[1]

Materials. Medical grade poly(L-lactide-co-ε-caprolactone) (PLCL) with the comonomer ratio of 70/30 and M_w of 246,000 g/mol was purchased from Purac Biomaterials. β-tricalcium phosphate (β-TCP) (granule size $<$ 38 μm) was purchased from Plasma Biotal Ltd. Rifampicin antibiotic (molecular structure shown in **Fig. 3**) was purchased from Orion Pharma. Sörensen buffer solution was prepared according to the standard ISO 15814[38] and the chemicals used for the buffer solution (Na_2HPO_4 and KH_2PO_4) were purchased from J.T. Baker. The chemicals used for the bioluminescence bacterial cultures were: Gentamicin sulfate (Sigma-Aldrich), Isopropyl-β-D-thiogalaktopyranoside (IPTG) (Fermentas), Trypton (Lab M Limited), Yeast extract (Lab M Limited), Sodium Chloride (Merck), Agar (Merck).

Processing and sterilization. Dried polymer, β-TCP powder, and rifampicin (72 h in vacuum at room temperature) were processed into rod-shaped billets with a diameter of approximately 2.5 mm with a co-rotating custom-built intermeshing twin-screw extruder (L/D ratio = 22.5) in a nitrogen atmosphere. PLCL copolymer, β-TCP and rifampicin antibiotic were delivered to the process with separate gravimetric screw feeders. The mixing of the components took place in the extruder. A haul-off unit was used to guide the extrudate from the die and the diameter of the billets was fine-tuned adjusting the speed of the haul-off unit. Three different composites were processed. Each composite had 8 wt% rifampicin antibiotic in feed and different β-TCP contents (0, 50 and 60 wt%). These composites are denoted PLCL + R, PLCL + TCP50 + R and PLCL + TCP60 + R, respectively. Pellet-shaped samples (length approximately 2.5 mm) were cut from the billets. Before degradation tests were performed, the samples were packed and sterilized using gamma irradiation (minimum dose 25 kGy).

Drug release study. Weighed test samples (each test sample consisted of 15 pellets, approximately 300 mg in total) were placed in brown glass bottles along with 20 ml Sörensen buffer solution. Five parallel test samples were tested for each composite material. The bottles were placed in an incubator shaker at 37°C. At predetermined time intervals, the buffer solution was withdrawn from each of the bottles and replaced with fresh solution. The amount of buffer solution and the periodical change to fresh buffer solution enabled sink conditions to be valid throughout the test series. The amount of released rifampicin was determined from the buffer solution using a Unicam UV 500 spectrometer (ThermoSpectronic) at isosbestic point at wavelength of 226 nm. A wavelength area from 190 to 650 nm was scanned in order to detect possible changes in the rifampicin molecular structure which cause deviation in the UV-spectrum. Rifampicin is known to oxidize to rifampicin quinone in mildly alkaline aqueous solutions and in the presence of atmospheric oxygen. This can be seen as a change in the UV-spectrum of a rifampicin solution as well as a change in the color of the solution. Rifampicin quinone has a partly similar UV-spectrum to rifampicin and it also possesses antibacterial properties.[25] At a wavelength of 226 nm, an isosbestic point was found that could be used in the rifampicin content measurements. At this point, we can calculate the initial rifampicin content of the solution despite

the fact that it has partly oxidized to rifampicin quinone, because the absorbance of these compounds is the same at this wavelength. The fact that rifampicin quinone degrades further to other compounds without UV-absorbance, may affect the accuracy of this method. The accuracy is at its best if the measurements are made at short intervals, not letting the dissolution medium stay unchanged for long periods.

Inhibition zone testing using bioluminescence imaging. The effect of the antibiotic releasing composite materials against one of the common osteomyelitis causing bacteria *Pseudomonas aeruginosa*, which was used as a non-pathogenic model organism, was tested using bioluminescence imaging based on the ability of genetically engineered bacteria to emit light. The antibiotic containing composite material chosen for this study was the composite containing 50 wt% of β-TCP (PLCL + TCP50 + R) based on the most promising drug release results. Composite of PLCL and 50 wt % β-TCP without antibiotics was used as control.

An engineered bacteria strain of *Pseudomonas aeruginosa* PAO-LAC carrying plasmid pUCP24GW[39] was used as the biosensor. The bacteria were cultured on antibiotic plates overnight at 30°C and 300 rpm (1 mM IPTG, 10 μg/ml gentamycin), and suitable colonies were moved into liquid culturing in LB (5 g/l yeast extract, 10 g/l tryptone and 5 g/l NaCl). If the bacteria did not produce luminescence as wished in the morning, 1/50 dilution was made in a culture tube and it was incubated at 37°C and 300 rpm for three hours. The level of luminescence of the cultures was measured by using Plate Chameleon™ multilabel counter 1.001 (Hidex Ltd.), and at volume of 200 μl. Counts of 1.1–2.3 × 10^6 were found satisfying.

Layers of LB-agar (agar 15 g/l, 2 ml) were cast into 6-well plate, and the controls and antibiotic containing composite pellets were placed on top of them (each pellet into its own well). Bacteria were mixed with soft LB-agar (7.5 g/l) solution and cast on top of the first layers. The amount of bacterial culture was dependent on the luminescence level. It was 350–500 μl/well. After solidification, the plate was taken to the imaging station of Xenogen VivoVision IVIS® Lumina luminescence camera (Caliper LifeSciences). Pictures were taken every 20 min for 16 h with exposure time of 30 sec. The pictures were analyzed using Living Image® 3.1 program (Caliper LifeSciences).

In vitro degradation study. Degradation tests were conducted at 37°C in vitro following the standard ISO 15814.[38] First, weighed test samples (each test sample consisted of 15 pellets) were placed in brown glass bottles along with 20 ml Sörensen buffer solution. Five parallel test samples of each composite material were tested at each time point. The bottles were placed in an incubator shaker at 37°C. The pH of the buffer solution was measured periodically with a calibrated pH meter and the buffer solutions were changed every two weeks at the beginning of the test series and once a week as the degradation accelerated. Test samples were withdrawn at predetermined time points of 2, 4, 6, 8, 10, 12, 16, 20, 26, 30 and 52 weeks.

Methods of analysis. *Residual monomer.* The determination of residual L-lactide and ε-caprolactone monomer contents before and after processing was performed by Ramboll Analytics Oy. The ε-caprolactone and L-lactide contents were measured after chloroform extraction of the samples using gas chromatography (DC8000, CE Instruments) and after chloroform dilution using an FI-detector. The measuring resolution was 0.02%.

Initial drug content measurements. Samples of about 150 mg were weighed from each manufactured composition and dissolved in 50 ml of chloroform (J.T. Baker). The amount of rifampicin in the chloroform solution was determined using a Unicam UV 540 Spectrophotometer (ThermoSpectronic) at a maximum absorption wavelength of 349 nm. The rifampicin concentration in the solution was calculated using Beer-Lambert law and standard curves prepared with known concentrations of rifampicin.

Mass loss, water absorption and pH. After the test samples were withdrawn from the incubator shaker, they were rinsed twice with distilled water and the surfaces were carefully wiped with tissue paper. The test samples were weighed immediately after wiping. The weighed test samples were dried for at least three days at ambient conditions and for one week in vacuum. Finally, the test samples were reweighed to obtain the dry masses. The dried test samples were stored in a desiccator for further analysis.

The mass loss was calculated as the difference between the initial mass of the test sample and the mass of the dried test sample divided by the initial mass of the test sample. The water absorption was calculated as the difference between the mass of the wet test sample and the mass of the dried test sample divided by the mass of the dried test sample.

Molecular weights. The molecular weights (number average, M_n, and weight average, M_w, molecular weights) and polydispersity (PD) of the copolymer were determined at room temperature by size exclusion chromatography (SEC) (Waters Associates system equipped with a Waters 717plus autosampler, a Waters 510 HPLC solvent pump, four linear PL gel columns (10^4, 10^5, 10^3 and 100 Å) connected in series, and a Waters 2414 differential refractometer). Chloroform (Riedel-de Haën Ag, stabilized with 1% ethanol) was used as a solvent and eluent. The samples were filtered through a 0.5 μm Millex SR (Millipore) filter. The injected volume was 200 μl and the flow rate was 1.0 ml/min. Monodisperse polystyrene standards were used for primary calibration.

Thermal properties. Thermal analysis was performed using differential scanning calorimeter DSC Q1000 (TA Instruments). Nitrogen was used as the sweeping gas. To ensure the samples (4–6 mg) had a similar thermal history, they were heated twice and cooled rapidly in between. The heating rate was 20°C/min, the cooling rate was 50°C/min and the temperature range was -60°C to +200°C. Glass transition temperatures (T_g) were obtained from the second heating and melting temperatures and enthalpies (T_m and ΔH_f respectively) were obtained from the first heating cycle. Two to five parallel samples were tested for each composite material and time point. The results were analyzed using Universal Analysis Software and averages and standard deviations were calculated.

Ceramic content. The β-TCP content of the test samples was measured using thermogravimetric analysis (TA Instruments). Approximately 20 mg of a sample was used and the samples were heated at a rate of 20°C/min up to 700°C. The results were analyzed using Universal Analysis Software. Five parallel samples

of each composition at each time point were analyzed and the results were calculated as averages and standard deviations.

Molecular structure. The proton spectra of the samples were measured using Varian Mercury 300 MHz NMR Spectrometer (Varian Associates Inc.) at room temperature. Tetramethylsilane (TMS) was used as an internal standard, and chemical shifts were measured relative to TMS. The ^{1}H NMR spectra were measured in standard 5 mm tubes in deuterochloroform. The data were acquired until the quality of the spectrum was sufficient and the number of scans was about 512. The proton NMR spectra of the samples were processed and analyzed using SpinWorks 3.1 and ACD/Spectrus software. Phase correction and baseline correction were applied to all spectra. Information on the molecular composition of rifampicin and the comonomer ratio of the copolymer was obtained.

Microstructure of the samples. The microstructure of the composites was observed using scanning electron microscopy (Philips XL-30 SEM equipped with a LaB6 filament, Philips) with an acceleration voltage of 12.0 kV. The micrographs were taken both on the surface of the samples and on fractured samples that were coated with gold (Edwards S150 Sputter Coater) prior to microstructure examination.

Disclosure of Potential Conflicts of Interest

No potential conflicts of interest were disclosed.

Acknowledgments

Research collaboration with Bioretec Ltd. and financial support from the Finnish Funding Agency for Technology and Innovation (TEKES) and National Graduate School of Musculoskeletal Disorders and Biomaterials (N.A. and M.V.) are gratefully appreciated. MSc Kalle Räsänen, Raija Reinikainen, Kaija Honkavaara, Eija Ahonen and MSc Vuokko Heino are warmly thanked for technical assistance. Peter Heath is thanked for checking the language of the manuscript.

Supplemental Materials

Supplemental materials may be found here:
www.landesbioscience.com/journals/biomatter/article/22793

References

1. Ahola N, Männistö N, Veiranto M, Karp M, Rich J, Efimov A, et al. An in vitro study of composites of poly (L-lactide-co-epsilon-caprolactone), β-tricalcium phosphate, and ciprofloxacin intended for local treatment of osteomyelitis. Biomatter 2013; In press.
2. Ginebra MP, Traykova T, Planell JA. Calcium phosphate cements as bone drug delivery systems: a review. J Control Release 2006; 113:102-10; PMID: 16740332; http://dx.doi.org/10.1016/j.jconrel.2006.04.007
3. Chihara S, Segreti J. Osteomyelitis. Dis Mon 2010; 56: 6-31; http://dx.doi.org/10.1016/j.disamonth.2009.07.001
4. Parsons B, Strauss E. Surgical management of chronic osteomyelitis. Am J Surg 2004; 188(Suppl):57-66; PMID:15223504; http://dx.doi.org/10.1016/S0002-9610(03)00292-7
5. Zilberman M, Elsner JJ. Antibiotic-eluting medical devices for various applications. J Control Release 2008; 130:202-15; PMID:18687500; http://dx.doi.org/10.1016/j.jconrel.2008.05.020
6. Arruebo M, Vilaboa N, Santamaria J. Drug delivery from internally implanted biomedical devices used in traumatology and in orthopedic surgery. Expert Opin Drug Deliv 2010; 7:589-603; PMID:20230306; http://dx.doi.org/10.1517/17425241003671544
7. Perlroth J, Kuo M, Tan J, Bayer AS, Miller LG. Adjunctive use of rifampin for the treatment of Staphylococcus aureus infections: a systematic review of the literature. Arch Intern Med 2008; 168:805-19; PMID:18443255; http://dx.doi.org/10.1001/archinte.168.8.805
8. Zimmerli W, Widmer AF, Blatter M, Frei R, Ochsner PE, Foreign-Body Infection (FBI) Study Group. Role of rifampin for treatment of orthopedic implant-related staphylococcal infections: a randomized controlled trial. JAMA 1998; 279:1537-41; PMID:9605897; http://dx.doi.org/10.1001/jama.279.19.1537
9. Khanlari B, Elzi L, Estermann L, Weisser M, Brett W, Grapow M, et al. A rifampicin-containing antibiotic treatment improves outcome of staphylococcal deep sternal wound infections. J Antimicrob Chemother 2010; 65:1799-806; PMID:20542908; http://dx.doi.org/10.1093/jac/dkq182
10. Bliziotis IA, Ntziora F, Lawrence KR, Falagas ME. Rifampin as adjuvant treatment of Gram-positive bacterial infections: a systematic review of comparative clinical trials. Eur J Clin Microbiol Infect Dis 2007; 26: 849-56; PMID:17712583; http://dx.doi.org/10.1007/s10096-007-0378-1
11. Mäkinen TJ, Veiranto M, Lankinen P, Moritz N, Jalava J, Törmälä P, et al. In vitro and in vivo release of ciprofloxacin from osteoconductive bone defect filler. J Antimicrob Chemother 2005; 56:1063-8; PMID: 16234335; http://dx.doi.org/10.1093/jac/dki366
12. Alvarez H, Castro C, Moujir L, Perera A, Delgado A, Soriano I, et al. Efficacy of ciprofloxacin implants in treating experimental osteomyelitis. J Biomed Mater Res B Appl Biomater 2008; 85:93-104; PMID: 17696153; http://dx.doi.org/10.1002/jbm.b.30921
13. Mäkinen TJ, Veiranto M, Knuuti J, Jalava J, Törmälä P, Aro HT. Efficacy of bioabsorbable antibiotic containing bone screw in the prevention of biomaterial-related infection due to Staphylococcus aureus. Bone 2005; 36:292-9; PMID:15780955; http://dx.doi.org/10.1016/j.bone.2004.11.009
14. Miyai T, Ito A, Tamazawa G, Matsuno T, Sogo Y, Nakamura C, et al. Antibiotic-loaded poly-ε-caprolactone and porous β-tricalcium phosphate composite for treating osteomyelitis. Biomaterials 2008; 29:350-8; PMID: 17977596; http://dx.doi.org/10.1016/j.biomaterials.2007.09.040
15. Tiainen J, Knuutila K, Veiranto M, Suokas E, Törmälä P, Kaarela O, et al. Pull-out strength of multifunctional bioabsorbable ciprofloxacin-releasing polylactide-polyglycolide 80/20 tacks: an experimental study allograft cranial bone. J Craniofac Surg 2009; 20:58-61; PMID: 19164990; http://dx.doi.org/10.1097/SCS.0b013e318190df48
16. Garvin KL, Miyano JA, Robinson D, Giger D, Novak J, Radio S. Polylactide/polyglycolide antibiotic implants in the treatment of osteomyelitis. A canine model. J Bone Joint Surg Am 1994; 76:1500-6; PMID:7929497
17. Waknis V, Jonnalagadda S. Novel poly-DL-lactide-polycaprolactone copolymer based flexible drug delivery system for sustained release of ciprofloxacin. Drug Deliv 2011; 18:236-45; PMID:21189060; http://dx.doi.org/10.3109/10717544.2010.528070
18. Castro C, Évora C, Baro M, Soriano I, Sánchez E. Two-month ciprofloxacin implants for multibacterial bone infections. Eur J Pharm Biopharm 2005; 60:401-6; PMID:15996581; http://dx.doi.org/10.1016/j.ejpb.2005.02.005
19. Castro C, Sánchez E, Delgado A, Soriano I, Núñez P, Baro M, et al. Ciprofloxacin implants for bone infection. In vitro-in vivo characterization. J Control Release 2003; 93:341-54; PMID:14644584; http://dx.doi.org/10.1016/j.jconrel.2003.09.004
20. Koort JK, Mäkinen TJ, Suokas E, Veiranto M, Jalava J, Knuuti J, et al. Efficacy of ciprofloxacin-releasing bioabsorbable osteoconductive bone defect filler for treatment of experimental osteomyelitis due to Staphylococcus aureus. Antimicrob Agents Chemother 2005; 49:1502-8; PMID:15793132; http://dx.doi.org/10.1128/AAC.49.4.1502-1508.2005
21. Koort JK, Suokas E, Veiranto M, Mäkinen TJ, Jalava J, Törmälä P, et al. In vitro and in vivo testing of bioabsorbable antibiotic containing bone filler for osteomyelitis treatment. J Biomed Mater Res A 2006; 78:532-40; PMID:16736479; http://dx.doi.org/10.1002/jbm.a.30766
22. Koort JK, Makinen TJ, Suokas E, Veiranto M, Jalava J, Tormala P, et al. Sustained release of ciprofloxacin from an osteoconductive poly(DL)-lactide implant. Acta Orthop 2008; 79:295-301; PMID:18484258; http://dx.doi.org/10.1080/17453670710015111
23. Daculsi G, Goyenvalle E, Cognet R, Aguado E, Suokas EO. Osteoconductive properties of poly(96L/4D-lactide)/beta-tricalcium phosphate in long term animal model. Biomaterials 2011; 32:3166-77; PMID: 21315446; http://dx.doi.org/10.1016/j.biomaterials.2011.01.033
24. Paakinaho K, Ellä V, Syrjälä S, Kellomäki M. Melt spinning of poly(l/d)lactide 96/4: Effects of molecular weight and melt processing on hydrolytic degradation. Polym Degrad Stabil 2009; 94:438-42; http://dx.doi.org/10.1016/j.polymdegradstab.2008.11.010

25. Bain DF, Munday DL, Cox PJ. Evaluation of biodegradable rifampicin-bearing microsphere formulations using a stability-indicating high-performance liquid chromatographic assay. Eur J Pharm Sci 1998; 7:57-65; PMID:9845778; http://dx.doi.org/10.1016/S0928-0987(98)00005-0
26. Jindal KC, Chaudhary RS, Singla AK, Gangwal SS, Khanna S. Effects of buffers and pH on rifampicin stability. Pharm Ind 1995; 57:420-2.
27. Le Guellec C, Gaudet ML, Lamanetre S, Breteau M. Stability of rifampin in plasma: consequences for therapeutic monitoring and pharmacokinetic studies. Ther Drug Monit 1997; 19:669-74; PMID:9421109; http://dx.doi.org/10.1097/00007691-199712000-00011
28. Baker R. Controlled Release of Biologically Active Agents. New York: John Wiley & Sons, 1987.
29. Ritger PL, Peppas NA. A simple equation for desciption of solute release I. fickian and non-fickian release from non-swellable devices in the form of slabs, spheres, cylinders or discs. J Control Release 1987; 5:23-36; http://dx.doi.org/10.1016/0168-3659(87)90034-4
30. Jones DS, McCoy CP, Andrews GP. Physicochemical and drug diffusion analysis of rifampicin containing polyethylene glycol-poly(ε-caprolactone) networks designed for medical device applications. Chem Eng J 2011; 172:1088-95; http://dx.doi.org/10.1016/j.cej.2011.05.024
31. Jeong SI, Kim BS, Lee YM, Ihn KJ, Kim SH, Kim YH. Morphology of elastic poly(L-lactide-co-ε-caprolactone) copolymers and in vitro and in vivo degradation behavior of their scaffolds. Biomacromolecules 2004; 5:1303-9; PMID:15244444; http://dx.doi.org/10.1021/bm049921i
32. Herbert IR. Statistical analysis of copolymer sequence distribution. In: Ibbet RN, ed. NMR Spectroscopy of Polymers. London: Blackie Academic & Professional, 1993:50-79.
33. Fernández J, Etxeberria A, Sarasua JR. Synthesis, structure and properties of poly(L-lactide-co-ε-caprolactone) statistical copolymers. J Mech Behav Biomed Mater 2012; 9:100-12; PMID:22498288; http://dx.doi.org/10.1016/j.jmbbm.2012.01.003
34. Cellai L, Cerrini S, Segre A, Brufani M, Fedeli W, Vaciago A. Comparative study of the conformations of rifamycins in solution and in the solid state by proton nuclear magnetic resonance and X-rays. J Org Chem 1982; 47:2652-61; http://dx.doi.org/10.1021/jo00134a028
35. Ragaert K, Dekeyser A, Cardon L, Degrieck J. Quantification of thermal material degradation during the processing of biomedical thermoplastics. J Appl Polym Sci 2011; 120:2872-80; http://dx.doi.org/10.1002/app.33323
36. Li S, Garreau H, Vert M. Structure-property relationships in the case of the degradation of massive poly(α-hydroxy acids) in aqueous media - part 3 influence of the morphology of poly(l-lactic acid). J Mater Sci Mater Med 1990; 1:198-206; http://dx.doi.org/10.1007/BF00701077
37. Pitt CG, Chasalow FI, Hibionada YM, Klimas DM, Schindler A. Aliphatic Polyesters - 1. the Degradation of Poly(epsilon-caprolactone) in vivo. J Appl Polym Sci 1981; 26:3779-87; http://dx.doi.org/10.1002/app.1981.070261124
38. ISO 15814. Implants for surgery – copolymers and blends based in polylactide – *in vitro* degradation testing.
39. Moir DT, Ming Di, Opperman T, Schweizer HP, Bowlin TL. A high-throughput, homogeneous, bioluminescent assay for Pseudomonas aeruginosa gyrase inhibitors and other DNA-damaging agents. J Biomol Screen 2007; 12:855-64; PMID:17644773; http://dx.doi.org/10.1177/1087057107304729
40. Ahola N, Veiranto M, Rich J, Efimov A, Seppälä J, et al. Hydrolytic degradation of composites of poly(L-lactide-co-epsilon-caprolactone) 70/30 and beta-tricalcium phosphate. J Biomater Appl 2012; In press; PMID:23048066; http://dx.doi.org/10.1177/0885328212462258

Publication IV

Männistö, N., Ahola, N., Karp, M., Veiranto, M., Kellomäki, M.

In vitro bioluminescence used as a method for real-time inhibition zone testing for antibiotic-releasing composites

British Microbiology Research Journal, 4 (2014) 235-254

British Microbiology Research Journal
4(2): 235-254, 2014

SCIENCEDOMAIN *international*
www.sciencedomain.org

In vitro Bioluminescence Used as a Method for Real-Time Inhibition Zone Testing for Antibiotic-Releasing Composites

Noora M. Mannisto[1], Niina Ahola[2,3*], Matti T. Karp[1], Minna Veiranto[4] and Minna Kellomaki[2,3]

[1]Department of Chemistry and Bioengineering, Tampere University of Technology, Korkeakoulunkatu 10, 33720 Tampere, Finland.
[2]Department of Electronics and Communications Engineering, Tampere University of Technology, Korkeakoulunkatu 3, 33720 Tampere, Finland.
[3]BioMediTech, Tampere, Finland.
[4]Bioretec Ltd., Hermiankatu 22, 33720 Tampere, Finland.

Authors' contributions

All authors took part in the design of the study. Author NA supervised the work and author NMM carried out the research work. The manuscript was written jointly by the authors NMM and NA. All authors read and approved the final manuscript.

Original Research Article

Received 30th August 2013
Accepted 2nd November 2013
Published 20th November 2013

ABSTRACT

Aims: This study describes the potential of real-time bioluminescence imaging in evaluating the antibiotic efficiency of two cylinder-shaped bioabsorbable antibiotic-releasing composites by *in vitro* inhibition zone tests. The bacterial infections of bone tissue can cause extensive hard and soft tissue damage and decrease the efficiency of oral antibiotic therapy due to the poor blood circulation in the infected area. To overcome this problem, new, locally antibiotic-releasing biodegradable composites have been developed.
Study Design & Methodology: The two composites evaluated in this study were composed of poly(L-lactide-co-ε-caprolactone) matrix, β-tricalcium phosphate ceramic and either ciprofloxacin or rifampicin antibiotic. The composites were tested with genetically modified model pathogens of osteomyelitis (*Pseudomonas aeruginosa* and *Staphylococcus epidermidis*) *in vitro* in inhibition zone tests using a method of real-time bioluminescence.
Results: The first signs of the effect of the released ciprofloxacin or rifampicin became visible after four hours of incubation and were seen as changed bioluminescence around

**Corresponding author: Email: niina.ahola@tut.fi;*

the composite pellet on a culture dish. Both of the composite types showed excellent effects against the sensor bacteria within the diffusion area. Bioluminescence measurements suggested that no survivor bacteria capable of evolving resistant strains were left inside the inhibition zones. The *S. epidermidis* bacterial strain was an inhibition sensor and *P. aeruginosa* was a stress sensor.

Conclusion: These results highlight the potential of the composite materials against the pathogens of osteomyelitis. The approach allows continuous visual inspection of the efficacy of the antibiotics against the bacteria.

Keywords: Bioluminescence; ciprofloxacin; controlled drug delivery; inhibition zone; rifampicin.

1. INTRODUCTION

Osteomyelitis is a severe bacterial infection that can cause bone and soft tissue necrosis [1,2]. A major problem in the treatment of osteomyelitis is the wide spectrum of pathogens, i.e. staphylococcal, enterococcal, *Pseudomonas*and *Salmonella* species [1-4]. It is common that infected bone has degenerated blood circulation that greatly affects the efficacy of parenteral or intravascular antibiotics. To overcome this problem, local drug delivery systems have been developed to deliver the antibiotics directly to the infected tissue. Local antibiotic release, in the form of antibiotic-releasing implants, provides high local antibiotic concentrations and also reduces side effects [1,4]. Additionally, they can reduce the cost of drug therapy, increase the efficiency of drugs, and enhance patient compliance [4,5]. Osteomyelitis often requires surgical debridement of infected tissues that leaves a defect in the bone called a dead space. Currently, dead spaces are often treated with gentamycin-releasing poly(methyl methacrylate) beads that need to be removed later because they are not bioabsorbable and require bone grafting after bead removal [6]. This method of treatment is not optimal because it involves two surgeries. Bioabsorbable, osteconductive and antibiotic-releasing composites offer the possibility to treat osteomyelitis in one stage and to reduce both the risks for the patient and the costs. Such materials have been requested in the literature and the research is going on to achieve these goals [7].

In the development phase of antibiotic-releasing materials, screening the materials before preclinical testing is important to find the most promising materials. Often, the functionality of such materials is evaluated by inhibition zone testing. Typically, inhibition zones are measured using over-night-grown bacterial cultures, where the inhibition zone can be simply measured [8,9]. In this study, real-time bioluminescence imaging was used to investigate the potential and the antimicrobial activity of two bioabsorbable, antibiotic-releasing and cylinder-shaped composites in *in vitro* inhibition zone tests.

Bioluminescence imaging has been used successfully, for example, to monitor the antimicrobial efficacy of wound dressings *in vitro* [10], stem cell differentiation [11,12], vascularization [13,14], apoptosis [12], gene therapy [15,16], inflammation of tissue [17], implant-related bacterial infections [18,19] and in osteomyelitis animal model (mouse) [20]. The method, using whole bacteria cells as biosensors, offers several advantages: it is easy to use, it is non-invasive, and it has high throughput and low costs [12,21]. In the case of inhibition zone testing, bioluminescence imaging provides more information than the conventional method because information on the bacteria and their reactions can be followed in real time when exposed to the antibiotics [22]. Due to the light-emitting nature of bioluminescent bacteria, the number of emitted photons can be detected real-time and the

changes in light levels are proportional to the changes in the metabolism of the cells under study [10,23-27].

The osteoconductive, bioabsorbable, and antibiotic-releasing composites used in this study were developed for the treatment of osteomyelitis and their drug release and degradation properties *in vitro* were tested in our earlier studies [28,29]. A steady-state drug release period was observed after the initial burst in the beginning of the release [28,29]. Because the materials have been tested only in *in vitro* conditions, it is possible that the actual concentrations in tissue would be different due to differences in clearance from the tissue.

2. MATERIALS AND METHODS

2.1 Materials

Medical grade poly(L-lactide-co-ε-caprolactone) (PLCL) with the comonomer ratio of 70/30 and M_w of 246,000 g/mol was purchased from Purac Biomaterials (Gorinchem, the Netherlands). β-Tricalcium phosphate (β-TCP) (granule size < 38 µm) was purchased from Plasma Biotal Ltd. (Buxton, Derbyshire, United Kingdom). Rifampicin was purchased from Oriola (Espoo, Finland) and ciprofloxacin from Uquifa (Civac, Jiutepec-Morelos, Mexico). Sörensen phosphate buffer solution was prepared and used according to the ISO 15814 standard [30]. The chemicals used for the buffer solution (Na_2HPO_4 and KH_2PO_4) were purchased from J.T. Baker (Deventer, the Netherlands).

2.2 Processing of Composite Materials

Processing was done according to Ahola et al. [28,29]. In short: dried polymer (PLCL), β-TCP (50 wt-%) and antibiotics (either rifampicin or ciprofloxacin) were processed with a custom-built co-rotating twin-screw extruder in nitrogen atmosphere into rod-shaped billets, with a diameter of approximately 2.5 mm. Three different composites were processed: one composite had 8 wt-% of ciprofloxacin, one 8 wt-% of rifampicin and one with no antibiotic served as a control material. Cylindrical-shaped samples (length approx. 2.5 mm) were cut from the billets. Before inhibition zone testing, the samples were packed and gamma irradiated (28.7-34.0 kGy) for sterility.

2.3 Bacteria and Plasmids

Two engineered, non-pathogenic bacterial strains cloned with bacterial luciferase reporter genes were used as biosensor cells: *Pseudomonas aeruginosa* PAO-LAC carrying plasmid pUCP24GW and integrated mini-Tn*7*-Gm-GW-LUX carrying the PA0614 promoter [31] and *Staphylococcus epidermidis*ATCC-14990 carrying plasmid pAT19-lux-hlaP-frp. Minimum inhibitory concentrations (MIC) of ciprofloxacin against *P. aeruginosa* has been reported to be 0.1-1.2 µg/ml [32,33] and against *S. epidermidis* 0.1-0.8 µg/ml [34]. For rifampicin, the MIC reported against *S. epidermidis* is 0.015 µg/ml [35]. The values against *P. aeruginosa* vary greatly and values of 32-64 µg/ml [36] and 8-16 µg/ml [37] have been reported.

2.4 Bioluminescence Imaging

Bacteria were cultured on antibiotic L-agar plates (10 g/L tryptone, 5 g/L yeast extract, 5 g/L NaCl, 15 g/L agar; 10 g/L gentamycin for *P. aeruginosa* and 5 g/L erythromycin for *S. epidermidis*) overnight at 30°C and suitable colonies were placed into 5 ml of liquid Luria-

Bertani medium (LB; 5 g/L yeast extract, 10 g/L tryptone, 5 g/l NaCl in 1L). The bacteria were cultured overnight at 30°C, shaken at 300 rpm, and suitable antibiotics were added. The level of luminescence of the cultures was measured by using a Plate Chameleon^{TM}multilabel counter 1.001 (Hidex Ltd, Turku, Finland). At a volume of 200 µl, 1.1-2.3×10^6 counts for *S. epidermidis* and1.1-2 and 3×10^6 counts for *P. aeruginosa* were found to be optimal for subsequent steps.

Plates were prepared by casting two layers of LB-agar into a 6-well plate. Controls and antibiotic-containing composites were placed in the center of the bottom layer, one pellet per well. Bacteria culture of 350-500 µl per well was mixed with 1 ml of soft LB-agar (agar concentration 7.5 g/L) solution and cast on top. After solidification, the plate was taken to the imaging station of a Xenogen Vivo Vision IVIS® Lumina CCD camera (Caliper Life Sciences, USA). Images were taken every 20 minutes for 16 hours with an exposure time of 30 seconds. The images were analyzed using the Living Image® 3.1 program (Caliper Life Sciences, USA). The ciprofloxacin and rifampicin-releasing composite pellets were tested with both strains of bacteria after sterilization with gamma irradiation as well as after one and two weeks immersion in Sörensen phosphate buffer solution (pH 7.4) at 37°C.

After each 16-h measurement cycle, the outcome of bioluminescence was verified by visual inspection (halo around the antibiotic-releasing pellet showing no visual bacterial growth).

2.5 Interpretation of the Results

The results are presented as false color photos, where dark blue and purple were interpreted as dead bacteria with no bioluminescence. The dark blue color resulted from internal reflection from the high light levels in the stress zones. The red and yellow colors were interpreted to indicate a situation where the bacteria are in contact with sub-inhibitory concentrations of the antibiotics and produce a strong light emission that is presumably due to the nonspecific activation of central metabolic pathways [22]. These red and yellow zones are called stress zones (SZ). Green color was considered to be unaffected bacteria because this was the usual intensity in the control wells.

3. RESULTS

We have previously introduced the preliminary results of ciprofloxacin releasing composites [28] and rifampicin releasing composites[29] against *Pseudomonas aeruginosa* in connection with the *in vitro* drug release results. Here, we want to show the differences between the two bacteria *Pseudomonas aeruginosa* and *Staphylococcus epidermidis*. In addition, we want to show the results of the antibiotic releasing composites after 1 week immersion in Sörensen phosphate buffer solution (pH 7.4) at 37°C to simulate situation, when the composites have been implanted in tissue and the antibiotic release has been stabilized after the initial burst in the release. It is intended that the two composites will be used together in the local treatment of osteomyelitis in such a way that the surgeon treating the patient can decide the exact ratio of the antibiotics to be used.

The results of the bioluminescence imaging for the pellets tested directly after processing and sterilization are presented in Figs. 1-4 as part A. The light emission levels for the same samples are shown as photon counts in Figs. 1-4 as part B. The results of bioluminescence imaging for the pellets that were kept immersed in Sörensen phosphate buffer solution (pH 7.4) at 37°C for one week are presented in Appendix as Figs. 1-4 part A and the light

emission levels in Appendix as Figs. 1-4 part B. Because there were no major differences in the antibiotic activity between the samples that had been in *in vitro* conditions for one or two weeks, only the results for the samples that had been in *in vitro* conditions for one week are presented.

Both *S. epidermidis*and *P. aeruginosa* responded to ciprofloxacin released from the composite pellets that were tested directly after processing and sterilization (Figs. 1A and 2A, respectively). The yellow-red stress zone preceded the expanding inhibition zone that was seen as an increasing blue zone in the middle of the well. The decrease in the bioluminescence that suggested the death of bacteria near the composite material was clearly visible after 6 hours for *P. aeruginosa* and after 10 hours for *S. epidermidis*. At the time point of 12 hours, the inhibition zones had reached their maximum. After this, changes were mainly detected in the light emission levels, which can be seen in Figs. 1B and 2B as photon counts. In these graphs, high light emission, which represented the appearance of a SZ, was seen at the edges of the inhibition zones.

When the ciprofloxacin-releasing composites that had been immersed in Sörensen phosphate buffer solution (pH 7.4) at 37°C for a week were compared with those tested directly after sterilization, the stress zones (SZ) appeared earlier (Appendix Figs. 1 and 2). The SZs were, however, no larger in size, which indicated a longer presence of sub-inhibitory concentration areas. The initial burst, as seen in the results of the pellets tested directly after the sterilization step, was not present and the release of ciprofloxacin was steadier but yet strong enough to kill the bacteria. The ciprofloxacin release resulted in narrower inhibition zones that correlated well with the *in vitro* ciprofloxacin release study conducted earlier [28].

Both bacteria also responded to rifampicin release (Figs. 3 and 4), but the inhibition zones produced were much smaller than the zones produced by ciprofloxacin (Figs. 1 and 2). Due to the larger molecular size of rifampicin compared with ciprofloxacin, the diffusion in agar is probably slower and limited when compared with the diffusion of ciprofloxacin and, as a result, the inhibition zone was smaller. The first signs of decreased bioluminescence could already be seen after 4 hours for both of the studied bacteria. In the case of *S. epidermidis*, the formation of inhibition zones began as an appearance of red and yellow SZs around the antibiotic composites, but such behavior was not seen in the case of *P. aeruginosa*. The light emission levels of *S. epidermidis* and *P. aeruginosa* are shown in Figs. 3B and 4B, respectively.

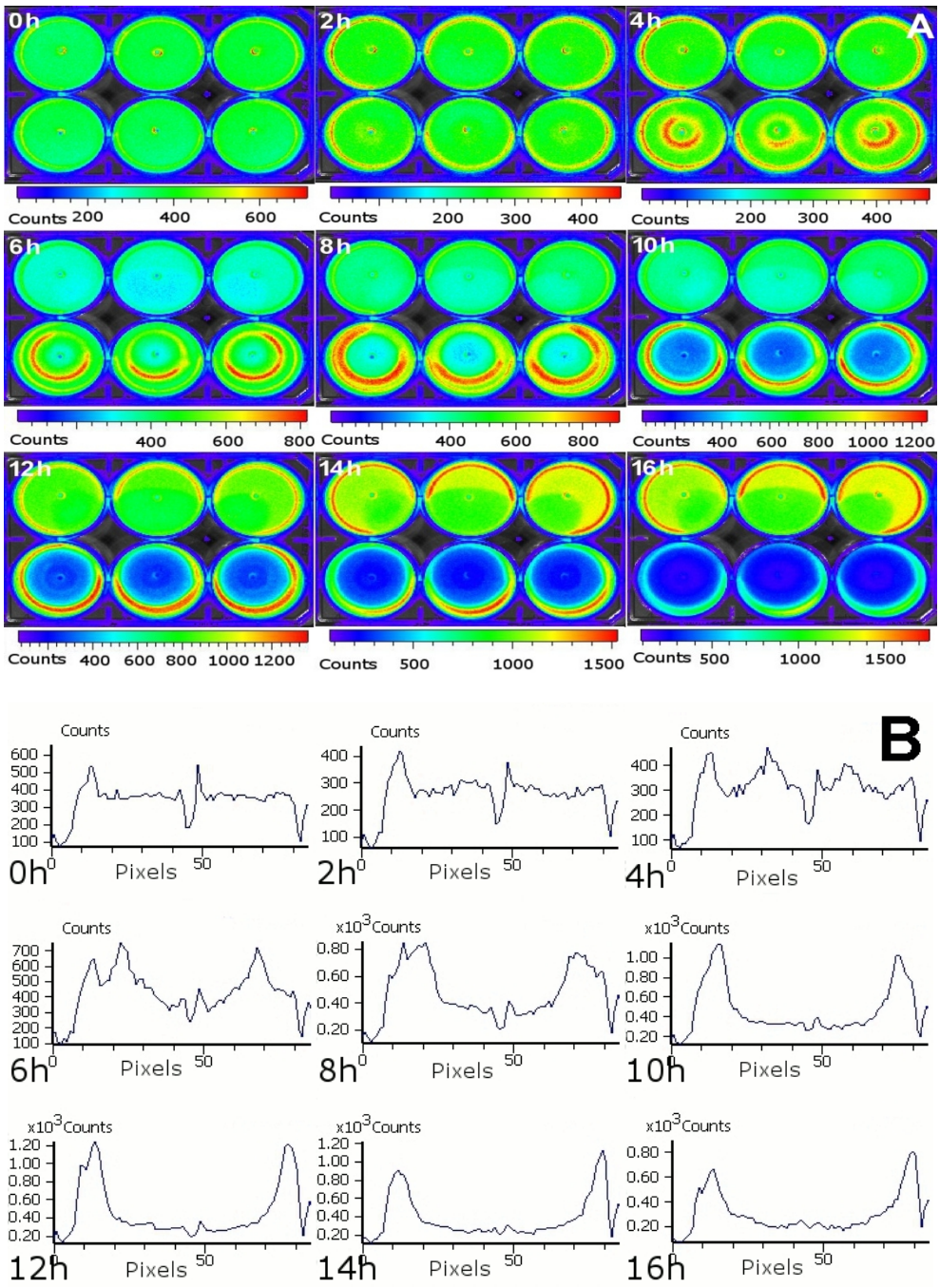

Fig. 1.(A) The development of the inhibitory zones was seen as growing blue areas in the middle of the wells of cultured S. epidermidis and ciprofloxacin composite pellets (in triplicate on the lower row). Pellets without antibiotic were used as controls (in triplicate on the top row). The plate was photographed at time points of 0, 2, 4, 6, 8, 10, 12, 14, and 16 hours. The diameter of one well is 35 mm. (B) Light intensity levels as photon counts of S. epidermidis exposed to one ciprofloxacin releasing composite pellet in the middle of the well. The results are presented at time points of 0, 2, 4, 6, 8, 10, 12, 14, and 16 hours. Note the different scales of the y-axes.

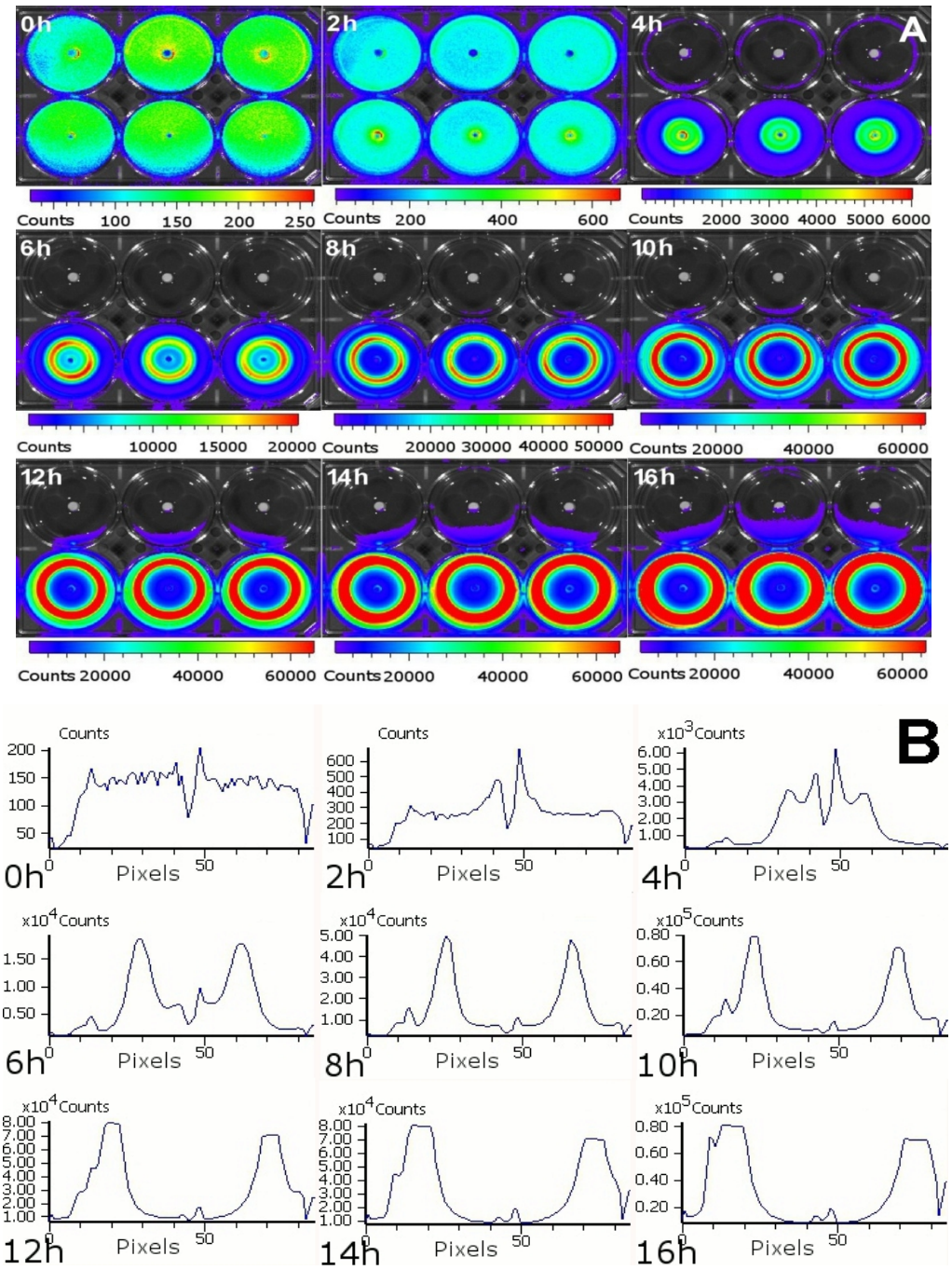

Fig. 2.(A) The development of the inhibitory zone was seen as growing blue areas in the middle of the wells of cultured P. aeruginosa and ciprofloxacin composite pellets (in triplicate on the lower row). Pellets without antibiotic were used as controls (in triplicate on the top row). The plate was photographed at time points of 0, 2, 4, 6, 8, 10, 12, 14, and 16 hours. The diameter of one well is 35 mm. (B) Light intensity levels as photon counts of P. aeruginosa exposed to one ciprofloxacin releasing composite pellet in the middle of the well. The results are presented at time points of 0, 2, 4, 6, 8, 10, 12, 14, and 16 hours. Note the different scales of the y-axes.

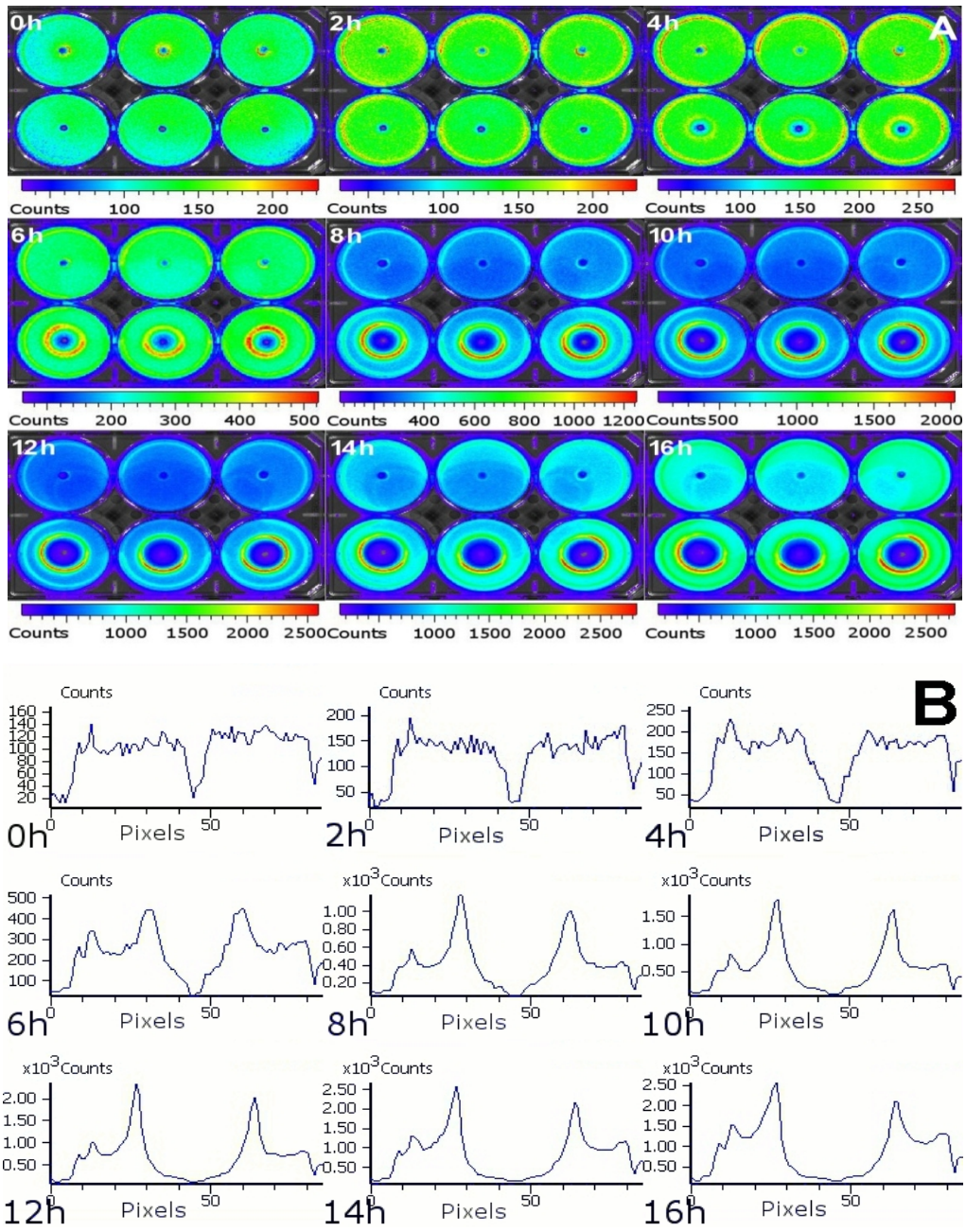

Fig. 3.(A) The development of the inhibitory zones was seen as growing blue areas in the middle of the wells of cultured S. epidermidis and rifampicin composite pellets (in triplicate on the lower row). Pellets without antibiotics were used as controls (in triplicate on the top row). The plate was photographed at time points of 0, 2, 4, 6, 8, 10, 12, 14, and 16 hours. The diameter of one well is 35 mm.(B) Light intensity levels as photon counts of S. epidermidis exposed to one rifampicin releasing composite pellet in the middle of the well. The results are presented at time points of 0, 2, 4, 6, 8, 10, 12, 14, and 16 hours. Note the different scales of the y-axes.

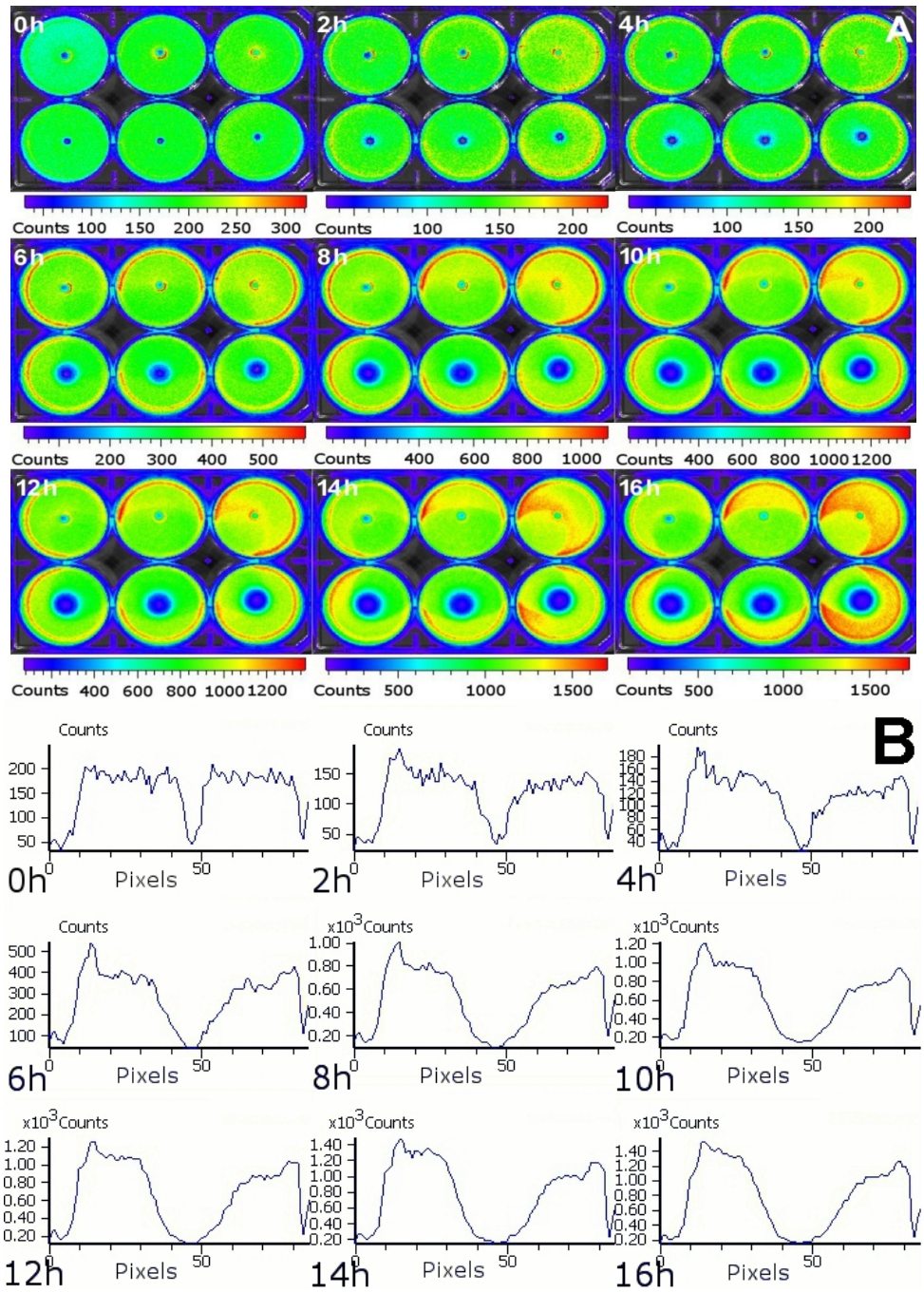

Fig. 4.(A) The development of the inhibitory zone was seen as growing blue areas in the middle of the wells of cultures P. aeruginosa and rifampicin composite pellets (in triplicate on the lower row). Pellets without antibiotic were used as controls (in triplicate on the top row). The plate was photographed at time points of 0, 2, 4, 6, 8, 10, 12, 14, and 16 hours. The diameter of one well is 35 mm. (B) Light intensity levels as photon counts of P. aeruginosa exposed to one rifampicin releasing composite pellet in the middle of the well. The results are presented at time points of 0, 2, 4, 6, 8, 10, 12, 14, and 16 hours. Note the different scales of the y-axes.

In the case of the rifampicin-releasing samples kept immersed in Sörensen phosphate buffer solution (pH 7.4) at 37°C for one week, the initial burst was not present, as was also the case with ciprofloxacin. There was also no significant change in light emission levels (Appendix Figs. 3B and 4B), which indicated no clear inhibition.

In Fig. 5, the growth of the area of the inhibition zones is shown as a function of time. The graphs indicate the size of the inhibition zone that one composite pellet, releasing either ciprofloxacin or rifampicin, is capable of producing. The inhibition zone areas are presented without and with stress zones (5 A and C without stress zones and 5 B and D with stress zones). The graphs also show the differences in the effects between the different bacterial species. With ciprofloxacin (Figure 5A), the inhibition zone of *S. epidermidis*was around 9.0 cm^2, but with *P. aeruginosa*the area was only half the size. When the ciprofloxacin-releasing composites had been immersed in the Sörensen phosphate buffer solution at 37°C for a week, the zone area decreased to around 8.0 cm^2 for *S. epidermidis* and to 2.0 cm^2 for *P. aeruginosa*. With *S. epidermidis*, the inhibition zone of rifampicin was around 2.3 cm^2 (Fig.5C),and only 0.4 cm^2 after immersion in Sörensen phosphate buffer solution at 37°C. For *P. aeruginosa*, the values were 1.5 and 0.2 cm^2, respectively. When the stress zones were included in the inhibition zones (Figs. 5B and 5D), the areas differed only slightly for *S. epidermidis*. With *P. aeruginosa* the stress zones made a larger difference, which indicated larger stress zones for *P. aeruginosa*.

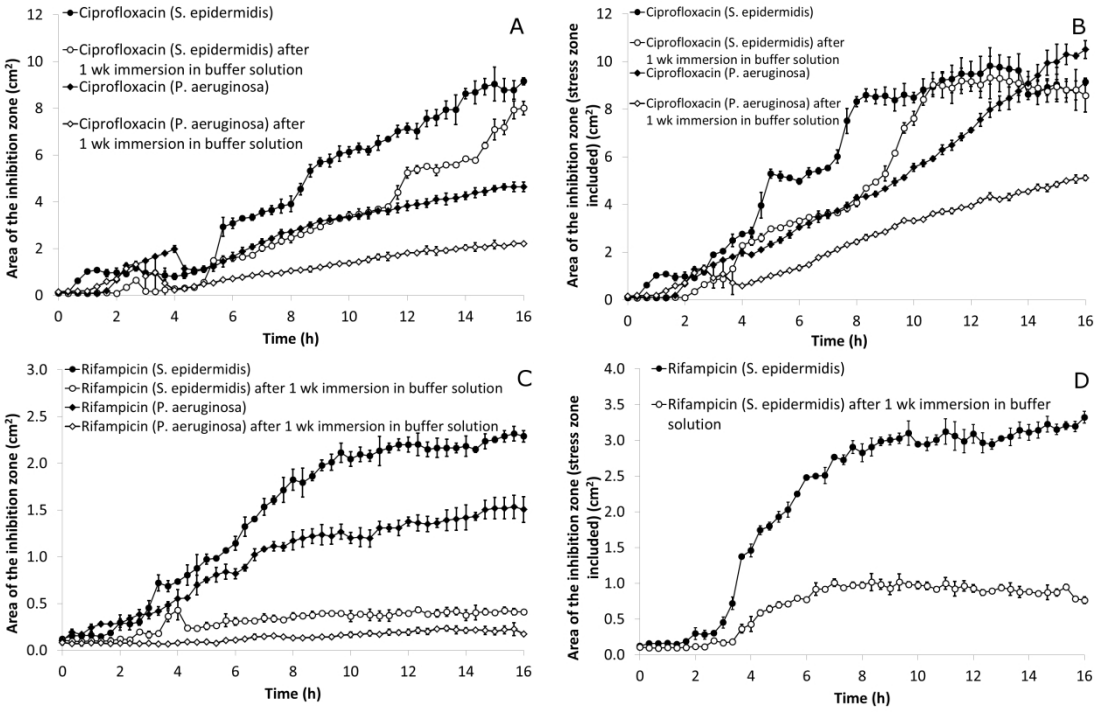

Fig. 5. Measured area of the bioluminescence inhibitory zones with (A) ciprofloxacin, (B) ciprofloxacin with stress zones included in the inhibitory zones, (C) rifampicin and (D) rifampicin with stress zones included in the inhibitory zones (n=3). Results using pellets that had been immersed in Sörensen phosphate buffer solution (pH 7.4) at 37°C for one week prior to testing are shown as well.

4. DISCUSSION

The aim of this study was to demonstrate the potential of bioluminescence in inhibition zone tests and to show that bioluminescence provides more information about the effects of antibiotics on bacteria than the conventional over-night-grown inhibition zone measurements. The possibility for real-time observation of the evolving inhibition zones and so-called stress zones provides an insight in to how the antibiotics affect the bacteria.

The antibiotic-releasing composites studied here were cylindrical in shape and were composed of bioabsorbable poly(L-lactide-co-ε-caprolactone) (PLCL) as the polymer matrix, 50 wt-% β-tricalciumphosphate (β-TCP), and either 8 wt-% of ciprofloxacin or rifampicin. It is intended that the composites will be used together in the local treatment of osteomyelitis in such a way that the surgeon treating the patient can decide the exact ratio of the antibiotics to be used. The main advantage of this kind of composite implant is that removal after treatment is not required due to the bioabsorbability of the composites. β-TCP acts as an osteoconductive material and is capable of attracting osteoblasts. This can both facilitate controlled drug release and enhance bone repair and regeneration [4,38-41].

The antibiotics used in this study, rifampicin and ciprofloxacin, have been widely used because they are known to form an effective, synergistic combination even against bacterial strains that are not susceptible to, for example, β-lactams or tetracyclines. A quinolone-rifampicin treatment is safe and well tolerated by patients [2,4,42,43]. Ciprofloxacin is used as the main antibiotic because it is an active fluoroquinolone that inhibits DNA gyrase and stops DNA replication [22,44]. Rifampicin supports ciprofloxacin by inhibiting the emerging resistant strains. It also penetrates biofilm well [45,46], which is an advantage because osteomyelitis is often caused by bacteria forming biofilms. Some bacteria are more resistant to antibiotics than others, a good example being the MRSA strain of *S. aureus*[22]. The use of two or more antibiotics that have a synergistic action is frequently employed [22,47] because this seems to prevent or inhibit the development of resistance.

The antibiotics used in the treatment of osteomyelitis must be active against a broad spectrum of common disease-causing pathogens [4]. The treatment must also ensure that no bacteria survive. If the duration of the treatment is too short or the antibiotic reaches the infection site in sub-inhibitory concentrations, the remaining bacteria can cause clinical failure and potentially develop resistance [1-3,48]. Often, two antibiotics are used together because of their synergistic effect against the causative bacteria. The benefits of this kind of treatment are accelerated bacterial count decline, a wider antibacterial spectrum and reduction in the risk of resistant strain development to one of the antibiotics [49].

In the bioluminescence measurements conducted in this study, it was shown that both ciprofloxacin and rifampicin caused very strong, non-specific activation of bioluminescence in both of the model bacteria. The same kinds of reactions have been previously reported several times in solution-based assays in the high-throughput assays of antimicrobial agents in microtitreplate format [23,50,51]. Even though ciprofloxacin-releasing composite pellets were shown to be more effective against bacteria than rifampicin-releasing ones, it was noticed that rifampicin composites reached the level of total eradication earlier. This was seen, when using rifampicin-releasing composites, as a faster decrease in luminescence in the middle of inhibition zones (Figs. 3B and 4B). The fast response was most probably due to the burst in the release that is caused when the composite materials first release the antibiotic molecules on or near the surface as they are exposed to fluids. Here, rifampicin caused a stronger burst than ciprofloxacin, as was seen in the *in vitro* drug release test

conducted earlier [28,29]. The burst effect is a well-known phenomenon in controlled drug delivery and is sometimes considered to be unwanted [52]. In the case of antibiotics, however, reaching drug concentrations over the minimum inhibition concentration quickly is crucial because antibiotic resistance is a serious problem worldwide. In this sense, a moderate burst in the beginning of the release is useful. After the burst, the drug may be released in a continuous manner that can last for weeks [4,28].

The formation of stress zones was more visible for the ciprofloxacin-releasing composites. Within these zones, the concentration of antibiotic was considered to be too low to kill bacteria, but still able to cause the up-regulation of certain promoters. As a part of this regulation, the bacteria were presumably partially shutting down some of their metabolic pathways and thus liberated more energy for the bioluminescence reaction.

*S. epidermidis*is a metabolic inhibition sensor and *P. aeruginosa*is a stress sensor. *P. aeruginosa* is constructed to respond to the threat caused by gyrase inhibitors such as ciprofloxacin: up-regulation of luminescence genes only results if expression of the *gyrA*gene is reduced and gyrase is inhibited by ciprofloxacin [31]. The shut-down of light emission, especially in control wells (Fig. 2), may occur when the bacteria have reached the stationary phase and the quantity of active gyrase is not reduced by inhibition [31]. Therefore, the promoter in front of the luciferase reporter genes is efficiently shut down in non-stressing conditions and results in a dark background over the control pellets. Another explanation may be that the light emission levels of the wells affected by ciprofloxacin were very high and because of the internal recalibration system of the equipment, the low background light emission was under the detection limit. Thus, it may have seemed that there was no light emission. The blue light that was seen in the control wells in Fig. 2 was probably only a reflection of the strong light emission produced by the bacteria in contact with ciprofloxacin. Because *P. aeruginosa*is a stress and inhibition sensor, the light emission was up-regulated as ciprofloxacin diffusion proceeded and turned off as bacteria died. This was seen as the inhibition zone expanded within stress zone progression. Rifampicin being a transcriptional inhibitor did not produce a similar stress effect with *P. aeruginosa*.

Because sub-inhibitory concentration levels of quinolones are enough to promote an SOS response that regulates several promoters, sub-inhibitory concentration levels can lead to a possible increased tolerance to DNA damage [44]. As a result, an inadequate antibiotic release of the composites can cause the development of resistant bacterial strains. Most promoters regulate virulence genes and survival and some promoters are also sensitive to low concentrations of rifampicin [53]. It is, therefore, vital to decrease the formation of low concentration release barriers in order to lower the mutation rate of these promoters.

Because the bioluminescence method uses light-emitting bacterial cultures from which the range of the antibiotic release and the level of inhibition inside the zones formed can be estimated and measured, the method can be used to screen the potency of antibiotic-releasing systems before preclinical studies. Direct correlation between the light production and viable light emitting bacteria has been reported several times and with several different bacteria [10,23-27]. If toxic substances such as antibiotics kill the sensor bacteria, the decrease in light emission correlates directly to the number of viable bacteria [24-26]. Thus, bioluminescence seems to be a very suitable method for assessing the antimicrobial effects of antibiotic-releasing materials.

By imaging the antibiotic release utilizing bioluminescence and a CCD camera in real-time, it is easy to demonstrate whether the antibiotic-releasing capacity of the material is high

enough to eradicate the bacteria without any potential survivors developing antibiotic resistance. The antibiotic release from a small, ciprofloxacin-containing pellet seems to be sufficient to kill all the bacteria inside the inhibition zones. The inhibition zones formed by rifampicin-releasing material may, however, pose the risk of resistant strain formation if used alone. Therefore, the materials must be used together in order to support each other and to decrease the risk of resistance. In this study, we investigated the antibiotics separately in order to highlight the differences more clearly. According to the results, the composite materials have good potential to release antibiotics in concentrations high enough to eradicate bacteria from tissues infected by pathogens of osteomyelitis.

5. CONCLUSION

The *in vitro* inhibition zone test using real-time bioluminescence was demonstrated to be an efficient tool to observe the effects of the released antibiotics on the model pathogens of osteomyelitis. The method provides more information on the effects against the bacteria than the conventional over-night-grown bacterial cultures. Additionally, the potential of the new antibiotic-releasing biodegradable composites were shown to be adequate on model pathogens. However, it has to be kept in mind that the results presented here were obtained using single antibiotic-releasing composite pellets. In real clinical cases, several of these kinds of composite pellets would be used together. The therapeutic value of the release of ciprofloxacin and rifampicin from composites needs to be demonstrated carefully in order to validate the potential of new antibiotic-releasing composites in efficient antibiotic release. Studying the composite material with bioluminescence inhibition tests helped to monitor the efficiency of antibiotic release.

ACKNOWLEDGEMENTS

The authors thank Bioretec Ltd. for their co-operation in material processing. Peter Heath is thanked for language editing.

COMPETING INTERESTS

Authors have declared that no competing interest exists.

REFERENCES

1. Haidar R, Boghossian AD, Atiyeh B. Duration of post-surgical antibiotics in chronic osteomyelitis: Empiric or evidence-based? Int J Infect Dis. 2010;14(9):e752-e758.
2. Sia IG, Berbari EF. Osteomyelitis. Best Pract Res Clin Rheumatol 2006;20:1065-1081.
3. Lazzarini L, Lipsky BA, Mader JT. Antibiotic treatment of osteomyelitis: What have we learned from 30 years of clinical trials? Int J Infect Dis. 2005;9:127-138.
4. Nandi SK, Mukherjee P, Roy S, Kundu B, De DK, Basu D. Local antibiotic delivery systems for the treatment of osteomyelitis - A review. Mater Sci Eng C. 2009;29:2478-2485.
5. Tiainen J, Veiranto M, Koort JK, Suokas E, Kaarela O, Törmälä P, Waris T, Ashammakhi N. Bone tissue concentrations of ciprofloxacin released from biodegradable screws implanted in rabbits skull. Eur J Plast Surg. 2007;1-5.
6. Zilberman M, Elsner JJ. Antibiotic-eluting medical devices for various applications. J Control Release. 2008;130:202-215.

7. Jiang J, Li Y, Fang T, Zhou J, Li X, Wang Y, Dong J. Vancomycin-loaded nano-hydroxyapatite pellets to treat MRSA-induced chronic osteomyelitis with bone defect in rabbits. Inflamm Res. 2012;61:207-215.
8. Greene AH, Bumgardner JD, Yang Y, Moseley J, Haggard WO. Chitosan-coated stainless steel screws for fixation in contaminated fractures. Clin Orthop Relat Res. 2008;466:1699-1704.
9. Ashammakhi N, Veiranto M, Suokas E, Tiainen J, Niemelä S, Törmälä P. Innovation in multifunctional bioabsorbable osteoconductive drug-releasing hard tissue fixation devices. J Mater Sci Mater Med. 2006;17:1275-1282.
10. Thorn RMS, Nelson SM, Greenman J. Use of a bioluminescent Pseudomonas aeruginosa strain within an in vitro microbiological system, as a model of wound infection, to assess the antimicrobial efficacy of wound dressings by monitoring light production. Antimicrob Agents Chemother. 2007;51:3217-3224.
11. Vilalta M, Jorgensen C, Dégano IR, Chernajovsky Y, Gould D, Noël D, Andrades JA, Becerra J, Rubio N, Blanco J. Dual luciferase labelling for non-invasive bioluminescence imaging of mesenchymal stromal cell chondrogenic differentiation in demineralized bone matrix scaffolds. Biomaterials. 2009;30:4986-4995.
12. De Boer J, Van Blitterswijk C, Löwik C. Bioluminescent imaging: Emerging technology for non-invasive imaging of bone tissue engineering. Biomaterials. 2006;27:1851-1858.
13. Gafni Y, Zilberman Y, Ophir Z, Abramovitch R, Jaffe M, Gazit Z, Domb Jr. A, Gazit D. Design of a filamentous polymeric scaffold for in vivo guided angiogenesis. Tissue Eng. 2006;12:3021-3034.
14. Zhang N, Fang Z, Contag PR, Purchio AF, West DB. Tracking angiogenesis induced by skin wounding and contact hypersensitivity using a Vegfr2-luciferase transgenic mouse. Blood. 2004;103:617-626.
15. Shin S, Shea LD. Lentivirus immobilization to nanoparticles for enhanced and localized delivery from hydrogels. Mol Ther. 2010;18:700-706.
16. Peterson CY, Shaterian A, Borboa AK, Gonzalez AM, Potenza BM, Coimbra R, Eliceiri BP, Baird A. The noninvasive, quantitative, in vivo assessment of adenoviral-mediated gene delivery in skin wound biomaterials. Biomaterials. 2009;30:6788-6793.
17. Hanada T, Yoshimura A. Regulation of cytokine signaling and inflammation. Cytokine Growth Factor Rev. 2002;13:413-421.
18. Engelsman AF, Van Der Mei HC, Francis KP, Busscher HJ, Ploeg RJ, Van Dam GM. Real time noninvasive monitoring of contaminating bacteria in a soft tissue implant infection model. J Biomed Mater Res Part B Appl Biomater. 2009;88:123-129.
19. Kadurugamuwa JL, Sin L, Albert E, Yu J, Francis K, DeBoer M, Rubin M, Bellinger-Kawahara C, Parr Jr. TR, Contag PR. Direct continuous method for monitoring biofilm infection in a mouse model. Infect Immun. 2003;71:882-890.
20. Funao H, Ishii K, Nagai S, Sasaki A, Hoshikawa T, Aizawa M, Okada Y, Chiba K, Koyasu S, Toyama Y, Matsumoto M. Establishment of a real-time, quantitative, and reproducible mouse model of staphylococcus osteomyelitis using bioluminescence imaging. Infect Immun. 2012;80:733-741.
21. Close DM, Xu T, Sayler GS, Ripp S. In vivo bioluminescent imaging (BLI): Noninvasive visualization and interrogation of biological processes in living animals. Sensors. 2011;11:180-206.
22. Mesak LR, Davies J. Phenotypic changes in ciprofloxacin-resistant Staphylococcus aureus. Res Microbiol. 2009;160:785-791.
23. Tenhami M, Hakkila K, Karp M. Measurement of effects of antibiotics in bioluminescent Staphylococcus aureus RN4220. Antimicrob Agents Chemother. 2001;45:3456-3461.

24. Virta M, Lineri S, Kankaanpää P, Karp M, Peltonen K, Nuutila J, Lilius E-. Determination of complement-mediated killing of bacteria by viability staining and bioluminescence. Appl Environ Microbiol. 1998;64:515-519.
25. Atosuo JT, Lilius E. The real-time-based assessment of the microbial killing by the antimicrobial compounds of neutrophils. TheScientificWorldJournal. 2011;11:2382-2390.
26. Atosuo J, Lehtinen J, Vojtek L, Lilius E. Escherichia coli K-12 (pEGFPluxABCDEamp): A tool for analysis of bacterial killing by antibacterial agents and human complement activities on a real-time basis. Lumin, 2012;(in press).
27. Lampinen J, Korpela M, Saviranta P, Kroneld R, Karp M. Use of Escherichia coli cloned with genes encoding bacterial luciferase for evaluation of chemical toxicity. TOXIC ASSESS. 1990;5:337-350.
28. Ahola N, Männistö N, Veiranto M, Karp M, Rich J, Efimov A, Seppälä J, Kellomäki M. An in vitro study of composites of poly(L-lactide-co-ε-caprolactone), β-tricalcium phosphate and ciprofloxacin intended for local treatment of osteomyelitis. Biomatter. 2013;3:e23162.
29. Ahola N, Veiranto M, Männistö N, Karp M, Rich J, Efimov A, Seppälä J, Kellomäki M. Processing and sustained in vitro release of rifampicin containing composites to enhance the treatment of osteomyelitis. Biomatter. 2012;2:213-225.
30. ISO 15814. Implants for surgery – Copolymers and blends based in polylactide – *In vitro* degradation testing.
31. Moir DT, Di M, Opperman T, Schweizer HP, Bowlin TL. A high-throughput, homogeneous, bioluminescent assay for Pseudomonas aeruginosa gyrase inhibitors and other DNA-damaging agents. J Biomol Screen. 2007;12:855-864.
32. Kwok CS, Wan C, Hendricks S, Bryers JD, Horbett TA, Ratner BD. Design of infection-resistant antibiotic-releasing polymers: I. Fabrication and formulation. J Control Release. 1999;62:289-299.
33. MacGowan AP, Wootton M, Holt HA. The antibacterial efficacy of levofloxacin and ciprofloxacin against Pseudomonas aeruginosaassessed by combining antibiotic exposure and bacterial susceptibility. Journal of Antimicrobial Chemotherapy. 1999;43:345-349.
34. Chin NX, Neu HC. Ciprofloxacin, a quinolone carboxylic acid compound active against aerobic and anaerobic bacteria. Antimicrob Agents Chemother. 1984;25:319-326.
35. Leite B, Gomes F, Teixeira P, Souza C, Pizzolitto E, Oliveira R. In vitro activity of daptomycin, linezolid and rifampicin on Staphylococcus epidermidis biofilms. Curr Microbiol. 2011;63:313-317.
36. Yee YC, Kisslinger B, Yu VL, Jin DJ. A mechanism of rifamycin inhibition and resistance in Pseudomonas aeruginosa. J Antimicrob Chemother. 1996;38:133-137.
37. Timurkaynak F, Can F, Azap ÖK, Demirbilek M, Arslan H, Karaman SÖ. In vitro activities of non-traditional antimicrobials alone or in combination against multidrug-resistant strains of Pseudomonas aeruginosa and Acinetobacter baumannii isolated from intensive care units. Int J Antimicrob Agents. 2006;27:224-228.
38. Kanellakopoulou K, Giamarellos-Bourboulis EJ. Carrier systems for the local delivery of antibiotics in bone infections. Drugs. 2000;59:1223-1232.
39. Koort JK, Mäkinen TJ, Suokas E, Veiranto M, Jalava J, Knuuti J, Törmälä P, Aro HT. Efficacy of ciprofloxacin-releasing bioabsorbable osteoconductive bone defect filler for treatment of experimental osteomyelitis due to Staphylococcus aureus. Antimicrob Agents Chemother. 2005;49:1502-1508.
40. Anker CJ, Holdridge SP, Baird B, Cohen H, Damron TA. Ultraporous ß-tricalcium phosphate is well incorporated in small cavitary defects. Clin Orthop Relat Res. 2005:251-257.

41. Arai E, Nakashima H, Tsukushi S, Shido Y, Nishida Y, Yamada Y, Sugiura H, Katagiri H. Regenerating the fibula with beta-tricalcium phosphate minimizes morbidity after fibula resection. Clin Orthop Relat Res. 2005:233-237.
42. Coe CJ, Doss SA, Tillotson GS, Amyes SGB. Interaction of sub-inhibitory concentrations of ciprofloxacin and rifampicin against Staphylococcus aureus. Int J Antimicrob Agents. 1995;5:135-139.
43. Trampuz A, Zimmerli W. Antimicrobial agents in orthopaedic surgery: Prophylaxis and treatment. Drugs. 2006;66:1089-1105.
44. Yim G, McClure J, Surette MG, Davies JE. Modulation of Salmonella gene expression by subinhibitory concentrations of quinolones. J Antibiot. 2011;64:73-78.
45. Perlroth J, Kuo M, Tan J, Bayer AS, Miller LG. Adjunctive use of rifampin for the treatment of Staphylococcus aureus infections: A systematic review of the literature. Arch Intern Med. 2008;168:805-819.
46. Kiedrowski MR, Horswill AR. New approaches for treating staphylococcal biofilm infections. Ann New York Acad Sci. 2011;1241(1):104-121.
47. Chusri S, Villanueva I, Voravuthikunchai SP, Davies J. Enhancing antibiotic activity: A strategy to control Acinetobacter infections. J Antimicrob Chemother. 2009;64:1203-1211.
48. Blázquez J, Couce A, Rodríguez-Beltrán J, Rodríguez-Rojas A. Antimicrobials as promoters of genetic variation. Curr Opin Microbiol. 2012;15:561-569.
49. Coiffier G, Albert J-, Arvieux C, Guggenbuhl P. Optimizing combination rifampin therapy for staphylococcal osteoarticular infections. Jt Bone Spine. 2013;80:11-17.
50. Änko M-, Kurittu J, Karp M. An Escherichia coli biosensor strain for amplified and high throughput detection of antimicrobial agents. J Biomol Screen. 2002;7:119-125.
51. Galluzzi L, Karp M. Amplified detection of transcriptional and translational inhibitors in bioluminescent Escherichia coli K-12. J Biomol Screen. 2003;8:340-346.
52. Kankilic B, Bayramli E, Kilic E, Dağdeviren S, Korkusuz F. Vancomycin containing PLLA/β-TCP controls MRSA in vitro. Clin Orthop Relat Res. 2011;469:3222-3228.
53. Yim G, De La Cruz F, Spiegelman GB, Davies J. Transcription modulation of Salmonella enterica serovar typhimurium promoters by sub-MIC levels of rifampin. J Bacteriol. 2006;188:7988-7991.

APPENDIX

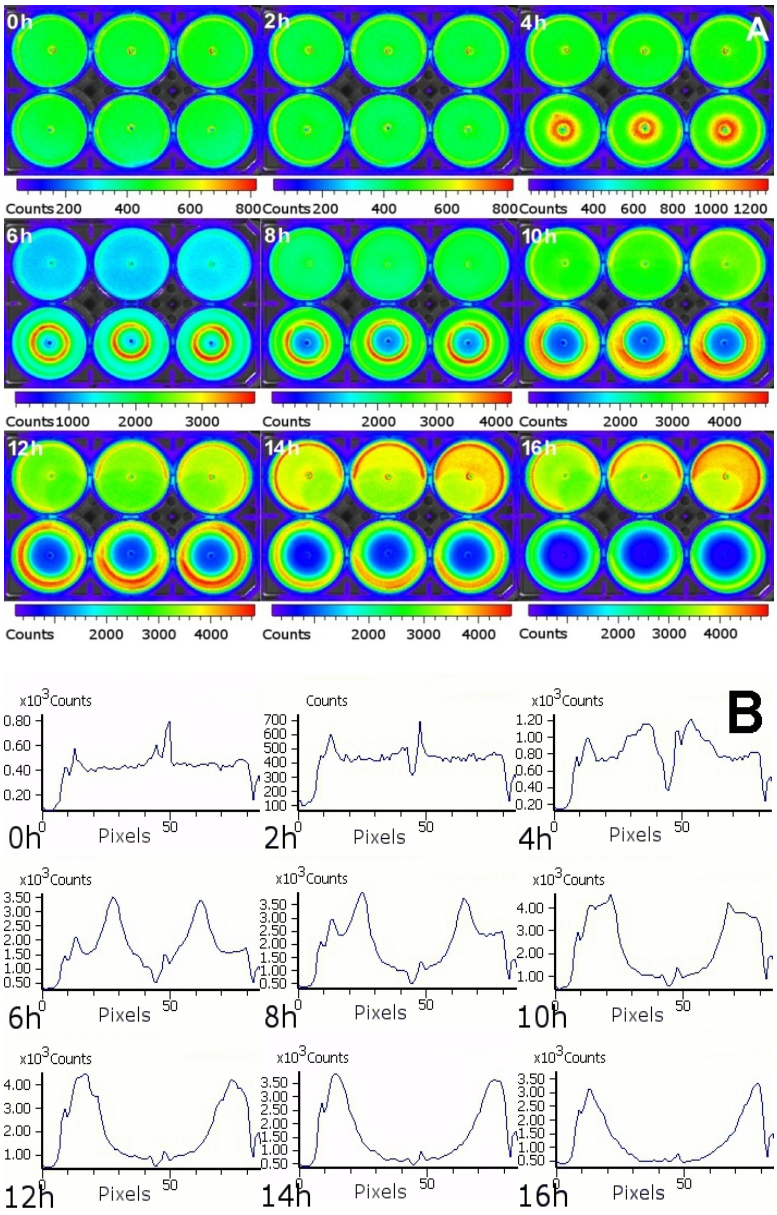

Figure. 1. (A) The development of the inhibitory zones was seen as growing blue areas in the middle of the wells of cultured S. epidermidis and ciprofloxacin composite pellets, which had been immersed in Sörensen phosphate buffer solution (pH 7.4) at 37°C for one week (in triplicate on the lower row). Pellets without antibiotic were used as controls (in triplicate on the top row). The plate was photographed at time points of 0, 2, 4, 6, 8, 10, 12, 14, and 16 hours. The diameter of one well is 35 mm. (B) Light intensity levels as photon counts of S. epidermidis exposed to one ciprofloxacin releasing composite pellet in the middle of the well. The pellet had been immersed in Sörensen phosphate buffer solution (pH 7.4) at 37°C for one week before the experiment. The results are presented at time points of 0, 2, 4, 6, 8, 10, 12, 14, and 16 hours. Note the different scales of the y-axes.

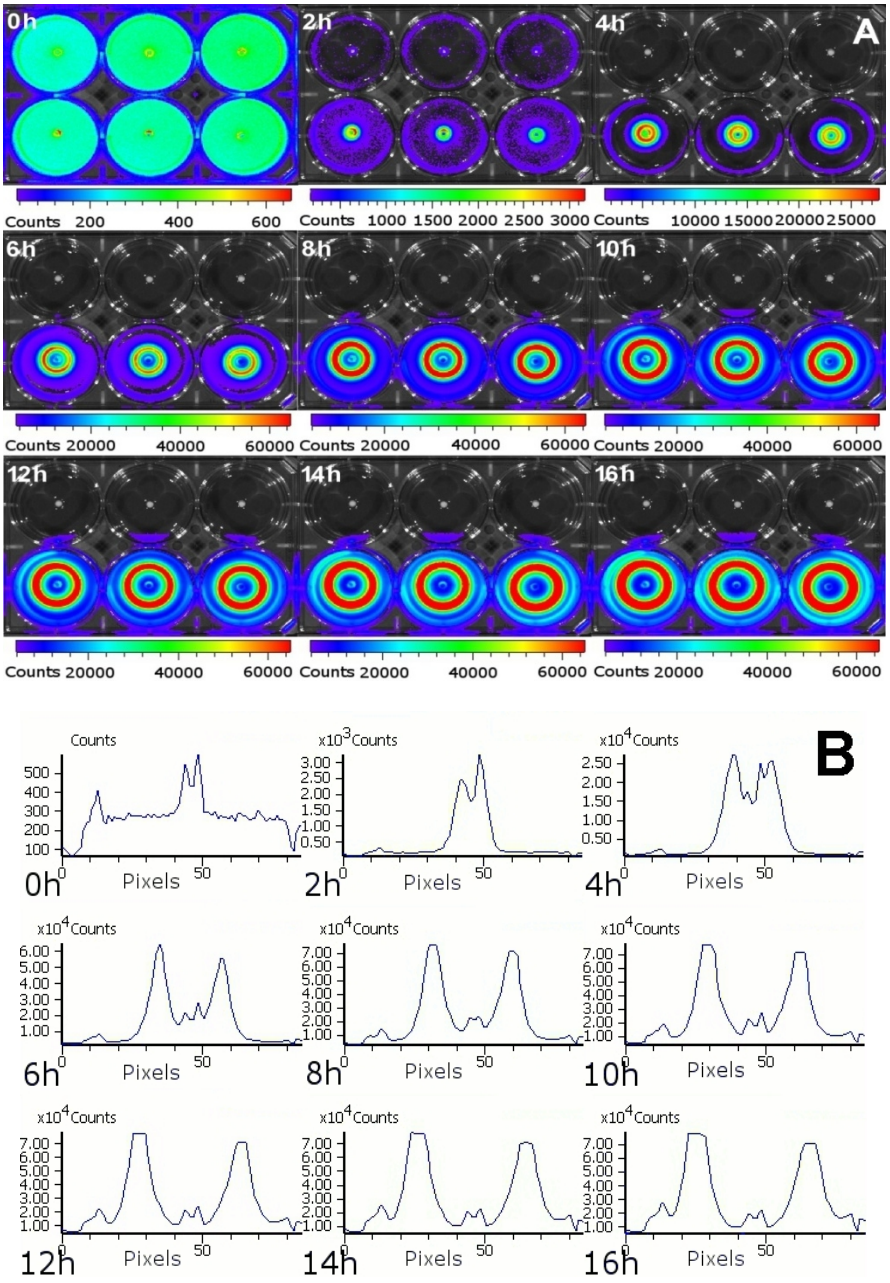

Figure 2.(A) The development of the inhibitory zones was seen as growing blue areas in the middle of the wells of cultured P. aeruginosa and ciprofloxacin composite pellets, which had been immersed in Sörensen phosphate buffer solution (pH 7.4) at 37°C for one week (in triplicate on the lower row). Pellets without antibiotic were used as controls (in triplicate on the top row). The plate was photographed at time points of 0, 2, 4, 6, 8, 10, 12, 14, and 16 hours. The diameter of one well is 35 mm. (B) Light intensity levels as photon counts of P. aeruginosa exposed to one ciprofloxacin releasing composite pellet in the middle of the well. The pellet had been immersed in Sörensen phosphate buffer solution (pH 7.4) at 37°C for one week before the experiment. The results are presented at time points of 0, 2, 4, 6, 8, 10, 12, 14, and 16 hours. Note the different scales of the y-axes.

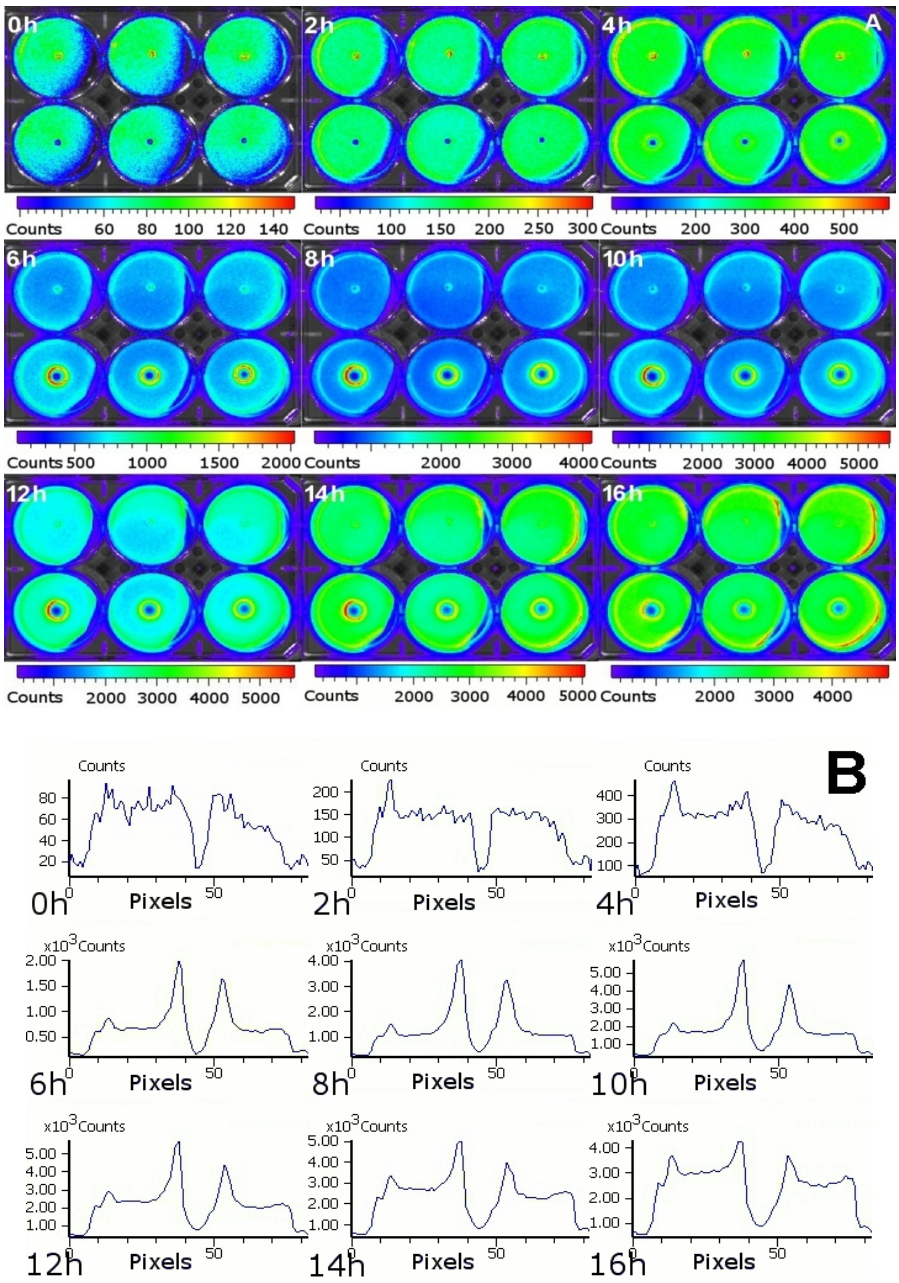

Figure 3.(A) The development of the inhibitory zones was seen as growing blue areas in the middle of the wells of cultured S. epidermidis and rifampicin composite pellets, which had been immersed in Sörensen phosphate buffer solution (pH 7.4) at 37°C for one week (in triplicate on the lower row). Pellets without antibiotic were used as controls (in triplicate on the top row). The plate was photographed at time points of 0, 2, 4, 6, 8, 10, 12, 14, and 16 hours. The diameter of one well is 35 mm. (B) Light intensity levels as photon counts of S. epidermidis exposed to one rifampicin releasing composite pellet in the middle of the well. The pellet had been immersed in Sörensen phosphate buffer solution (pH 7.4) at 37°C for one week before the experiment. The results are presented at time points of 0, 2, 4, 6, 8, 10, 12, 14, and 16 hours. Note the different scales of the y-axes.

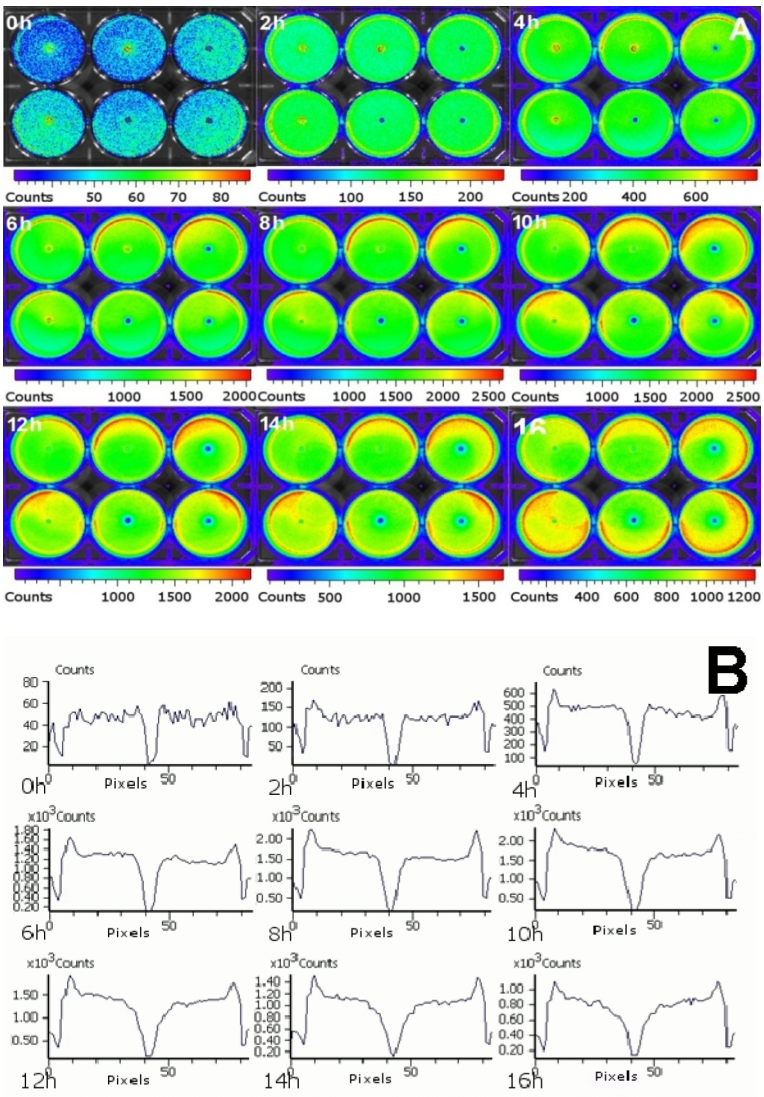

Figure 4.(A) The development of the inhibitory zones was seen as growing blue areas in the middle of the wells of cultured P. aeruginosa and rifampicin composite pellets, which had been immersed in Sörensen phosphate buffer solution (pH 7.4) at 37°C for one week (in triplicate on the lower row). Pellets without antibiotic were used as controls (in triplicate on the top row). The plate was photographed at time points of 0, 2, 4, 6, 8, 10, 12, 14, and 16 hours. The diameter of one well is 35 mm. (B) Light intensity levels as photon counts of P. aeruginosa exposed to one rifampicin releasing composite pellet in the middle of the well. The pellet had been immersed in Sörensen phosphate buffer solution (pH 7.4) at 37°C for one week before the experiment. The results are presented at time points of 0, 2, 4, 6, 8, 10, 12, 14, and 16 hours. Note the different scales of the y-axes.

Peer-review history:
The peer review history for this paper can be accessed here:
http://www.sciencedomain.org/review-history.php?iid=305&id=8&aid=2569

Tampereen teknillinen yliopisto
PL 527
33101 Tampere

Tampere University of Technology
P.O.B. 527
FI-33101 Tampere, Finland

ISBN 978-952-15-3211-5
ISSN 1459-2045